École doctorale MSTIC

Mathématiques et Sciences et Techniques de l'Information et de la Communication

Thèse de doctorat

Spécialité : Traitement du signal

Présentée par :

Florian DUPUY

Étude des systèmes MIMO pour émetteurs mono-porteuses dans le contexte de canaux sélectifs en fréquence

Analysis of MIMO systems for single-carrier transmitters in frequency-selective channels

À soutenir le 16 décembre 2011 devant les membres du jury :

Rapporteur	Prof. Wolfgang GERSTACKER,	Universität Erlangen-Nürnberg
Rapporteur	Prof. Eduard JORSWIECK,	Technische Universität Dresden
Directeur de thèse	Prof. Philippe LOUBATON,	Université Paris Est
Co-directeur de thèse	Prof. Pascal CHEVALIER,	CNAM/Thales Communications
Examinateur	Dr. Walid HACHEM,	CNRS/Telecom ParisTech
Examinateur	Prof. Dirk SLOCK,	Eurecom

Table des matières

Introduction

La présente thèse s'est déroulée dans le cadre d'un contrat CIFRE entre l'université de Paris Est (Marne-la-Vallée) et Thales Communications (Colombes). Cette thèse s'articule autour des canaux MIMO sélectifs en fréquence pour des émetteurs mono-porteuses. Il est connu depuis longtemps que les systèmes multi-antennes, ou systèmes MIMO, permettent d'augmenter substantiellement les débits de transmission des systèmes mono-antenne, ou systèmes SISO ; un premier axe de recherche concerne ainsi l'optimisation de la capacité ergodique dans les canaux sélectifs en fréquence. L'utilisation de plusieurs antennes d'émission permet également d'augmenter les performances en réception grâce à la diversité de transmission induite ; un second axe s'attache donc à étudier la diversité pour des récepteurs MMSE dans des canaux sélectifs en fréquence.

Capacité ergodique

Depuis une quinzaine d'années de nombreux travaux s'attachent à utiliser les systèmes MIMO (Multiple Input / Multiple Output), c'est-à-dire des systèmes équipés de plusieurs antennes d'émission et de plusieurs antennes de réception, afin d'augmenter la capacité de Shannon associée aux traditionnels systèmes SISO (Single Input / Single Output). Dans ce but, un problème crucial consiste en la conception de l'émetteur optimal au sens de la capacité de Shannon, c'est-à-dire en la relation optimale entre le vecteur $\mathbf{x}(n)$ transmis sur les antennes d'émission et les symboles d'information à transmettre. Ces problématiques ont fait l'objet de nombreuses études dans le cas où le canal de transmission MIMO est non sélectif en fréquence ; elles sont cependant nettement moins matures dans le cadre d'un canal MIMO sélectif en fréquence. Cette thèse s'intéresse ainsi dans cette première partie à l'optimisation, au sens de la capacité ergodique, de la matrice de covariance du vecteur transmis dans le cas où seules les statistiques du canal, et non la valeur instantanée du canal, sont connues à l'émetteur.

État de l'art des cas non sélectifs en fréquence

Dans le cas d'un canal non sélectif en fréquence on peut représenter le canal MIMO par une matrice $\mathbf{H}$ de taille $r \times t$, où r est le nombre d'antennes en réception et t le nombre d'antennes en émission. Le vecteur $\mathbf{y}(n)$ obtenu en échantillonnant le signal reçu à la période symbole sur les antennes de réception peut donc s'écrire sous la forme :

$$\mathbf{y}(n) = \mathbf{H}\mathbf{x}(n) + \mathbf{b}(n), \tag{1}$$

où $\mathbf{x}(n)$ est le vecteur transmis sur les antennes d'émission et $\mathbf{b}(n)$ un bruit additif supposé Gaussien de variance σ^2. Telatar a établi le premier la formule explicite de l'information mutuelle entre $\mathbf{x}(n)$ et $\mathbf{y}(n)$ pour une matrice $\mathbf{H}$ donnée [1, 2] :

$$\log\det\left(\mathbf{I}_r + \frac{1}{\sigma^2}\mathbf{H}\mathbf{Q}\mathbf{H}^H\right), \tag{2}$$

où $\mathbf{Q}$ est la covariance du vecteur émis $\mathbf{x}$ supposé Gaussien, i.e. $\mathbf{Q} = \mathbb{E}\left[\mathbf{x}\mathbf{x}^H\right]$, qui vérifie la contrainte de puissance $\frac{1}{t}\mathrm{Tr}\,\mathbf{Q} \leq 1$. Lorsque l'on a accès à la valeur de $\mathbf{H}$, le maximum sur $\mathbf{Q}$ de l'information mutuelle (2) correspond à la capacité du canal MIMO et représente le débit maximum auquel on peut transmettre de façon fiable l'information. Il est bien connu [3] que les vecteurs propres de la matrice $\mathbf{Q}$ optimale, notée $\mathbf{Q}_*$, coïncident avec les vecteurs singuliers à droite de $\mathbf{H}$ et les valeurs propres de $\mathbf{Q}_*$ s'obtiennent grâce à un algorithme de type "waterfilling" – la connaissance du canal instantané $\mathbf{H}$ est donc requise à l'émetteur. Il est peu réaliste dans le cas des communications mobiles de supposer disposer de la matrice $\mathbf{H}$ à l'émetteur. Le canal de transmission est en pratique versatile, à cause notamment de la mobilité des utilisateurs et de la diversité des trajets de propagation. Il est donc d'usage de modéliser $\mathbf{H}$ comme la réalisation d'une matrice aléatoire Gaussienne de statistiques connues. On s'intéresse alors non plus à l'optimisation de (2) lui-même mais à l'optimisation de l'espérance de l'information mutuelle, appelée information mutuelle ergodique et que nous noterons $I(\mathbf{Q})$:

$$I(\mathbf{Q}) = \mathbb{E}\left[\log\det\left(\mathbf{I}_r + \frac{1}{\sigma^2}\mathbf{H}\mathbf{Q}\mathbf{H}^H\right)\right]. \tag{3}$$

L'optimisation de l'information mutuelle ergodique ne nécessite alors que la connaissance des statistiques du canal à l'émetteur. Ceci est une hypothèse plus réaliste dans le cadre des communications sans fil que la connaissance du canal instantané. En effet, les statistiques du canal varient en pratique de manière beaucoup plus lente que le canal lui-même. Une première étape consiste à étudier le cas où les entrées de la matrice $\mathbf{H}$ sont i.i.d. Gaussiennes complexes de moyenne nulle et de variance $1/\sqrt{t}$, qui est un modèle simplifié d'un canal de Rayleigh. Telatar a montré dans [2] que pour un tel modèle de canal la matrice de covariance optimale au sens de l'information mutuelle ergodique était $\mathbf{Q}_* = \mathbf{I}_t$. L'information mutuelle ergodique vaut alors

$$I(\mathbf{Q}_*) = \mathbb{E}\left[\log\det\left(\mathbf{I}_r + \frac{1}{\sigma^2}\mathbf{H}\mathbf{H}^H\right)\right]. \tag{4}$$

Ce problème d'optimisation a ensuite été étudié pour des modèles de canaux plus élaborés, comme le modèle de Kronecker ou le canal de Rice. Le modèle de Kronecker prend en compte la corrélation spatiale entre les différents trajets en considérant que la matrice $\mathbf{H}$ peut s'écrire sous la forme $\mathbf{C}^{\frac{1}{2}}\mathbf{W}\tilde{\mathbf{C}}^{\frac{1}{2}}$, où $\mathbf{W}$ est une matrice dont les entrées sont i.i.d. Gaussiennes complexes de moyenne nulle et de variance $1/\sqrt{t}$; on suppose dans ce modèle une séparation des corrélations à l'émetteur $\tilde{\mathbf{C}}$ et au récepteur $\mathbf{C}$ – d'où le nom également de covariance séparable. Dans le cas d'un canal de Kronecker, il a été montré par de nombreux auteurs que les vecteurs propres de la covariance optimale $\mathbf{Q}_*$ doivent coïncider avec les vecteurs propres de la matrice de corrélation à l'émission $\tilde{\mathbf{C}}$ (voir, entre autres, [4, 5]). Un canal de Rice à corrélation séparable correspond à un modèle de Kronecker avec une moyenne non nulle, i.e. la matrice $\mathbf{H}$ peut être modélisée de la sorte : $\mathbf{H} = \mathbf{A} + \mathbf{C}^{\frac{1}{2}}\mathbf{W}\tilde{\mathbf{C}}^{\frac{1}{2}}$, où $\mathbf{A}$ déterministe est la composante en ligne de vue (ou LOS - Line Of Sight). On parle de canal de Rice décorrélé lorsque $\mathbf{C} = \mathbf{I}_r$ et $\tilde{\mathbf{C}} = \mathbf{I}_t$. De manière similaire au cas du modèle de Kronecker, [6] a montré pour un canal de Rice décorrélé que les vecteurs propres de la covariance optimale $\mathbf{Q}_*$ doivent coïncider avec les vecteurs singuliers à droite de la matrice $\mathbf{A}$. Il suffit alors, dans les deux cas précédemment cités, d'estimer les valeurs propres de $\mathbf{Q}_*$ par des algorithmes classiques d'optimisation, de type "waterfilling". Dans le cas du canal de Rice à corrélation séparable, l'optimisation est plus complexe ; les vecteurs propres de la covariance optimale $\mathbf{Q}_*$ n'ont pas d'expression explicite. Une approche directe a cependant été étudiée dans [7], où les entrées de la matrice $\mathbf{Q}_*$ sont estimés par un algorithme de Newton, associé à une méthode de barrière, appliqué directement sur l'expression de l'information mutuelle ergodique (3). Cette méthode d'optimisation directe de l'information mutuelle ergodique nécessite l'utilisation de méthodes de Monte-Carlo, très coûteuses en terme de calculs numériques, pour estimer l'information mutuelle ergodique $I(\mathbf{Q})$ au cours de l'algorithme d'optimisation – ainsi que pour estimer les vecteurs gradient et les matrices Hessiennes pour l'algorithme de Newton.

Afin d'éviter l'utilisation de méthodes basées sur des simulations de Monte-Carlo, divers auteurs ont proposé de remplacer l'optimisation de $I(\mathbf{Q})$ par l'optimisation d'un approximant en grande dimension, c'est-à-dire pour r et t tendant vers l'infini de sorte que $r/t \to c$ avec $c \in]0, +\infty[$. Le point de départ est de remarquer que $\frac{1}{r}\log\det\left(\mathbf{I} + \frac{1}{\sigma^2}\mathbf{H}\mathbf{Q}\mathbf{H}^H\right)$ se met sous la forme

$$\frac{1}{r}\sum_{i=1}^{r}\log\left(1+\frac{\lambda_i}{\sigma^2}\right), \tag{5}$$

où les $(\lambda_i)_{i=1,\ldots,r}$ représentent les valeurs propres de $\mathbf{H}\mathbf{Q}\mathbf{H}^H$. Dans nombre de situation d'intérêt pratique (5) a le même comportement asymptotique qu'une quantité déterministe ne dépendant que de $\mathbf{Q}$ et des statistiques de $\mathbf{H}$. Dès lors, on peut approximer $I(\mathbf{Q})$ par une fonction $\overline{I}(\mathbf{Q})$ dont l'expression dépend du canal considéré. Par exemple, il a été montré par [8, 9] que, dans le cas d'un modèle de Kronecker, $\overline{I}(\mathbf{Q})$ peut s'écrire sous la forme suivante :

$$\overline{I}(\mathbf{Q}) = \log\det\left(\mathbf{I}_r + \tilde{\delta}\mathbf{C}\right) + \log\det\left(\mathbf{I}_t + \delta\mathbf{Q}\tilde{\mathbf{C}}\right) - \sigma^2 t\delta\tilde{\delta}, \tag{6}$$

où δ et $\tilde{\delta}$ sont deux réels strictement positifs solutions d'un système d'équations couplées. Le calcul de Moustakas et al. [8] se base cependant sur la méthode des répliques, dont la pertinence mathématique n'a pas été prouvée à ce jour dans le cas présent. Il est par ailleurs intéressant d'étudier le rythme de convergence de l'approximant $\overline{I}(\mathbf{Q})$ vers $I(\mathbf{Q})$; il a été montré par [8, 10] que $I(\mathbf{Q}) - \overline{I}(\mathbf{Q}) = \mathcal{O}(1/t)$. La preuve de [8] repose à nouveau sur les méthodes des répliques, tandis que l'approche simple et rigoureuse de [10] utilise les méthodes dites Gaussiennes, qui utilisent le caractère Gaussien du modèle de canal considéré. Un résultat similaire est également obtenu pour un canal de Rice à corrélation séparable, comme il a été montré dans [11] par la méthode des répliques, puis dans [12] par les méthodes Gaussiennes : l'approximant $\overline{I}(\mathbf{Q})$ peut dans ce cas s'écrire

$$\overline{I}(\mathbf{Q}) = \log\det\left(\mathbf{I}_r + \tilde{\delta}\mathbf{C}\right) + \log\det\left(\mathbf{I}_t + \delta\mathbf{Q}\tilde{\mathbf{C}} + \frac{1}{\sigma^2}\mathbf{Q}\mathbf{A}^H\left(\mathbf{I}_r + \tilde{\delta}\mathbf{C}\right)^{-1}\mathbf{A}\right) - \sigma^2 t\delta\tilde{\delta}, \quad (7)$$

où δ et $\tilde{\delta}$ sont à nouveau deux réels strictement positifs solutions d'un système d'équations couplées non linéaires.

Cet approximant permet alors une approche indirecte d'optimisation de l'information mutuelle ergodique consistant à utiliser l'approximant $\overline{I}(\mathbf{Q})$ pour optimiser la covariance, plutôt que d'utiliser directement l'information mutuelle ergodique $I(\mathbf{Q})$. Les expressions de $\overline{I}(\mathbf{Q})$ sont explicites ce qui permet d'éviter l'utilisation des méthodes de Monte-Carlo pour estimer $I(\mathbf{Q})$. La mise en œuvre de l'optimisation de $\overline{I}(\mathbf{Q})$ est donc plus aisée que pour $I(\mathbf{Q})$ et le gain en terme de complexité de calcul important. Dans le cas du modèle de Kronecker, [13] propose ainsi un algorithme itératif d'optimisation basé sur l'approximant de l'information mutuelle ergodique. Une extension de cet algorithme au canal de Rice à corrélation séparable est proposée dans [12], qui montre également la stricte concavité de l'approximant et donne des résultats partiels de convergence. L'approche indirecte est également justifiée dans [12] : il y est montré que

$$I(\overline{\mathbf{Q}}_*) = I(\mathbf{Q}_*) + \mathcal{O}\left(\frac{1}{t}\right). \quad (8)$$

où $\overline{\mathbf{Q}}_*$ est la matrice de covariance maximisant $\overline{I}(\mathbf{Q})$ et où $\mathbf{Q}_*$ est la matrice de covariance maximisant $I(\mathbf{Q})$. Pour ce type de canal un algorithme similaire a été introduit par [14] avant d'être étudié tout récemment plus en détail par [15]. Il est notamment prouvé par [15] que l'algorithme considéré converge dans le cas d'un canal de Rayleigh et des cas d'oscillation de l'algorithme introduit par [12] sont exhibés.

Cas sélectif en fréquence

La première contribution de cette thèse est l'optimisation de l'information mutuelle ergodique pour les canaux sélectifs en fréquence. Lorsque le canal est sélectif en fréquence et que l'émetteur utilise des modulation mono-porteuses, le modèle de réception (1) n'est plus valable. Le signal reçu $\mathbf{y}(n)$ se met

alors sous la forme :

$$\begin{aligned}\mathbf{y}(n) &= \sum_{l=1}^{L} \mathbf{H}^{(l)}\mathbf{x}(n-l+1) + \mathbf{b}(n) \\ &= [\mathbf{H}(z)]\mathbf{x}(n) + \mathbf{b}(n),\end{aligned} \tag{9}$$

où l'on note désormais $\mathbf{H}(z)$ la fonction de transfert du canal équivalent à temps discret défini par $\mathbf{H}(z) = \sum_{l=1}^{L} \mathbf{H}^{(l)}\, z^{-(l-1)}$, chaque matrice $\mathbf{H}^{(l)}$ correspondant à un trajet. Un modèle répandu (voir par ex. [16, 17]) pour ces matrices $\mathbf{H}^{(l)}$ consiste à considérer qu'elles sont indépendantes, ce qui correspond à des trajets indépendants, et qu'elles suivent chacune un modèle de Kronecker : $\mathbf{H}^{(l)} = \frac{1}{\sqrt{t}}(\mathbf{C}^{(l)})^{1/2}\mathbf{W}_l(\tilde{\mathbf{C}}^{(l)})^{1/2}$, où $\mathbf{W}_l$ est une matrice aléatoire dont les entrées sont Gaussiennes complexes standards. On note $\mathbf{Q}(e^{2i\pi\nu})$ la densité spectrale de la matrice de covariance du vecteur transmis $\mathbf{x}$. L'information mutuelle ergodique du canal peut alors s'écrire

$$I(\mathbf{Q}(e^{2i\pi\nu})) = \mathbb{E}\left[\int_0^1 \log\det\left(\mathbf{I}_r + \frac{1}{\sigma^2}\mathbf{H}(e^{2i\pi\nu})\mathbf{Q}(e^{2i\pi\nu})\mathbf{H}(e^{2i\pi\nu})^H\right) d\nu\right]. \tag{10}$$

Nous avons montré que dans le cadre de l'optimisation de $I(\mathbf{Q}(e^{2i\pi\nu}))$ on pouvait se ramener au cas de matrices de covariance $\mathbf{Q}(e^{2i\pi\nu})$ ne dépendant pas de la fréquence. On considère désormais $\mathbf{Q}(e^{2i\pi\nu}) = \mathbf{Q}\,\forall\nu$. Un approximant de $I(\mathbf{Q})$ en grande dimension noté $\overline{I}(\mathbf{Q})$ a été établi par [17] en utilisant la méthode des répliques :

$$\overline{I}(\mathbf{Q}) = \log\det\left(\mathbf{I}_r + \sum_{l=1}^{L}\tilde{\delta}_l\mathbf{C}^{(l)}\right) + \log\det\left(\mathbf{I}_t + \mathbf{Q}\left(\sum_{l=1}^{L}\delta_l\tilde{\mathbf{C}}^{(l)}\right)\right) - \sigma^2 t\sum_{l=1}^{L}\delta_l\tilde{\delta}_l, \tag{11}$$

où les δ_l et $\tilde{\delta}_l$, $l = 1,\ldots,L$, sont les réels positifs solutions d'un système non linéaire de $2L$ équations couplées. Nous vérifions dans un premier temps la pertinence de cet approximant en utilisant une approche rigoureuse inspirée des résultats de [12] précédemment évoqués. Nous justifions tout d'abord l'existence et l'unicité des δ_l et $\tilde{\delta}_l$, un point qui n'avait pas été abordé par [17]. Nous précisons également les hypothèses techniques nécessaires à la convergence de $I(\mathbf{Q})$ vers l'approximant ainsi que la vitesse de cette convergence :

$$I(\mathbf{Q}) = \overline{I}(\mathbf{Q}) + \mathcal{O}\left(\frac{1}{t}\right). \tag{12}$$

Nous nous intéressons dans un second temps à l'optimisation de $I(\mathbf{Q})$ via son approximation $\overline{I}(\mathbf{Q})$. Pour cela nous justifions la stricte concavité de la fonction $\mathbf{Q} \mapsto \overline{I}(\mathbf{Q})$, avant d'établir le résultat suivant :

$$I(\overline{\mathbf{Q}}_*) = I(\mathbf{Q}_*) + \mathcal{O}\left(\frac{1}{t}\right), \tag{13}$$

où $\overline{\mathbf{Q}}_*$ est la matrice maximisant $\overline{I}(\mathbf{Q})$ sous la contrainte de puissance $\mathrm{Tr}\,\mathbf{Q} = t$, et où $\mathbf{Q}_*$ est la matrice maximisant $\mathbf{I}(\mathbf{Q})$ sous la contrainte de puissance $\mathrm{Tr}\,\mathbf{Q} = t$. Autrement dit, il est cohérent de maximiser

l'approximation $\overline{I}(\mathbf{Q})$ au lieu de $I(\mathbf{Q})$. Nous proposons ainsi un algorithme de maximisation de $\overline{I}(\mathbf{Q})$ qui se base sur un waterfilling itératif : chaque itération résout le système de $2L$ équations couplées évoqué précédemment ainsi qu'un problème classique de waterfilling [18]. Cet algorithme peut être vu comme une extension de celui proposé par [13] dans le cas d'un canal de Rayleigh et par [12] dans le cas d'un canal de Rice. Nous prouvons également que s'il converge l'algorithme converge vers la covariance optimale $\overline{\mathbf{Q}}_*$ – la convergence en elle-même n'a pu être prouvée.

Diversité des récepteurs MMSE

Pour ce second axe de la thèse, nous nous intéressons aux récepteurs MMSE. A l'inverse des récepteurs du maximum de vraisemblance (ou ML pour Maximum Likelihood) ces récepteurs sont sous-optimaux mais plus simples à mettre en œuvre. Dans un premier temps, nous étudions la diversité de tels récepteurs à haut SNR pour des canaux sélectifs en fréquence. Nous nous attardons dans un second temps sur un facteur de diversité, l'utilisation des codes spatio-temporels en bloc (STBC), plus spécifiquement l'utilisation du code d'Alamouti. Ainsi, nous proposons et analysons un nouveau récepteur MMSE adapté à la non-circularité des signaux qu'occasionne l'utilisation du codage d'Alamouti. Cette dernière analyse a cependant été limitée au cas des canaux non sélectifs en fréquence – ou de manière équivalente au cas des canaux sélectifs en fréquence avec une forme d'onde OFDM.

Analyse de l'ordre de diversité

On définit l'ordre de diversité d d'un système par la pente de la décroissance exponentielle de la probabilité d'erreur P_e en fonction du SNR ρ, à haut SNR :

$$d = -\lim_{\rho \to +\infty} \frac{\log P_e}{\log \rho} \tag{14}$$

On a alors, pour $\rho \gg 1$, $P_e \sim k\rho^{-d}$. Il existe deux approches pour étudier la diversité d'un système. La plus répandue (voir entre autres [19–21]) consiste à analyser le rythme de décroissance de la probabilité d'erreur par paire (PEP) en fonction du SNR. Cette approche nécessite cependant l'élaboration de schémas de codage spécifique pour atteindre la diversité maximale. Nous nous intéressons ici à la seconde approche qui est basée sur la probabilité d'outage $P_{out}(R)$, où R est le débit cible :

$$P_{out}(R) = \mathbb{P}\left(I < R\right), \tag{15}$$

où I représente l'information mutuelle du système. Pour un système bien conçu, la probabilité d'outage correspond à la probabilité que la transmission soit non fiable. Il est alors pertinent d'étudier la décroissance exponentielle non pas de la probabilité d'erreur P_e mais de la probabilité d'outage P_{out}.

Cette approche est également commode car elle permet d'éviter le problème de conception du codage à l'émetteur. On définit alors la diversité de la manière suivante :

$$d(R) = -\lim_{\rho \to +\infty} \frac{\log P_{out}(R)}{\log \rho}. \tag{16}$$

Cette approche est utilisée par de nombreux auteurs, dans le cadre de l'analyse du compromis diversité-multiplexage (ou Diversity-Multiplexing Trade-off – DMT), introduit par Zheng et Tse [22]. L'étude de ce compromis permet d'obtenir la diversité maximale atteignable. Nous nous attardons donc désormais sur l'étude du DMT.

Le compromis diversité-multiplexage :
Comme évoqué dans la section précedente, les systèmes MIMO permettent à haut SNR un gain linéaire en capacité par rapport aux systèmes SISO [2] :

$$I(\rho) \sim \min\{M, N\} \log \rho \text{ pour } \rho \gg 1, \tag{17}$$

où $I(\rho)$ est l'information mutuelle, M le nombre d'antennes en émission, N le nombre d'antennes en réception. La capacité croît donc en $\log \rho$ à haut SNR. Il est donc pertinent d'écrire le débit cible sous la forme

$$R = r \log \rho, \tag{18}$$

où $r \leq \min\{M, N\}$ est le coefficient – ou l'ordre, le gain – de multiplexage. Ce gain correspond au multiplexage spatial : le canal MIMO peut être décomposé en sous-canaux SISO indépendants dont le nombre est le rang de la matrice canal $\mathbf{H}$, qui est $\min\{M, N\}$ si $\mathbf{H}$ est bien conditionnée. Le multiplexage spatial revient à utiliser les degrés de liberté disponibles pour transmettre des signaux indépendants sur ces canaux parallèles, au lieu de les utiliser pour améliorer la fiabilité de la transmission : il existe un compromis fondamental entre le coefficient de multiplexage r et la diversité $d(R)$, appelé DMT ou compromis diversité-multiplexage [22]. Il est alors intéressant d'étudier la dépendance en r de la diversité $d(R) = d(r \log \rho)$ défini par (16) ; on notera désormais $d(r)$ la fonction donnant la diversité en fonction du coefficient de multiplexage r :

$$d(r) = -\lim_{\rho \to +\infty} \frac{\log P_{out}(r \log \rho)}{\log \rho}. \tag{19}$$

On obtient alors, a priori, l'ordre de diversité maximal atteignable d_{max} en prenant $r = 0$. Zheng et Tse ont établi $d(r)$ pour un canal MIMO non sélectif en fréquence dans [22] :

$$d(r) = (M - r)(N - r). \tag{20}$$

On a donc $d_{max} = MN$ pour R fixé. Une extension de ce résultat au cas SISO sélectif en fréquence a rapidement suivi [23, 24], puis le cas du canal MIMO sélectif en fréquence a été analysé [25–27].

En notant L le nombre de trajets indépendants, il est montré que, sous certaines conditions, l'ordre de diversité $d(r)$ vérifie

$$d(r) = L(M - r)(N - r), \tag{21}$$

d'où un ordre de diversité maximal $d_{max} = LMN$. Ces calculs de diversité supposent cependant un récepteur optimal, c'est-à-dire un récepteur ML. Un tel récepteur est en pratique trop complexe à mettre en œuvre. On lui préfère des récepteurs linéaires sous-optimaux tel le récepteur MMSE, ce qui nous amène à l'étude qui suit.

Étude du DMT pour les récepteurs MMSE :
La seconde contribution de la thèse est l'étude du DMT pour les récepteurs MMSE pour un débit cible R fixe, i.e. pour un coefficient de multiplexage $r = 0$. Il a été montré par [28] que dans le cas d'un canal MIMO non sélectif en fréquence les récepteurs MMSE détériorent grandement le DMT : en effet, l'expression suivante de $d(r)$ est obtenue :

$$d(r) = (N - M + 1)\left(1 - \frac{r}{M}\right)^{+}, \tag{22}$$

où $(\cdot)^{+} = \max\{0, \cdot\}$. On s'attend donc au mieux à une diversité de $d_{max} = N - M + 1$. Cependant, pour un débit cible R fini, i.e. pour $r = 0$, il a été observé par Hedayat et al. dans [29] que les récepteurs MMSE exhibent des ordres de diversité qui diffèrent selon le débit cible R choisi (voir également [30, 31]). En particulier, la diversité maximale LMN évoquée précédemment est atteinte pour des débits R suffisamment faibles, d'où le grand intérêt de ces récepteurs simples à mettre en œuvre. Ce comportement inattendu a été expliqué dans [28, 32] pour des canaux MIMO non sélectifs en fréquence et dans [33] pour des canaux MIMO sélectifs en fréquence, mais dans les deux cas l'explication est malheureusement partielle. Nous mettons en exergue le caractère inexact de la preuve donnée par [32] dans le cas d'un canal non sélectif en fréquence et donnons une preuve rigoureuse de la diversité pour un tel système. Par ailleurs, en ce qui concerne les canaux sélectifs en fréquence avec préfixe cyclique, Mehana et Nosratinia [33] n'établissent la diversité que dans le cas particulier d'un nombre de trajets L égal à la longueur du bloc de données émis. Par conséquent nous établissons la diversité dans le cas sélectif en fréquence avec préfixe cyclique – nous supposons toutefois une longueur de bloc de données émis suffisamment grande.

Diversité apportée par les STBC

Le compromis diversité-multiplexage se retrouve au niveau de la conception des systèmes MIMO : on peut par exemple privilégier le multiplexage en utilisant le schéma V-BLAST (Vertical Bell Layered Space-Time [34, 35]) ou préférer maximiser le gain en diversité en utilisant un Code Spatio-Temporel en Bloc (ou STBC pour Space-Time Block Code [36]) en émission. Zheng et Tse [22] ont d'ailleurs mis en évidence les comportements opposés de ces deux schémas par l'étude de leur DMT. Comme dans

cette partie nous nous intéressons avant tout à la diversité, qui permet d'augmenter la portée et la fiabilité des communications, nous nous penchons ici sur l'utilisation des STBC. Les STBC orthogonaux [37] sont particulièrement attractifs ; ils permettent d'atteindre la diversité spatiale maximale pour un nombre fixe d'antennes d'émission et de réception. Nous nous pencherons sur l'utilisation du premier STBC orthogonal, qui est également le plus simple et le plus connu, présenté par Alamouti dans [38]. Il est standardisé dans les normes UMTS, GSM, EDGE, IEEE 802.11n, IEEE 802.16 [39].

Afin d'exploiter au mieux le spectre disponible et la diversité inhérente au canal de transmission nous nous intéressons dans cette thèse au cas multi-utilisateur Alamouti, c'est-à-dire au cas où plusieurs utilisateurs partagent les mêmes ressources spectrales et utilisent chacun un codage Alamouti. Ce contexte requiert le développement de techniques d'annulation d'interférences (Interference Cancellation - IC) pour permettre aux utilisateurs de partager les mêmes ressources spectrales sans avoir d'incidence sur la qualité de transmission de chacun. Plusieurs schémas d'annulation d'interférences [40–47] ont été introduits permettant à P utilisateurs équipés de M antennes en émission et utilisant un STBC de partager le même canal. Winters et al. ont montré [48] que l'ordre de diversité de chaque utilisateur était M si le nombre d'antennes en réception est $N = M(P-1)+1$. Cependant, si la structure du STBC est exploitée, on peut montrer que $N = P$ antennes de réception suffisent pour un même ordre de diversité de M. Ce résultat a d'abord été prouvé par Naguib et al. dans [40, 42] pour le cas du codage Alamouti et $M = N = P = 2$. Une généralisation de ce résultat à un nombre d'antennes de réception $N \geq P$ a ensuite été établie par [43] (voir également [47] pour une approche alternative). Kazemitabar et Jafarkhani ont finalement présenté dans [46] un schéma d'annulation d'interférences pour des STBC quasi-orthogonaux (voir [49, 50]) qui permet de séparer P utilisateurs équipés de $M > 2$ antennes d'émission à partir de $N \geq P$ antennes de réception. Toutes ces techniques d'annulation d'interférences requièrent donc $N > 1$, i.e. plusieurs antennes en réception, ce qui reste un point bloquant au niveau du terminal mobile pour des raisons de coût et de dimensions. Ceci justifie le développement des techniques d'annulation d'interférences dites SAIC (Single Antenna Interference Cancellation), qui ne nécessitent qu'une seule antenne en réception et sont une alternative aux techniques complexes d'estimation ML multi-utilisateur [51].

Les techniques SAIC ont tout d'abord été développées pour des utilisateurs équipés d'une seule antenne d'émission et des transmissions mono-porteuses [52–56]. La plupart [52, 54–56] de ces techniques exploitent la non-circularité au second ordre [57] des modulations à valeurs réelles (BPSK, ASK) ou des modulations quasi-rectilignes (c'est-à-dire correspondant à la filtrée complexe de modulations à valeurs réelles) après une opération de dérotation (MSK, GMSK, OQAM [58]). Ces techniques implémentent un filtrage linéaire au sens large (LSL, ou encore WL pour Widely Linear [59]) optimal des observations et permettent la séparation de deux utilisateurs à partir d'une unique antenne de réception [54]. Ce concept, simple et efficace, est rapidement devenu populaire dans les réseaux 2G-3G :

- 3G Americas [60] a présenté le concept de SAIC comme une grande amélioration pour les récepteurs GSM des terminaux mobiles,
- cette technologie a été standardisé en 2005 pour le GSM et est donc désormais opérationnelle dans la plupart des terminaux mobiles GSM,
- une nouvelle normalisation de cette technologie permettant à plusieurs utilisateurs GSM d'utiliser le même slot TDMA (Multi-User Reusing One Slot - MUROS) est actuellement à l'étude,
- une extension de ce concept à plusieurs antennes de réception, dite MAIC (Muliple Antenna Interference Cancellation) [54], est d'un grand intérêt notamment pour les réseaux GPRS [61].

Dans le cadre des réseaux 4G, les réseaux d'antennes pour le terminal mobile ont été standardisés, ce qui suppose donc l'emploi des techniques MAIC uniquement. Cependant la mise en œuvre de ces réseaux d'antennes reste un point bloquant ; les techniques SAIC sont donc toujours d'actualité pour les réseaux 4G. Ainsi, une extension à l'OFDM de ces techniques a été récemment présentée par [62], pour des utilisateurs munis d'une antenne d'émission et utilisant la modulation ASK. Par ailleurs, le concept SAIC/MAIC est également d'un grand intérêt pour les réseaux militaires ad hoc, qui demandent avant tout des systèmes simples et robustes.

La modulation ASK est certes moins efficace en terme de puissance que la modulation QAM : seule la dimension réelle est utilisée pour l'émission. Cependant, dans un contexte multi-utilisateur, la modulation ASK peut être plus avantageuse qu'une modulation QAM par l'utilisation des degrés de liberté disponibles en réception pour séparer les différents utilisateurs. Les degrés de liberté non utilisés en émission dans la modulation sont en quelque sorte retrouvés en réception par un traitement adéquat : le filtrage LSL. Plusieurs travaux [62–64] semblent d'ailleurs mettre en évidence, toujours dans le contexte multi-utilisateur, une plus grande efficacité spectrale des modulations à valeurs réelles couplées à des récepteurs LSL par rapport à des modulations à valeurs complexes couplées à des récepteurs linéaires.

Les concepts de SAIC et MAIC concernent uniquement les systèmes SISO et SIMO. Nous étendons dans cette partie ces concepts aux systèmes MISO et MIMO, grâce à l'utilisation d'un STBC, plus spécifiquement du codage Alamouti, pour des constellations à valeurs réelles. Nous introduisons à cette fin un nouveau récepteur MMSE LSL (qui a cependant déjà été introduit par [65] pour des fins d'égalisation). Ce récepteur permet de traiter les interférences internes aux réseau (c'est-à-dire les autres utilisateurs Alamouti) mais également les interférences externes. Nous montrons que dans le cas d'interférence internes ce récepteur est optimal au sens ML, contrairement aux récepteurs existants. Nous étudions ensuite, toujours pour des interférences internes, les performances d'un tel récepteur en terme de capacité de rejet d'interférences, de SINR et de SER afin de mettre en évidence sa supériorité par rapport aux récepteurs MMSE existant. Nous montrons notamment qu'il peut rejeter $2N - 1$ interférences

internes à partir de N antennes de réception. Nous donnons également une interprétation géométrique simple de son fonctionnement.

Plan de la thèse

La première partie de ce document s'intéresse à l'optimisation de la capacité ergodique dans les canaux sélectifs en fréquence ; elle est traitée dans le chapitre 1. Nous y établissons dans un premier temps un approximant en grande dimension de l'information mutuelle ergodique avant de s'attacher dans un second temps à son optimisation vis-à-vis de la covariance en émission. Nous proposons ainsi un algorithme performant pour obtenir la covariance optimale. La seconde partie de ce manuscrit traite des questions de diversité en présence d'un récepteur MMSE : dans le chapitre 2 nous nous intéressons ainsi à la diversité maximale atteignable du récepteur MMSE pour des débits fixes dans le cadre des canaux non sélectifs en fréquence puis dans le cadre des canaux sélectifs en fréquence, tandis que dans le chapitre 3 nous nous intéressons à la diversité assurée par le codage d'Alamouti. Dans ce dernier chapitre nous proposons un nouveau récepteur MMSE exploitant au mieux les degrés de liberté du canal en contexte multi-utilisateur. Ce récepteur est ainsi robuste aux interférences et permet d'élargir le concept de SAIC/MAIC aux systèmes MIMO, d'où le nom de concept SAIC/MAIC Alamouti.

Contributions

Les différents travaux menés au cours de ces trois années de thèse ont donné naissance aux deux articles de revue suivants :

- F. Dupuy et P. Loubaton, "*On the capacity achieving covariance matrix for frequency selective MIMO channels using the asymptotic approach*," IEEE Transactions on Information Theory, vol. 57, n° 9, pp 5737–5753 , Septembre 2011
- P. Chevalier et F. Dupuy, "*Widely linear Alamouti receivers for the reception of real-valued signals corrupted by interferences - the Alamouti-SAIC/MAIC concept*," IEEE Transactions on Signal Processing, vol. 59, n° 7, pp 3339–3354, Juillet 2011.

L'article de revue IEEE IT correspond au chapitre 1, tandis que l'article de revue IEEE SP sert de base au chapitre 3. Les cinq articles suivants ont également été présentés lors de conférences :

- F. Dupuy et P. Loubaton, "*Diversity of the MMSE receiver in flat fading and frequency selective MIMO channels at fixed rate*," Forty-Fifth Asilomar Conference on Signals, Systems and Computers, Pacific Grove, Californie, Novembre 2011,

- F. Dupuy et P. Chevalier, "*Fonctionnement et performance des récepteurs Alamouti linéaires au sens large pour la réception de constellations réelles en contexte multi-utilisateur - Analyse du concept SAIC/MAIC Alamouti*," GRETSI Conference, Bordeaux, France, Septembre 2011,
- F. Dupuy et P. Chevalier, "*Performance Analysis of WL Alamouti Receivers for real-valued constellations in Multiuser Context*," European Signal Processing Conference (EUSIPCO), Barcelone, Espagne, Septembre 2011,
- F. Dupuy et P. Loubaton, "*On the capacity achieving covariance matrix for frequency selective MIMO channels using the asymptotic approach*," IEEE International Symposium on Information Theory (ISIT), Austin, Texas, Juin 2010,
- P. Chevalier et F. Dupuy, "*Single and multiple antennas Alamouti receivers for the reception of real-valued signals corrupted by interferences - the Alamouti SAIC/MAIC concept*," Forty-Third Asilomar Conference on Signals, Systems and Computers, Pacific Grove, Californie, Novembre 2009.

Les résultats du chapitre 2 seront ainsi présentés à la conférence d'Asilomar 2011. Un brevet a par ailleurs été déposé dans le cadre de cette thèse, correspondant au récepteur présenté au chapitre 3 :

- P. Chevalier et F. Dupuy, "*Procédé et dispositif de réception mono et multi-antennes pour liaisons de type Alamouti*," n° FR 09.05263, 3 Novembre 2009.

Introduction

THIS thesis has been carried out within the framework of a CIFRE convention between Thales Communications and Université Paris Est. It is dedicated to the frequency selective MIMO channels with single-carrier transmitters. It is acknowledged that the multi-antenna systems, also known as MIMO (Multiple In / Multiple Out) systems, allow to increase the transmission rate of single antenna systems significantly; the first area of research is thus the optimization of the ergodic capacity in frequency selective channels. Using multiple transmitting antennas also gives rise to transmit diversity, thus improving the receiving performance; the second area of research is therefore the analysis of diversity for MMSE (Minimum Mean-Square Error) receivers in frequency selective channels.

Ergodic capacity

For fifteen years many studies have sought to use MIMO (Multiple Input / Multiple Output) systems, that is, systems equipped with several transmitting antennas and several receiving antennas, in order to increase the Shannon capacity related to the usual SISO (Single Input / Single Output) systems. To that end, conceiving the optimal transmitter in terms of the Shannon capacity, i.e. the optimal relation between the transmitted vector $\mathbf{x}(n)$ and the information symbols to transmit, is a crucial issue. This problem has been studied extensively in the case of flat fading MIMO channels. Nevertheless, few authors have tackled the case of frequency selective channels. Hence, the first part of this thesis focuses on the optimization of the ergodic capacity w.r.t. the covariance matrix of the transmit vector $\mathbf{x}(n)$, when only the channel statistics are known at the transmitter side instead of the instantaneous channel state information.

Flat fading channels

In the case of flat fading channels one can describe the MIMO channel with a $r \times t$ matrix $\mathbf{H}$, where r is the number of transmitting antennas and t the number of receiving antennas. The vector $\mathbf{y}(n)$ obtained

by sampling the signal received at the symbol period can then be written under the following form

$$\mathbf{y}(n) = \mathbf{H}\mathbf{x}(n) + \mathbf{b}(n), \tag{23}$$

where $\mathbf{x}(n)$ is the transmitted vector and $\mathbf{b}(n)$ an additive noise, assumed Gaussian with variance σ^2. The first results about the MIMO mutual information have been obtained by Telatar; in [1, 2] he derived the explicit expression of the mutual information between vectors $\mathbf{x}(n)$ and $\mathbf{y}(n)$ for a given matrix $\mathbf{H}$:

$$\log\det\left(\mathbf{I}_r + \frac{1}{\sigma^2}\mathbf{H}\mathbf{Q}\mathbf{H}^H\right), \tag{24}$$

where $\mathbf{Q} = \mathbb{E}\left[\mathbf{x}\mathbf{x}^H\right]$, verifying the power constraint $\frac{1}{t}\mathrm{Tr}\,\mathbf{Q} \leq 1$, is the covariance matrix of the input vector $\mathbf{x}$, which is assumed Gaussian. When the instantaneous channel state information (CSI), i.e. matrix $\mathbf{H}$, is available, the maximum over $\mathbf{Q}$ of the mutual information (24) corresponds to the MIMO capacity and accounts for the maximum rate at which the information can be transmitted in a reliable way. It is well known [3] that the eigenvectors of the optimal input covariance matrix, which we denote $\mathbf{Q}_*$, correspond to the right singular vectors of $\mathbf{H}$ – as for the eigenvalues of $\mathbf{Q}_*$, they can be obtained by a "waterfilling" type algorithm. The value of $\mathbf{H}$, i.e. the instantaneous CSI, is therefore needed at the transmitter. Nonetheless, within the framework of mobile communications, knowing the value of $\mathbf{H}$ at the transmitter is not realistic. Indeed, the transmission channel varies quickly in practice, due in particular to the user mobility and to the diversity of propagation paths. Therefore, one usually models $\mathbf{H}$ as the realization of a Gaussian random matrix with known statistics. It is then more relevant to tackle the optimization of the expectation of the mutual information, instead of the optimization of (24) itself. The expectation of the mutual information is called ergodic mutual information and is here denoted by $I(\mathbf{Q})$:

$$I(\mathbf{Q}) = \mathbb{E}\left[\log\det\left(\mathbf{I}_r + \frac{1}{\sigma^2}\mathbf{H}\mathbf{Q}\mathbf{H}^H\right)\right]. \tag{25}$$

Optimizing the ergodic mutual information only requires the knowledge of the channel statistics at the transmitter, which is a more realistic assumption than the instantaneous CSI knowledge within the framework of wireless communications. Indeed, the statistics of the channel vary in practice a lot more slowly than the channel itself. A first step for this approach is to study the case of a channel matrix $\mathbf{H}$ whose entries are zero mean i.i.d. Gaussian random variables with $1/\sqrt{t}$ variance, which corresponds to a simplified Rayleigh channel. Telatar proved in [2] that, for such a channel, the optimal input covariance matrix is $\mathbf{Q}_* = \mathbf{I}_t$. The ergodic mutual information then becomes

$$I(\mathbf{Q}_*) = \mathbb{E}\left[\log\det\left(\mathbf{I}_r + \frac{1}{\sigma^2}\mathbf{H}\mathbf{H}^H\right)\right]. \tag{26}$$

This optimization problem has then been studied for more elaborate channel models, like the Kronecker channel model or the Rician channel. The Kronecker channel model takes into account the spatial correlation between paths by considering that matrix $\mathbf{H}$ can be written as $\mathbf{C}^{\frac{1}{2}}\mathbf{W}\tilde{\mathbf{C}}^{\frac{1}{2}}$, where $\mathbf{W}$ is a matrix

whose entries are zero mean i.i.d. complex Gaussian with a $1/\sqrt{t}$ variance. This model assumes that the correlations at the transmitter $\tilde{\mathbf{C}}$ and at the receiver $\mathbf{C}$ are separable – hence its alternative name of separable covariance model. In the case of a Kronecker channel, numerous authors have shown that the optimal input covariance matrix $\mathbf{Q}_*$ has the same eigenvectors as the transmitting correlation matrix $\tilde{\mathbf{C}}$ (see, e.g., [4, 5]). The Rician channel model with separable correlation corresponds to the Kronecker channel model but with a non-zero mean, that is, matrix $\mathbf{H}$ can be written under the following form: $\mathbf{H} = \mathbf{A} + \mathbf{C}^{\frac{1}{2}}\mathbf{W}\tilde{\mathbf{C}}^{\frac{1}{2}}$, where the deterministic matrix $\mathbf{A}$ corresponds to the Line Of Sight (LOS) component of the channel. The so-called decorrelated Rician channel model corresponds to the specific case of $\mathbf{C} = \mathbf{I}_r$, $\tilde{\mathbf{C}} = \mathbf{I}_t$. Similarly to the Kronecker channel case, it has been shown by [6] that, for decorrelated Rician channels, the eigenvectors of the optimal covariance $\mathbf{Q}_*$ correspond to the right singular vectors of matrix $\mathbf{A}$. In both optimization cases mentioned previously, the eigenvalues of the optimal matrix $\mathbf{Q}_*$ are then simply estimated by classical "waterfilling" type optimization algorithms. The optimization is more complex for Rician channels with separable correlation. The eigenvectors of the optimal input covariance $\mathbf{Q}_*$ have no explicit expression and thus have to be numerically evaluated. A direct approach has been proposed and analyzed by [7]: the entries of $\mathbf{Q}_*$ are estimated by a Newton algorithm, associated with a barrier interior-point method, which directly optimizes the ergodic mutual information (25). Yet, this direct approach requires the use of Monte-Carlo simulations, which are computationally costly, to estimate the ergodic mutual information $I(\mathbf{Q})$, together with the gradient and Hessian of $I(\mathbf{Q})$ for the Newton algorithm, along the optimization algorithm.

In order to avoid the use of Monte-Carlo simulation, various authors have proposed to optimize not $I(\mathbf{Q})$ itself but rather a large system approximation of $I(\mathbf{Q})$, i.e. an approximation for $t \to \infty$, $r \to \infty$ in such a way that $t/r \to c \in]0, \infty[$. The starting point is to notice that $\frac{1}{r}\log\det\left(\mathbf{I} + \frac{1}{\sigma^2}\mathbf{H}\mathbf{Q}\mathbf{H}^H\right)$ can be written as

$$\frac{1}{r}\sum_{i=1}^{r}\log\left(1+\frac{\lambda_i}{\sigma^2}\right), \tag{27}$$

where the $(\lambda_i)_{i=1,\ldots,r}$ are the eigenvalues of $\mathbf{H}\mathbf{Q}\mathbf{H}^H$. In numerous situations of practical interest, (27) has the same asymptotic behavior as a deterministic quantity which depends only on $\mathbf{Q}$ and on the statistics of $\mathbf{H}$. Hence, $I(\mathbf{Q})$ can be approximated by a function denoted $\overline{I}(\mathbf{Q})$ whose expression depends on the considered channel. For instance [8,9] have shown that for a Kronecker channel the approximation $\overline{I}(\mathbf{Q})$ can be written as

$$\overline{I}(\mathbf{Q}) = \log\det\left(\mathbf{I}_r + \tilde{\delta}\mathbf{C}\right) + \log\det\left(\mathbf{I}_t + \delta\mathbf{Q}\tilde{\mathbf{C}}\right) - \sigma^2 t\delta\tilde{\delta}, \tag{28}$$

where δ and $\tilde{\delta}$ are the positive solutions of a coupled equations system. Nonetheless, the proof of Moustakas et al. [8] is based on the replica method, whose mathematical relevance has not yet been proved in this context. Furthermore, it is interesting to study the convergence speed of the approximation $\overline{I}(\mathbf{Q})$ towards $I(\mathbf{Q})$; it has been proved by [8, 10] that $I(\mathbf{Q}) - \overline{I}(\mathbf{Q}) = \mathcal{O}\left(1/t\right)$. The approach of [8] is based

once again on the replica methods, while the simple and rigorous approach of [10] uses the so-called Gaussian methods, which use the Gaussian nature of the considered channel model. A similar result is also obtained for Rician channels with separable correlation, as shown by [11] through the replica methods and later by [12] with the Gaussian methods. In this case the approximation $\overline{I}(\mathbf{Q})$ can be written as

$$\overline{I}(\mathbf{Q}) = \log\det\left(\mathbf{I}_r + \tilde{\delta}\mathbf{C}\right) + \log\det\left(\mathbf{I}_t + \delta\mathbf{Q}\tilde{\mathbf{C}} + \frac{1}{\sigma^2}\mathbf{Q}\mathbf{A}^H\left(\mathbf{I}_r + \tilde{\delta}\mathbf{C}\right)^{-1}\mathbf{A}\right) - \sigma^2 t\delta\tilde{\delta}, \qquad (29)$$

where δ and $\tilde{\delta}$ are this time the positive solutions of a coupled nonlinear equations system.

The large system approximation $\overline{I}(\mathbf{Q})$ of $I(\mathbf{Q})$ gives rise to an indirect approach to optimize the ergodic mutual information: the input covariance is optimized using the approximation $\overline{I}(\mathbf{Q})$ instead of using the ergodic mutual information $I(\mathbf{Q})$ directly. One great advantage of this approach comes from the explicit expressions of $\overline{I}(\mathbf{Q})$, which avoid in particular the use of Monte-Carlo methods to estimate $I(\mathbf{Q})$. The optimization implementation is thus easier for $\overline{I}(\mathbf{Q})$ than for $I(\mathbf{Q})$ and computationally much more efficient. For Kronecker channels [13] proposed this way an iterative optimization algorithm based on the large system approximation of the ergodic mutual information. This algorithm has been extended to Rician channels with separable correlation by [12], which also proves the strict concavity of the approximation and gives some details about the convergence. The indirect approach is also legitimized in [12] by showing that

$$I(\overline{\mathbf{Q}}_*) = I(\mathbf{Q}_*) + \mathcal{O}\left(\frac{1}{t}\right). \qquad (30)$$

where $\overline{\mathbf{Q}}_*$ is the input covariance matrix maximizing $\overline{I}(\mathbf{Q})$ and where $\mathbf{Q}_*$ is the input covariance matrix maximizing $I(\mathbf{Q})$ – both maximizations under the power constraint $\mathrm{Tr}\,\mathbf{Q} = t$. Taricco and Riegler have introduced a similar algorithm in [14] and have analyzed it more thoroughly very recently in [15]. In particular, they have proved in the case of Rayleigh channels that their algorithm converges and that the algorithm introduced by [12] may not converge in some particular cases.

Frequency selective channels

The first contribution of this thesis is the optimization of the ergodic mutual information for frequency selective channels. When the channel is frequency selective and when the transmitter uses a single-carrier waveform, the receiving model (23) is not valid anymore. The received signal $\mathbf{y}(n)$ then takes the following form

$$\begin{aligned}\mathbf{y}(n) &= \sum_{l=1}^{L}\mathbf{H}^{(l)}\mathbf{x}(n-l+1) + \mathbf{b}(n) \qquad (31)\\ &= [\mathbf{H}(z)]\mathbf{x}(n) + \mathbf{b}(n),\end{aligned}$$

where $\mathbf{H}(z)$ now denotes the transfer function of the discrete-time equivalent channel defined by $\mathbf{H}(z) = \sum_{l=1}^{L} \mathbf{H}^{(l)} z^{-(l-1)}$, where matrix $\mathbf{H}^{(l)}$ is associated to the l^{th} channel tap. A common model (see, e.g., [16, 17]) for these matrices $\mathbf{H}^{(l)}$ is to consider that they are independent, which corresponds to independent paths, and that they each follow a Kronecker model: $\mathbf{H}^{(l)} = \frac{1}{\sqrt{t}}(\mathbf{C}^{(l)})^{1/2}\mathbf{W}_l(\tilde{\mathbf{C}}^{(l)})^{1/2}$, where $\mathbf{W}_l$ is a random matrix whose entries are i.i.d. standard complex Gaussian. Denoting $\mathbf{Q}(e^{2i\pi\nu})$ the spectral density of the transmitted vector $\mathbf{x}$, the ergodic mutual information can be written as

$$I(\mathbf{Q}(e^{2i\pi\nu})) = \mathbb{E}\left[\int_0^1 \log\det\left(\mathbf{I}_r + \frac{1}{\sigma^2}\mathbf{H}(e^{2i\pi\nu})\mathbf{Q}(e^{2i\pi\nu})\mathbf{H}(e^{2i\pi\nu})^H\right) d\nu\right]. \tag{32}$$

We have shown that for the optimization of $I(\mathbf{Q}(e^{2i\pi\nu}))$ we could restrict ourselves to the covariance matrices $\mathbf{Q}(e^{2i\pi\nu})$ which do not depend on the frequency. Hence, we consider hereafter $\mathbf{Q}(e^{2i\pi\nu}) = \mathbf{Q}\,\forall\nu$. A large system approximation $\overline{I}(\mathbf{Q})$ of $I(\mathbf{Q})$ was derived by [17] using the replica method:

$$\overline{I}(\mathbf{Q}) = \log\det\left(\mathbf{I}_r + \sum_{l=1}^{L}\tilde{\delta}_l\mathbf{C}^{(l)}\right) + \log\det\left(\mathbf{I}_t + \mathbf{Q}\left(\sum_{l=1}^{L}\delta_l\tilde{\mathbf{C}}^{(l)}\right)\right) - \sigma^2 t\sum_{l=1}^{L}\delta_l\tilde{\delta}_l, \tag{33}$$

where the δ_l and $\tilde{\delta}_l$, $l = 1, \ldots, L$, are the positive solutions of a system of $2L$ coupled nonlinear equations. We confirm in the first place the relevance of this approximation by using a rigorous approach inspired by the results of [12] previously mentioned. We justify in particular the existence and uniqueness of the δ_l and $\tilde{\delta}_l$, which had not been discussed in [17]. We also specify the technical assumptions needed for the convergence of $I(\mathbf{Q})$ towards its approximation $\overline{I}(\mathbf{Q})$. Furthermore, we provide the speed of this convergence:

$$I(\mathbf{Q}) = \overline{I}(\mathbf{Q}) + \mathcal{O}\left(\frac{1}{t}\right). \tag{34}$$

We can then tackle the optimization of the ergodic mutual information $I(\mathbf{Q})$ via its large system approximation $\overline{I}(\mathbf{Q})$. To that end, we justify the strict concavity of function $\mathbf{Q} \mapsto \overline{I}(\mathbf{Q})$. Similarly to the Rician case, we establish the following key result which legitimizes our indirect approach:

$$I(\overline{\mathbf{Q}}_*) = I(\mathbf{Q}_*) + \mathcal{O}\left(\frac{1}{t}\right), \tag{35}$$

where $\overline{\mathbf{Q}}_*$ is the input covariance matrix maximizing $\overline{I}(\mathbf{Q})$ under the power constraint $\mathrm{Tr}\,\mathbf{Q} = t$ and where $\mathbf{Q}_*$ is the input covariance matrix maximizing $I(\mathbf{Q})$ under the power constraint $\mathrm{Tr}\,\mathbf{Q} = t$. In other words, it is relevant, up to $\mathcal{O}(1/t)$ term, to maximize the approximation $\overline{I}(\mathbf{Q})$ instead of the ergodic mutual information $I(\mathbf{Q})$ itself. We then propose a maximization algorithm for $\overline{I}(\mathbf{Q})$ which is based on an iterative waterfilling: each iteration solves first the mentioned system of $2L$ coupled equations, then a classical waterfilling problem [18]. This algorithm is to some extent an extension of the algorithm introduced by [13] for a Kronecker channel and by [12] for a Rician channel. We finally prove that, if the algorithm converges, it converges towards the optimal input covariance $\overline{\mathbf{Q}}_*$ – yet the convergence itself has not been proved.

MMSE receivers diversity

In this second area of research we consider the MMSE (Minimum Mean-Square Error) receivers. Unlike the ML (Maximum Likelihood) receivers, these receivers are sub-optimal yet simpler to implement. In the first place we analyze the diversity of the MMSE receivers at high SNR (Signal to Noise Ratio) for frequency selective channels. Secondly, we focus on systems enhancing diversity through the use of Space-Time Block Codes (STBC), more specifically through the use of the Alamouti code. In particular, we propose and analyze a new MMSE receiver in multiuser context, which is robust to the encountered intra-network but also external interferences. This latter analysis has however been limited to the case of flat fading channels – or, equivalently, to the case of frequency selective channels with an OFDM waveform.

Diversity order

The diversity order d of a system is by definition the exponential decrease slope of the error probability P_e as a function of the SNR ρ, for high SNRs:

$$d = -\lim_{\rho \to +\infty} \frac{\log P_e}{\log \rho}. \tag{36}$$

The probability error then verifies $P_e \sim k\rho^{-d}$ for $\rho \gg 1$, where k does not depend on ρ. There are two approaches to study the diversity of a system. The most common one (see, e.g., [19–21]) is based on the analysis of the Pairwise Error Probability (PEP) decrease rate w.r.t. the SNR. Nevertheless, this approach requires the design of specific coding schemes to achieve the maximum diversity. We here consider the second approach which is based on the outage probability $P_{out}(R)$, R being the target rate:

$$P_{out}(R) = \mathbb{P}\left(I < R\right), \tag{37}$$

where I denotes the mutual information of the system. For a well designed system, the outage probability corresponds to the probability of a non reliable transmission. It is therefore consistent to study the exponential decrease of the outage probability P_{out} instead of the error probability P_e. This approach is moreover convenient as it bypasses the coding design issue at the transmitter. In this case the diversity is defined as

$$d(R) = -\lim_{\rho \to +\infty} \frac{\log P_{out}(R)}{\log \rho}. \tag{38}$$

This approach is used by many authors within the framework of the DMT (Diversity-Multiplexing Trade-off) analysis introduced by Zheng and Tse [22]. Hence, we now focus on studying the DMT.

The Diversity-Multiplexing Trade-off:
As mentioned in previous section, MIMO systems enable at high SNR a linear capacity gain compared

to SISO systems [2]:

$$I(\rho) \sim \min\{M, N\} \log \rho \text{ for } \rho \gg 1, \tag{39}$$

where $I(\rho)$ stands for the mutual information, M for the number of transmitting antennas, N for the number of receiving antennas. The capacity thus increases like $\log \rho$ at high SNR. It is therefore relevant to write the target rate under the following form:

$$R = r \log \rho, \tag{40}$$

where $r \leq \min\{M, N\}$ is called the multiplexing coefficient – or multiplexing order, multiplexing gain. Parameter r corresponds to the spatial multiplexing gain: the MIMO channel can be decoupled into independent SISO subchannels which amount to the rank of channel matrix $\mathbf{H}$, which is $\min\{M, N\}$ if $\mathbf{H}$ is well conditioned. Spatial multiplexing is equivalent to using the available degrees of freedom to transmit independent signals on these parallel channels instead of using them to improve the transmission reliability; there is a fundamental trade-off between the multiplexing coefficient r and the diversity $d(R)$, which is called Diversity-Multiplexing Trade-off (DMT) [22]. It is then interesting to analyze how the diversity order $d(R) = d(r \log \rho)$ defined by (38) depends on the multiplexing gain r; hence, we hereafter consider the diversity order as a function of r and denote it $d(r)$:

$$d(r) = -\lim_{\rho \to +\infty} \frac{\log P_{out}(r \log \rho)}{\log \rho}. \tag{41}$$

We then obtain a priori the maximum achievable diversity d_{max} for $r = 0$. Zheng and Tse have derived $d(r)$ for a flat fading MIMO channel in [22]:

$$d(r) = (M - r)(N - r). \tag{42}$$

For a fixed target rate R, i.e. for $r = 0$, the diversity is then $d_{max} = MN$. This result has been extended rapidly to the frequency selective SISO channel [23, 24], followed by the analysis of the frequency selective MIMO channel [25–27]. Noting L the number of independent paths, it has been shown that, under certain conditions, the diversity order $d(r)$ verifies

$$d(r) = L(M - r)(N - r), \tag{43}$$

hence, a maximum diversity order $d_{max} = LMN$. Nevertheless, these results assume an optimal receiver, that is a Maximum Likelihood (ML) receiver. Such a receiver is in practice complex to implement. Sub-optimal linear receivers such as the MMSE receivers are then preferred.

Analysis of the DMT for MMSE receivers:

The second contribution of the thesis is the DMT analysis for MMSE receivers, for a fixed target rate R, i.e. for a multiplexing coefficient $r = 0$. In the case of a flat fading MIMO channel it has been shown

by [28] that the MMSE receivers considerably damage the DMT. Indeed, the following expression of $d(r)$ is then obtained:

$$d(r) = (N - M + 1)\left(1 - \frac{r}{M}\right)^+, \tag{44}$$

with $(\cdot)^+ = \max\{0, \cdot\}$. Hence, we expect at most a diversity of $d_{max} = N - M + 1$. Nonetheless, for a finite target rate R, i.e. for $r = 0$, Hedayat et al. have observed in [29] that the MMSE receivers give rise to several diversity orders depending on the value of target rate R (see also [30, 31]). In particular, the maximum diversity LMN previously mentioned is achieved for sufficiently low values of R, hence the great interest of these receivers simple to implement. This unexpected behavior has been explained in [28, 32] for flat fading MIMO channels and in [33, 66] for frequency selective channels, yet in both cases the explanations are incomplete. We highlight the inaccuracy of the proof given in [32] for a flat fading channel and give a rigorous proof of the diversity for such a system. As for the frequency selective channels with cyclic prefix, Mehana and Nosratinia [33, 66] have only derived the diversity for the specific case of a number of paths L equal to the transmission data block length. Hence, we derive the diversity order in the general case – yet we assume that the transmission data block length is large enough.

Diversity through STBC

The diversity-multiplexing trade-off mentioned previously occurs naturally at the system design level: one can for instance favor multiplexing by using the V-BLAST scheme (Vertical Bell Layered Space-Time [34,35]), or favor the diversity gain by using a STBC (Space-Time Block Code [36]) at the transmitter. Zheng et Tse [22] have in fact highlighted the opposite behavior of these two schemes by analyzing their DMT. As we focus in this part on diversity, which helps increasing the transmission range and reliability, we here concentrate on the use of STBC. The orthogonal STBCs are particularly attractive as they achieve maximum spatial diversity for a given number of transmitting and receiving antennas. We tackle the use of the first orthogonal STBC, which is also the simplest and most-known, introduced by Alamouti in [38]. It has been standardized in the following norms: UMTS, GSM, EDGE, IEEE 802.11n, IEEE 802.16 [39].

In order to make the most of the available spectrum and of the diversity inherent in the transmission channel, we focus in this thesis on the multiuser Alamouti case, that is to say the case where several users share the same spectral resources and all use the Alamouti scheme. In this context Interference Cancellation (IC) schemes are required to allow users to share the same spectral resources without impacting the transmission quality. Several IC schemes [40–47] have been introduced allowing P users, all having M transmitting antennas and using a STBC, to share the same channel. Winters et al. have shown [48] that the diversity order of each user is M for $N = M(P - 1) + 1$ receiving antennas. However, if the STBC structure is used properly, $N = P$ receiving antennas are sufficient to provide this diversity order

of M. This result was first proved by Naguib et al. in [40, 42] for the case of the Alamouti scheme with $M = N = P = 2$. The latter has been generalized to a number of receiving antennas $N \geq P$ by [43] (see also [47] for an alternative approach). Eventually, Kazemitabar and Jafarkhani have presented in [46] an IC scheme for quasi-orthogonal STBC (see [49, 50]), allowing a receiver with $N \geq P$ antennas to separate P users, all equipped with $M > 2$ transmitting antennas. Nonetheless, all these IC techniques require $N > 1$, that is several receiving antennas, which remains a challenge at the handset level due to cost and size limitations. This supports the development of the so-called SAIC techniques (Single Antenna Interference Cancellation), which only require one receiving antenna and which are an alternative to the complex ML multiuser demodulation techniques [51].

The SAIC techniques were first developed for users with only one transmitting antenna using single carrier transmission [52–56]. Most of these techniques [52, 54–56] use the second order non-circularity property [57] of real-valued modulations, such as BPSK and ASK, or of quasi-rectilinear modulations (that is, corresponding to a complex filtering of real-valued constellations) after a derotation operation, such as MSK, GMSK, OQAM [58]. They implement an optimal WL (Widely Linear [59]) filtering of the observations and allow a receiver to separate two users from only one receiving antenna [54]. This simple and efficient concept has received significant attention within the framework of 2G-3G networks:

- 3G Americas [60] has presented the SAIC technology as a great improvement for GSM mobile station receivers allowing significant network capacity gains for the GSM system [55, 67],
- this technology has been standardized in 2005 for GSM and is currently operational in most of GSM handsets,
- a new standardization of this technology, called MUROS (Multi-User Reusing One Slot), which enables several GSM users reuse the same TDMA slot, is currently under investigation,
- an extension of the SAIC concept for several receiving antennas, called MAIC (Multiple Antenna Interference Cancellation) [54], is of great interest for GPRS networks in particular [61].

As for the 4G networks, antenna arrays have been standardized at the handset. The MAIC concept, which assumes several receiving antennas but is still of great interest, can then be used instead of the SAIC concept. Nevertheless, the implementation of antenna arrays at the handset level remains a challenge; hence, the SAIC techniques are still relevant and of great interest for 4G networks. In fact, an extension of these techniques to OFDM has been recently introduced by [62] for users with one single transmitting antenna using ASK modulation. Note, moreover, that the SAIC/MAIC concept is also very attractive for military ad hoc networks, which require most of all simple and robust systems.

The real-valued modulations, such as the ASK modulation, are certainly less power efficient than the traditional QAM modulation: the transmitter only uses the real dimension. Yet, in a multiuser context, the ASK modulation may become more attractive than a QAM modulation by properly using the available

degree of freedom to separate the users at the receiver. The degree of freedom which have not been used by the transmitter are somehow recovered at the receiver, where they can be used if an appropriate processing is used, that is, WL filtering. Several studies [62–64] seem to show that, in multiuser contexts, transmissions using real-valued modulations together with WL receivers may provide a higher spectral efficiency compared to transmissions using complex-valued modulation together with linear receivers. As a consequence, the use of ASK constellations coupled with WL receivers, instead of complex ones with linear receivers, does not seem to be a limitation and may even bring advantages in terms of error probability and spectral efficiency in multiuser environments.

The SAIC/MAIC concepts only concern SISO and SIMO systems. We propose in this thesis an extension of these concepts to MISO and MIMO systems, thanks to the Alamouti orthogonal STBC used with real-valued constellations. To that end we introduce in multiuser context a new WL MMSE receiver – which has already been introduced by [65] but for equalization purposes. This receiver, called the F-WL-MMSE receiver, is robust to intra-network interferences (that is, interferences which arise from the other users of the network), but also to external interferences. We prove that, contrary to the receivers of the literature, this receiver is optimal in the ML sense for internal interferences. We then analyze its performance, in terms of interferences rejection capability, of SINR and of SER, in order to highlight its great interest compared to the receivers of the literature. In particular, we show that the F-WL-MMSE receiver can reject $2N-1$ internal interferences from N receiving antennas and provide a simple geometrical interpretation of its behavior. We also propose an adaptive implementation of this receiver.

Thesis outline

The first part of this manuscript focuses on the ergodic capacity optimization for frequency selective channels and is discussed in chapter 1. We establish in the first place a large system approximation of the ergodic mutual information before secondly tackling its optimization w.r.t. the input covariance matrix. To that end we propose an efficient iterative algorithm to obtain the optimal covariance. The second part of this thesis deals with diversity issues in the presence of a MMSE receiver: in chapter 2 we focus on the maximum achievable diversity of the MMSE receiver for flat fading and frequency selective channels, while in chapter 3 we focus on systems enhancing diversity through the use of the Alamouti scheme. In this latter chapter we introduce a new MMSE receiver in multiuser contexts, which makes the most of the degrees of freedom available in the channel. This receiver is robust to interferences and extends the SAIC/MAIC concept to MIMO systems, hence the name of SAIC/MAIC Alamouti concept.

Contributions

The two following journal articles arose from the work carried out during this thesis:

- F. Dupuy and P. Loubaton, "*On the capacity achieving covariance matrix for frequency selective MIMO channels using the asymptotic approach*," IEEE Transactions on Information Theory, vol. 57, n° 9, pp 5737–5753 , September 2011
- P. Chevalier and F. Dupuy, "*Widely linear Alamouti receivers for the reception of real-valued signals corrupted by interferences - the Alamouti-SAIC/MAIC concept*," IEEE Transactions on Signal Processing, vol. 59, n° 7, pp 3339–3354, July 2011.

The IEEE IT journal article corresponds to chapter 1, whereas the IEEE SP journal article serves as a basis for chapter 3. Moreover, the five following articles have been presented at various conferences:

- F. Dupuy and P. Loubaton, "*Diversity of the MMSE receiver in flat fading and frequency selective MIMO channels at fixed rate*," Forty-Fifth Asilomar Conference on Signals, Systems and Computers, Pacific Grove, California, November 2011,
- F. Dupuy and P. Chevalier, "*Fonctionnement et performance des récepteurs Alamouti linéaires au sens large pour la réception de constellations réelles en contexte multi-utilisateur - Analyse du concept SAIC/MAIC Alamouti*," GRETSI Conference, Bordeaux, France, September 2011,
- F. Dupuy and P. Chevalier, "*Performance Analysis of WL Alamouti Receivers for real-valued constellations in Multiuser Context*," European Signal Processing Conference (EUSIPCO), Barcelona, Spain, September 2011,
- F. Dupuy and P. Loubaton, "*On the capacity achieving covariance matrix for frequency selective MIMO channels using the asymptotic approach*," IEEE International Symposium on Information Theory (ISIT), Austin, Texas, June 2010,
- P. Chevalier and F. Dupuy, "*Single and multiple antennas Alamouti receivers for the reception of real-valued signals corrupted by interferences - the Alamouti SAIC/MAIC concept*," Forty-Third Asilomar Conference on Signals, Systems and Computers, Pacific Grove, California, November 2009.

In particular, chapter 2 corresponds to the results which will be presented at Asilomar conference 2011. A patent has also been filed within the framework of this thesis, corresponding to the receiver introduced in chapter 3:

- P. Chevalier and F. Dupuy, "*Procédé et dispositif de réception mono et multi-antennes pour liaisons de type Alamouti*," n° FR 09.05263, 3 November 2009.

Chapter 1

Capacity optimization

In this chapter we propose an algorithm for evaluating the capacity-achieving input covariance matrices for frequency selective Rayleigh MIMO channels. In contrast with the flat fading Rayleigh case, no closed-form expressions for the eigenvectors of the optimum input covariance matrix are available. Classically, both the eigenvectors and eigenvalues are computed numerically and the corresponding optimization algorithms remain computationally very demanding. In this chapter, it is proposed to optimize (w.r.t. the input covariance matrix) a large system approximation of the average mutual information derived by Moustakas and Simon. The validity of this asymptotic approximation is clarified thanks to Gaussian large random matrices methods. It is shown that the approximation is a strictly concave function of the input covariance matrix and that the average mutual information evaluated at the argmax of the approximation is equal to the capacity of the channel up to a $\mathcal{O}\left(1/t\right)$ term, where t is the number of transmit antennas. An algorithm based on an iterative waterfilling scheme is proposed to maximize the average mutual information approximation, and its convergence studied. Numerical simulation results show that, even for a moderate number of transmit and receive antennas, the new approach provides the same results as direct maximization approaches of the average mutual information.

1.1 Introduction

When the channel state information is available at both the receiver and the transmitter of a MIMO system, the problem of designing the transmitter in order to maximize the (Gaussian) mutual information of the system has been addressed successfully in a number of chapters. This problem is, however, more difficult when the transmitter has the knowledge of the statistical properties of the channel, the channel state information being still available at the receiver side, a more realistic assumption in the context of mobile systems. In this case, the mutual information is replaced by the average mutual information

(EMI), which, of course, is more complicated to optimize.

The optimization problem of the EMI has been addressed extensively in the case of certain flat fading Rayleigh channels. In the context of the so-called Kronecker model, it has been shown by various authors (see, e.g., [68] for a review) that the eigenvectors of the optimal input covariance matrix must coincide with the eigenvectors of the transmit correlation matrix. It is therefore sufficient to evaluate the eigenvalues of the optimal matrix, a problem which can be solved by using standard optimization algorithms. Similar results have been obtained for flat fading uncorrelated Rician channels ([6]).

In this chapter, we consider this EMI maximization problem in the case of popular frequency selective MIMO channels (see, e.g., [16, 17]) with independent paths. In this context, the eigenvectors of the optimum transmit covariance matrix have no closed-form expressions, so that both the eigenvalues and the eigenvectors of the matrix have to be evaluated numerically. For this, it is possible to adapt the approach of [7] developed in the context of correlated Rician channels. However, the corresponding algorithms are computationally very demanding as they heavily rely on intensive Monte-Carlo simulations. We therefore propose to optimize the approximation of the EMI, derived by Moustakas and Simon ([17]), in principle valid when the number of transmit and receive antennas converge to infinity at the same rate, but accurate for realistic numbers of antennas. This will turn out to be a simpler problem. We mention that, while [17] contains some results related to the structure of the argument of the maximum of the EMI approximation, [17] does not propose any optimization algorithm.

We first review the results of [17] related to the large system approximation of the EMI. The analysis of [17] is based on the so-called replica method, an ingenious trick whose mathematical relevance has not yet been established mathematically. Using a generalization of the rigorous analysis of [10], we verify the validity of the approximation of [17] and provide the convergence speed under certain technical assumptions. Besides, the expression of the approximation depends on the solutions of a non linear system. The existence and the uniqueness of the solutions are not addressed in [17]. As our optimization algorithm needs to solve this system, we clarify this crucial point. We show in particular that the system admits a unique solution that can be evaluated numerically using the fixed point algorithm. Next, we study the properties of the EMI approximation, and briefly justify that it is a strictly concave function of the input covariance matrix. We show that the mutual information corresponding to the argmax of the EMI approximation is equal to the channel capacity up to a $\mathcal{O}\left(\frac{1}{t}\right)$ term, where t is the number of transmit antennas. Therefore it is relevant to optimize the EMI approximation to evaluate the capacity achieving covariance matrix. We finally present our maximization algorithm of the EMI approximation. It is based on an iterative waterfilling algorithm which, in some sense, can be seen as a generalization of [13] devoted to the Rayleigh context and of [12, 69] devoted to the correlated Rician case: Each iteration will be devoted to solve the above mentioned system of nonlinear equations as well as a standard waterfilling problem. It is proved that the algorithm converges towards the optimum input covariance matrix as long

as it converges[1].

The chapter is organized as follows. Section 1.2 is devoted to the presentation of the channel model, the underlying assumptions, the problem statement. In section 1.3, we rigorously derive the large system approximation of the EMI with Gaussian methods and establish some properties of the asymptotic approximation as a function of the covariance matrix of the input signal. The maximization problem of the EMI approximation is then studied in section 1.4. Numerical results are provided in section 1.5.

1.2 Problem Statement

1.2.1 General Notations

In this chapter, the notations s, $\mathbf{x}$, $\mathbf{M}$, stand for scalars, vectors and matrices, respectively. As usual, $\|\mathbf{x}\|$ represents the Euclidian norm of vector $\mathbf{x}$, and $\|\mathbf{M}\|$, $\rho(\mathbf{M})$ and $|\mathbf{M}|$ respectively stand for the spectral norm, the spectral radius and the determinant of matrix $\mathbf{M}$. The superscripts $(.)^T$ and $(.)^H$ represent respectively the transpose and transpose conjugate. The trace of $\mathbf{M}$ is denoted by $\mathrm{Tr}(\mathbf{M})$. The mathematical expectation operator is denoted by $\mathbb{E}(\cdot)$. We denote by $\delta_{i,j}$ the Kronecker delta, i.e. $\delta_{i,j} = 1$ if $i = j$ and 0 otherwise.

All along this chapter, r and t stand for the number of receive and transmit antennas. Certain quantities will be studied in the asymptotic regime $t \to \infty$, $r \to \infty$ in such a way that $t/r \to c \in (0, \infty)$. In order to simplify the notations, $t \to \infty$ should be understood from now on as $t \to \infty$, $r \to \infty$ and $t/r \to c \in (0, \infty)$. A matrix $\mathbf{M}_t$ whose size depends on t is said to be uniformly bounded if $\sup_t \|\mathbf{M}_t\| < \infty$.

Several variables used throughout this chapter depend on various parameters, e.g., the number of antennas, the noise level, the covariance matrix of the transmitter, etc. In order to simplify the notations, we may not always mention all these dependencies.

1.2.2 Channel Model

We consider a wireless MIMO link with t transmit and r receive antennas corrupted by a multipath propagation channel. The discrete-time propagation channel between the transmitter and the receiver is characterized by the input-output equation

$$\mathbf{y}(n) = \sum_{l=1}^{L} \mathbf{H}^{(l)} \mathbf{s}(n - l + 1) + \mathbf{n}(n) = [\mathbf{H}(z)]\mathbf{s}(n) + \mathbf{n}(n), \tag{1.1}$$

[1]Note however that we have been unable to prove formally its convergence.

where $\mathbf{s}(n) = [s_1(n), \ldots, s_t(n)]^T$ and $\mathbf{y}(n) = [y_1(n), \ldots, y_r(n)]^T$ represent the transmit and the receive vector at time n respectively. $\mathbf{n}(n)$ is an additive Gaussian noise such that $\mathbb{E}[\mathbf{n}\mathbf{n}^H] = \sigma^2\mathbf{I}$. $\mathbf{H}(z)$ denotes the transfer function of the discrete-time equivalent channel defined by

$$\mathbf{H}(z) = \sum_{l=1}^{L} \mathbf{H}^{(l)}\, z^{-(l-1)}. \tag{1.2}$$

Each coefficient $\mathbf{H}^{(l)}$ is assumed to be a Gaussian random matrix given by

$$\mathbf{H}^{(l)} = \frac{1}{\sqrt{t}} (\mathbf{C}^{(l)})^{1/2} \mathbf{W}_l (\tilde{\mathbf{C}}^{(l)})^{1/2}, \tag{1.3}$$

where $\mathbf{W}_l$ is a $r \times t$ random matrix whose entries are independent and identically distributed complex circular Gaussian random variables, with zero mean and unit variance. The matrices $\mathbf{C}^{(l)}$ and $\tilde{\mathbf{C}}^{(l)}$ are positive definite, and respectively account for the receive and transmit antenna correlation. This correlation structure is called a separable or Kronecker correlation model. We also assume that for each $k \neq l$, matrices $\mathbf{H}^{(k)}$ and $\mathbf{H}^{(l)}$ are independent. Note that our assumptions imply that $\mathbf{H}^{(l)} \neq 0$ for $l = 1, \ldots, L$. However, it can be checked easily that the results stated in this chapter remain valid if some coefficients $(\mathbf{H}^{(l)})_{l=1,\ldots,L}$ are zero.

In this chapter the channel matrices are assumed perfectly known at the receiver side. However, only the statistics of the $(\mathbf{H}^{(l)})_{l=1,\ldots,L}$, i.e. matrices $(\tilde{\mathbf{C}}^{(l)}, \mathbf{C}^{(l)})_{l=1,\ldots,L}$, are available at the transmitter side.

1.2.3 Ergodic Capacity of the Channel.

Let $\mathbf{Q}(e^{2i\pi\nu})$ be the $t \times t$ spectral density matrix of the transmit signal $\mathbf{s}(n)$, which is assumed to verify the transmit power condition

$$\frac{1}{t} \int_0^1 \mathrm{Tr}(\mathbf{Q}(e^{2i\pi\nu}))d\nu = 1. \tag{1.4}$$

Then, the (Gaussian) ergodic mutual information $I(\mathbf{Q}(.))$ between the transmitter and the receiver is defined as

$$I(\mathbf{Q}(.)) = \mathbb{E}_{\mathcal{W}} \left[\int_0^1 \log \left| \mathbf{I}_r + \frac{1}{\sigma^2} \mathbf{H}(\cdot)\mathbf{Q}(\cdot)\mathbf{H}(\cdot)^H \right| d\nu \right], \tag{1.5}$$

where $\mathbb{E}_{\mathcal{W}}[.] = \mathbb{E}_{(\mathbf{W}_l)_{l=1,\ldots,L}}[.]$. The ergodic capacity of the MIMO channel is equal to the maximum of $I(\mathbf{Q}(.))$ over the set of all spectral density matrices satisfying the constraint (1.4). The hypotheses formulated on the statistics of the channel allow however to limit the optimization to the set of positive matrices which are independent of the frequency ν. This is because the probability distribution of matrix $\mathbf{H}(e^{2i\pi\nu})$ is clearly independent of the frequency ν. More precisely, the mutual information $\mathbf{I}(\mathbf{Q}(.))$ is also given by

$$I(\mathbf{Q}(.)) = \mathbb{E}_{\mathbf{H}} \left[\int_0^1 \log \left| \mathbf{I}_r + \frac{1}{\sigma^2} \mathbf{H}\mathbf{Q}(e^{2i\pi\nu})\mathbf{H}^H \right| d\nu \right],$$

where $\mathbf{H} = \sum_{l=1}^{L} \mathbf{H}^{(l)} = \mathbf{H}(1)$. Using the concavity of the logarithm, we obtain that

$$I(\mathbf{Q}(.)) \leq \mathbb{E}_{\mathbf{H}} \left[\log \left| \mathbf{I}_r + \frac{1}{\sigma^2} \mathbf{H} \left(\int_0^1 \mathbf{Q}(e^{2i\pi\nu}) d\nu \right) \mathbf{H}^H \right| \right].$$

We denote by $\mathcal{C}$ the cone of non negative hermitian matrices, and by $\mathcal{C}_1$ the subset of all matrices $\mathbf{Q}$ of $\mathcal{C}$ satisfying $\frac{1}{t}\mathrm{Tr}(\mathbf{Q}) = 1$. If $\mathbf{Q}$ is an element of $\mathcal{C}_1$, the mutual information $I(\mathbf{Q})$ reduces to

$$I(\mathbf{Q}) = \mathbb{E}_{\mathbf{H}} \left[\log \left| \mathbf{I}_r + \frac{1}{\sigma^2} \mathbf{H}\mathbf{Q}\mathbf{H}^H \right| \right]. \tag{1.6}$$

$\mathbf{Q} \mapsto I(\mathbf{Q})$ is strictly concave on the convex set $\mathcal{C}_1$ and reaches its maximum at a unique element $\mathbf{Q}_* \in \mathcal{C}_1$. It is clear that if $\mathbf{Q}(e^{2i\pi\nu})$ is any spectral density matrix satisfying (1.4), then the matrix $\int_0^1 \mathbf{Q}(e^{2i\pi\nu})d\nu$ is an element of $\mathcal{C}_1$. Therefore,

$$\mathbb{E}_{\mathbf{H}} \left[\log \left| \mathbf{I}_r + \frac{1}{\sigma^2} \mathbf{H} \left(\int_0^1 \mathbf{Q}(e^{2i\pi\nu}) d\nu \right) \mathbf{H}^H \right| \right] \leq \mathbb{E}_{\mathbf{H}} \left[\log \left| \mathbf{I}_r + \frac{1}{\sigma^2} \mathbf{H}\mathbf{Q}_*\mathbf{H}^H \right| \right].$$

In other words,

$$I(\mathbf{Q}(.)) \leq I(\mathbf{Q}_*)$$

for each spectral density matrix verifying (1.4). This shows that the maximum of function I over the set of all spectral densities satisfying (1.4) is reached on the set $\mathcal{C}_1$. The ergodic capacity $\mathcal{C}_E$ of the channel is thus equal to

$$\mathcal{C}_E = \max_{\mathbf{Q} \in \mathcal{C}_1} I(\mathbf{Q}). \tag{1.7}$$

We note that property (1.7) also holds if the time delays of the channel are non integer multiples of the symbol period, provided that the receiving filter coincides with the ideal low-pass filter on the $[-\frac{1}{2T}, \frac{1}{2T}]$ frequency interval, where T denotes the symbol period. If this is the case, the transfer function $\mathbf{H}(e^{2i\pi\nu})$ is equal to $\mathbf{H}(e^{2i\pi\nu}) = \sum_{l=1}^{L} \mathbf{H}^{(l)} e^{-2i\pi\nu\tau_l}$, where τ_l is the delay associated to path l for $l = 1, \ldots, L$. The probability distribution of $\mathbf{H}(e^{2i\pi\nu})$ does not depend on ν and this leads immediately to (1.7).

If the matrices $(\mathbf{C}^{(l)})_{l=1,\ldots,L}$ all coincide with a matrix $\mathbf{C}$, matrix $\mathbf{H}$ follows a Kronecker model with transmit and receive covariance matrices $\frac{1}{L}\sum_{l=1}^{L} \tilde{\mathbf{C}}^{(l)}$ and $\mathbf{C}$ respectively [70]. In this case, the eigenvectors of the optimum matrix $\mathbf{Q}_*$ coincide with the eigenvectors of $\frac{1}{L}\sum_{l=1}^{L} \tilde{\mathbf{C}}^{(l)}$. The situation is similar if the transmit covariance matrices $(\tilde{\mathbf{C}}^{(l)})_{l=1,\ldots,L}$ coincide. In the most general case, the eigenvectors of $\mathbf{Q}_*$ have however no closed-form expression. The evaluation of $\mathbf{Q}_*$ and of the channel capacity $\mathcal{C}_E$ is thus a more difficult problem. A possible solution consists in adapting the Vu-Paulraj approach ([7]) to the present context. However, the algorithm presented in [7] is very demanding since the needed evaluations of $I(\mathbf{Q})$ gradient and Hessian require intensive Monte-Carlo simulations.

1.2.4 The Large System Approximation of $I(\mathbf{Q})$

When t and r converge to ∞ while $t/r \to c$, $c \in (0,\infty)$, [17] showed that $I(\mathbf{Q})$ can be approximated by $\overline{I}(\mathbf{Q})$ defined by

$$\overline{I}(\mathbf{Q}) = \log\left|\mathbf{I}_r + \sum_{l=1}^{L} \tilde{\delta}_l(\mathbf{Q})\mathbf{C}^{(l)}\right| + \log\left|\mathbf{I}_t + \mathbf{Q}\left(\sum_{l=1}^{L}\delta_l(\mathbf{Q})\tilde{\mathbf{C}}^{(l)}\right)\right| - \sigma^2 t\left(\sum_{l=1}^{L}\delta_l(\mathbf{Q})\tilde{\delta}_l(\mathbf{Q})\right), \quad (1.8)$$

where $(\delta_1(\mathbf{Q}),\ldots,\delta_L(\mathbf{Q}))^T = \boldsymbol{\delta}(\mathbf{Q})$ and $(\tilde{\delta}_1(\mathbf{Q}),\ldots,\tilde{\delta}_L(\mathbf{Q}))^T = \tilde{\boldsymbol{\delta}}(\mathbf{Q})$ are the positive solutions of the system of $2L$ equations:

$$\begin{cases} \kappa_l = f_l(\tilde{\boldsymbol{\kappa}}) \\ \tilde{\kappa}_l = \tilde{f}_l(\boldsymbol{\kappa},\mathbf{Q}) \end{cases} \text{ for } l = 1,\ldots,L, \quad (1.9)$$

with $\boldsymbol{\kappa} = (\kappa_1,\ldots,\kappa_L)^T$ and $\tilde{\boldsymbol{\kappa}} = (\tilde{\kappa}_1,\ldots,\tilde{\kappa}_L)^T$, and with

$$\begin{cases} f_l(\tilde{\boldsymbol{\kappa}}) = \frac{1}{t}\mathrm{Tr}\left[\mathbf{C}^{(l)}\mathbf{T}(\tilde{\boldsymbol{\kappa}})\right], \\ \tilde{f}_l(\boldsymbol{\kappa},\mathbf{Q}) = \frac{1}{t}\mathrm{Tr}\left[\mathbf{Q}^{1/2}\tilde{\mathbf{C}}^{(l)}\mathbf{Q}^{1/2}\tilde{\mathbf{T}}(\boldsymbol{\kappa},\mathbf{Q})\right]. \end{cases} \quad (1.10)$$

The $r \times r$ matrix $\mathbf{T}(\tilde{\boldsymbol{\kappa}})$ and the $t \times t$ matrix $\tilde{\mathbf{T}}(\boldsymbol{\kappa},\mathbf{Q})$ are respectively defined by:

$$\mathbf{T}(\tilde{\boldsymbol{\kappa}}) = \left[\sigma^2\left(\mathbf{I}_r + \sum_{j=1}^{L}\tilde{\kappa}_j\mathbf{C}^{(j)}\right)\right]^{-1}, \quad (1.11)$$

$$\tilde{\mathbf{T}}(\boldsymbol{\kappa},\mathbf{Q}) = \left[\sigma^2\left(\mathbf{I}_t + \sum_{j=1}^{L}\kappa_j\mathbf{Q}^{1/2}\tilde{\mathbf{C}}^{(j)}\mathbf{Q}^{1/2}\right)\right]^{-1}. \quad (1.12)$$

1.3 Deriving the Large System Approximation

1.3.1 The Canonical Equations

In [17], the existence and the uniqueness of positive solutions to (1.9) is assumed without justification. Moreover no algorithm is given for the calculation of the δ_l and $\tilde{\delta}_l$, $l = 1,\ldots,L$. We therefore clarify below these important points. We consider the case $\mathbf{Q} = \mathbf{I}$ in order to simplify the notations. To address the general case it is sufficient to change matrices $(\tilde{\mathbf{C}}^{(l)})_{l=1,\ldots,L}$ into $(\mathbf{Q}^{1/2}\tilde{\mathbf{C}}^{(l)}\mathbf{Q}^{1/2})_{l=1,\ldots,L}$ in what follows.

Theorem 1. *The system of equations (1.9) admits unique positive solutions $(\delta_l)_{l=1,\ldots,L}$ and $(\tilde{\delta}_l)_{l=1,\ldots,L}$, which are the limits of the following fixed point algorithm:*

- *Initialization:* $\delta_l^{(0)} > 0$, $\tilde{\delta}_l^{(0)} > 0$, $l = 1,\ldots,L$.

- *Evaluation of the* $\delta_l^{(n+1)}$ *and* $\tilde{\delta}_l^{(n+1)}$ *from* $\boldsymbol{\delta}^{(n)} = (\delta_1^{(n)}, \ldots, \delta_L^{(n)})^T$ *and* $\tilde{\boldsymbol{\delta}}^{(n)} = (\tilde{\delta}_1^{(n)}, \ldots, \tilde{\delta}_L^{(n)})^T$*:*

$$\begin{cases} \delta_l^{(n+1)} = f_l(\tilde{\boldsymbol{\delta}}^{(n)}), \\ \tilde{\delta}_l^{(n+1)} = \tilde{f}_l(\boldsymbol{\delta}^{(n)}, \mathbf{I}). \end{cases} \tag{1.13}$$

Proof: We prove the existence and uniqueness of positive solutions.

Existence: Using analytic continuation technique, we show in Appendix 1.A that the fixed point algorithm introduced converges to positive coefficients δ_l and $\tilde{\delta}_l$, $l = 1, \ldots, L$. As functions $\tilde{\boldsymbol{\kappa}} \mapsto f_l(\tilde{\boldsymbol{\kappa}})$ and $\boldsymbol{\kappa} \mapsto \tilde{f}_l(\boldsymbol{\kappa}, \mathbf{I})$ are clearly continuous, the limit of $(\boldsymbol{\delta}^{(n)}, \tilde{\boldsymbol{\delta}}^{(n)})$ when $n \to \infty$ satisfies (1.9). Hence, the convergence of the algorithm yields the existence of a positive solution to (1.9).

Uniqueness: Let $(\boldsymbol{\delta}, \tilde{\boldsymbol{\delta}})$ and $(\boldsymbol{\delta}', \tilde{\boldsymbol{\delta}}')$ be two solutions of the canonical equation (1.9) with $\mathbf{Q} = \mathbf{I}$. We denote $(\mathbf{T}, \tilde{\mathbf{T}})$ and $(\mathbf{T}', \tilde{\mathbf{T}}')$ the associated matrices defined by (1.11) and (1.12), where $(\boldsymbol{\kappa}, \tilde{\boldsymbol{\kappa}})$ respectively coincide with $(\boldsymbol{\delta}, \tilde{\boldsymbol{\delta}})$ and $(\boldsymbol{\delta}', \tilde{\boldsymbol{\delta}}')$. Introducing $\mathbf{e} = \boldsymbol{\delta} - \boldsymbol{\delta}' = (e_1, \ldots, e_L)^T$ we have:

$$\begin{aligned} e_l &= \frac{1}{t}\mathrm{Tr}\left[\mathbf{C}^{(l)}\mathbf{T}(\mathbf{T}'^{-1} - \mathbf{T}^{-1})\mathbf{T}'\right] \\ &= \frac{\sigma^2}{t}\sum_{k=1}^{L}(\tilde{\delta}_k' - \tilde{\delta}_k)\mathrm{Tr}\left(\mathbf{C}^{(l)}\mathbf{T}\mathbf{C}^{(k)}\mathbf{T}'\right). \end{aligned} \tag{1.14}$$

Similarly, with $\tilde{\boldsymbol{e}} = \tilde{\boldsymbol{\delta}} - \tilde{\boldsymbol{\delta}}' = (\tilde{e}_1, \ldots, \tilde{e}_L)^T$,

$$\tilde{e}_k = \frac{\sigma^2}{t}\sum_{l=1}^{L}(\delta_l' - \delta_l)\mathrm{Tr}\left(\tilde{\mathbf{C}}^{(k)}\tilde{\mathbf{T}}\tilde{\mathbf{C}}^{(l)}\tilde{\mathbf{T}}'\right). \tag{1.15}$$

And (1.14) and (1.15) can be written together as

$$\begin{bmatrix} \mathbf{I} & \sigma^2\mathbf{A}(\mathbf{T}, \mathbf{T}') \\ \sigma^2\tilde{\mathbf{A}}(\tilde{\mathbf{T}}, \tilde{\mathbf{T}}') & \mathbf{I} \end{bmatrix} \begin{bmatrix} \mathbf{e} \\ \tilde{\mathbf{e}} \end{bmatrix} = \mathbf{0}, \tag{1.16}$$

where $L \times L$ matrices $\mathbf{A}(\mathbf{T}, \mathbf{T}')$ and $\tilde{\mathbf{A}}(\tilde{\mathbf{T}}, \tilde{\mathbf{T}}')$ are defined by $\mathbf{A}_{kl}(\mathbf{T}, \mathbf{T}') = \frac{1}{t}\mathrm{Tr}\left(\mathbf{C}^{(k)}\mathbf{T}\mathbf{C}^{(l)}\mathbf{T}'\right)$ and $\tilde{\mathbf{A}}_{kl}(\tilde{\mathbf{T}}, \tilde{\mathbf{T}}') = \frac{1}{t}\mathrm{Tr}(\tilde{\mathbf{C}}^{(k)}\tilde{\mathbf{T}}\tilde{\mathbf{C}}^{(l)}\tilde{\mathbf{T}}')$. We will now prove that $\rho(\mathbf{M}) < 1$, where matrix $\mathbf{M}$ is defined by

$$\mathbf{M} = \sigma^4\tilde{\mathbf{A}}(\tilde{\mathbf{T}}, \tilde{\mathbf{T}}')\mathbf{A}(\mathbf{T}, \mathbf{T}').$$

This will imply that the matrix governing the linear system (1.16) is invertible, and thus that $\mathbf{e} = \tilde{\mathbf{e}} = \mathbf{0}$, i.e. the uniqueness.

$$\begin{aligned} |\mathbf{M}_{kl}| &= \left|\frac{\sigma^4}{t^2}\sum_{j=1}^{L}\mathrm{Tr}(\tilde{\mathbf{C}}^{(k)}\tilde{\mathbf{T}}\tilde{\mathbf{C}}^{(j)}\tilde{\mathbf{T}}')\mathrm{Tr}(\mathbf{C}^{(j)}\mathbf{T}\mathbf{C}^{(l)}\mathbf{T}')\right| \\ &\leq \frac{\sigma^4}{t^2}\sum_{j=1}^{L}\left|\mathrm{Tr}(\tilde{\mathbf{C}}^{(k)}\tilde{\mathbf{T}}\tilde{\mathbf{C}}^{(j)}\tilde{\mathbf{T}}')\right|\left|\mathrm{Tr}(\mathbf{C}^{(j)}\mathbf{T}\mathbf{C}^{(l)}\mathbf{T}')\right|. \end{aligned} \tag{1.17}$$

Using Cauchy-Schwarz inequality $|\mathrm{Tr}(\mathbf{AB})|^2 \leq \mathrm{Tr}(\mathbf{AA}^H) \cdot \mathrm{Tr}(\mathbf{BB}^H)$, we have:

$$\begin{cases} \frac{1}{t}\left|\mathrm{Tr}(\tilde{\mathbf{C}}^{(k)}\tilde{\mathbf{T}}\tilde{\mathbf{C}}^{(j)}\tilde{\mathbf{T}}')\right| \leq \sqrt{\tilde{\mathbf{A}}_{kj}(\tilde{\mathbf{T}},\tilde{\mathbf{T}})\tilde{\mathbf{A}}_{kj}(\tilde{\mathbf{T}}',\tilde{\mathbf{T}}')}, \\ \frac{1}{t}\left|\mathrm{Tr}(\mathbf{C}^{(j)}\mathbf{T}\mathbf{C}^{(l)}\mathbf{T}')\right| \leq \sqrt{\mathbf{A}_{jl}(\mathbf{T},\mathbf{T})\mathbf{A}_{jl}(\mathbf{T}',\mathbf{T}')}. \end{cases}$$

Using these two inequalities in (1.17) gives

$$|\mathbf{M}_{kl}| \leq \sigma^4 \sum_{j=1}^{L} \sqrt{\tilde{\mathbf{A}}_{kj}(\tilde{\mathbf{T}})\tilde{\mathbf{A}}_{kj}(\tilde{\mathbf{T}}')\mathbf{A}_{jl}(\mathbf{T})\mathbf{A}_{jl}(\mathbf{T}')},$$

where matrices $\mathbf{A}(\mathbf{T})$ and $\tilde{\mathbf{A}}(\tilde{\mathbf{T}})$ are defined by

$$\begin{cases} \mathbf{A}_{kl}(\mathbf{T}) = \frac{1}{t}\mathrm{Tr}(\mathbf{C}^{(k)}\mathbf{T}\mathbf{C}^{(l)}\mathbf{T}) = \mathbf{A}_{kl}(\mathbf{T},\mathbf{T}), \\ \tilde{\mathbf{A}}_{kl}(\tilde{\mathbf{T}}) = \frac{1}{t}\mathrm{Tr}(\tilde{\mathbf{C}}^{(k)}\tilde{\mathbf{T}}\tilde{\mathbf{C}}^{(l)}\tilde{\mathbf{T}}) = \tilde{\mathbf{A}}_{kl}(\tilde{\mathbf{T}},\tilde{\mathbf{T}}). \end{cases} \tag{1.18}$$

Using Cauchy-Schwarz inequality then yields:

$$|\mathbf{M}_{kl}| \leq \mathbf{P}_{kl},$$

where $\mathbf{P}$ is the $L \times L$ matrix whose entries are defined by

$$\mathbf{P}_{kl} = \sqrt{\left(\sigma^4\tilde{\mathbf{A}}(\tilde{\mathbf{T}})\mathbf{A}(\mathbf{T})\right)_{kl}}\sqrt{\left(\sigma^4\tilde{\mathbf{A}}(\tilde{\mathbf{T}}')\mathbf{A}(\mathbf{T}')\right)_{kl}}.$$

Theorem 8.1.18 of [71] then yields $\rho(\mathbf{M}) \leq \rho(\mathbf{P})$. Besides, Lemma 5.7.9 of [72] used on the definition of $\mathbf{P}$ gives:

$$\rho(\mathbf{P}) \leq \sqrt{\rho\left(\sigma^4\tilde{\mathbf{A}}(\tilde{\mathbf{T}})\mathbf{A}(\mathbf{T})\right)}\sqrt{\rho\left(\sigma^4\tilde{\mathbf{A}}(\tilde{\mathbf{T}}')\mathbf{A}(\mathbf{T}')\right)}. \tag{1.19}$$

Lemma 1 (ii) in Appendix 1.C implies that $\rho(\sigma^4\tilde{\mathbf{A}}(\tilde{\mathbf{T}})\mathbf{A}(\mathbf{T})) < 1$ and $\rho(\sigma^4\tilde{\mathbf{A}}(\tilde{\mathbf{T}}')\mathbf{A}(\mathbf{T}')) < 1$, so that (1.19) finally implies:

$$\rho(\mathbf{M}) \leq \rho(\mathbf{P}) < 1.$$

This completes the proof of Theorem 1. □

1.3.2 Deriving the Approximation of $I(\mathbf{Q} = \mathbf{I}_t)$ With Gaussian Methods

We consider in this section the case $\mathbf{Q} = \mathbf{I}_t$. We note $I = I(\mathbf{I}_t)$, $\overline{I} = \overline{I}(\mathbf{I}_t)$. We have proved in the previous section the consistency of $\overline{I}(\mathbf{Q})$ definition. To establish the approximation of $I(\mathbf{Q})$, [17] used the replica method, a useful and simple trick whose mathematical relevance is not yet proved in the present context. Moreover, no assumptions were specified for the convergence of $I(\mathbf{Q})$ towards $\overline{I}(\mathbf{Q})$. However, using large random matrix techniques similar to those of [10] and [12], it is possible to prove rigorously the following theorem, in which the (mild) suitable technical assumptions are clarified.

Theorem 2. *If we assume that, for every* $j \in \{1, \dots, L\}$, $\sup_t \|\mathbf{C}^{(j)}\| < +\infty$, $\sup_t \|\tilde{\mathbf{C}}^{(j)}\| < +\infty$, $\inf_t \left(\frac{1}{t}\mathrm{Tr}\, \mathbf{C}^{(j)}\right) > 0$ *and* $\inf_t \left(\frac{1}{t}\mathrm{Tr}\, \tilde{\mathbf{C}}^{(j)}\right) > 0$, *then*

$$I = \overline{I} + \mathcal{O}\left(\frac{1}{t}\right).$$

Sketch of proof: The proof is done in three steps:

1. In a first step we derive a large system approximation of $\mathbb{E}_{\mathbf{H}}[\mathrm{Tr}\, \mathbf{S}]$, where $\mathbf{S} = (\mathbf{H}\mathbf{H}^H + \sigma^2 \mathbf{I}_r)^{-1}$ is the resolvent of $\mathbf{H}\mathbf{H}^H$ at point $-\sigma^2$. Nonetheless the approximation is expressed with the terms $\alpha_l = \frac{1}{t}\mathbb{E}_{\mathbf{H}}[\mathrm{Tr}\left(\mathbf{C}^{(l)}\mathbf{S}\right)]$, $l = 1, \dots, L$, which still depend on the entries of $\mathbb{E}_{\mathbf{H}}[\mathbf{S}]$.

2. A second step refines the previous approximation to obtain an approximation which this time only depends on the variance structure of the channels, i.e. matrices $(\mathbf{C}^{(l)})_{l\in\{1,\dots,L\}}$ and $(\tilde{\mathbf{C}}^{(l)})_{l\in\{1,\dots,L\}}$.

3. The previous approximation is used to get the asymptotic behavior of mutual information by a proper integration.

Proof: We now sketch the three steps stated above. We provide the missing details in the Appendix.

a) A first large system approximation of $\mathbb{E}_{\mathbf{H}}[\mathrm{Tr}\, \mathbf{S}]$

We introduce vectors $\boldsymbol{\alpha} = [\alpha_1, \dots, \alpha_L]^T$ and $\tilde{\boldsymbol{\alpha}} = [\tilde{\alpha}_1, \dots, \tilde{\alpha}_L]^T$ defined by

$$\begin{cases} \alpha_l = \frac{1}{t}\mathrm{Tr}\left[\mathbf{C}^{(l)}\mathbb{E}_{\mathbf{H}}[\mathbf{S}]\right] \\ \tilde{\alpha}_l = \frac{1}{t}\mathrm{Tr}\big[\tilde{\mathbf{C}}^{(l)}\tilde{\mathbf{R}}\big] \end{cases} \text{for } l = 1, \dots, L, \tag{1.20}$$

where $t \times t$ matrix $\tilde{\mathbf{R}}$ is defined by $\tilde{\mathbf{R}}(\boldsymbol{\alpha}) = \left[\sigma^2\big(\mathbf{I}_t + \sum_{j=1}^L \alpha_j \tilde{\mathbf{C}}^{(j)}\big)\right]^{-1}$. Using large random matrix techniques similar to those of [10] and [12], the following proposition is proved in Appendix 1.B.

Proposition 1. *Assume that, for every* $j \in \{1, \dots, L\}$, $\sup_t \|\mathbf{C}^{(j)}\| < +\infty$, $\sup_t \|\tilde{\mathbf{C}}^{(j)}\| < +\infty$. *Then* $\mathbb{E}_{\mathbf{H}}[\mathbf{S}]$ *can be written as*

$$\mathbb{E}_{\mathbf{H}}[\mathbf{S}] = \mathbf{R} + \boldsymbol{\Upsilon}, \tag{1.21}$$

where matrix $\boldsymbol{\Upsilon}$ *is such that* $\frac{1}{t}\mathrm{Tr}(\boldsymbol{\Upsilon}\mathbf{A}) = \mathcal{O}\left(\frac{1}{t^2}\right)$ *for any uniformly bounded matrix* $\mathbf{A}$ *and where matrix* $\mathbf{R}$ *is defined by* $\mathbf{R}(\tilde{\boldsymbol{\alpha}}) = \left[\sigma^2\big(\mathbf{I}_r + \sum_{j=1}^L \tilde{\alpha}_j \mathbf{C}^{(j)}\big)\right]^{-1}$.

One can check that the entries of matrix $\boldsymbol{\Upsilon}$ are $\mathcal{O}\left(\frac{1}{t^{3/2}}\right)$; nevertheless this result is not needed here. It follows from Proposition 1 that, for any $r \times r$ matrix $\mathbf{A}$ uniformly bounded in r,

$$\frac{1}{t}\mathbb{E}_{\mathbf{H}}[\mathrm{Tr}(\mathbf{S}\mathbf{A})] = \frac{1}{t}\mathrm{Tr}(\mathbf{R}\mathbf{A}) + \mathcal{O}\left(\frac{1}{t^2}\right). \tag{1.22}$$

Taking $\mathbf{A} = \mathbf{I}$ gives a first approximation of $\mathbb{E}_{\mathbf{H}}[\mathrm{Tr}\,\mathbf{S}]$:

$$\mathbb{E}_{\mathbf{H}}[\mathrm{Tr}\,\mathbf{S}] = \mathrm{Tr}\,\mathbf{R} + \mathcal{O}\left(\frac{1}{t}\right). \tag{1.23}$$

Nonetheless matrix $\mathbf{R}$ depends on $\mathbb{E}_{\mathbf{H}}[\mathbf{S}]$ through vector $\boldsymbol{\alpha}$.

b) A refined large system approximation of $\mathbb{E}_{\mathbf{H}}[\mathrm{Tr}\,\mathbf{S}]$

We first recall from Section 1.3.1 that $\mathbf{T}$ is the matrix defined by (1.11) associated to the solutions $(\boldsymbol{\delta}, \tilde{\boldsymbol{\delta}})$ of the canonical equation (1.9) with $\mathbf{Q} = \mathbf{I}_t$: $\mathbf{T} = \left(\sigma^2\left(\mathbf{I}_r + \sum_{l=1}^{L} \tilde{\delta}_l \mathbf{C}^{(l)}\right)\right)^{-1}$. We introduce the following proposition which will lead to the desired approximation of $\mathbb{E}_{\mathbf{H}}[\mathrm{Tr}\,\mathbf{S}]$:

Proposition 2. *Assume that, for every $j \in \{1, \ldots, L\}$, $\sup_t \|\mathbf{C}^{(j)}\| < +\infty$, $\sup_t \|\tilde{\mathbf{C}}^{(j)}\| < +\infty$, $\inf_t \left(\frac{1}{t}\mathrm{Tr}\,\mathbf{C}^{(j)}\right) > 0$ and $\inf_t \left(\frac{1}{t}\mathrm{Tr}\,\tilde{\mathbf{C}}^{(j)}\right) > 0$. Let $\mathbf{A}$ be a $r \times r$ matrix uniformly bounded in r, then*

$$\frac{1}{t}\mathrm{Tr}(\mathbf{R}\mathbf{A}) = \frac{1}{t}\mathrm{Tr}(\mathbf{T}\mathbf{A}) + \mathcal{O}\left(\frac{1}{t^2}\right). \tag{1.24}$$

The proof is given in Appendix 1.C. It relies on the similarity of the systems of equations verified by the $(\alpha_l, \tilde{\alpha}_l)$ and the $(\delta_l, \tilde{\delta}_l)$. Actually, taking $\mathbf{A} = \mathbf{C}^{(l)}$ in (1.22) yields $\alpha_l = \frac{1}{t}\mathrm{Tr}(\mathbf{C}^{(l)}\mathbf{R}) + \mathcal{O}\left(\frac{1}{t^2}\right)$ and therefore

$$\begin{cases} \alpha_l = \frac{1}{t}\mathrm{Tr}\left[\mathbf{C}^{(l)}\left[\sigma^2(\mathbf{I} + \sum_{j=1}^{L} \tilde{\alpha}_j \mathbf{C}^{(j)})\right]^{-1}\right] + \mathcal{O}\left(\frac{1}{t^2}\right) \\ \tilde{\alpha}_l = \frac{1}{t}\mathrm{Tr}\left[\tilde{\mathbf{C}}^{(l)}\left[\sigma^2(\mathbf{I} + \sum_{j=1}^{L} \alpha_j \tilde{\mathbf{C}}^{(j)})\right]^{-1}\right] \end{cases}$$

for $l = 1, \ldots, L$. Taking $\mathbf{A} = \mathbf{I}_r$ in (1.24) together with (1.23) leads to

$$\mathbb{E}_{\mathbf{H}}[\mathrm{Tr}\,\mathbf{S}] = \mathrm{Tr}\,\mathbf{T} + \mathcal{O}\left(\frac{1}{t}\right) \tag{1.25}$$

c) The resulting large system approximation of I

The ergodic mutual information I can be written in terms of the resolvent $\mathbf{S}$:

$$I = \mathbb{E}_{\mathbf{H}}\left[\log\left|\mathbf{I}_r + \frac{\mathbf{H}\mathbf{H}^H}{\sigma^2}\right|\right] = \mathbb{E}_{\mathbf{H}}\left[\log\left|\sigma^2\mathbf{S}(\sigma^2)\right|^{-1}\right].$$

As the differential of $g(\mathbf{A}) = \log|\mathbf{A}|$ is given by $g(\mathbf{A} + \delta\mathbf{A}) = g(\mathbf{A}) + \mathrm{Tr}[\mathbf{A}^{-1}\delta\mathbf{A}] + o(\|\delta\mathbf{A}\|)$, we obtain:

$$\begin{aligned} \frac{dI}{d\sigma^2} &= -\mathbb{E}_{\mathbf{H}}\left[\frac{\mathrm{Tr}[\mathbf{S}(\sigma^2)\mathbf{H}\mathbf{H}^H]}{\sigma^2}\right] \\ &= -\mathbb{E}_{\mathbf{H}}\left[\frac{\mathrm{Tr}[\mathbf{I}_r - \sigma^2\mathbf{S}(\sigma^2)]}{\sigma^2}\right], \end{aligned}$$

where the last equality follows from the so-called resolvent identity

$$\sigma^2\mathbf{S}(\sigma^2) = \mathbf{I}_r - \mathbf{S}(\sigma^2)\mathbf{H}\mathbf{H}^H. \tag{1.26}$$

The resolvent identity is inferred easily from the definition of $\mathbf{S}(\sigma^2)$. As $I(\sigma^2 = +\infty) = 0$, we now have the following expression of mutual information:

$$I(\sigma^2) = \int_{\sigma^2}^{+\infty} \left(\frac{r}{\rho} - \mathbb{E}_{\mathbf{H}} \left[\mathrm{Tr}\, \mathbf{S}(\rho) \right] \right) d\rho.$$

This equality clearly justifies the search of a large system equivalent of $\mathbb{E}_{\mathbf{H}} \left[\mathrm{Tr}\, \mathbf{S} \right]$ done in the previous sections. The term under the integral sign can be written as

$$\frac{r}{\sigma^2} - \mathbb{E}_{\mathbf{H}} \left[\mathrm{Tr}\, \mathbf{S} \right] = t \sum_{l=1}^{L} \tilde{\delta}_l \delta_l + \mathbb{E}_{\mathbf{H}} \left[\mathrm{Tr}\, (\mathbf{T} - \mathbf{S}) \right],$$

as $\frac{r}{\sigma^2} - \mathrm{Tr}\, \mathbf{T} = \mathrm{Tr}\big[((\sigma^2\mathbf{T})^{-1} - \mathbf{I}_r)\mathbf{T}\big] = \mathrm{Tr}\big[(\sum_l \tilde{\delta}_l \mathbf{C}^{(l)})\mathbf{T}\big] = t \sum_l \tilde{\delta}_l \delta_l$. We need to integrate $\varepsilon(t, \sigma^2) = \mathbb{E}_{\mathbf{H}} \left[\mathrm{Tr}\, (\mathbf{T} - \mathbf{S}) \right]$ with respect to σ^2 on $(\rho > 0, +\infty)$. We therefore introduce the following proposition:

Proposition 3. *$\varepsilon(t, \sigma^2) = \mathbb{E}_{\mathbf{H}} \left[\mathrm{Tr}\, (\mathbf{T} - \mathbf{S}) \right]$ is integrable with respect to σ^2 on $(\rho > 0, +\infty)$ and*

$$\int_{\rho}^{+\infty} \varepsilon(t, \sigma^2) d\sigma^2 = \mathcal{O}\left(\frac{1}{t} \right).$$

Proof: We prove in Appendix 1.D that there exists t_0 such that, for $t > t_0$, $|\varepsilon(t, \sigma^2)| \leq \frac{1}{\sigma^8 t} P\left(\frac{1}{\sigma^2}\right)$, where P is a polynomial whose coefficients are real positive and do not depend on σ^2 nor on t. Therefore $\int_{\rho}^{+\infty} \varepsilon(t, \sigma^2) d\sigma^2 = \mathcal{O}\left(\frac{1}{t}\right)$.

□

We now prove that the term $t \sum_l \tilde{\delta}_l \delta_l$ corresponds to the derivative of $\overline{I}(\sigma^2)$ with respect to σ^2. To this end, we consider the function $\mathcal{V}_0(\sigma^2, \boldsymbol{\kappa}, \tilde{\boldsymbol{\kappa}})$ defined by

$$\mathcal{V}_0(\sigma^2, \boldsymbol{\kappa}, \tilde{\boldsymbol{\kappa}}) = \log |\mathbf{I} + \mathbf{C}(\tilde{\boldsymbol{\kappa}})| + \log |\mathbf{I} + \tilde{\mathbf{C}}(\boldsymbol{\kappa})| - \sigma^2 t \sum_{l=1}^{L} \kappa_l \tilde{\kappa}_l,$$

where $\tilde{\mathbf{C}}(\boldsymbol{\kappa}) = \sum_{l=1}^{L} \kappa_l \tilde{\mathbf{C}}^{(l)}$ and $\mathbf{C}(\tilde{\boldsymbol{\kappa}}) = \sum_{l=1}^{L} \tilde{\kappa}_l \mathbf{C}^{(l)}$. Note that $\mathcal{V}_0(\sigma^2, \boldsymbol{\delta}, \tilde{\boldsymbol{\delta}}) = \overline{I}(\sigma^2)$. The derivative of $\overline{I}(\sigma^2)$ can then be expressed in terms of the partial derivatives of $\mathcal{V}_0$.

$$\begin{aligned} \frac{d\overline{I}}{d\sigma^2} =& \frac{\partial \mathcal{V}_0}{\partial \sigma^2}(\sigma^2, \boldsymbol{\delta}, \tilde{\boldsymbol{\delta}}) + \sum_{l=1}^{L} \frac{\partial \mathcal{V}_0}{\partial \kappa_l}(\sigma^2, \boldsymbol{\delta}, \tilde{\boldsymbol{\delta}}) \cdot \frac{d\delta_l}{d\sigma^2} \\ &+ \sum_{l=1}^{L} \frac{\partial \mathcal{V}_0}{\partial \tilde{\kappa}_l}(\sigma^2, \boldsymbol{\delta}, \tilde{\boldsymbol{\delta}}) \cdot \frac{d\tilde{\delta}_l}{d\sigma^2}. \end{aligned}$$

It is straightforward to check that

$$\begin{cases} \dfrac{\partial \mathcal{V}_0}{\partial \kappa_l}(\sigma^2, \boldsymbol{\kappa}, \tilde{\boldsymbol{\kappa}}) = -\sigma^2 t\big(\tilde{f}_l(\boldsymbol{\kappa}, \mathbf{I}_t) - \tilde{\kappa}_l\big), \\ \dfrac{\partial \mathcal{V}_0}{\partial \tilde{\kappa}_l}(\sigma^2, \boldsymbol{\kappa}, \tilde{\boldsymbol{\kappa}}) = -\sigma^2 t\big(f_l(\tilde{\boldsymbol{\kappa}}) - \kappa_l\big). \end{cases} \tag{1.27}$$

Both partial derivatives are equal to zero at point $(\sigma^2, \boldsymbol{\delta}, \tilde{\boldsymbol{\delta}})$, as $(\boldsymbol{\delta}, \tilde{\boldsymbol{\delta}})$ verifies by definition (1.9) with $\mathbf{Q} = \mathbf{I}_t$. Therefore,

$$\frac{d\overline{I}}{d\sigma^2} = \frac{\partial \mathcal{V}_0}{\partial \sigma^2}(\sigma^2, \boldsymbol{\delta}, \tilde{\boldsymbol{\delta}}) = -t \sum_{l=1}^{L} \delta_l \tilde{\delta}_l,$$

which, together with Proposition 3, leads to $I = \overline{I} + \mathcal{O}\left(\frac{1}{t}\right)$.

□

1.3.3 The Approximation $\overline{I}(\mathbf{Q})$

We now consider the dependency in $\mathbf{Q}$ of the approximation $\bar{I}(\mathbf{Q})$. We previously considered the case $\mathbf{Q} = \mathbf{I}_t$; to address the general case it is sufficient to change matrix $\tilde{\mathbf{C}}^{(l)}$ into $\mathbf{Q}^{1/2}\tilde{\mathbf{C}}^{(l)}\mathbf{Q}^{1/2}$ for every $l = 1, \ldots, L$ in 1.3.1 and 1.3.2. Hence the following Corollary of Theorem 2:

Corollary 1. *Assume that, for every* $j \in \{1, \ldots, L\}$, $\sup_t \|\mathbf{C}^{(j)}\| < +\infty$, $\sup_t \|\tilde{\mathbf{C}}^{(j)}\| < +\infty$, $\inf_t \left(\frac{1}{t}\mathrm{Tr}\, \mathbf{C}^{(j)}\right) > 0$ *and* $\inf_t \lambda_{\min}(\tilde{\mathbf{C}}^{(j)}) > 0$. *Then, for* $\mathbf{Q}$ *such as* $\sup_t \|\mathbf{Q}\| < +\infty$,

$$I(\mathbf{Q}) = \overline{I}(\mathbf{Q}) + \mathcal{O}\left(\frac{1}{t}\right).$$

Note that the technical assumptions on matrices $(\tilde{\mathbf{C}}^{(l)})_{l=1,\ldots,L}$ are slightly stronger than in Theorem 2 in order to ensure that $\inf_t \left(\frac{1}{t}\mathrm{Tr}\left[\mathbf{Q}\tilde{\mathbf{C}}^{(j)}\right]\right) > 0$.

We can now state an important result about the concavity of the function $\mathbf{Q} \mapsto \overline{I}(\mathbf{Q})$, a result which will be highly needed for its optimization in section 1.4.

Theorem 3. $\mathbf{Q} \mapsto \overline{I}(\mathbf{Q})$ *is a strictly concave function over the compact set* $\mathcal{C}_1$.

Proof: We here only prove the concavity of $\overline{I}(\mathbf{Q})$. The proof of the strict concavity is quite tedious, but essentially the same as in [12] section IV (see also the extended version [69]). It is therefore omitted.

Denote by $\otimes$ the Kronecker product of matrices. Let us introduce the following matrices:

$$\boldsymbol{\Delta}^{(l)} = \mathbf{I}_m \otimes \mathbf{C}^{(l)},\ \tilde{\boldsymbol{\Delta}}^{(l)} = \mathbf{I}_m \otimes \tilde{\mathbf{C}}^{(l)},\ \check{\mathbf{Q}} = \mathbf{I}_m \otimes \mathbf{Q}.$$

We now denote $\check{\mathbf{H}}(z) = \sum_{l=1}^{L} \check{\mathbf{H}}^{(l)} z^{-(l-1)}$ with $\check{\mathbf{H}}^{(l)} = \frac{1}{\sqrt{mt}} (\mathbf{\Delta}^{(l)})^{1/2} \check{\mathbf{W}}_l (\tilde{\mathbf{\Delta}}^{(l)})^{1/2}$. where $\check{\mathbf{W}}$ is a $rm \times tm$ matrix whose entries are independent and identically distributed complex circular Gaussian random variables with variance 1. Introducing $I_m(\check{\mathbf{Q}})$ the ergodic mutual information associated with channel $\check{\mathbf{H}}(z)$:

$$I_m(\check{\mathbf{Q}}) = \mathbb{E}_{\check{\mathbf{H}}} \log \left| \mathbf{I} + \frac{\check{\mathbf{H}} \check{\mathbf{Q}} \check{\mathbf{H}}^H}{\sigma^2} \right|,$$

where $\check{\mathbf{H}} = \check{\mathbf{H}}(1) = \sum_l \check{\mathbf{H}}^{(l)}$. Using the results of [17] and Theorem 2, it is clear that $I_m(\check{\mathbf{Q}})$ admits an asymptotic approximation $\bar{I}_m(\check{\mathbf{Q}})$. Due to the block-diagonal nature of matrices $\mathbf{\Delta}^{(l)}$, $\tilde{\mathbf{\Delta}}^{(l)}$ and $\check{\mathbf{Q}}$, it is straightforward to show that $\delta_l(\mathbf{Q}) = \delta_l(\check{\mathbf{Q}})$, $\tilde{\delta}_l(\mathbf{Q}) = \tilde{\delta}_l(\check{\mathbf{Q}})$ and that, as a consequence,

$$\frac{1}{m} \bar{I}_m(\check{\mathbf{Q}}) = \bar{I}(\mathbf{Q}),$$

and thus

$$\lim_{m \to \infty} \frac{1}{m} I_m(\check{\mathbf{Q}}) = \bar{I}(\mathbf{Q}).$$

As $\check{\mathbf{Q}} \mapsto I_m(\check{\mathbf{Q}})$ is concave, we can conclude that $\bar{I}(\mathbf{Q})$ is concave as a pointwise limit of concave functions. □

As $\overline{I}(\mathbf{Q})$ is strictly concave on $\mathcal{C}_1$ by Theorem 3, it admits a unique argmax that we denote $\overline{\mathbf{Q}}_*$. We recall that $I(\mathbf{Q})$ is strictly concave on $\mathcal{C}_1$ and that we denoted $\mathbf{Q}_*$ its argmax. In order to clarify the relation between $\overline{\mathbf{Q}}_*$ and $\mathbf{Q}_*$ we introduce the following proposition which establishes that the maximization of $\overline{I}(\mathbf{Q})$ is equivalent to the maximization of $I(\mathbf{Q})$ over $\mathcal{C}_1$, up to a $\mathcal{O}\left(\frac{1}{t}\right)$ term.

Proposition 4. *Assume that, for every* $j \in \{1, \ldots, L\}$, $\sup_t \|\mathbf{C}^{(j)}\| < +\infty$, $\sup_t \|\tilde{\mathbf{C}}^{(j)}\| < +\infty$, $\inf_t \lambda_{\min}(\mathbf{C}^{(j)}) > 0$ *and* $\inf_t \lambda_{\min}(\tilde{\mathbf{C}}^{(j)}) > 0$. *Then*

$$I(\overline{\mathbf{Q}}_*) = I(\mathbf{Q}_*) + \mathcal{O}\left(\frac{1}{t}\right).$$

Proof: The proof is very similar to the one of [12, Proposition 3]. Assuming that $\sup_t \|\overline{\mathbf{Q}}_*\| < +\infty$ and $\sup_t \|\mathbf{Q}_*\| < +\infty$ we can apply Theorem 1 on $\overline{\mathbf{Q}}_*$ and $\mathbf{Q}_*$, hence

$$\Big(I(\mathbf{Q}_*) - I(\overline{\mathbf{Q}}_*)\Big) + \Big(\overline{I}(\overline{\mathbf{Q}}_*) - \overline{I}(\mathbf{Q}_*)\Big) = \Big(I(\mathbf{Q}_*) - \overline{I}(\mathbf{Q}_*)\Big) + \Big(\overline{I}(\overline{\mathbf{Q}}_*) - I(\overline{\mathbf{Q}}_*)\Big) = \mathcal{O}\left(\frac{1}{t}\right).$$

Besides $I(\mathbf{Q}_*) - I(\overline{\mathbf{Q}}_*) \geq 0$ and $\overline{I}(\overline{\mathbf{Q}}_*) - \overline{I}(\mathbf{Q}_*) \geq 0$, as $\mathbf{Q}_*$ and $\overline{\mathbf{Q}}_*$ respectively maximize $I(\mathbf{Q})$ and $\overline{I}(\mathbf{Q})$. Therefore $I(\mathbf{Q}_*) - I(\overline{\mathbf{Q}}_*) = \mathcal{O}\left(\frac{1}{t}\right)$.

One can prove $\sup_t \|\overline{\mathbf{Q}}_*\| < +\infty$ using the same arguments as in [12, Appendix III]. It essentially lies in the fact that $\overline{\mathbf{Q}}_*$ is the solution of a waterfilling algorithm, which will be shown independently from this result in next section (see Proposition 7).

Concerning $\sup_t \|\mathbf{Q}_*\| < +\infty$, the proof is identical to [12, Appendix III]; one just needs to replace

$$\begin{array}{ccc} \frac{\sqrt{K}}{\sqrt{K+1}}\mathbf{A} & \text{by} & \frac{1}{\sqrt{t}}\sum_{l=2}^{L}(\mathbf{C}^{(l)})^{1/2}\mathbf{W}_l(\tilde{\mathbf{C}}^{(l)})^{1/2}, \\ \frac{1}{\sqrt{K+1}}\frac{1}{\sqrt{t}}\mathbf{C}_R^{1/2}\mathbf{W}\mathbf{C}_T^{1/2} & \text{by} & \frac{1}{\sqrt{t}}(\mathbf{C}^{(1)})^{1/2}\mathbf{W}_1(\tilde{\mathbf{C}}^{(1)})^{1/2} \end{array}$$

in the definition of $\mathbf{H}$. Then S_j, defined in [12, (134)], can be written as

$$\begin{aligned} S_j = 2\mathrm{Re}\left\{\frac{1}{t}\mathbf{u}_j^{\perp H}\big(\mathbf{C}^{(1)}\big)^{1/2}\mathbf{R}_j\left(\sum_{l=2}^{L}\big(\mathbf{C}^{(l)}\big)^{1/2}\mathbf{z}_{l,j} + \big(\mathbf{C}^{(1)}\big)^{1/2}\mathbf{u}_j\right)\right\} \\ + \frac{1}{t}\mathbf{u}_j^{\perp H}\big(\mathbf{C}^{(1)}\big)^{1/2}\mathbf{R}_j\big(\mathbf{C}^{(1)}\big)^{1/2}\mathbf{u}_j^{\perp}, \end{aligned} \tag{1.28}$$

where $\mathbf{R}_j$ has the same definition as in [12], $\mathbf{z}_{l,j}$ is the j^{th} column of matrix $\mathbf{W}_l(\tilde{\mathbf{C}}^{(l)})^{1/2}$ and $\mathbf{z}_j = \mathbf{z}_{1,j} = \mathbf{u}_j + \mathbf{u}_j^{\perp}$ with $\mathbf{u}_j$ the conditional expectation $\mathbf{u}_j = \mathbb{E}\big[\mathbf{z}_{1,j}\big|(\mathbf{z}_{1,k})_{1\le k\le t, k\neq j}\big]$. As the vector $\mathbf{u}_j^{\perp}$ is independent from $\mathbf{R}_j$ and from $\mathbf{z}_{l,k}$, $k = 1,\ldots,t$, $l = 2,\ldots,L$, we can easily prove that the first term of the right-hand side of (1.28) is a $\mathcal{O}\left(\frac{1}{t}\right)$. The second term of the right-hand side of (1.28) is moreover close from $\rho_j = \frac{1}{t}\big[(\tilde{\mathbf{C}}^{(1)})^{-1}\big]_{jj}^{-1}\mathrm{Tr}(\mathbf{R}_j\mathbf{C}^{(1)})$. In fact it is possible to prove that there exists a constant C_1 such that $\mathbb{E}\big[(S_j-\rho_j)^2\big] < \frac{C_1}{t}$ (see [12] for more details).

The rest of the proof of [12, Proposition 3 (ii)] can then follow.

□

1.4 Maximization Algorithm

Proposition 4 shows that it is relevant to maximize $\overline{I}(\mathbf{Q})$ over $\mathcal{C}_1$. In this section we propose a maximization algorithm for the large system approximation $\overline{I}(\mathbf{Q})$. We first introduce some classical concepts and results needed for the optimization of $\mathbf{Q} \mapsto \overline{I}(\mathbf{Q})$.

Definition 1. *Let ϕ be a function defined on the convex set $\mathcal{C}_1$. Let $\mathbf{P},\mathbf{Q} \in \mathcal{C}_1$. Then ϕ is said to be differentiable in the Gâteaux sense (or Gâteaux differentiable) at point $\mathbf{Q}$ in the direction $\mathbf{P}-\mathbf{Q}$ if the following limit exists:*

$$\lim_{\lambda\to 0^+}\frac{\phi(\mathbf{Q}+\lambda(\mathbf{P}-\mathbf{Q})) - \phi(\mathbf{Q})}{\lambda}.$$

In this case, this limit is noted $\langle \phi'(\mathbf{Q}), \mathbf{P}-\mathbf{Q}\rangle$.

Note that $\phi(\mathbf{Q}+\lambda(\mathbf{P}-\mathbf{Q}))$ makes sense for $\lambda \in [0,1]$, as $\mathbf{Q}+\lambda(\mathbf{P}-\mathbf{Q}) = (1-\lambda)\mathbf{Q}+\lambda\mathbf{P}$ naturally belongs to $\mathcal{C}_1$. We now establish the following result:

Proposition 5. *For each $\mathbf{P},\mathbf{Q} \in \mathcal{C}_1$, functions $\mathbf{Q} \mapsto \delta_l(\mathbf{Q})$, $\mathbf{Q} \mapsto \tilde{\delta}_l(\mathbf{Q})$, $l = 1,\ldots,L$, as well as function $\mathbf{Q} \mapsto \overline{I}(\mathbf{Q})$ are Gâteaux differentiable at $\mathbf{Q}$ in the direction $\mathbf{P}-\mathbf{Q}$.*

Proof: See Appendix 1.E. □

In order to characterize the matrix $\overline{\mathbf{Q}}_*$ maximizing $\overline{I}(\mathbf{Q})$, we recall the following result:

Proposition 6. *Let $\phi : \mathcal{C}_1 \to \mathbb{R}$ be a strictly concave function. Then,*

(i) ϕ is Gâteaux differentiable at $\mathbf{Q}$ in the direction $\mathbf{P} - \mathbf{Q}$ for each $\mathbf{P}, \mathbf{Q} \in \mathcal{C}_1$,

(ii) $\mathbf{Q}_{opt}$ is the unique argmax of ϕ on $\mathcal{C}_1$ if and only if it verifies:

$$\forall \mathbf{Q} \in \mathcal{C}_1,\ \langle \phi'(\mathbf{Q}_{opt}), \mathbf{Q} - \mathbf{Q}_{opt} \rangle \leq 0. \tag{1.29}$$

This proposition is standard (see for example [73, Chapter 2]).

In order to introduce our maximization algorithm, we consider the function $\mathcal{V}(\mathbf{Q}, \boldsymbol{\kappa}, \tilde{\boldsymbol{\kappa}})$ defined by:

$$\begin{aligned}\mathcal{V}(\mathbf{Q}, \boldsymbol{\kappa}, \tilde{\boldsymbol{\kappa}}) =& \log|\mathbf{I}_r + \mathbf{C}(\tilde{\boldsymbol{\kappa}})| + \log|\mathbf{I}_t + \mathbf{Q}\tilde{\mathbf{C}}(\boldsymbol{\kappa})| \\ &- \sigma^2 t \sum_{l=1}^{L} \kappa_l \tilde{\kappa}_l.\end{aligned} \tag{1.30}$$

We recall that $\tilde{\mathbf{C}}(\boldsymbol{\kappa}) = \sum_l \kappa_l \tilde{\mathbf{C}}^{(l)}$ and $\mathbf{C}(\tilde{\boldsymbol{\kappa}}) = \sum_l \tilde{\kappa}_l \mathbf{C}^{(l)}$. Note that we have $\mathcal{V}(\mathbf{Q}, \boldsymbol{\delta}(\mathbf{Q}), \tilde{\boldsymbol{\delta}}(\mathbf{Q})) = \overline{I}(\mathbf{Q})$. We then have the following result:

Proposition 7. *Denote by $\boldsymbol{\delta}_*$ and $\tilde{\boldsymbol{\delta}}_*$ the quantities $\boldsymbol{\delta}(\overline{\mathbf{Q}}_*)$ and $\tilde{\boldsymbol{\delta}}(\overline{\mathbf{Q}}_*)$. Matrix $\overline{\mathbf{Q}}_*$ is the solution of the standard waterfilling problem: maximize over $\mathbf{Q} \in \mathcal{C}_1$ the function $\log|\mathbf{I}_t + \mathbf{Q}\tilde{\mathbf{C}}(\boldsymbol{\delta}_*)|$.*

Proof: We first remark that maximizing function $\mathbf{Q} \mapsto \log|\mathbf{I} + \mathbf{Q}\tilde{\mathbf{C}}(\boldsymbol{\delta}_*)|$ is equivalent to maximizing function $\mathbf{Q} \mapsto \mathcal{V}(\mathbf{Q}, \boldsymbol{\delta}_*, \tilde{\boldsymbol{\delta}}_*)$ by (1.30). The proof then relies on the observation hereafter proven that, for each $\mathbf{P} \in \mathcal{C}_1$,

$$\langle \overline{I}'(\overline{\mathbf{Q}}_*), \mathbf{P} - \overline{\mathbf{Q}}_* \rangle = \langle \mathcal{V}'(\overline{\mathbf{Q}}_*, \boldsymbol{\delta}_*, \tilde{\boldsymbol{\delta}}_*), \mathbf{P} - \overline{\mathbf{Q}}_* \rangle, \tag{1.31}$$

where $\langle \mathcal{V}'(\overline{\mathbf{Q}}_*, \boldsymbol{\delta}_*, \tilde{\boldsymbol{\delta}}_*), \mathbf{P} - \overline{\mathbf{Q}}_* \rangle$ is the Gâteaux differential of function $\mathbf{Q} \mapsto \mathcal{V}(\mathbf{Q}, \boldsymbol{\delta}_*, \tilde{\boldsymbol{\delta}}_*)$ at point $\overline{\mathbf{Q}}_*$ in direction $\mathbf{P} - \overline{\mathbf{Q}}_*$. Assuming (1.31) is verified, (1.29) yields that $\langle \mathcal{V}'(\overline{\mathbf{Q}}_*, \boldsymbol{\delta}_*, \tilde{\boldsymbol{\delta}}_*), \mathbf{P} - \overline{\mathbf{Q}}_* \rangle \leq 0$ for each matrix $\mathbf{P} \in \mathcal{C}_1$. And as the function $\mathbf{Q} \mapsto \mathcal{V}(\mathbf{Q}, \boldsymbol{\delta}_*, \tilde{\boldsymbol{\delta}}_*)$ is strictly concave on $\mathcal{C}_1$, its unique argmax on $\mathcal{C}_1$ coincides with $\overline{\mathbf{Q}}_*$.

It now remains to prove (1.31). Consider $\mathbf{P}$, $\mathbf{Q} \in \mathcal{C}_1$. Then,

$$\begin{aligned}\langle \overline{I}'(\mathbf{Q}), \mathbf{P} - \mathbf{Q} \rangle =& \langle \mathcal{V}'(\mathbf{Q}, \boldsymbol{\delta}(\mathbf{Q}), \tilde{\boldsymbol{\delta}}(\mathbf{Q})), \mathbf{P} - \mathbf{Q} \rangle + \sum_{l=1}^{L} \frac{\partial \mathcal{V}}{\partial \kappa_l}(\mathbf{Q}, \boldsymbol{\delta}(\mathbf{Q}), \tilde{\boldsymbol{\delta}}(\mathbf{Q})) \langle \delta_l'(\mathbf{Q}), \mathbf{P} - \mathbf{Q} \rangle \\ &+ \sum_{l=1}^{L} \frac{\partial \mathcal{V}}{\partial \tilde{\kappa}_l}(\mathbf{Q}, \boldsymbol{\delta}(\mathbf{Q}), \tilde{\boldsymbol{\delta}}(\mathbf{Q})) \langle \tilde{\delta}_l'(\mathbf{Q}), \mathbf{P} - \mathbf{Q} \rangle.\end{aligned} \tag{1.32}$$

Similarly to (1.27), partial derivatives $\frac{\partial \mathcal{V}}{\partial \kappa_l}(\mathbf{Q}, \boldsymbol{\kappa}, \tilde{\boldsymbol{\kappa}}) = -\sigma^2 t\big(\tilde{f}_l(\boldsymbol{\kappa}, \mathbf{Q}) - \tilde{\kappa}_l\big)$ and $\frac{\partial \mathcal{V}}{\partial \tilde{\kappa}_l}(\mathbf{Q}, \boldsymbol{\kappa}, \tilde{\boldsymbol{\kappa}}) = -\sigma^2 t$ $\big(f_l(\tilde{\boldsymbol{\kappa}}) - \kappa_l\big)$ are equal to zero at point $(\mathbf{Q}, \boldsymbol{\delta}(\mathbf{Q}), \tilde{\boldsymbol{\delta}}(\mathbf{Q}))$, as $(\boldsymbol{\delta}(\mathbf{Q}), \tilde{\boldsymbol{\delta}}(\mathbf{Q}))$ verifies (1.9) by definition. Therefore, letting $\mathbf{Q} = \overline{\mathbf{Q}}_*$ in (1.32) yields:

$$\langle \overline{I}'(\overline{\mathbf{Q}}_*), \mathbf{P} - \overline{\mathbf{Q}}_* \rangle = \langle \mathcal{V}'(\overline{\mathbf{Q}}_*, \boldsymbol{\delta}(\overline{\mathbf{Q}}_*), \tilde{\boldsymbol{\delta}}(\overline{\mathbf{Q}}_*)), \mathbf{P} - \overline{\mathbf{Q}}_* \rangle.$$

□

Proposition 7 shows that the optimum matrix is solution of a waterfilling problem associated to the covariance matrix $\tilde{\mathbf{C}}(\boldsymbol{\delta}_*)$. This result cannot be used to evaluate $\overline{\mathbf{Q}}_*$, because the matrix $\tilde{\mathbf{C}}(\boldsymbol{\delta}_*)$ itself depends on $\overline{\mathbf{Q}}_*$. However, it provides some insight on the structure of the optimum matrix: the eigenvectors of $\overline{\mathbf{Q}}_*$ coincide with the eigenvectors of a linear combination of matrices $\tilde{\mathbf{C}}^{(l)}$, the $\delta_l(\mathbf{Q}_*)$ being the coefficients of this linear combination. This is in line with the result of [17, Appendix VI].

We now introduce our iterative algorithm for optimizing $\overline{I}(\mathbf{Q})$:

- Initialization: $\mathbf{Q}_0 = \mathbf{I}$.
- Evaluation of $\mathbf{Q}_k$ from $\mathbf{Q}_{k-1}$: $(\boldsymbol{\delta}^{(k)}, \tilde{\boldsymbol{\delta}}^{(k)})$ is defined as the unique solution of (1.9) in which $\mathbf{Q} = \mathbf{Q}_{k-1}$. Then $\mathbf{Q}_k$ is defined as the maximum of function $\mathbf{Q} \mapsto \log\big|\mathbf{I}_t + \mathbf{Q}\tilde{\mathbf{C}}(\boldsymbol{\delta}^{(k)})\big|$ on $\mathcal{C}_1$.

We now establish a result which implies that, if the algorithm converges, then it converges towards the optimal covariance matrix $\overline{\mathbf{Q}}_*$.

Proposition 8. *Assume that*

$$\lim_{k\to\infty} \boldsymbol{\delta}^{(k)} - \boldsymbol{\delta}^{(k-1)} = \lim_{k\to\infty} \tilde{\boldsymbol{\delta}}^{(k)} - \tilde{\boldsymbol{\delta}}^{(k-1)} = 0. \tag{1.33}$$

Then, the algorithm converges towards matrix $\overline{\mathbf{Q}}_*$.

Proof: The sequence $(\mathbf{Q}_k)$ belongs to the set $\mathcal{C}_1$. As $\mathcal{C}_1$ is compact, we just have to verify that every convergent subsequence $(\mathbf{Q}_{\psi(k)})_{k\in\mathbb{N}}$ extracted from $(\mathbf{Q}_k)_{k\in\mathbb{N}}$ converges towards $\overline{\mathbf{Q}}_*$. For this, we denote by $\overline{\mathbf{Q}}_{\psi,*}$ the limit of the above subsequence, and prove that this matrix verifies property (1.29) with $\phi = \overline{I}$. Vectors $\boldsymbol{\delta}^{\psi(k)+1}$ and $\tilde{\boldsymbol{\delta}}^{\psi(k)+1}$ are defined as the solutions of (1.9) with $\mathbf{Q} = \mathbf{Q}_{\psi(k)}$. Hence, due to the continuity of functions $\mathbf{Q} \mapsto \delta_l(\mathbf{Q})$ and $\mathbf{Q} \mapsto \tilde{\delta}_l(\mathbf{Q})$, sequences $(\boldsymbol{\delta}^{\psi(k)+1})_{k\in\mathbb{N}}$ and $(\tilde{\boldsymbol{\delta}}^{\psi(k)+1})_{k\in\mathbb{N}}$ converge towards $\boldsymbol{\delta}^{\psi,*} = \boldsymbol{\delta}(\overline{\mathbf{Q}}_{\psi,*})$ and $\tilde{\boldsymbol{\delta}}^{\psi,*} = \tilde{\boldsymbol{\delta}}(\overline{\mathbf{Q}}_{\psi,*})$ respectively. Moreover, $(\boldsymbol{\delta}^{\psi,*}, \tilde{\boldsymbol{\delta}}^{\psi,*})$ is solution of system (1.9) in which matrix $\mathbf{Q}$ coincides with $\overline{\mathbf{Q}}_{\psi,*}$. Therefore,

$$\frac{\partial \mathcal{V}}{\partial \kappa_l}\left(\overline{\mathbf{Q}}_{\psi,*}, \boldsymbol{\delta}^{\psi,*}, \tilde{\boldsymbol{\delta}}^{\psi,*}\right) = \frac{\partial \mathcal{V}}{\partial \tilde{\kappa}_l}\left(\overline{\mathbf{Q}}_{\psi,*}, \boldsymbol{\delta}^{\psi,*}, \tilde{\boldsymbol{\delta}}^{\psi,*}\right) = 0.$$

As in the proof of Proposition 7, this leads to

$$\langle \overline{I}'(\overline{\mathbf{Q}}_{\psi,*}), \mathbf{P} - \overline{\mathbf{Q}}_{\psi,*} \rangle = \langle \mathcal{V}'(\overline{\mathbf{Q}}_{\psi,*}, \boldsymbol{\delta}_{\psi,*}, \tilde{\boldsymbol{\delta}}_{\psi,*}), \mathbf{P} - \overline{\mathbf{Q}}_{\psi,*} \rangle \tag{1.34}$$

for every $\mathbf{P} \in \mathcal{C}_1$. It remains to show that the right-hand side of (1.34) is negative to complete the proof. For this, we use that $\mathbf{Q}_{\psi(k)}$ is the argmax over $\mathcal{C}_1$ of function $\mathbf{Q} \mapsto \mathcal{V}\big(\mathbf{Q}, \boldsymbol{\delta}^{\psi(k)}, \tilde{\boldsymbol{\delta}}^{\psi(k)}\big)$. Therefore,

$$\langle \mathcal{V}'(\mathbf{Q}_{\psi(k)}, \boldsymbol{\delta}_{\psi(k)}, \tilde{\boldsymbol{\delta}}_{\psi(k)}), \mathbf{P} - \mathbf{Q}_{\psi(k)} \rangle \leq 0 \ \ \forall\, \mathbf{P} \in \mathcal{C}_1. \tag{1.35}$$

By condition (1.33), sequences $(\boldsymbol{\delta}_{\psi(k)})$ and $(\tilde{\boldsymbol{\delta}}_{\psi(k)})$ also converge towards $\boldsymbol{\delta}^{\psi,*}$ and $\tilde{\boldsymbol{\delta}}^{\psi,*}$ respectively. Taking the limit of (1.35) when $k \to \infty$ eventually shows that $\langle \mathcal{V}'(\overline{\mathbf{Q}}_{\psi,*}, \boldsymbol{\delta}_{\psi,*}, \tilde{\boldsymbol{\delta}}_{\psi,*}), \mathbf{P} - \overline{\mathbf{Q}}_{\psi,*} \rangle \leq 0$ as required. □

To conclude, if the algorithm is convergent, that is, if the sequence of $(\mathbf{Q}_k)_{k\in\mathbb{N}}$ converges towards a certain matrix, then the $\delta_l^{(k)} = \delta_l(\mathbf{Q}_{k-1})$ and the $\tilde{\delta}_l^{(k)} = \tilde{\delta}_l(\mathbf{Q}_{k-1})$ converge as well when $k \to \infty$. Condition (1.33) is then verified, hence, if the algorithm is convergent, it converges towards $\overline{\mathbf{Q}}_*$. Although the convergence of the algorithm has not been proved, this result is encouraging and suggests that the algorithm is reliable. In particular, in all the conducted simulations the algorithm was converging. In any case, condition (1.33) can be easily checked. If it is not satisfied, it is possible to modify the initial point $\mathbf{Q}_0$ as many times as needed to ensure the convergence.

1.5 Numerical Results

We provide here some simulations results to evaluate the performance of the proposed approach. We use the propagation model introduced in [16], in which each path corresponds to a scatterer cluster characterized by a mean angle of departure, a mean angle of arrival and an angle spread for each of these two angles.

In the featured simulations for Fig. 1.1(a) (respectively Fig. 1.1(b)), we consider a frequency selective MIMO system with $r = t = 4$ (respectively $r = t = 8$), a carrier frequency of 2GHz, a number of paths $L = 5$. The paths share the same power, and their mean departure angles and angles spreads are given in Table 1.1 in radians. In both Fig. 1.1(a) and 1.1(b), we have represented the EMI $I(\mathbf{I}_t)$ (i.e. without optimization), and the optimized EMI $I(\overline{\mathbf{Q}}_*)$ (i.e. with an input covariance matrix maximizing the approximation $\overline{I}$). The EMI are evaluated by Monte-Carlo simulations, with $2 \cdot 10^4$ channel realizations. The EMI optimized with Vu-Paulraj algorithm [7] is also represented for comparison.

Vu-Paulraj's algorithm is composed of two nested iterative loops. The inner loop evaluates $\mathbf{Q}_*^{(n)} = \operatorname{argmax} \{I(\mathbf{Q}) + k_{\text{barrier}} \log|\mathbf{Q}|\}$ thanks to the Newton algorithm with the constraint $\frac{1}{t}\operatorname{Tr}\mathbf{Q} = 1$, for a given value of k_{barrier} and a given starting point $\mathbf{Q}_0^{(n)}$. Maximizing $I(\mathbf{Q}) + k_{\text{barrier}} \log|\mathbf{Q}|$ instead of $I(\mathbf{Q})$ ensures that $\mathbf{Q}$ remains positive semi-definite through the steps of the Newton algorithm; this is the so-called barrier interior-point method. The outer loop then decreases k_{barrier} by a certain constant factor μ and gives the inner loop the next starting point $\mathbf{Q}_0^{(n+1)} = \mathbf{Q}_*^{(n)}$. The algorithm stops when the desired precision is obtained, or, as the Newton algorithm requires heavy Monte-Carlo simulations for

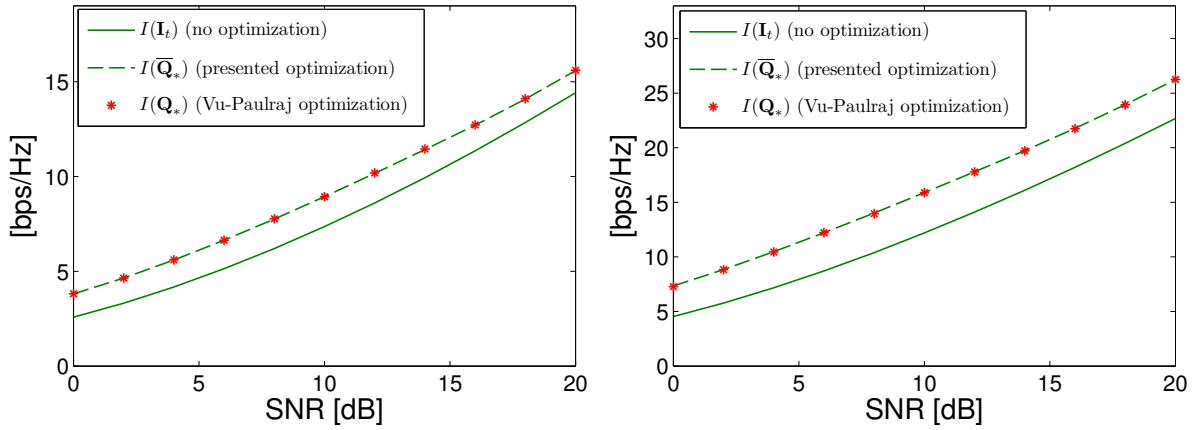

(a) $r = t = 4$ (b) $r = t = 8$

Figure 1.1: Comparison with Vu-Paulraj algorithm

Table 1.1: Paths angular parameters *(in radians)*

	$l = 1$	$l = 2$	$l = 3$	$l = 4$	$l = 5$
mean departure angle	6.15	3.52	4.04	2.58	2.66
departure angle spread	0.06	0.09	0.05	0.05	0.03
mean arrival angle	4.85	3.48	1.71	5.31	0.06
arrival angle spread	0.06	0.08	0.05	0.02	0.11

the evaluation of the gradient and of the Hessian of $I(\mathbf{Q})$, when the number of iterations of the outer loop reaches a given number $N_{\max}$. As in [7] we took $N_{\max} = 10$, $\mu = 100$, $2 \cdot 10^4$ trials for the Monte-Carlo simulations, and we started with $k_{\text{barrier}} = \frac{1}{100}$.

Both Fig. 1.1(a) and 1.1(b) show that maximizing $\overline{I}(\mathbf{Q})$ over the input covariance leads to significant improvement for $I(\mathbf{Q})$. Our approach provides the same results as Vu-Paulraj's algorithm. Moreover our algorithm is computationally much more efficient: in Vu-Paulraj's algorithm, the evaluation of the gradient and of the Hessian of $I(\mathbf{Q})$ needs heavy Monte-Carlo simulations. Table 1.2 gives for both algorithms the average execution time in seconds to obtain the input covariance matrix, on a 3.16GHz Intel Xeon CPU with 8GB of RAM, for a number of paths $L = 3$, $L = 4$ and $L = 5$, given $r = t = 4$.

Table 1.2: Average execution time *(in seconds)*

	$L = 3$	$L = 4$	$L = 5$
Vu-Paulraj	681	884	1077
New algorithm	$7.0 \cdot 10^{-3}$	$7.4 \cdot 10^{-3}$	$8.3 \cdot 10^{-3}$

1.6 Conclusion

In this chapter we have addressed the evaluation of the capacity achieving covariance matrices of frequency selective MIMO channels. We have first clarified the definition of the large system approximation of the EMI and rigorously proved its expression and convergence speed with Gaussian methods. We have then proposed to optimize the EMI through this approximation, and have introduced an attractive iterative algorithm based on an iterative waterfilling scheme. Numerical results have shown that our approach provides the same results as a direct approach, but in a more efficient way in terms of computation time.

Appendices

1.A Proof of the existence of a solution

To study (1.9), it is quite useful to interpret functions f_l and $\tilde{f}_l$ as functions of the parameter $-\sigma^2 \in \mathbb{R}^-$, to extend their domain of validity from $\mathbb{R}^-$ to $\mathbb{C} - \mathbb{R}^+$, and to use powerful results concerning certain class of analytic functions. We therefore define the functions $g(\tilde{\boldsymbol{\psi}})(z)$ and $g(\boldsymbol{\psi})(z)$, with $\boldsymbol{\psi}(z) = [\psi_1(z), ..., \psi_L(z)]^T$, $\tilde{\boldsymbol{\psi}}(z) = [\tilde{\psi_1}(z), ..., \tilde{\psi_L}(z)]^T$, as

$$g(\tilde{\boldsymbol{\psi}})(z) = \begin{bmatrix} g_1(\tilde{\boldsymbol{\psi}})(z) \\ ... \\ g_L(\tilde{\boldsymbol{\psi}})(z) \end{bmatrix}, \; \tilde{g}(\boldsymbol{\psi})(z) = \begin{bmatrix} \tilde{g_1}(\boldsymbol{\psi})(z) \\ ... \\ \tilde{g_L}(\boldsymbol{\psi})(z) \end{bmatrix},$$

where functions $g_l(\tilde{\boldsymbol{\psi}})$ and $\tilde{g}_l(\boldsymbol{\psi})$ are defined by

$$g_l(\tilde{\boldsymbol{\psi}})(z) = \frac{1}{t}\mathrm{Tr}\big[\mathbf{C}^{(l)}\mathbf{T}^{\tilde{\boldsymbol{\psi}}}(z)\big],$$
$$\tilde{g}_l(\boldsymbol{\psi})(z) = \frac{1}{t}\mathrm{Tr}\big[\tilde{\mathbf{C}}^{(l)}\tilde{\mathbf{T}}^{\boldsymbol{\psi}}(z)\big].$$

Matrices $\mathbf{T}^{\tilde{\boldsymbol{\psi}}}(z)$ and $\tilde{\mathbf{T}}^{\boldsymbol{\psi}}(z)$ are defined by

$$\mathbf{T}^{\tilde{\boldsymbol{\psi}}}(z) = \Big[-z\Big(\mathbf{I}_r + \sum_{j=1}^{L} \tilde{\psi_j}(z)\mathbf{C}^{(j)}\Big)\Big]^{-1}, \tag{1.36}$$

$$\tilde{\mathbf{T}}^{\boldsymbol{\psi}}(z) = \Big[-z\Big(\mathbf{I}_t + \sum_{j=1}^{L} \psi_j(z)\tilde{\mathbf{C}}^{(j)}\Big)\Big]^{-1}. \tag{1.37}$$

In order to explain the following results, we now have to introduce the concept of Stieltjès transforms.

Definition 2. *Let μ be a finite[2] positive measure carried by $\mathbb{R}^+$. The Stieltjès transform of μ is the function $s(z)$ defined for $z \in \mathbb{C} - \mathbb{R}^+$ by*

$$s(z) = \int_{\mathbb{R}^+} \frac{d\mu(\lambda)}{\lambda - z}. \tag{1.38}$$

In the following, the class of all Stieltjès transforms of finite positive measures carried by $\mathbb{R}^+$ is denoted $\mathcal{S}(\mathbb{R}^+)$. We now state some of the properties of the elements of $\mathcal{S}(\mathbb{R}^+)$.

Proposition 9. *Let $s(z) \in \mathcal{S}(\mathbb{R}^+)$, and μ its associated measure. Then we have the following results:*

[2] finite means that $\mu(\mathbb{R}^+) < \infty$

(i) $s(z)$ *is analytic on* $\mathbb{C} - \mathbb{R}^+$,

(ii) $\mathrm{Im}(s(z)) > 0$ *if* $\mathrm{Im}(z) > 0$, *and* $\mathrm{Im}(s(z)) < 0$ *if* $\mathrm{Im}(z) < 0$,

(iii) $\mathrm{Im}(zs(z)) > 0$ *if* $\mathrm{Im}(z) > 0$, *and* $\mathrm{Im}(zs(z)) < 0$ *if* $\mathrm{Im}(z) < 0$,

(iv) $s(-\sigma^2) > 0$ *for* $\sigma^2 > 0$,

(v) $|s(z)| \leq \frac{\mu(\mathbb{R}^+)}{d(z,\mathbb{R}^+)}$ *for* $z \in \mathbb{C} - \mathbb{R}^+$,

(vi) $\mu(\mathbb{R}^+) = \lim_{y\to\infty} -iy\, s(iy)$.

Proof: All the stated properties are standard material, see e.g. Appendix of [74]. □

Conversely, a useful tool to prove that a certain function belongs to $\mathcal{S}(\mathbb{R}^+)$ is the following proposition:

Proposition 10. *Let* s *be a function holomorphic on* $\mathbb{C} - \mathbb{R}^+$ *which verifies the three following properties:*

(i) $\mathrm{Im}(s(z)) > 0$ *if* $\mathrm{Im}(z) > 0$,

(ii) $\mathrm{Im}(zs(z)) > 0$ *if* $\mathrm{Im}(z) > 0$,

(iii) $\sup_{y>0} |iy\, s(iy)| < \infty$.

Then $s \in \mathcal{S}(\mathbb{R}^+)$ *and, if* μ *represents the corresponding positive measure,*

$$\mu(\mathbb{R}^+) = \lim_{y\to\infty} (-iy\, s(iy)).$$

Proof: see Appendix of [74]. □

Now that we have recalled the notion of Stieltjès transforms and its associated basic properties we can introduce the following proposition:

Proposition 11. *Let* $(\psi_l, \tilde{\psi}_l)_{l=1,\dots,L} \in \mathcal{S}(\mathbb{R}^+)$. *We define functions* $\varphi_l(z)$ *and* $\tilde{\varphi}_l(z)$, $l = 1, \dots, L$, *as*

$$\begin{cases} \varphi_l(z) = \frac{1}{t}\mathrm{Tr}\big[\mathbf{C}^{(l)}\mathbf{T}^{\tilde{\psi}}(z)\big], \\ \tilde{\varphi}_l(z) = \frac{1}{t}\mathrm{Tr}\big[\tilde{\mathbf{C}}^{(l)}\tilde{\mathbf{T}}^{\psi}(z)\big]. \end{cases}$$

Then we have the following results:

(i) $\mathbf{T}^{\tilde{\psi}}$, $\tilde{\mathbf{T}}^{\psi}$ *are holomorphic on* $\mathbb{C} - \mathbb{R}^+$,

(ii) $\|\mathbf{T}^{\tilde{\boldsymbol{\psi}}}(z)\| \leq \frac{1}{d(z,\mathbb{R}^+)}$, $\|\tilde{\mathbf{T}}^{\boldsymbol{\psi}}(z)\| \leq \frac{1}{d(z,\mathbb{R}^+)}$ *on* $\mathbb{C}-\mathbb{R}^+$,

(iii) $\varphi_l \in \mathcal{S}(\mathbb{R}^+)$ *with the corresponding mass* μ_l *verifying* $\mu_l(\mathbb{R}^+) = \frac{1}{t}\mathrm{Tr}\,\mathbf{C}^{(l)}$, $\tilde{\varphi}_l \in \mathcal{S}(\mathbb{R}^+)$ *with the corresponding mass* $\tilde{\mu}_l$ *verifying* $\tilde{\mu}_l(\mathbb{R}^+) = \frac{1}{t}\mathrm{Tr}\,\tilde{\mathbf{C}}^{(l)}$.

Proof: For item (i) we only have to check that $z\big(\mathbf{I}_r + \sum_{j=1}^L \tilde{\psi}_j(z)\mathbf{C}^{(j)}\big)$ is invertible for every $z \in \mathbb{C}-\mathbb{R}^+$ to prove that $\mathbf{T}^{\tilde{\boldsymbol{\psi}}}$ is holomorphic on $\mathbb{C}-\mathbb{R}^+$. The key point is to notice that, for any vector $\mathbf{v}$, for z such that $\mathrm{Im}(z) > 0$,

$$\mathrm{Im}\Big\{\mathbf{v}^H z\Big(\mathbf{I}_r + \sum_{j=1}^L \tilde{\psi}_j(z)\mathbf{C}^{(j)}\Big)\mathbf{v}\Big\} = \mathrm{Im}\{z\}\mathbf{v}^H\mathbf{v} + \sum_{j=1}^L \mathrm{Im}\left\{z\tilde{\psi}_j(z)\right\}\mathbf{v}^H\mathbf{C}^{(j)}\mathbf{v} > 0.$$

A similar inequality holds for $\mathrm{Im}(z) < 0$, and the case $z \in \mathbb{R}^-$ is straightforward.

Item (iii) can easily be proved thanks to Proposition 10.

As for item (ii), the proof is essentially the same as the proof of Proposition 5.1 item 3 in [75], and is therefore omitted. □

We consider the following iterative scheme:

$$\begin{cases} \boldsymbol{\psi}^{(n+1)}(z) = g(\tilde{\boldsymbol{\psi}}^{(n)})(z), \\ \tilde{\boldsymbol{\psi}}^{(n+1)}(z) = \tilde{g}(\boldsymbol{\psi}^{(n)})(z), \end{cases} \tag{1.39}$$

with a starting point $(\boldsymbol{\psi}^{(0)}(z), \tilde{\boldsymbol{\psi}}^{(0)}(z))$ in $(\mathcal{S}(\mathbb{R}^+))^{2L}$. Item (iii) of Proposition 11 then ensures that, for each $n \geq 1$, $\boldsymbol{\psi}^{(n)}(z)$ and $\tilde{\boldsymbol{\psi}}^{(n)}(z)$ belong to $(\mathcal{S}(\mathbb{R}^+))^L$. Moreover,

$$\begin{aligned} \left|(\psi_l^{(n+1)} - \psi_l^{(n)})(z)\right| &= \left|g_l(\boldsymbol{\psi}^{(n)})(z) - g_l(\boldsymbol{\psi}^{(n-1)})(z)\right| \\ &= \frac{1}{t}\left|\mathrm{Tr}\Big[\mathbf{C}^{(l)}(\mathbf{T}^{(n)}(z) - \mathbf{T}^{(n-1)}(z))\Big]\right|, \end{aligned} \tag{1.40}$$

where matrices $\mathbf{T}^{(n)}(z)$ and $\tilde{\mathbf{T}}^{(n)}(z)$ are defined by $\mathbf{T}^{(n)}(z) = \mathbf{T}^{\tilde{\boldsymbol{\psi}}^{(n)}}(z)$, $\tilde{\mathbf{T}}^{(n)}(z) = \tilde{\mathbf{T}}^{\boldsymbol{\psi}^{(n)}}(z)$. Note that in the following we may not always mention the dependency in z of $\mathbf{T}^{(n)}$, $\tilde{\mathbf{T}}^{(n)}$, $\psi_j^{(n)}$ and $\tilde{\psi}_j^{(n)}$ for reading ease. Using the equality $\mathbf{A}-\mathbf{B} = \mathbf{A}\left(\mathbf{B}^{-1}-\mathbf{A}^{-1}\right)\mathbf{B}$, we then obtain:

$$\mathbf{T}^{(n)} - \mathbf{T}^{(n-1)} = \mathbf{T}^{(n)}\Big(-z\sum_{j=1}^L\left(\tilde{\psi}_j^{(n-1)} - \tilde{\psi}_j^{(n)}\right)\mathbf{C}^{(j)}\Big)\mathbf{T}^{(n-1)}. \tag{1.41}$$

Using (1.41) in (1.40) then yields:

$$\begin{aligned} \left|\psi_l^{(n+1)} - \psi_l^{(n)}\right| &= \frac{|z|}{t}\left|\sum_{j=1}^L\left(\tilde{\psi}_j^{(n-1)} - \tilde{\psi}_j^{(n)}\right)\mathrm{Tr}\left[\mathbf{C}^{(l)}\mathbf{T}^{(n)}\mathbf{C}^{(j)}\mathbf{T}^{(n-1)}\right]\right| \\ &\leq \frac{|z|}{t}\sum_{j=1}^L\left|\tilde{\psi}_j^{(n-1)} - \tilde{\psi}_j^{(n)}\right|\left|\mathrm{Tr}\left[\mathbf{C}^{(l)}\mathbf{T}^{(n)}\mathbf{C}^{(j)}\mathbf{T}^{(n-1)}\right]\right|. \end{aligned}$$

The trace in the above expression can be bounded with the help of $C_{\max} = \max_j\{\|\mathbf{C}^{(j)}\|, \|\tilde{\mathbf{C}}^{(j)}\|\}$:

$$\begin{aligned}\left|\psi_l^{(n+1)} - \psi_l^{(n)}\right| &\leq |z|\frac{r}{t}\sum_{j=1}^{L}\left|\tilde{\psi}_j^{(n)} - \tilde{\psi}_j^{(n-1)}\right| \|\mathbf{C}^{(l)}\|\|\mathbf{T}^{(n)}\|\|\mathbf{C}^{(j)}\|\|\mathbf{T}^{(n-1)}\| \\ &\leq |z|C_{\max}^2\frac{r}{t}\|\mathbf{T}^{(n)}\|\|\mathbf{T}^{(n-1)}\|\sum_{j=1}^{L}\left|\tilde{\psi}_j^{(n)} - \tilde{\psi}_j^{(n-1)}\right|.\end{aligned}$$

For $z \in \mathbb{C} - \mathbb{R}^+$, $\mathbf{T}^{(n)}(z)$ and $\mathbf{T}^{(n-1)}(z)$ have a spectral norm less than $1/d(z,\mathbb{R}^+)$ by item (ii) of Proposition 11. Therefore,

$$\left|(\psi_l^{(n+1)} - \psi_l^{(n)})(z)\right| \leq \frac{rC_{\max}^2}{t}\frac{|z|}{(d(z,\mathbb{R}^+))^2}\sum_{j=1}^{L}\left|\left(\tilde{\psi}_j^{(n)} - \tilde{\psi}_j^{(n-1)}\right)(z)\right|. \tag{1.42}$$

A similar computation leads to

$$\left|(\tilde{\psi}_j^{(n+1)} - \tilde{\psi}_j^{(n)})(z)\right| \leq C_{\max}^2\frac{|z|}{(d(z,\mathbb{R}^+))^2}\sum_{l=1}^{L}\left|\left(\psi_l^{(n)} - \psi_l^{(n-1)}\right)(z)\right|. \tag{1.43}$$

We now introduce the following maximum:

$$M^{(n)}(z) = \max_j\left\{\left|(\psi_j^{(n+1)} - \psi_j^{(n)})(z)\right|, \left|(\tilde{\psi}_j^{(n+1)} - \tilde{\psi}_j^{(n)})(z)\right|\right\}$$

Equations (1.42) and (1.43) can then be combined into:

$$M^{(n)}(z) \leq \varepsilon(z)M^{(n-1)}(z),$$

where $\varepsilon(z) = \frac{\varepsilon_1|z|}{(d(z,\mathbb{R}^+))^2}$, with $\varepsilon_1 = LC_{\max}^2\max\left\{\frac{r}{t}, 1\right\}$. We now define the following domain: $U = \left\{z \in \mathbb{C}, d(z,\mathbb{R}^+) \geq \frac{2\varepsilon_1}{K}, \frac{|z|}{d(z,\mathbb{R}^+)} \leq 2\right\}$, with $0 \leq K < 1$. On this domain U we have $M^{(n)}(z) \leq KM^{(n-1)}(z)$. Hence, for $z \in U$, $\psi_l^{(n)}(z)$ and $\tilde{\psi}_j^{(n)}(z)$ are Cauchy sequences and, as such, converge. We denote by $\psi_l(z)$ and $\tilde{\psi}_j(z)$ their respective limit.

One wants to extend this convergence result on $\mathbb{C} - \mathbb{R}^+$. We first notice that, as $\psi_l^{(n)}$ is a Stieltjès transform whose associated measure has mass $\frac{1}{t}\mathrm{Tr}\,\mathbf{C}^{(l)}$ by Proposition 11 item (iii), item (v) of Proposition 9 implies

$$\psi_l^{(n)}(z) \leq \frac{\frac{1}{t}\mathrm{Tr}\mathbf{C}^{(l)}}{d(z,\mathbb{R}^+)}.$$

The $\psi_l^{(n)}$ are thus bounded on any compact set included in $\mathbb{C} - \mathbb{R}^+$, uniformly in n. By Montel's theorem, $\left(\psi_l^{(n)}\right)_{n\in\mathbb{N}}$ is a normal family. Therefore one can extract a subsequence converging uniformly on compact sets of $\mathbb{C} - \mathbb{R}^+$, whose limit is thus analytic over $\mathbb{C} - \mathbb{R}^+$. This limit coincides with ψ_l on domain U. The limit of any converging subsequence of $\left(\psi_l^{(n)}\right)$ thus coincides with ψ_l on U. Therefore,

these limits all coincide on $\mathbb{C}-\mathbb{R}^+$ with a function analytic on $\mathbb{C}-\mathbb{R}^+$, that we still denote ψ_l. The converging subsequences of $\left(\psi_l^{(n)}\right)$ have thus the same limit. We have therefore shown the convergence of the whole sequence $\left(\psi_l^{(n)}\right)_{n\geq 0}$ on $\mathbb{C}-\mathbb{R}^+$ towards an analytic function ψ_l. Moreover, as one can check that ψ_l verifies Proposition 10, we have $\psi_l(z)\in\mathcal{S}(\mathbb{R}^+)$. The same arguments hold for the $\tilde{\psi}_l(z)$.

We have proved the convergence of iterative sequence (1.39). Taking $z=-\sigma^2$ then yields the convergence of the fixed point algorithm (1.13). Note that the starting point $(\boldsymbol{\delta}^{(0)},\tilde{\boldsymbol{\delta}}^{(0)})$ only needs to verify $\delta_l^{(0)}>0$, $\tilde{\delta}_l^{(0)}>0$ ($l=1,\ldots,L$), as any positive real number can be interpreted as the value at point $z=-\sigma^2$ of some element $s(z)\in\mathcal{S}(\mathbb{R}^+)$. Moreover, the limits $\psi_l(z)$, $\tilde{\psi}_l(z)$ ($l=1,\ldots,L$) of the iterative sequence (1.39) are positive for any $z=-\sigma^2$ by item (iv) of Proposition 9, as they all are Stieltjès transforms. Therefore, the limits δ_l, $\tilde{\delta}_l$ ($l=1,\ldots,L$) are positive.

1.B A first large system approximation of $\mathbb{E}_{\mathbf{H}}[\mathrm{Tr}\,\mathbf{S}]$

We will prove Proposition 1 by deriving the matrix $\boldsymbol{\Upsilon}$ defined by (1.21), before proving that it satisfies $\frac{1}{t}\mathrm{Tr}\left(\boldsymbol{\Upsilon}\mathbf{A}\right)=\mathcal{O}\left(\frac{1}{t^2}\right)$ for any uniformly bounded matrix $\mathbf{A}$. To that end, as the entries of matrices $\mathbf{H}^{(l)}$ are Gaussian, we can use the classical Gaussian methods: we introduce here two Gaussian tools, an Integration by Parts formula and the Nash-Poincaré inequality, both widely used in Random Matrix Theory (see e.g. [76]).

In this section, if x is a random variable we denote by $\mathring{x}$ the zero mean random variable $\mathring{x}=x-\mathbb{E}(x)$.

We first present an Integration by Parts formula which provides the expectation of some functionals of Gaussian vectors (see e.g. [77]).

Theorem 4. *Let $\boldsymbol{\xi}=[\xi_1,\ldots,\xi_M]^T$ a complex Gaussian random vector such that $\mathbb{E}[\boldsymbol{\xi}]=\mathbf{0}$, $\mathbb{E}[\boldsymbol{\xi}\boldsymbol{\xi}^T]=\mathbf{0}$ and $\mathbb{E}[\boldsymbol{\xi}\boldsymbol{\xi}^H]=\boldsymbol{\Omega}$. If $\Gamma=\Gamma(\boldsymbol{\xi},\boldsymbol{\xi}^*)$ is a $\mathcal{C}^1$ complex function polynomially bounded together with its derivatives, then*

$$\mathbb{E}[\xi_p\Gamma(\boldsymbol{\xi})]=\sum_{m=1}^{M}\boldsymbol{\Omega}_{pm}\mathbb{E}\left[\frac{\partial\Gamma(\boldsymbol{\xi})}{\partial\xi_m^*}\right]. \tag{1.44}$$

In the present context we consider $\boldsymbol{\xi}$ being the vector of the stacked columns of matrices $\mathbf{H}^{(l)}$, where the channels $\mathbf{H}^{(l)}$ are independent and follow the Kronecker model, i.e. $\mathbb{E}_{\mathbf{H}}\left[\mathbf{H}_{ij}^{(k)}\mathbf{H}_{mn}^{(l)*}\right]=\delta_{k,l}\frac{1}{t}\mathbf{C}_{im}^{(l)}\tilde{\mathbf{C}}_{jn}^{(l)}$. Then (1.44) becomes

$$\mathbb{E}_{\mathbf{H}}\left[\mathbf{H}_{ij}^{(l)}\Gamma\left((\mathbf{H}^{(l)})_{l=1,\ldots,L}\right)\right]=\frac{1}{t}\sum_{m=1}^{r}\sum_{n=1}^{t}\mathbf{C}_{im}^{(l)}\tilde{\mathbf{C}}_{jn}^{(l)}\mathbb{E}_{\mathbf{H}}\left[\frac{\partial\Gamma}{\partial\mathbf{H}_{mn}^{(l)*}}\right]. \tag{1.45}$$

The second useful tool is the Poincaré Nash inequality which bounds the variance of certain functionals of Gaussian vectors (see e.g. [10, 76]).

Theorem 5. *Let $\boldsymbol{\xi} = [\xi_1, \ldots, \xi_M]^T$ a complex Gaussian random vector such that $\mathbb{E}[\boldsymbol{\xi}] = \mathbf{0}$, $\mathbb{E}[\boldsymbol{\xi}\boldsymbol{\xi}^T] = \mathbf{0}$ and $\mathbb{E}[\boldsymbol{\xi}\boldsymbol{\xi}^H] = \boldsymbol{\Omega}$. If $\Gamma = \Gamma(\boldsymbol{\xi}, \boldsymbol{\xi}^*)$ is a $\mathcal{C}^1$ complex function polynomially bounded together with its derivatives, then, noting $\nabla_{\boldsymbol{\xi}}\Gamma = [\frac{\partial\Gamma}{\partial\xi_1}, \ldots, \frac{\partial\Gamma}{\partial\xi_M}]^T$ and $\nabla_{\boldsymbol{\xi}^*}\Gamma = [\frac{\partial\Gamma}{\partial\xi_1^*}, \ldots, \frac{\partial\Gamma}{\partial\xi_M^*}]^T$,*

$$\mathrm{var}(\Gamma(\boldsymbol{\xi})) \leq \mathbb{E}\left[\nabla_{\boldsymbol{\xi}}\Gamma(\boldsymbol{\xi})^T\, \boldsymbol{\Omega}\, \overline{\nabla_{\boldsymbol{\xi}}\Gamma(\boldsymbol{\xi})}\right] + \mathbb{E}\left[\nabla_{\boldsymbol{\xi}^*}\Gamma(\boldsymbol{\xi})^H\, \boldsymbol{\Omega}\, \nabla_{\boldsymbol{\xi}^*}\Gamma(\boldsymbol{\xi})\right]. \tag{1.46}$$

In the following we will use the Nash-Poincaré inequality with $\boldsymbol{\xi}$ being the vector of the stacked columns of independent matrices $\mathbf{H}^{(l)}$, where the channels $\mathbf{H}^{(l)}$ follow the Kronecker model. Then (1.46) can be written under the following form:

$$\mathrm{var}\left(\Gamma\big((\mathbf{H}^{(l)})_{l=1,\ldots,L}\big)\right) \leq \frac{1}{t}\sum_{i,m=1}^{r}\sum_{j,n=1}^{t}\sum_{l=1}^{L}\mathbf{C}_{im}^{(l)}\tilde{\mathbf{C}}_{jn}^{(l)}\mathbb{E}_{\mathbf{H}}\left[\frac{\partial\Gamma}{\partial\mathbf{H}_{ij}^{(l)}}\left(\frac{\partial\Gamma}{\partial\mathbf{H}_{mn}^{(l)}}\right)^* + \left(\frac{\partial\Gamma}{\partial\mathbf{H}_{ij}^{(l)*}}\right)^*\frac{\partial\Gamma}{\partial\mathbf{H}_{mn}^{(l)*}}\right]. \tag{1.47}$$

Using these two Gaussian tools we now prove Proposition 1. In order to derive the matrix $\boldsymbol{\Upsilon}$ defined by $\mathbb{E}_{\mathbf{H}}[\mathbf{S}] = \mathbf{R} + \boldsymbol{\Upsilon}$ we study the entries of $\mathbb{E}_{\mathbf{H}}[\mathbf{S}]$. Using the resolvent identity (1.26) we have $\sigma^2\mathbb{E}_{\mathbf{H}}[\mathbf{S}_{pq}] = (\mathbf{I} - \mathbb{E}_{\mathbf{H}}[\mathbf{S}\mathbf{H}\mathbf{H}^H])_{pq}$. We evaluate $\mathbb{E}_{\mathbf{H}}[(\mathbf{S}\mathbf{H}\mathbf{H}^H)_{pq}]$ by first studying $\mathbb{E}_{\mathbf{H}}\left[\mathbf{S}_{pi}\mathbf{H}_{ij}^{(l)}\mathbf{H}_{qk}^{(l')*}\right]$. Calculation begins with an integration by parts on $\mathbf{H}_{ij}^{(l)}$ (1.45):

$$\begin{aligned}\mathbb{E}_{\mathbf{H}}\left[\mathbf{S}_{pi}\mathbf{H}_{ij}^{(l)}\mathbf{H}_{qk}^{(l')*}\right] &= \frac{1}{t}\sum_{m,n}\mathbf{C}_{im}^{(l)}\tilde{\mathbf{C}}_{jn}^{(l)}\mathbb{E}_{\mathbf{H}}\left[\frac{\partial(\mathbf{S}_{pi}\mathbf{H}_{qk}^{(l')*})}{\partial\mathbf{H}_{mn}^{(l)*}}\right]\\ &= \frac{1}{t}\sum_{m,n}\mathbf{C}_{im}^{(l)}\tilde{\mathbf{C}}_{jn}^{(l)}\mathbb{E}_{\mathbf{H}}\left[\mathbf{S}_{pi}\delta_{l,l'}\delta_{q,m}\delta_{k,n} + \mathbf{H}_{qk}^{(l')*}\frac{\partial\mathbf{S}_{pi}}{\partial\mathbf{H}_{mn}^{(l)*}}\right].\end{aligned}$$

As $\frac{\partial\mathbf{S}_{pi}}{\partial\mathbf{H}_{mn}^{(l)*}} = -\left(\mathbf{S}\frac{\partial\mathbf{S}^{-1}}{\partial\mathbf{H}_{mn}^{(l)*}}\mathbf{S}\right)_{pi} = -(\mathbf{S}\mathbf{H})_{pn}\mathbf{S}_{mi}$, we obtain

$$\mathbb{E}_{\mathbf{H}}\left[\mathbf{S}_{pi}\mathbf{H}_{ij}^{(l)}\mathbf{H}_{qk}^{(l')*}\right] = \frac{1}{t}\mathbf{C}_{iq}^{(l)}\tilde{\mathbf{C}}_{jk}^{(l)}\mathbb{E}_{\mathbf{H}}[\mathbf{S}_{pi}]\delta_{l,l'} - \frac{1}{t}\sum_{n}\tilde{\mathbf{C}}_{jn}^{(l)}\mathbb{E}_{\mathbf{H}}\left[\mathbf{H}_{qk}^{(l')*}(\mathbf{S}\mathbf{H})_{pn}(\mathbf{C}^{(l)}\mathbf{S})_{ii}\right].$$

Summing over i, l and l' then leads to:

$$\mathbb{E}_{\mathbf{H}}\left[(\mathbf{S}\mathbf{H})_{pj}\mathbf{H}_{qk}^*\right] = \sum_{l}\frac{1}{t}\mathbb{E}_{\mathbf{H}}[(\mathbf{S}\mathbf{C}^{(l)})_{pq}]\tilde{\mathbf{C}}_{jk}^{(l)} - \sum_{n,l}\tilde{\mathbf{C}}_{jn}^{(l)}\mathbb{E}_{\mathbf{H}}\left[\mathbf{H}_{qk}^*(\mathbf{S}\mathbf{H})_{pn}\frac{1}{t}\mathrm{Tr}(\mathbf{S}\mathbf{C}^{(l)})\right].$$

To separate the terms under the last expectation, we denote $\eta_l = \frac{1}{t}\mathrm{Tr}(\mathbf{S}\mathbf{C}^{(l)}) = \alpha_l + \mathring{\eta}_l$, where $\alpha_l = \mathbb{E}_{\mathbf{H}}[\eta_l]$. We can then write $\mathbb{E}_{\mathbf{H}}\left[\mathbf{H}_{qk}^*(\mathbf{S}\mathbf{H})_{pn}\eta_l)\right] = \alpha_l\mathbb{E}_{\mathbf{H}}\left[\mathbf{H}_{qk}^*(\mathbf{S}\mathbf{H})_{pn}\right] + \mathbb{E}_{\mathbf{H}}\left[\mathbf{H}_{qk}^*(\mathbf{S}\mathbf{H})_{pn}\mathring{\eta}_l\right]$, hence

$$\mathbb{E}_{\mathbf{H}}\left[(\mathbf{S}\mathbf{H})_{pj}\mathbf{H}_{qk}^*\right] = \sum_{l}\frac{1}{t}\mathbb{E}_{\mathbf{H}}[(\mathbf{S}\mathbf{C}^{(l)})_{pq}]\tilde{\mathbf{C}}_{jk}^{(l)} - \sum_{n,l}\alpha_l\tilde{\mathbf{C}}_{jn}^{(l)}\mathbb{E}_{\mathbf{H}}\left[(\mathbf{S}\mathbf{H})_{pn}\mathbf{H}_{qk}^*\right] - \boldsymbol{\Xi}_{jk}^{(p,q)}, \tag{1.48}$$

where $\mathbf{\Xi}_{jk}^{(p,q)} = \sum_l \mathbb{E}_{\mathbf{H}}\big[\mathring{\eta}_l \mathbf{H}_{qk}^* (\mathbf{S}\mathbf{H}\tilde{\mathbf{C}}^{(l)T})_{pj}\big]$. We here notice the presence of $\mathbb{E}_{\mathbf{H}}\big[(\mathbf{S}\mathbf{H})_{p\_}\mathbf{H}_{qk}^*\big]$ on both sides of equation (1.48). Hence, let us denote $\Delta_{jk}^{(p,q)} = \mathbb{E}_{\mathbf{H}}\big[(\mathbf{S}\mathbf{H})_{pj}\mathbf{H}_{qk}^*\big]$. Then (1.48) becomes

$$\Delta_{jk}^{(p,q)} = \sum_l \frac{1}{t}\mathbb{E}_{\mathbf{H}}[(\mathbf{S}\mathbf{C}^{(l)})_{pq}]\tilde{\mathbf{C}}_{jk}^{(l)} - \Big(\sum_l \alpha_l \tilde{\mathbf{C}}^{(l)}\Delta^{(p,q)}\Big)_{jk} - \mathbf{\Xi}_{jk}^{(p,q)}.$$

Recalling that $\tilde{\mathbf{R}} = \big(\sigma^2\big(\mathbf{I}_t + \sum_l \alpha_l \tilde{\mathbf{C}}^{(l)}\big)\big)^{-1}$, this leads to

$$\Delta^{(p,q)} = \sigma^2 \sum_l \frac{1}{t}\mathbb{E}_{\mathbf{H}}[(\mathbf{S}\mathbf{C}^{(l)})_{pq}]\tilde{\mathbf{R}}\tilde{\mathbf{C}}^{(l)} - \sigma^2\tilde{\mathbf{R}}\mathbf{\Xi}^{(p,q)}.$$

Besides, noticing that $\mathbb{E}_{\mathbf{H}}[(\mathbf{S}\mathbf{H}\mathbf{H}^H)_{pq}] = \mathrm{Tr}(\Delta^{(p,q)})$ allows us to come back to the calculation of $\mathbb{E}_{\mathbf{H}}[\mathbf{S}_{pq}] = \frac{1}{\sigma^2}(\mathbf{I}_r - \mathbb{E}_{\mathbf{H}}[\mathbf{S}\mathbf{H}\mathbf{H}^H])_{pq}$:

$$\mathbb{E}_{\mathbf{H}}[\mathbf{S}_{pq}] = \frac{\delta_{p,q}}{\sigma^2} - \sum_l \tilde{\alpha}_l \mathbb{E}_{\mathbf{H}}[(\mathbf{S}\mathbf{C}^{(l)})_{pq}] + \mathrm{Tr}\left(\tilde{\mathbf{R}}\mathbf{\Xi}^{(p,q)}\right),$$

recalling from (1.20) that $\tilde{\alpha}_l = \frac{1}{t}\mathrm{Tr}\big(\tilde{\mathbf{R}}\tilde{\mathbf{C}}^{(l)}\big)$. Coming back to the definition of matrix $\mathbf{\Xi}^{(p,q)}$, we notice that $\mathrm{Tr}\big(\tilde{\mathbf{R}}\mathbf{\Xi}^{(p,q)}\big) = \sum_l \mathbb{E}_{\mathbf{H}}\big[\mathring{\eta}_l(\mathbf{S}\mathbf{H}\tilde{\mathbf{C}}^{(l)T}\tilde{\mathbf{R}}^T\mathbf{H}^H)_{pq}\big]$. Hence matrix $\mathbb{E}_{\mathbf{H}}[\mathbf{S}]$ can be written as

$$\mathbb{E}_{\mathbf{H}}[\mathbf{S}] = \frac{1}{\sigma^2}\mathbf{I}_r - \mathbb{E}_{\mathbf{H}}[\mathbf{S}]\sum_l \tilde{\alpha}_l \mathbf{C}^{(l)} + \sum_l \mathbb{E}_{\mathbf{H}}\left[\mathring{\eta}_l \mathbf{S}\mathbf{H}\tilde{\mathbf{C}}^{(l)T}\tilde{\mathbf{R}}^T\mathbf{H}^H\right].$$

And finally, $\mathbb{E}_{\mathbf{H}}[\mathbf{S}] = \mathbf{R} + \mathbf{\Upsilon}$, where we recall that $\mathbf{R} = \left(\sigma^2\left(\mathbf{I}_r + \sum_l \tilde{\alpha}_l \mathbf{C}^{(l)}\right)\right)^{-1}$ and where matrix $\mathbf{\Upsilon}$ is defined as

$$\mathbf{\Upsilon} = \sigma^2 \sum_l \mathbb{E}_{\mathbf{H}}\left[\mathring{\eta}_l \mathbf{S}\mathbf{H}\tilde{\mathbf{C}}^{(l)T}\tilde{\mathbf{R}}^T\mathbf{H}^H\right]\mathbf{R}. \tag{1.49}$$

To end Proposition 1 proof, we now need to prove that $\frac{1}{t}\mathrm{Tr}\left(\mathbf{\Upsilon}\mathbf{A}\right) = \mathcal{O}\left(\frac{1}{t^2}\right)$ for any uniformly bounded matrix $\mathbf{A}$. Let $\mathbf{A}$ be a $r \times r$ matrix uniformly bounded in r. Using (1.49),

$$\begin{aligned}\frac{1}{t}\mathrm{Tr}\left(\mathbf{\Upsilon}\mathbf{A}\right) &= \frac{\sigma^2}{t}\sum_l \mathbb{E}_{\mathbf{H}}\left[\mathring{\eta}_l \mathrm{Tr}\left(\mathbf{S}\mathbf{H}\tilde{\mathbf{C}}^{(l)T}\tilde{\mathbf{R}}^T\mathbf{H}^H\mathbf{R}\mathbf{A}\right)\right] \\ &= \frac{\sigma^2}{t}\sum_l \mathbb{E}_{\mathbf{H}}\left[\mathring{\eta}_l \overset{\circ}{\overbrace{\mathrm{Tr}(\mathbf{S}\mathbf{H}\tilde{\mathbf{C}}^{(l)T}\tilde{\mathbf{R}}^T\mathbf{H}^H\mathbf{R}\mathbf{A})}}\right].\end{aligned}$$

We can now bound $\frac{1}{t}\mathrm{Tr}\left(\mathbf{\Upsilon}\mathbf{A}\right)$ thanks to Cauchy-Schwartz inequality.

$$\begin{aligned}\left|\frac{1}{t}\mathrm{Tr}\left(\mathbf{\Upsilon}\mathbf{A}\right)\right| &\leq \frac{\sigma^2}{t}\sum_l \sqrt{\mathbb{E}_{\mathbf{H}}\left[\,|\mathring{\eta}_l|^2\,\right]\mathbb{E}_{\mathbf{H}}\left[\left|\overset{\circ}{\overbrace{\mathrm{Tr}(\mathbf{S}\mathbf{H}\tilde{\mathbf{C}}^{(l)T}\tilde{\mathbf{R}}^T\mathbf{H}^H\mathbf{R}\mathbf{A})}}\right|^2\right]} \\ &= \frac{\sigma^2}{t}\sum_l \sqrt{\mathrm{var}\left(\eta_l\right)\mathrm{var}\left(\mathrm{Tr}(\mathbf{S}\mathbf{H}\tilde{\mathbf{C}}^{(l)T}\tilde{\mathbf{R}}^T\mathbf{H}^H\mathbf{R}\mathbf{A})\right)},\end{aligned} \tag{1.50}$$

as $\mathbb{E}_{\mathbf{H}}\big[\,|\mathring{x}|^2\,\big] = \mathrm{var}\,(x)$ for any random variable x. We now prove that $\mathrm{var}(\eta_l) = \mathcal{O}\left(\frac{1}{t^2}\right)$. The Nash-Poincaré inequality (1.47) states that

$$\mathrm{var}(\eta_l) \leq \frac{1}{t} \sum_{i,j,m,n,k} \mathbf{C}^{(k)}_{im} \tilde{\mathbf{C}}^{(k)}_{jn} \mathbb{E}\Big[\frac{\partial \eta_l}{\partial \mathbf{H}^{(k)}_{ij}} \left(\frac{\partial \eta_l}{\partial \mathbf{H}^{(k)}_{mn}} \right)^* + \left(\frac{\partial \eta_l}{\partial \mathbf{H}^{(k)*}_{ij}} \right)^* \frac{\partial \eta_l}{\partial \mathbf{H}^{(k)*}_{mn}} \Big]. \tag{1.51}$$

As $\partial \mathbf{S}_{pq}/\partial \mathbf{H}^{(k)}_{ij} = -(\mathbf{S}(\partial \mathbf{S}^{-1}/\partial \mathbf{H}^{(k)}_{ij})\mathbf{S})_{pq} = -\mathbf{S}_{pi}(\mathbf{H}^H\mathbf{S})_{jq}$ the partial derivative $\partial \eta_l/\partial \mathbf{H}^{(k)}_{ij}$ can be written as

$$\begin{aligned} \frac{\partial \eta_l}{\partial \mathbf{H}^{(k)}_{ij}} &= \frac{1}{t} \mathrm{Tr}\Big(\frac{\partial \mathbf{S}}{\partial \mathbf{H}^{(k)}_{ij}} \mathbf{C}^{(l)} \Big) \\ &= \frac{1}{t} \sum_{p,q} \frac{\partial \mathbf{S}_{pq}}{\partial \mathbf{H}^{(k)}_{ij}} \mathbf{C}^{(l)}_{qp} \\ &= -\frac{1}{t} (\mathbf{H}^H \mathbf{S} \mathbf{C}^{(l)} \mathbf{S})_{ji}. \end{aligned}$$

Similarly we obtain $\partial \eta_l/\partial \mathbf{H}^{(k)*}_{ij} = -\frac{1}{t}(\mathbf{S}\mathbf{C}^{(l)}\mathbf{S}\mathbf{H})_{ij}$. Therefore (1.51) leads to

$$\begin{aligned} \mathrm{var}(\eta_l) \leq \frac{1}{t^3} \sum_k \mathbb{E}\Big[&\mathrm{Tr}\left((\mathbf{H}^H \mathbf{S} \mathbf{C}^{(l)} \mathbf{S}) \mathbf{C}^{(k)} (\mathbf{H}^H \mathbf{S} \mathbf{C}^{(l)} \mathbf{S})^H \tilde{\mathbf{C}}^{(k)T} \right) \\ &+ \mathrm{Tr}\left(\tilde{\mathbf{C}}^{(k)T} (\mathbf{S}\mathbf{C}^{(l)}\mathbf{S}\mathbf{H})^H \mathbf{C}^{(k)} (\mathbf{S}\mathbf{C}^{(l)}\mathbf{S}\mathbf{H}) \right) \Big]. \end{aligned} \tag{1.52}$$

Both traces in the right-hand side of (1.52) can be upper bounded thanks to the following inequality:

$$|\mathrm{Tr}(\mathbf{B}_1\mathbf{B}_2)| \leq \|\mathbf{B}_1\| \mathrm{Tr}\,\mathbf{B}_2,$$

where $\mathbf{B}_2$ is non-negative hermitian.

$$\begin{aligned} \mathrm{var}(\eta_l) &\leq \frac{2}{t^3} \|\mathbf{C}^{(l)}\|^2 \sum_k \|\mathbf{C}^{(k)}\| \, \mathbb{E}\left[\|\mathbf{S}\|^4 \mathrm{Tr}\left(\mathbf{H}\tilde{\mathbf{C}}^{(k)T}\mathbf{H}^H \right) \right] \\ &\leq \frac{2}{t^3} \|\mathbf{C}^{(l)}\|^2 \sum_k \|\mathbf{C}^{(k)}\| \|\tilde{\mathbf{C}}^{(k)}\| \, \mathbb{E}\left[\|\mathbf{S}\|^4 \mathrm{Tr}\left(\mathbf{H}\mathbf{H}^H \right) \right] \\ &\leq \frac{1}{t^2} \frac{2LC^4_{\sup}}{\sigma^8} \mathbb{E}\left[\frac{1}{t} \mathrm{Tr}\left(\mathbf{H}\mathbf{H}^H \right) \right], \end{aligned} \tag{1.53}$$

where the second inequality follows from $\|\mathbf{S}\| \leq \frac{1}{\sigma^2}$ and from the definition of $C_{\sup}$:

$$\begin{aligned} C_{\sup} &= \sup_t C_{\max} \\ &= \sup_t \left\{ \max_k \left\{ \|\mathbf{C}^{(k)}\|, \|\tilde{\mathbf{C}}^{(k)}\| \right\} \right\}. \end{aligned} \tag{1.54}$$

The hypotheses of Proposition 1 ensure that $C_{\sup} < +\infty$. We now prove that $\mathbb{E}\left[\frac{1}{t}\mathrm{Tr}\left(\mathbf{H}\mathbf{H}^H\right)\right] = \mathcal{O}(1)$. Using the fact that the channels $\mathbf{H}^{(l)}$ are independent and follow the Kronecker model, that is $\mathbb{E}_{\mathbf{H}}\left[\mathbf{H}_{ij}^{(k)}\mathbf{H}_{mn}^{(l)*}\right] = \delta_{k,l}\frac{1}{t}\mathbf{C}_{im}^{(l)}\tilde{\mathbf{C}}_{jn}^{(l)}$,

$$\begin{aligned}\mathbb{E}_{\mathbf{H}}\left[\frac{1}{t}\mathrm{Tr}\left(\mathbf{H}\mathbf{H}^H\right)\right] &= \frac{1}{t}\sum_{i,j,k,l}\mathbb{E}_{\mathbf{H}}\left[\mathbf{H}_{ij}^{(k)}\mathbf{H}_{ij}^{(l)*}\right] = \frac{1}{t^2}\sum_{i,j,l}\mathbf{C}_{ii}^{(l)}\tilde{\mathbf{C}}_{jj}^{(l)} \\ &= \frac{1}{t^2}\sum_{l}\mathrm{Tr}\,\mathbf{C}^{(l)}\mathrm{Tr}\,\tilde{\mathbf{C}}^{(l)} \leq \frac{r}{t}LC_{\sup}^2.\end{aligned}$$

We have therefore proved that $\mathbb{E}_{\mathbf{H}}\left[\frac{1}{t}\mathrm{Tr}\left(\mathbf{H}\mathbf{H}^H\right)\right] = \mathcal{O}(1)$. Coming back to (1.53) gives

$$\mathrm{var}(\eta_l) \leq \frac{1}{t^2}\left(\frac{r}{t}\frac{2C_{\sup}^6L^2}{\sigma^8}\right), \tag{1.55}$$

hence

$$\mathrm{var}(\eta_l) = \mathcal{O}\left(\frac{1}{t^2}\right). \tag{1.56}$$

We evaluate similarly the behavior of the second term of the right-hand side of (1.50) and we obtain

$$\mathrm{var}\big(\mathrm{Tr}(\mathbf{S}\mathbf{H}\tilde{\mathbf{C}}^{(l)T}\tilde{\mathbf{R}}^T\mathbf{H}^H\mathbf{R}\mathbf{A})\big) \leq \frac{k}{\sigma^{12}}\left(1+\frac{1}{\sigma^2}\right)\|\mathbf{A}\|^2, \tag{1.57}$$

where k does not depend on σ^2 nor on t. Therefore,

$$\mathrm{var}\big(\mathrm{Tr}(\mathbf{S}\mathbf{H}\tilde{\mathbf{C}}^{(l)T}\tilde{\mathbf{R}}^T\mathbf{H}^H\mathbf{R}\mathbf{A})\big) = \mathcal{O}(1). \tag{1.58}$$

Using (1.56) and (1.58) in (1.50), we eventually have:

$$\frac{1}{t}\mathrm{Tr}(\boldsymbol{\Upsilon}\mathbf{A}) = \mathcal{O}\left(\frac{1}{t^2}\right),$$

which completes the proof of Proposition 1.

Remark 1. *Note that using* (1.55) *and* (1.57) *in* (1.50) *leads to*

$$\frac{1}{t}\mathrm{Tr}(\boldsymbol{\Upsilon}\mathbf{A}) \leq \frac{1}{\sigma^8t^2}P\left(\frac{1}{\sigma^2}\right), \tag{1.59}$$

where P is a polynomial with real positive coefficients which do not depend on σ^2 nor on t.

1.C A refined large system approximation of $\mathbb{E}_{\mathbf{H}}[\mathrm{Tr}\,\mathbf{S}]$

We prove in this section Proposition 2, i.e. that, under the technical assumptions made in the Proposition statement,

$$\frac{1}{t}\mathrm{Tr}(\mathbf{RA}) = \frac{1}{t}\mathrm{Tr}(\mathbf{TA}) + \mathcal{O}\left(\frac{1}{t^2}\right)$$

for any $r \times r$ matrix $\mathbf{A}$ uniformly bounded in r.

We first note that the difference $\frac{1}{t}\mathrm{Tr}\left(\mathbf{RA}\right) - \frac{1}{t}\mathrm{Tr}\left(\mathbf{TA}\right)$ can be written as

$$\begin{aligned}\frac{1}{t}\mathrm{Tr}\left((\mathbf{R}-\mathbf{T})\mathbf{A}\right) &= \frac{1}{t}\mathrm{Tr}\left(\mathbf{R}\left(\mathbf{T}^{-1}-\mathbf{R}^{-1}\right)\mathbf{TA}\right)\\ &= -\frac{\sigma^2}{t}\sum_l(\tilde{\alpha}_l-\tilde{\delta}_l)\mathrm{Tr}(\mathbf{RC}^{(l)}\mathbf{TA}).\end{aligned} \tag{1.60}$$

As $\|\mathbf{T}\| \leq \frac{1}{\sigma^2}$ and $\|\mathbf{R}\| \leq \frac{1}{\sigma^2}$, equation (1.60) yields

$$\frac{1}{t}\left|\mathrm{Tr}\left((\mathbf{R}-\mathbf{T})\mathbf{A}\right)\right| \leq \frac{r}{t}\frac{C_{\sup}\|\mathbf{A}\|}{\sigma^2}\sum_l\left|\tilde{\alpha}_l-\tilde{\delta}_l\right|, \tag{1.61}$$

where $C_{\sup} < +\infty$ is defined by (1.54). We derive similarly the difference $\frac{1}{t}\mathrm{Tr}(\tilde{\mathbf{R}}\tilde{\mathbf{A}}) - \frac{1}{t}\mathrm{Tr}(\tilde{\mathbf{T}}\tilde{\mathbf{A}})$ for any $t \times t$ matrix $\tilde{\mathbf{A}}$ uniformly bounded in t.

$$\frac{1}{t}\left|\mathrm{Tr}\left(\left(\tilde{\mathbf{R}}-\tilde{\mathbf{T}}\right)\tilde{\mathbf{A}}\right)\right| \leq \frac{C_{\sup}\|\tilde{\mathbf{A}}\|}{\sigma^2}\sum_l|\alpha_l-\delta_l| \tag{1.62}$$

Taking $\mathbf{A} = \mathbf{C}^{(k)}$ in (1.61), $\tilde{\mathbf{A}} = \tilde{\mathbf{C}}^{(k)}$ in (1.62) and using Proposition 1 gives

$$\left|\alpha_k-\delta_k\right| \leq \frac{r}{t}\frac{C_{\sup}^2}{\sigma^2}\sum_l\left|\tilde{\alpha}_l-\tilde{\delta}_l\right| + \mathcal{O}\left(\frac{1}{t^2}\right), \tag{1.63}$$

$$\left|\tilde{\alpha}_k-\tilde{\delta}_k\right| \leq \frac{C_{\sup}^2}{\sigma^2}\sum_l\left|\alpha_l-\delta_l\right|, \tag{1.64}$$

which leads to

$$\left(1-\frac{r}{t}\frac{C_{\sup}^4L^2}{\sigma^4}\right)\sum_k\left|\alpha_k-\delta_k\right| \leq \mathcal{O}\left(\frac{1}{t^2}\right).$$

Therefore it is clear that there exists σ_0^2 such that $\left|\alpha_k-\delta_k\right| = \mathcal{O}\left(\frac{1}{t^2}\right)$ for $\sigma^2 > \sigma_0^2$ for any $k \in \{1,\ldots,L\}$. In particular, $\left|\alpha_k-\delta_k\right| \xrightarrow{t\to\infty} 0$ for $\sigma^2 > \sigma_0^2$. We now extend this result to any $\sigma^2 > 0$. To this end, similarly to Appendix 1.A, it is useful to consider α_l and δ_l as functions of the parameter $(-\sigma^2) \in \mathbb{R}^-$ and to extend their domain of validity from $\mathbb{R}^-$ to $\mathbb{C}-\mathbb{R}^+$ in order to use the results about Stieltjès transforms. The function $\delta_l(z)$ then corresponds to the function $\psi_l(z)$ of Appendix 1.A and therefore

belongs to $\mathcal{S}(\mathbb{R}^+)$ with an associated measure of mass $\frac{1}{t}\mathrm{Tr}\,\mathbf{C}^{(l)}$, for $l = 1, \ldots, L$. It is easy to check that function $\alpha_l(z)$ also belongs to $\mathcal{S}(\mathbb{R}^+)$ with an associated measure of mass $\frac{1}{t}\mathrm{Tr}\,\mathbf{C}^{(l)}$ for any $l \in \{1, \ldots, L\}$. Hence, by Proposition 9 (v), we can upper bound the Stieltjès transforms $\alpha_l(z)$ and $\delta_l(z)$ on $\mathbb{C} - \mathbb{R}^+$, yielding:

$$|\alpha_l(z) - \delta_l(z)| \leq 2\frac{\frac{1}{t}\mathrm{Tr}\,\mathbf{C}^{(l)}}{d(z, \mathbb{R}^+)} \leq 2\frac{\frac{r}{t}C_{\sup}}{d(z, \mathbb{R}^+)}.$$

The $(\alpha_l(z) - \delta_l(z))_{t\in\mathbb{N}}$ are thus bounded on any compact set included in $\mathbb{C} - \mathbb{R}^+$, uniformly in t. Moreover $(\alpha_l(z) - \delta_l(z))_{t\in\mathbb{N}}$ is a family of analytic functions. Using Montel's theorem similarly to Appendix 1.A, we obtain that $\left|\alpha_l(z) - \delta_l(z)\right| \xrightarrow{t\to\infty} 0$ on $\mathbb{C} - \mathbb{R}^+$ for any $l \in \{1, \ldots, L\}$, thus in particular

$$\left|\alpha_l - \delta_l\right| \xrightarrow{t\to\infty} 0 \tag{1.65}$$

for any $\sigma^2 > 0$, $l \in \{1, \ldots, L\}$. And (1.64) then yields

$$\left|\tilde{\alpha}_l - \tilde{\delta}_l\right| \xrightarrow{t\to\infty} 0 \tag{1.66}$$

for any $\sigma^2 > 0$, $l \in \{1, \ldots, L\}$. Using (1.66) in (1.61) and (1.65) in (1.62) gives

$$\frac{1}{t}\mathrm{Tr}\left(\mathbf{A}(\mathbf{R} - \mathbf{T})\right) \xrightarrow{t\to\infty} 0, \tag{1.67}$$

$$\frac{1}{t}\mathrm{Tr}\left(\tilde{\mathbf{A}}(\tilde{\mathbf{R}} - \tilde{\mathbf{T}})\right) \xrightarrow{t\to\infty} 0. \tag{1.68}$$

We now refine (1.67) and (1.68) to prove that these two traces are $\mathcal{O}\left(\frac{1}{t^2}\right)$. Taking $\mathbf{A} = \mathbf{C}^{(l)}$ in (1.60) leads to $\alpha_k - \delta_k = \frac{\sigma^2}{t}\sum_l(\tilde{\delta}_l - \tilde{\alpha}_l)\mathrm{Tr}\left(\mathbf{C}^{(l)}\mathbf{T}\mathbf{C}^{(k)}\mathbf{R}\right) + \frac{1}{t}\mathrm{Tr}\left(\mathbf{C}^{(k)}\boldsymbol{\Upsilon}\right)$, where $\boldsymbol{\Upsilon} = \mathbb{E}_{\mathbf{H}}[\mathbf{S}] - \mathbf{R}$, and similarly $\tilde{\delta}_k - \tilde{\alpha}_k = \frac{\sigma^2}{t}\sum_l(\alpha_l - \delta_l)\mathrm{Tr}\big(\tilde{\mathbf{C}}^{(l)}\tilde{\mathbf{T}}\tilde{\mathbf{C}}^{(k)}\tilde{\mathbf{R}}\big)$. We can rewrite these two equalities under the following matrix form:

$$\left(\mathbf{I}_{2L} - \mathbf{N}(\mathbf{R}, \mathbf{T}, \tilde{\mathbf{R}}, \tilde{\mathbf{T}})\right)\begin{bmatrix}\boldsymbol{\alpha} - \boldsymbol{\delta} \\ \tilde{\boldsymbol{\delta}} - \tilde{\boldsymbol{\alpha}}\end{bmatrix} = \begin{bmatrix}\boldsymbol{\varepsilon} \\ \mathbf{0}\end{bmatrix}, \tag{1.69}$$

where $\boldsymbol{\varepsilon}$ is a $L \times 1$ vector whose entries defined by $\boldsymbol{\varepsilon}_k = \frac{1}{t}\mathrm{Tr}\left(\mathbf{C}^{(k)}\boldsymbol{\Upsilon}\right)$ verify $\boldsymbol{\varepsilon}_k = \mathcal{O}\left(\frac{1}{t^2}\right)$, $k = 1, \ldots, L$, by Proposition 1, and where matrix $\mathbf{N}(\mathbf{R}, \mathbf{T}, \tilde{\mathbf{R}}, \tilde{\mathbf{T}})$ is defined by

$$\mathbf{N}(\mathbf{R}, \mathbf{T}, \tilde{\mathbf{R}}, \tilde{\mathbf{T}}) = \sigma^2\begin{bmatrix}\mathbf{0} & \mathbf{B}(\mathbf{R}, \mathbf{T}) \\ \tilde{\mathbf{B}}(\tilde{\mathbf{R}}, \tilde{\mathbf{T}}) & \mathbf{0}\end{bmatrix}, \tag{1.70}$$

where matrices $\mathbf{B}(\mathbf{R}, \mathbf{T})$ and $\tilde{\mathbf{B}}(\tilde{\mathbf{R}}, \tilde{\mathbf{T}})$ are $L \times L$ matrices whose entries are defined by $\mathbf{B}_{kl}(\mathbf{R}, \mathbf{T}) = \frac{1}{t}\mathrm{Tr}\left(\mathbf{C}^{(l)}\mathbf{T}\mathbf{C}^{(k)}\mathbf{R}\right)$ and $\tilde{\mathbf{B}}_{kl}(\tilde{\mathbf{R}}, \tilde{\mathbf{T}}) = \frac{1}{t}\mathrm{Tr}\big(\tilde{\mathbf{C}}^{(l)}\tilde{\mathbf{T}}\tilde{\mathbf{C}}^{(k)}\tilde{\mathbf{R}}\big)$. Besides, taking $\mathbf{A} = \mathbf{C}^{(l)}\mathbf{T}\mathbf{C}^{(k)}$ in (1.67) and $\tilde{\mathbf{A}} = \tilde{\mathbf{C}}^{(l)}\tilde{\mathbf{T}}\tilde{\mathbf{C}}^{(k)}$ in (1.68) leads to

$$\begin{cases}\mathbf{B}_{kl}(\mathbf{R}, \mathbf{T}) \xrightarrow{t\to\infty} \frac{1}{t}\mathrm{Tr}\left(\mathbf{C}^{(l)}\mathbf{T}\mathbf{C}^{(k)}\mathbf{T}\right), \\ \tilde{\mathbf{B}}_{kl}(\tilde{\mathbf{R}}, \tilde{\mathbf{T}}) \xrightarrow{t\to\infty} \frac{1}{t}\mathrm{Tr}\left(\tilde{\mathbf{C}}^{(l)}\tilde{\mathbf{T}}\tilde{\mathbf{C}}^{(k)}\tilde{\mathbf{T}}\right).\end{cases} \tag{1.71}$$

We now introduce the following lemma:

Lemma 1. *Let* $\mathbf{T}$, $\tilde{\mathbf{T}}$ *be the matrices defined by* (1.11) *and* (1.12) *with* $(\boldsymbol{\delta}, \tilde{\boldsymbol{\delta}})$ *verifying the canonical equation (1.9) with* $\mathbf{Q} = \mathbf{I}_t$. *Let* $\mathbf{A}(\mathbf{T})$ *and* $\tilde{\mathbf{A}}(\mathbf{T})$ *be the* $L \times L$ *matrices whose entries are defined by* $\mathbf{A}_{kl}(\mathbf{T}) = \frac{1}{t}\mathrm{Tr}\left(\mathbf{C}^{(k)}\mathbf{T}\mathbf{C}^{(l)}\mathbf{T}\right)$ *and* $\tilde{\mathbf{A}}_{kl}(\tilde{\mathbf{T}}) = \frac{1}{t}\mathrm{Tr}(\tilde{\mathbf{C}}^{(k)}\tilde{\mathbf{T}}\tilde{\mathbf{C}}^{(l)}\tilde{\mathbf{T}})$ *and* $\mathbf{M}(\mathbf{T}, \tilde{\mathbf{T}})$ *the matrix defined by*

$$\mathbf{M}(\mathbf{T}, \tilde{\mathbf{T}}) = \sigma^2 \begin{bmatrix} 0 & \mathbf{A}(\mathbf{T}) \\ \tilde{\mathbf{A}}(\tilde{\mathbf{T}}) & 0 \end{bmatrix}.$$

Assume that, for every $l \in \{1, \ldots, L\}$, $\sup_t \|\mathbf{C}^{(l)}\| < +\infty$, $\sup_t \|\tilde{\mathbf{C}}^{(l)}\| < +\infty$, $\inf_t \left(\frac{1}{t}\mathrm{Tr}\,\mathbf{C}^{(l)}\right) > 0$ *and* $\inf_t \left(\frac{1}{t}\mathrm{Tr}\,\tilde{\mathbf{C}}^{(l)}\right) > 0$. *Then there exists* $k_0 > 0$ *and* $k_1 < \infty$ *both independent of* σ^2 *such that*

(i) $\sup_t \left[\rho\left(\mathbf{M}\right)\right] \leq 1 - \frac{k_0\sigma^4}{(\sigma^2+k_1)^2} < 1$,

(ii) $\sup_t \left[\rho\left(\sigma^4 \tilde{\mathbf{A}}(\tilde{\mathbf{T}})\mathbf{A}(\mathbf{T})\right)\right] \leq \left(1 - \frac{k_0\sigma^4}{(\sigma^2+k_1)^2}\right)^2 < 1$,

(iii) $\sup_t \left[\left|\!\left|\!\left| (\mathbf{I}_{2L} - \mathbf{M}(\mathbf{T}, \tilde{\mathbf{T}}))^{-1} \right|\!\right|\!\right|_\infty \right] \leq \frac{(\sigma^2+k_1)^2}{k_0\sigma^4}$,

where $\left|\!\left|\!\left| \cdot \right|\!\right|\!\right|_\infty$ *is the max-row* ℓ_1 *norm defined by* $\left|\!\left|\!\left| \mathbf{P} \right|\!\right|\!\right|_\infty = \max_{j\in\{1,\ldots,M\}} \sum_{k=1}^N |\mathbf{P}_{jk}|$ *for a* $M \times N$ *matrix* $\mathbf{P}$.

Proof: Using the expression of $\mathbf{T}^{-1} = \sigma^2(\mathbf{I}_r + \sum_k \tilde{\delta}_k \mathbf{C}^{(k)})$, δ_l can be written as:

$$\begin{aligned}\delta_l &= \frac{1}{t}\mathrm{Tr}(\mathbf{C}^{(l)}\mathbf{T}\mathbf{T}^{-1}\mathbf{T}) \\ &= \frac{\sigma^2}{t}\mathrm{Tr}(\mathbf{C}^{(l)}\mathbf{T}\mathbf{T}) + \frac{\sigma^2}{t}\sum_{k=1}^L \tilde{\delta}_k \mathrm{Tr}(\mathbf{C}^{(l)}\mathbf{T}\mathbf{C}^{(k)}\mathbf{T}).\end{aligned}$$

Similarly $\tilde{\delta}_l$ verifies

$$\tilde{\delta}_l = \frac{\sigma^2}{t}\mathrm{Tr}\big(\tilde{\mathbf{C}}^{(l)}\tilde{\mathbf{T}}\tilde{\mathbf{T}}\big) + \frac{\sigma^2}{t}\sum_k \delta_k \mathrm{Tr}\big(\tilde{\mathbf{C}}^{(l)}\tilde{\mathbf{T}}\tilde{\mathbf{C}}^{(k)}\tilde{\mathbf{T}}\big).$$

Thus,

$$\begin{bmatrix}\boldsymbol{\delta} \\ \tilde{\boldsymbol{\delta}}\end{bmatrix} = \sigma^2 \begin{bmatrix} 0 & \mathbf{A}(\mathbf{T}) \\ \tilde{\mathbf{A}}(\tilde{\mathbf{T}}) & 0 \end{bmatrix} \begin{bmatrix}\boldsymbol{\delta} \\ \tilde{\boldsymbol{\delta}}\end{bmatrix} + \begin{bmatrix}\mathbf{w} \\ \tilde{\mathbf{w}}\end{bmatrix},$$

where $\mathbf{w}$ and $\tilde{\mathbf{w}}$ are $L \times 1$ vectors such that $\mathbf{w}_l = \frac{\sigma^2}{t}\mathrm{Tr}(\mathbf{C}^{(l)}\mathbf{T}\mathbf{T})$ and $\tilde{\mathbf{w}}_l = \frac{\sigma^2}{t}\mathrm{Tr}(\tilde{\mathbf{C}}^{(l)}\tilde{\mathbf{T}}\tilde{\mathbf{T}})$. This equality is of the form $\mathbf{u} = \mathbf{M}(\mathbf{T}, \tilde{\mathbf{T}})\mathbf{u} + \mathbf{v}$, with $\mathbf{u} = \left[\boldsymbol{\delta}^T, \tilde{\boldsymbol{\delta}}^T\right]^T$ and $\mathbf{v} = \left[\mathbf{w}^T, \tilde{\mathbf{w}}^T\right]^T$, the entries of $\mathbf{u}$ and $\mathbf{v}$ being positive, and the entries of $\mathbf{M}(\mathbf{T}, \tilde{\mathbf{T}})$ non-negative. A direct application of Corollary 8.1.29 of [71] then implies $\rho(\mathbf{M}(\mathbf{T}, \tilde{\mathbf{T}})) \leq 1 - \frac{\min \mathbf{v}_l}{\max \mathbf{u}_l}$.

We first consider $\sup_t \left\{ \max \mathbf{u}_l \right\}$. As $\mathbf{u} = \left[\boldsymbol{\delta}^T, \tilde{\boldsymbol{\delta}}^T\right]^T$ we need to upper bound δ_k and $\tilde{\delta}_k$. As $\|\mathbf{T}\| \leq \frac{1}{\sigma^2}$ and $\|\mathbf{C}^{(l)}\| \leq C_{\sup}$ we have

$$\delta_k = \frac{1}{t}\mathrm{Tr}\left(\mathbf{C}^{(k)}\mathbf{T}\right) \leq \frac{r}{\sigma^2 t} C_{\sup}. \tag{1.72}$$

Similarly, as $\|\tilde{\mathbf{T}}\| \leq \frac{1}{\sigma^2}$ and $\|\tilde{\mathbf{C}}^{(l)}\| \leq C_{\text{sup}}$,

$$\tilde{\delta}_k = \frac{1}{t}\text{Tr}\left(\tilde{\mathbf{C}}^{(k)}\tilde{\mathbf{T}}\right) \leq \frac{1}{\sigma^2}C_{\text{sup}}. \tag{1.73}$$

As $t/r \xrightarrow{t\to\infty} c > 0$ we have that $\sup_t [r/t] < +\infty$. Therefore $\sup_t \{\max \mathbf{u}_l\} \leq \frac{\lambda_0}{\sigma^2} < +\infty$, where $\lambda_0 = C_{\text{sup}} \max\{1, \sup_t [r/t]\}$.

We now consider $\inf_t \{\min_l \mathbf{v}_l\}$. As $\min_l \mathbf{v}_l = \min_k \left\{\frac{\sigma^2}{t}\text{Tr}(\mathbf{C}^{(k)}\mathbf{T}\mathbf{T}), \frac{\sigma^2}{t}\text{Tr}(\tilde{\mathbf{C}}^{(k)}\tilde{\mathbf{T}}\tilde{\mathbf{T}})\right\}$, we need to lower bound $\frac{\sigma^2}{t}\text{Tr}(\mathbf{C}^{(k)}\mathbf{T}\mathbf{T})$ and $\frac{\sigma^2}{t}\text{Tr}(\tilde{\mathbf{C}}^{(k)}\tilde{\mathbf{T}}\tilde{\mathbf{T}})$. We use the Cauchy-Schwarz inequality:

$$|\text{Tr}(\mathbf{A}\mathbf{B})| \leq \sqrt{\text{Tr}(\mathbf{A}\mathbf{A}^H)}\sqrt{\text{Tr}(\mathbf{B}\mathbf{B}^H)}. \tag{1.74}$$

Taking $\mathbf{A} = \left(\mathbf{C}^{(l)}\right)^{1/2}\mathbf{T}$ and $\mathbf{B} = \left(\mathbf{C}^{(l)}\right)^{1/2}$ in (1.74) leads to

$$\frac{\sigma^2}{t}\text{Tr}\left(\mathbf{C}^{(l)}\mathbf{T}\mathbf{T}\right) \geq \frac{\sigma^2\left(\frac{1}{t}\text{Tr}\left(\mathbf{C}^{(l)}\mathbf{T}\right)\right)^2}{\frac{1}{t}\text{Tr}\,\mathbf{C}^{(l)}} = \frac{\sigma^2\delta_l^2}{\frac{1}{t}\text{Tr}\,\mathbf{C}^{(l)}}. \tag{1.75}$$

We now need to lower bound δ_l. Using again inequality (1.74) with $\mathbf{A} = \left(\mathbf{C}^{(l)}\right)^{1/2}\mathbf{T}^{1/2}$ and $\mathbf{B} = \mathbf{T}^{-1/2}\left(\mathbf{C}^{(l)}\right)^{1/2}$ yields

$$\delta_l = \frac{1}{t}\text{Tr}\left(\mathbf{C}^{(l)}\mathbf{T}\right) \geq \frac{\left(\frac{1}{t}\text{Tr}\,\mathbf{C}^{(l)}\right)^2}{\frac{1}{t}\text{Tr}\left(\mathbf{C}^{(l)}\mathbf{T}^{-1}\right)}. \tag{1.76}$$

Thanks to (1.73), $\|\mathbf{T}^{-1}\| = \|\sigma^2(\mathbf{I}_r + \sum_l \tilde{\delta}_l\mathbf{C}^{(l)})\| \leq \sigma^2 + LC_{\text{sup}}^2$. Hence (1.76) leads to

$$\delta_l \geq \frac{\frac{1}{t}\text{Tr}\,\mathbf{C}^{(l)}}{\|\mathbf{T}^{-1}\|} \geq \frac{\frac{1}{t}\text{Tr}\,\mathbf{C}^{(l)}}{\sigma^2 + LC_{\text{sup}}^2}. \tag{1.77}$$

Eventually, using (1.77) in (1.75) gives

$$\frac{\sigma^2}{t}\text{Tr}\left(\mathbf{C}^{(l)}\mathbf{T}\mathbf{T}\right) \geq \frac{\sigma^2\frac{1}{t}\text{Tr}\,\mathbf{C}^{(l)}}{\left(\sigma^2 + LC_{\text{sup}}^2\right)^2}. \tag{1.78}$$

Similarly, we prove that

$$\frac{\sigma^2}{t}\text{Tr}\left(\tilde{\mathbf{C}}^{(l)}\tilde{\mathbf{T}}\tilde{\mathbf{T}}\right) \geq \frac{\sigma^2\frac{1}{t}\text{Tr}\,\tilde{\mathbf{C}}^{(l)}}{\left(\sigma^2 + \frac{r}{t}LC_{\text{sup}}^2\right)^2}.$$

Therefore $\inf_t\left\{\min_l \mathbf{v}_l\right\} \geq \frac{\sigma^2\lambda_1}{(\sigma^2+k_1)^2}$, where $\lambda_1 = \min_l\left\{\inf_t\left[\frac{1}{t}\text{Tr}\,\mathbf{C}^{(l)}\right], \inf_t\left[\frac{1}{t}\text{Tr}\,\tilde{\mathbf{C}}^{(l)}\right]\right\} > 0$ and $k_1 = LC_{\text{sup}}^2\max\{1, \inf_t[r/t]\} = LC_{\text{sup}}\lambda_0 < +\infty$. Noting $k_0 = \frac{\lambda_1}{\lambda_0} > 0$ we can now conclude about statement (i) of the lemma:

$$\begin{aligned}\sup_t \rho(\mathbf{M}(\mathbf{T}, \tilde{\mathbf{T}})) &\leq 1 - \frac{\inf_t(\min_l \mathbf{v}_l)}{\sup_t(\max_l \mathbf{u}_l)} \\ &\leq 1 - \frac{k_0\sigma^4}{(\sigma^2 + k_1)^2}.\end{aligned}$$

As for statement (ii) of the lemma, we note that $\left|\mathbf{M}(\mathbf{T},\tilde{\mathbf{T}}) - \lambda\mathbf{I}_{2L}\right| = \left|\sigma^4\tilde{\mathbf{A}}(\tilde{\mathbf{T}})\mathbf{A}(\mathbf{T}) - \lambda^2\mathbf{I}_L\right|$. Hence

$$\begin{aligned}\rho(\sigma^4\tilde{\mathbf{A}}(\tilde{\mathbf{T}})\mathbf{A}(\mathbf{T})) &= \Big(\rho(\mathbf{M}(\mathbf{T},\tilde{\mathbf{T}}))\Big)^2 \\ &\leq \big(1 - \frac{k_0\sigma^4}{(\sigma^2+k_1)^2}\big)^2 < 1.\end{aligned}$$

Concerning statement (iii), the proof is the same as in [78, Lemma 5.2]. Nonetheless we provide it here for the sake of completeness. As $\rho(\mathbf{M}(\mathbf{T},\tilde{\mathbf{T}})) < 1$, the series $\sum_{k\in\mathbb{N}}\mathbf{M}(\mathbf{T},\tilde{\mathbf{T}})^k$ converges, matrix $\mathbf{I}_{2L} - \mathbf{M}(\mathbf{T},\tilde{\mathbf{T}})$ is invertible and its inverse can be written as $\big(\mathbf{I}_{2L} - \mathbf{M}(\mathbf{T},\tilde{\mathbf{T}})\big)^{-1} = \sum_{k\in\mathbb{N}}\mathbf{M}(\mathbf{T},\tilde{\mathbf{T}})^k$. Therefore the entries of $\big(\mathbf{I}_{2L} - \mathbf{M}(\mathbf{T},\tilde{\mathbf{T}})\big)^{-1}$ are non-negative. Hence,

$$\begin{aligned}\mathbf{u}_k &= \sum_{l=1}^{2L}\Big[(\mathbf{I}_{2L} - \mathbf{M}(\mathbf{T},\tilde{\mathbf{T}}))^{-1}\Big]_{kl}\mathbf{v}_l \\ &\geq \min_l(\mathbf{v}_l)\sum_{l=1}^{2L}\Big[(\mathbf{I}_{2L} - \mathbf{M}(\mathbf{T},\tilde{\mathbf{T}}))^{-1}\Big]_{kl}.\end{aligned}$$

Therefore $\max_k\sum_{l=1}^{2L}\left[\big(\mathbf{I}_{2L} - \mathbf{M}(\mathbf{T},\tilde{\mathbf{T}})\big)^{-1}\right]_{kl} \leq \frac{\max_l(\mathbf{u}_l)}{\min_l(\mathbf{v}_l)}$ and it eventually follows that:

$$\begin{aligned}\sup_t\left[\left\|\left|\left(\mathbf{I}_{2L} - \mathbf{M}(\mathbf{T},\tilde{\mathbf{T}})\right)^{-1}\right|\right\|_\infty\right] &\leq \frac{\sup_t(\max_l\mathbf{u}_l)}{\inf_t(\min_l\mathbf{v}_l)} \\ &\leq \frac{(\sigma^2+k_1)^2}{k_0\sigma^4}.\end{aligned}$$

□

Remark 2. *Lemma 1* (ii) *is used in the proof of Theorem 1 for the uniqueness of solutions to* (1.9)*, but we took care not to use any consequences of this uniqueness in the proof above; this proof only requires the existence of solutions to* (1.9)*.*

Remark 3. *Unfortunately assumptions* $\inf_t\left(\frac{1}{t}\operatorname{Tr}\mathbf{C}^{(l)}\right) > 0$ *and* $\inf_t\left(\frac{1}{t}\operatorname{Tr}\tilde{\mathbf{C}}^{(l)}\right) > 0$ *made in Lemma 1 cannot be restrained, as* $\frac{1}{t}\operatorname{Tr}\big(\mathbf{C}^{(l)}\mathbf{T}\mathbf{T}\big) \leq \frac{1}{\sigma^4}\big(\frac{1}{t}\operatorname{Tr}\mathbf{C}^{(l)}\big)$ *and similarly* $\frac{1}{t}\operatorname{Tr}\big(\tilde{\mathbf{C}}^{(l)}\tilde{\mathbf{T}}\tilde{\mathbf{T}}\big) \leq \frac{1}{\sigma^4}\big(\frac{1}{t}\operatorname{Tr}\tilde{\mathbf{C}}^{(l)}\big)$.

Equation (1.71) shows that the entries of $\mathbf{B}(\mathbf{R},\mathbf{T})$ and $\tilde{\mathbf{B}}(\tilde{\mathbf{R}},\tilde{\mathbf{T}})$ respectively converge to the entries of $\mathbf{A}(\mathbf{T})$ and $\tilde{\mathbf{A}}(\tilde{\mathbf{T}})$. Hence there exists t_0 such that, for $t > t_0$,

- the matrix $\mathbf{I}_{2L} - \mathbf{N}(\mathbf{R},\mathbf{T},\tilde{\mathbf{R}},\tilde{\mathbf{T}})$ is invertible,
- $\sup_t\left[\left\|\left|(\mathbf{I}_{2L} - \mathbf{N}(\mathbf{R},\mathbf{T},\tilde{\mathbf{R}},\tilde{\mathbf{T}}))^{-1}\right|\right\|_\infty\right] \leq \frac{2(\sigma^2+k_1)^2}{k_0\sigma^4}$.

Then, for $t > t_0$, (1.69) yields

$$\begin{bmatrix} \boldsymbol{\alpha} - \boldsymbol{\delta} \\ \tilde{\boldsymbol{\delta}} - \tilde{\boldsymbol{\alpha}} \end{bmatrix} = \left(\mathbf{I}_{2L} - \mathbf{N}(\mathbf{R}, \mathbf{T}, \tilde{\mathbf{R}}, \tilde{\mathbf{T}}) \right)^{-1} \begin{bmatrix} \boldsymbol{\varepsilon} \\ \mathbf{0} \end{bmatrix}. \tag{1.79}$$

Thanks to (1.79) we can now upper bound all the $\alpha_l - \delta_l$ and $\tilde{\delta}_l - \tilde{\alpha}_l$.

$$\begin{aligned} \max_l \left\{ \left| \alpha_l - \delta_l \right|, \left| \tilde{\alpha}_l - \tilde{\delta}_l \right| \right\} &\leq \left\| \left(\mathbf{I}_{2L} - \mathbf{N}(\mathbf{R}, \mathbf{T}, \tilde{\mathbf{R}}, \tilde{\mathbf{T}}) \right)^{-1} \right\|_\infty \max_k |\boldsymbol{\varepsilon}_k| \\ &\leq \frac{2(\sigma^2 + k_1)^2}{k_0 \sigma^4} \max_k |\boldsymbol{\varepsilon}_k| \end{aligned}$$

As $\boldsymbol{\varepsilon}_l = \operatorname{Tr}\left(\mathbf{C}^{(l)} \boldsymbol{\Upsilon} \right) = \mathcal{O}\left(\frac{1}{t^2} \right)$ for $l = 1, \ldots, L$, we eventually have that

$$\tilde{\alpha}_l - \tilde{\delta}_l = \mathcal{O}\left(\frac{1}{t^2} \right). \tag{1.80}$$

Using (1.80) in (1.61) completes the proof of Proposition 2.

1.D Integrability of $\mathbb{E}_{\mathbf{H}}\left[\operatorname{Tr}\left(\mathbf{T} - \mathbf{S} \right) \right]$

We prove in this section Proposition 3, i.e. the integrability of $\mathbb{E}_{\mathbf{H}}\left[\operatorname{Tr}\left(\mathbf{T} - \mathbf{S} \right) \right]$.

We first consider $\mathbb{E}_{\mathbf{H}}\left[\operatorname{Tr}\left(\mathbf{R} - \mathbf{S} \right) \right]$, which is equal to $\operatorname{Tr} \boldsymbol{\Upsilon}$ by Proposition 1. As noted in Remark 1 of Appendix 1.B, we have $\left| \frac{1}{t} \operatorname{Tr}(\boldsymbol{\Upsilon} \mathbf{A}) \right| \leq \frac{1}{\sigma^8 t^2} P_0\left(\frac{1}{\sigma^2} \right)$, where P_0 is a polynomial with real positive coefficients which do not depend on σ^2 nor on t. Therefore

$$\left| \mathbb{E}_{\mathbf{H}}\left[\operatorname{Tr}\left(\mathbf{R} - \mathbf{S} \right) \right] \right| \leq \frac{P_0\left(\frac{1}{\sigma^2} \right)}{\sigma^8 t}. \tag{1.81}$$

We now consider $\operatorname{Tr}\left(\mathbf{R} - \mathbf{T} \right)$. We showed in Appendix 1.C that there exists t_0 such that, for $t > t_0$, $\mathbf{I}_{2L} - \mathbf{N}(\mathbf{R}, \mathbf{T}, \tilde{\mathbf{R}}, \tilde{\mathbf{T}})$ is invertible and such that $\left\| \left(\mathbf{I}_{2L} - \mathbf{N}(\mathbf{R}, \mathbf{T}, \tilde{\mathbf{R}}, \tilde{\mathbf{T}}) \right)^{-1} \right\|_\infty \leq \frac{2(\sigma^2 + k_1)^2}{k_0 \sigma^4}$, where k_0 and k_1 are given by Lemma 1. Equation (1.69) then implies

$$\begin{aligned} \left| \tilde{\alpha}_l - \tilde{\delta}_l \right| &\leq \left\| \left(\mathbf{I}_{2L} - \mathbf{N}(\mathbf{R}, \mathbf{T}, \tilde{\mathbf{R}}, \tilde{\mathbf{T}}) \right)^{-1} \right\|_\infty \max_k |\boldsymbol{\varepsilon}_k| \\ &\leq \frac{2(\sigma^2 + k_1)^2}{k_0 \sigma^4} \max_k |\boldsymbol{\varepsilon}_k|, \end{aligned}$$

where $\boldsymbol{\varepsilon}_k = \operatorname{Tr}\left(\mathbf{C}^{(k)} \boldsymbol{\Upsilon} \right)$. Besides, Remark 1 of Appendix 1.B ensures that $|\boldsymbol{\varepsilon}_k| \leq \frac{1}{\sigma^8 t^2} P_1\left(\frac{1}{\sigma^2} \right)$, where P_1 is a polynomial with real positive coefficients which do not depend on σ^2 nor on t. Hence, for $t > t_0$,

$$\left| \tilde{\alpha}_l - \tilde{\delta}_l \right| \leq \frac{P_1\left(\frac{1}{\sigma^2} \right)}{\sigma^8 t^2} \frac{2(\sigma^2 + k_1)^2}{k_0 \sigma^4} \tag{1.82}$$

for any $l \in \{1, \dots, L\}$. Using (1.82) in (1.61) with $\mathbf{A} = \mathbf{I}_r$ then gives, for $t > t_0$,

$$|\mathrm{Tr}\,(\mathbf{R} - \mathbf{T})| \leq \frac{1}{\sigma^8 t}\left(\frac{k_2}{\sigma^2}\left(1 + \frac{k_1}{\sigma^2}\right)^2 P_1\left(\frac{1}{\sigma^2}\right)\right) \tag{1.83}$$

where $k_2 = \frac{2LC_{\sup}}{k_0}\sup_t\{r/t\} < +\infty$.

Eventually, (1.81) and (1.83) yield $\left|\mathbb{E}_{\mathbf{H}}\left[\mathrm{Tr}\big(\mathbf{T} - \mathbf{S}\big)\right]\right| \leq \frac{1}{\sigma^8 t}P\big(\frac{1}{\sigma^2}\big)$ for $t > t_0$, where the coefficients of the polynomial $P\big(\frac{1}{\sigma^2}\big) = P_0\big(\frac{1}{\sigma^2}\big) + \frac{k_2}{\sigma^2}\big(1 + \frac{k_1}{\sigma^2}\big)^2 P_1\big(\frac{1}{\sigma^2}\big)$ are real positive coefficients and do not depend on σ^2 nor on t. This completes the proof of Proposition 3.

1.E Differentiability of $\mathbf{Q} \mapsto \boldsymbol{\delta}(\mathbf{Q})$, $\mathbf{Q} \mapsto \tilde{\boldsymbol{\delta}}(\mathbf{Q})$ and $\mathbf{Q} \mapsto \overline{I}(\mathbf{Q})$

We prove in this section Proposition 5, i.e. that for all $\mathbf{P}, \mathbf{Q} \in \mathcal{C}_1$ functions $\mathbf{Q} \mapsto \boldsymbol{\delta}(\mathbf{Q})$, $\mathbf{Q} \mapsto \tilde{\boldsymbol{\delta}}(\mathbf{Q})$ and $\mathbf{Q} \mapsto \overline{I}(\mathbf{Q})$ are Gâteaux differentiable at point $\mathbf{Q}$ in the direction $\mathbf{P} - \mathbf{Q}$, where $\boldsymbol{\delta}, \tilde{\boldsymbol{\delta}}$ are defined as the solutions of system (1.9) and where $\overline{I}(\mathbf{Q})$ is given by (1.8). The proof is based on the implicit function theorem.

Let $\mathbf{P}, \mathbf{Q} \in \mathcal{C}_1$. We introduce the function $\Gamma : \mathbb{R}_+^L \times \mathbb{R}_+^L \times [0,1] \to \mathbb{R}^{2L}$ defined by

$$\Gamma(\boldsymbol{\delta}, \tilde{\boldsymbol{\delta}}, \lambda) = \begin{bmatrix} \boldsymbol{\delta} - f(\tilde{\boldsymbol{\delta}}) \\ \tilde{\boldsymbol{\delta}} - \tilde{f}(\boldsymbol{\delta}, \mathbf{Q} + \lambda(\mathbf{P} - \mathbf{Q})) \end{bmatrix},$$

with $f(\tilde{\boldsymbol{\delta}}) = \big[f_1(\tilde{\boldsymbol{\delta}}), \dots, f_L(\tilde{\boldsymbol{\delta}})\big]^T$ and $\tilde{f}(\boldsymbol{\delta}, \mathbf{Q}) = \big[\tilde{f}_1(\boldsymbol{\delta}, \mathbf{Q}), \dots, \tilde{f}_L(\boldsymbol{\delta}, \mathbf{Q})\big]^T$, where the f_l and the $\tilde{f}_l$ are defined by (1.10). Note that $\boldsymbol{\delta}(\mathbf{Q} + \lambda(\mathbf{P} - \mathbf{Q}))$ and $\tilde{\boldsymbol{\delta}}(\mathbf{Q} + \lambda(\mathbf{P} - \mathbf{Q}))$ are defined by $\Gamma(\boldsymbol{\delta}, \tilde{\boldsymbol{\delta}}, \lambda) = 0$. We want to apply the implicit theorem on a neighbourhood of $\lambda = 0$; this requires the differentiability of Γ on this neighbourhood, and the invertibility of the partial Jacobian $D_{(\boldsymbol{\delta}, \tilde{\boldsymbol{\delta}})}(\Gamma(\boldsymbol{\delta}, \tilde{\boldsymbol{\delta}}, \lambda))$ at point $\lambda = 0$.

We first note that $f_l : \tilde{\boldsymbol{\delta}} \mapsto \frac{1}{\sigma^2 t}\mathrm{Tr}\big[\mathbf{C}^{(l)}\big(\mathbf{I}_r + \sum_k \tilde{\delta}_k \mathbf{C}^{(k)}\big)^{-1}\big]$ is clearly continuously differentiable on $\mathbb{R}_+^L$. Concerning $\tilde{f}_l$, we first need to use the matrix equality $(\mathbf{I} + \mathbf{AB})^{-1}\mathbf{B} = \mathbf{B}(\mathbf{I} + \mathbf{BA})^{-1}$, with $\mathbf{A} = \mathbf{Q}^{1/2}$ and $\mathbf{B} = \tilde{\mathbf{C}}\mathbf{Q}^{1/2}$:

$$\begin{aligned}\tilde{f}_l(\boldsymbol{\delta}, \mathbf{Q}) &= \frac{1}{\sigma^2 t}\mathrm{Tr}\left[\mathbf{Q}^{1/2}\tilde{\mathbf{C}}^{(l)}\mathbf{Q}^{1/2}\left(\mathbf{I}_t + \mathbf{Q}^{1/2}\tilde{\mathbf{C}}(\boldsymbol{\delta})\mathbf{Q}^{1/2}\right)^{-1}\right] \\ &= \frac{1}{\sigma^2 t}\mathrm{Tr}\left[\tilde{\mathbf{C}}^{(l)}\mathbf{Q}(\mathbf{I}_t + \tilde{\mathbf{C}}(\boldsymbol{\delta})\mathbf{Q})^{-1}\right]. \end{aligned} \tag{1.84}$$

Recall that $\tilde{\mathbf{C}}(\boldsymbol{\delta}) = \sum_k \delta_k \tilde{\mathbf{C}}^{(k)}$. Function $(\boldsymbol{\delta}, \lambda) \mapsto \tilde{f}(\boldsymbol{\delta}, \mathbf{Q} + \lambda(\mathbf{P} - \mathbf{Q}))$ is therefore clearly continuously differentiable on $\mathbb{R}_+^L \times [0,1]$. Nevertheless, as we want to use the implicit theorem for $\lambda = 0$, we need to enlarge the continuous differentiability on an open set including $\lambda = 0$. Note that for $\lambda < 0$, $\mathbf{Q} + \lambda(\mathbf{P} - \mathbf{Q})$ might have negative eigenvalues. Yet, $\det\big[\mathbf{I}_t + \tilde{\mathbf{C}}(\boldsymbol{\delta})(\mathbf{Q} + \lambda(\mathbf{P} - \mathbf{Q}))\big] > 0$ for $\boldsymbol{\delta} = \boldsymbol{\delta}(\mathbf{Q})$ and $\lambda = 0$.

Therefore it exists a neighbourhood V of $(\boldsymbol{\delta}(\mathbf{Q}),0)$ on which $\det\big[\mathbf{I}_t+\tilde{\mathbf{C}}(\boldsymbol{\delta})(\mathbf{Q}+\lambda(\mathbf{P}-\mathbf{Q}))\big]>0$. Defining $\tilde{f}_l$ by (1.84), the functions $(\boldsymbol{\delta},\lambda)\mapsto\tilde{f}_l(\boldsymbol{\delta},\mathbf{Q}+\lambda(\mathbf{P}-\mathbf{Q}))$ are continuously differentiable on V. Hence, $\Gamma(\boldsymbol{\delta},\tilde{\boldsymbol{\delta}},\lambda)$ is continuously differentiable on $\mathbb{R}_+^L\times V$.

We still have to check that the partial Jacobian $D_{(\boldsymbol{\delta},\tilde{\boldsymbol{\delta}})}(\Gamma(\boldsymbol{\delta},\tilde{\boldsymbol{\delta}},\lambda))$ is invertible at the point $\lambda=0$.

$$
\begin{aligned}
D_{(\boldsymbol{\delta},\tilde{\boldsymbol{\delta}})}\Gamma_{(\boldsymbol{\delta},\tilde{\boldsymbol{\delta}},0)} &= \begin{bmatrix} \mathbf{I}_L - D_{\boldsymbol{\delta}} f_{(\tilde{\boldsymbol{\delta}})} & -D_{\tilde{\boldsymbol{\delta}}} f_{(\tilde{\boldsymbol{\delta}})} \\ -D_{\boldsymbol{\delta}}\tilde{f}_{(\boldsymbol{\delta},0)} & \mathbf{I}_L - D_{\tilde{\boldsymbol{\delta}}}\tilde{f}_{(\boldsymbol{\delta},0)} \end{bmatrix} \\
&= \begin{bmatrix} \mathbf{I}_L & -\sigma^2\mathbf{A}(\mathbf{T}) \\ -\sigma^2\tilde{\mathbf{A}}(\tilde{\mathbf{T}}) & \mathbf{I}_L \end{bmatrix} = \mathbf{M}(\mathbf{T},\tilde{\mathbf{T}}),
\end{aligned}
$$

where the entries of matrices $\mathbf{A}(\mathbf{T})$ and $\tilde{\mathbf{A}}(\tilde{\mathbf{T}})$ are defined by $\mathbf{A}_{kl}(\mathbf{T}) = \frac{1}{t}\mathrm{Tr}(\mathbf{C}^{(k)}\mathbf{T}\mathbf{C}^{(l)}\mathbf{T})$ and $\tilde{\mathbf{A}}_{kl}(\tilde{\mathbf{T}}) = \frac{1}{t}\mathrm{Tr}(\mathbf{Q}^{1/2}\tilde{\mathbf{C}}^{(k)}\mathbf{Q}^{1/2}\tilde{\mathbf{T}}\mathbf{Q}^{1/2}\tilde{\mathbf{C}}^{(l)}\mathbf{Q}^{1/2}\tilde{\mathbf{T}})$, and where $\mathbf{T}=\mathbf{T}(\tilde{\boldsymbol{\delta}}(\mathbf{Q}))$ and $\tilde{\mathbf{T}}=\tilde{\mathbf{T}}(\boldsymbol{\delta}(\mathbf{Q}))$ are respectively defined by (1.11) and (1.12). Matrices $\mathbf{A}(\mathbf{T})$, $\tilde{\mathbf{A}}(\tilde{\mathbf{T}})$ and $\mathbf{M}(\mathbf{T},\tilde{\mathbf{T}})$ correspond to those defined in Lemma 1, but in which $\tilde{\mathbf{C}}^{(l)}$ is replaced by $\mathbf{Q}^{1/2}\tilde{\mathbf{C}}^{(l)}\mathbf{Q}^{1/2}$. Lemma 1 item (i) therefore gives the invertibility of $D_{(\boldsymbol{\delta},\tilde{\boldsymbol{\delta}})}\Gamma$ at point $\lambda=0$.

We now are in position to apply the implicit function theorem, which asserts that functions $\lambda\mapsto\boldsymbol{\delta}(\mathbf{Q}+\lambda(\mathbf{P}-\mathbf{Q}))$ and $\lambda\mapsto\tilde{\boldsymbol{\delta}}(\mathbf{Q}+\lambda(\mathbf{P}-\mathbf{Q}))$ are continuously differentiable on a neighbourhood of 0. Hence, $\boldsymbol{\delta}$ and $\tilde{\boldsymbol{\delta}}$ are Gâteaux differentiable at point $\mathbf{Q}$ in the direction $\mathbf{P}-\mathbf{Q}$. As $\overline{I}(\mathbf{Q}) = \log\big|\mathbf{I}_r+\sum_l\tilde{\delta}_l(\mathbf{Q})\mathbf{C}^{(l)}\big|+\log\big|\mathbf{I}_t+\mathbf{Q}\big(\sum_l\delta_l(\mathbf{Q})\tilde{\mathbf{C}}^{(l)}\big)\big|-\sigma^2t\big(\sum_l\delta_l(\mathbf{Q})\tilde{\delta}_l(\mathbf{Q})\big)$ it is clear that $\mathbf{Q}\mapsto\overline{I}(\mathbf{Q})$ is as well Gâteaux differentiable at point $\mathbf{Q}$ in the direction $\mathbf{P}-\mathbf{Q}$.

Chapter 2

MMSE Diversity Analysis

In this chapter, the evaluation of the diversity of the MIMO MMSE receiver is addressed for finite rates in both flat fading channels and frequency selective fading channels with cyclic prefix. It has been observed recently that in contrast with the other MIMO receivers, the MMSE receiver has a diversity depending on the target finite rate, and that for sufficiently low rates the MMSE receiver reaches the full diversity - that is, the diversity of the ML receiver. This behavior has so far only been partially explained. The purpose of this chapter is to provide complete proofs for flat fading MIMO channels, and to improve the partial existing results in frequency selective MIMO channels with cyclic prefix.

2.1 Introduction

The diversity-multiplexing trade-off (DMT) introduced by [22] studies the diversity function of the multiplexing gain in the high SNR regime. [28] showed that the MMSE linear receivers, widely used for their simplicity, exhibit a largely suboptimal DMT in flat fading MIMO channels. Nonetheless, for a finite data rate (i.e. when the rate does not increase with the signal to noise ratio), the MMSE receivers take several diversity values, depending on the target rate, as noticed earlier in [29], and also in [30, 31] for frequency-selective MIMO channels. In particular they achieve full diversity for sufficiently low data rates, hence their great interest. This behavior was partially explained in [28, 32] for flat fading MIMO channels and in [33] for frequency-selective MIMO channels. Indeed the proof of the upper bound on the diversity order for the flat fading case given in [32] contains a gap, and the approach of [32] based on the Specht bound seems to be unsuccessfull. As for MIMO frequency selective channels with cyclic prefix, [33] only derives the diversity in the particular case of a number of channel taps equal to the transmission data block length, and claims that this value provides an upper bound in more realistic cases, whose expression is however not explicitly given. In this chapter we provide a rigorous proof of

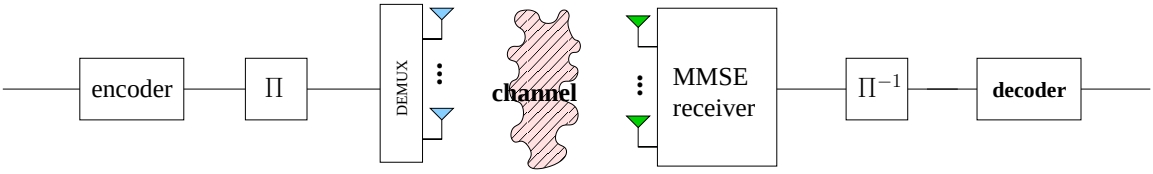

Figure 2.1: Considered MIMO system

the diversity for MMSE receivers in flat fading MIMO channels for finite data rates. We also derive the diversity in MIMO frequency selective channels with cyclic prefix for finite data rates if the transmission data block length is large enough. Simulations corroborate our derived diversity in the frequency selective channels case.

2.2 Problem statement

We consider a MIMO system with M transmitting, $N \geq M$ receiving antennas, with coding and ideal interleaving at the transmitter, and with a MMSE linear equalizer at the receiver, followed by a de-interleaver and a decoder (see Fig. 2.1). We evaluate in the following sections the achieved diversity by studying the outage probability, that is the probability that the capacity does not support the target data rate, at high SNR regimes. We denote ρ the SNR, I the capacity and R the target data rate. We use the notation $\doteq$ for *exponential equality* [22], i.e.

$$f(\rho) \doteq \rho^d \Leftrightarrow \lim_{\rho \to \infty} \frac{\log f(\rho)}{\log \rho} = d, \tag{2.1}$$

and the notations $\dot{\leq}$ and $\dot{\geq}$ for exponential inequalities, which are similarly defined. We note $\log$ the logarithm to base 2.

2.3 Flat fading MIMO channels

In this section we consider a flat fading MIMO channel. The output of the MIMO channel is given by

$$\mathbf{y} = \sqrt{\frac{\rho}{M}}\mathbf{H}\mathbf{x} + \mathbf{n}, \tag{2.2}$$

where $\mathbf{n} \sim \mathcal{CN}(\mathbf{0}, \mathbf{I}_N)$ is the additive white Gaussian noise and $\mathbf{x}$ the channel input vector, $\mathbf{H}$ the $N \times M$ channel matrix with i.i.d. entries $\sim \mathcal{CN}(0, 1)$.

Theorem 6. *For a rate R such that $\log \frac{M}{m} < \frac{R}{M} < \log \frac{M}{m-1}$, with $m \in \{1, \dots, M\}$, the outage probability verifies*

$$\mathbb{P}(I < R) \doteq \rho^{-m(N-M+m)}, \tag{2.3}$$

that is, a diversity of $m(N - M + m)$.

Note that for a rate $R < M \log \frac{M}{M-1}$ (i.e. $m = M$) full diversity MN is attained, while for a rate $R > M \log M$ the diversity corresponds to the one derived by DMT approach. This result was stated by [32]. Nevertheless the proof of the outage lower bound in [32] omits that the event noted $\mathcal{B}_a$ is not independent from the eigenvalues of $\mathbf{H}^*\mathbf{H}$, hence questioning the validity of the given proof. We thus provide an alternative proof based on an approach suggested by the analysis of [28] in the case where $R = r \log \rho$ with $r > 0$.

Proof. The capacity I of the MIMO MMSE considered system is given by

$$I = \sum_{j=1}^{M} \log(1 + \beta_j),$$

where β_j is the SINR for the jth stream:

$$\beta_j = \frac{1}{\left(\left[\mathbf{I} + \frac{\rho}{M}\mathbf{H}^*\mathbf{H}\right]^{-1}\right)_{jj}} - 1.$$

We lower bound in the first place $\mathbb{P}(I < R)$ and prove in the second place that the bound is tight by upper bounding $\mathbb{P}(I < R)$ with the same bound.

2.3.1 Outage probability lower bound

We here assume that $R/M > \log(M/m)$. In order to lower bound $\mathbb{P}(I < R)$ we need to upper bound the capacity I. Using Jensen's inequality on function $x \mapsto \log x$ yields

$$I \leq M \log \left[\frac{1}{M} \sum_{j=1}^{M} (1 + \beta_j) \right] \tag{2.4}$$

$$= M \log \left[\frac{1}{M} \sum_{j=1}^{M} \left(\left[\left(\mathbf{I} + \frac{\rho}{M}\mathbf{H}^*\mathbf{H} \right)^{-1} \right]_{jj} \right)^{-1} \right]. \tag{2.5}$$

We note $\mathbf{H}^*\mathbf{H} = \mathbf{U}^*\Lambda\mathbf{U}$ the SVD of $\mathbf{H}^*\mathbf{H}$ with $\Lambda = \mathrm{diag}(\lambda_1, \dots, \lambda_M)$, $\lambda_1 \leq \lambda_2 \dots \leq \lambda_M$. We recall that the $(\lambda_k)_{k=1,\dots,M}$ are independent from the entries of matrix $\mathbf{U}$ and that $\mathbf{U}$ is a Haar distributed

unitary random matrix, i.e. the probability distribution of $\mathbf{U}$ is invariant by left (or right) multiplication by deterministic matrices. Using this SVD we can write

$$\frac{1}{M}\sum_{j=1}^{M}\left(\left[\left(\mathbf{I}+\frac{\rho}{M}\mathbf{H}^{*}\mathbf{H}\right)^{-1}\right]_{jj}\right)^{-1}=\frac{1}{M}\sum_{j=1}^{M}\left(\sum_{k=1}^{M}\frac{|\mathbf{U}_{kj}|^{2}}{1+\frac{\rho}{M}\lambda_{k}}\right)^{-1}. \tag{2.6}$$

a) Case $m=1$

In order to better understand the outage probability behavior, we first consider the case $m=1$. In this case $R/M>\log M$. We review the approach of [28, III], which consists in upper bounding (2.6) by $\left(1+\frac{\rho}{M}\lambda_1\right)\frac{1}{M}\sum_{j=1}^{M}\frac{1}{|\mathbf{U}_{1j}|^2}$, as $\sum_{k=1}^{M}\frac{|\mathbf{U}_{kj}|^2}{1+\frac{\rho}{M}\lambda_k}\geq\frac{|\mathbf{U}_{1j}|^2}{1+\frac{\rho}{M}\lambda_1}$. Using this bound in (2.5) gives

$$I\leq M\log\left[\left(1+\frac{\rho}{M}\lambda_1\right)\frac{1}{M}\sum_{j=1}^{M}\frac{1}{|\mathbf{U}_{1j}|^2}\right].$$

Therefore

$$\left(\left(1+\frac{\rho}{M}\lambda_1\right)\frac{1}{M}\sum_{j=1}^{M}\frac{1}{|\mathbf{U}_{1j}|^2}<2^{R/M}\right)\subset(I<R).$$

In order to lower bound $\mathbb{P}(I<R)$, [28] introduced the set $\mathcal{A}_1$ defined by

$$\mathcal{A}_1=\left\{\frac{1}{M}\sum_{j=1}^{M}\frac{1}{|\mathbf{U}_{1j}|^2}<M+\varepsilon\right\}$$

for $\varepsilon>0$. Then,

$$\begin{aligned}\mathbb{P}(I<R)&\geq\mathbb{P}\left((I<R)\cap\mathcal{A}_1\right)\\&\geq\mathbb{P}\left[\left(\left(1+\frac{\rho}{M}\lambda_1\right)\frac{1}{M}\sum_{j=1}^{M}\frac{1}{|\mathbf{U}_{1j}|^2}<2^{R/M}\right)\cap\mathcal{A}_1\right]\\&\geq\mathbb{P}\left[\left(1+\frac{\rho}{M}\lambda_1<\frac{2^{R/M}}{M+\varepsilon}\right)\cap\mathcal{A}_1\right]\\&=\mathbb{P}(\mathcal{A}_1)\cdot\mathbb{P}\left[1+\frac{\rho}{M}\lambda_1<\frac{2^{R/M}}{M+\varepsilon}\right],\end{aligned}$$

where the last equality comes from the independence between eigenvectors and eigenvalues of Gaussian matrix $\mathbf{H}^{*}\mathbf{H}$. It is shown in [28, Appendix A] that $\mathbb{P}(\mathcal{A}_1)\neq 0$. Besides, as we supposed $2^{R/M}>M$, we can take ε such that $\frac{2^{R/M}}{M+\varepsilon}>1$, ensuring that $\mathbb{P}\left[\left(1+\frac{\rho}{M}\lambda_1\right)<\frac{2^{R/M}}{M+\varepsilon}\right]\neq 0$. Hence there exists $\kappa>0$ such that

$$\mathbb{P}(I<R)\dot{\geq}\,\mathbb{P}\left(\lambda_1<\frac{\kappa}{\rho}\right),$$

which is asymptotically equivalent to $\rho^{-(N-M+1)}$ in the sense of (2.1) (see, e.g., [79, Th. II.3]).

b) General case $1 \leq m \leq M$

By the same token as for $m = 1$ we now consider the general case – we recall that we assumed that $\log(M/m) < R/M$. We first lower bound $\sum_k \frac{|\mathbf{U}_{kj}|^2}{1+\frac{\rho}{M}\lambda_k}$ which appears in (2.6) by the m first terms of the sum and then use Jensen's inequality applied on $x \mapsto x^{-1}$, yielding

$$\begin{aligned}\sum_{k=1}^{M} \frac{|\mathbf{U}_{kj}|^2}{1+\frac{\rho}{M}\lambda_k} &\geq \sum_{k=1}^{m} \frac{|\mathbf{U}_{kj}|^2}{1+\frac{\rho}{M}\lambda_k} \\ &\geq \frac{\left(\sum_{l=1}^{m} |\mathbf{U}_{lj}|^2\right)^2}{\sum_{k=1}^{m} |\mathbf{U}_{kj}|^2 \left(1+\frac{\rho}{M}\lambda_k\right)}.\end{aligned}$$

Using this inequality in (2.6), we obtain that

$$\begin{aligned}\frac{1}{M}\sum_{j=1}^{M}\left(\left[\left(\mathbf{I}+\frac{\rho}{M}\mathbf{H}^*\mathbf{H}\right)^{-1}\right]_{jj}\right)^{-1} &\leq \frac{1}{M}\sum_{j=1}^{M}\frac{\sum_{k=1}^{m}|\mathbf{U}_{kj}|^2\left(1+\frac{\rho}{M}\lambda_k\right)}{\left(\sum_{l=1}^{m}|\mathbf{U}_{lj}|^2\right)^2} \\ &= \sum_{k=1}^{m}\left(1+\frac{\rho}{M}\lambda_k\right)\delta_k(\mathbf{U}), \qquad (2.7)\end{aligned}$$

where $\delta_k(\mathbf{U}) = \frac{1}{M}\sum_{j=1}^{M}\frac{|\mathbf{U}_{kj}|^2}{\left(\sum_{l=1}^{m}|\mathbf{U}_{lj}|^2\right)^2}$. Equation (2.7), together with (2.5), yields the following inclusion:

$$\left(\sum_{k=1}^{m}\delta_k(\mathbf{U})\left(1+\frac{\rho}{M}\lambda_k\right) < 2^{R/M}\right) \subset (I < R).$$

Similarly to the case $m = 1$, we introduce the set $\mathcal{A}_m$ defined by

$$\mathcal{A}_m = \left\{\delta_k(\mathbf{U}) < \frac{M}{m^2} + \varepsilon,\ k = 1, \ldots, m\right\}$$

for $\varepsilon > 0$. We now use this set to lower bound $\mathbb{P}(I < R)$.

$$\begin{aligned}\mathbb{P}(I < R) &\geq \mathbb{P}\left((I < R) \cap \mathcal{A}_m\right) \\ &\geq \mathbb{P}\left[\left(\sum_{k=1}^{m}\delta_k(\mathbf{U})\left(1+\frac{\rho}{M}\lambda_k\right) < 2^{R/M}\right) \cap \mathcal{A}_m\right] \\ &\geq \mathbb{P}\left[\left(\sum_{k=1}^{m}\left(1+\frac{\rho}{M}\lambda_k\right) < \frac{2^{R/M}}{\frac{M}{m^2}+\varepsilon}\right) \cap \mathcal{A}_m\right] \\ &= \mathbb{P}(\mathcal{A}_m) \cdot \mathbb{P}\left[\sum_{k=1}^{m}\left(1+\frac{\rho}{M}\lambda_k\right) < \frac{2^{R/M}}{\frac{M}{m^2}+\varepsilon}\right].\end{aligned}$$

The independence between eigenvectors and eigenvalues of Gaussian matrix $\mathbf{H}^*\mathbf{H}$ justifies the last equality. As we assumed that $\log(M/m) < R/M$, that is $m < \frac{2^{R/M}}{M/m^2}$, we can choose ε such that

$m < \frac{2^{R/M}}{M/m^2+\varepsilon}$. That ensures that $\mathbb{P}\left[\sum_{k=1}^{m}\left(1+\frac{\rho}{M}\lambda_k\right) < \frac{2^{R/M}}{M/m^2+\varepsilon}\right] \neq 0$. We show in Appendix 2.A that this probability is asymptotically equivalent to $\rho^{-m(N-M+m)}$ in the sense of (2.1), leading to

$$\mathbb{P}(I<R) \dot{\geq} \frac{\mathbb{P}(\mathcal{A}_m)}{\rho^{m(N-M+m)}}. \tag{2.8}$$

We still need to prove that $\mathbb{P}(\mathcal{A}_m) \neq 0$. Any Haar distributed random unitary matrix can be parameterized by M^2 independent angular random variables $(\alpha_1, \ldots, \alpha_{M^2}) = \boldsymbol{\alpha}$ whose probability distributions are almost surely positive (see [80, 81] and Appendix 2.C). We note Φ the function such that $\mathbf{U} = \Phi(\boldsymbol{\alpha})$. Consider a deterministic unitary matrix $\mathbf{U}_*$ such that $|(\mathbf{U}_*)_{ij}|^2 = \frac{1}{M}\ \forall i,j$, and denote by $\boldsymbol{\alpha}_*$ a corresponding M^2 dimensional vector. It is straightforward to check that $\delta_k \circ \Phi(\alpha_*) = M/m^2$. Functions $\boldsymbol{\alpha} \mapsto (\delta_k \circ \Phi)(\boldsymbol{\alpha})$ are continuous at point $\boldsymbol{\alpha}_*$ for $1 \leq k \leq m$ and therefore there exists $\eta > 0$ such that the ball $\mathcal{B}(\boldsymbol{\alpha}_*, \eta)$ is included in the set $\left\{\boldsymbol{\alpha},\ (\delta_k \circ \Phi)(\alpha) < \frac{M}{m^2} + \varepsilon,\ k = 1, \ldots, m\right\}$. We have therefore $\mathbb{P}(\mathcal{A}_m) \neq 0$ as

$$\begin{aligned}\mathbb{P}(\mathcal{A}_m) &= \int_{\left\{(\delta_k \circ \Phi)(\boldsymbol{\alpha}) < \frac{M}{m^2}+\varepsilon,\, k=1,\ldots,m\right\}} p(\boldsymbol{\alpha}) d\boldsymbol{\alpha} \\ &> \int_{\mathcal{B}(\boldsymbol{\alpha}_*,\eta)} p(\boldsymbol{\alpha}) d\boldsymbol{\alpha} > 0\end{aligned}$$

Coming back to (2.8), we eventually have

$$\mathbb{P}(I<R) \dot{\geq} \frac{1}{\rho^{m(N-M+m)}},$$

that is the diversity of the MMSE receiver is upper bounded by $m(N-M+m)$.

2.3.2 Outage probability upper bound

We now conclude by studying the upper bound of the outage probability, showing that $m(N-M+m)$ is also a lower bound for the diversity. Note that this lower bound has been derived in [28, 32] using however rather informal arguments; we provide a more rigorous proof here for the sake of completeness.

We now assume that $R/M < \log(M/(m-1))$, i.e. $m-1 < M2^{-R/M}$. Using Jensen inequality on function $y \mapsto \log(1/y)$, the capacity I can be lower bounded:

$$\begin{aligned}I &= -\sum_{j=1}^{M} \log\left(\left[\left(\mathbf{I} + \frac{\rho}{M}\mathbf{H}^*\mathbf{H}\right)^{-1}\right]_{jj}\right) \\ &\geq -M \log\left(\frac{1}{M}\mathrm{Tr}\left[\left(\mathbf{I} + \frac{\rho}{M}\mathbf{H}^*\mathbf{H}\right)^{-1}\right]\right),\end{aligned}$$

which leads to an upper bound for the outage probability:

$$\mathbb{P}(I < R) \leq \mathbb{P}\left[\mathrm{Tr}\left[\left(\mathbf{I} + \frac{\rho}{M}\mathbf{H}^*\mathbf{H}\right)^{-1}\right] > M2^{-R/M}\right]. \tag{2.9}$$

We need to derive the probability in the right-hand side of the above inequality. Noting $\mathcal{B}_0 = \Big\{\lambda_1 \leq \lambda_2 \ldots \leq \lambda_M,\ \sum_{k=1}^{M}\left(1+\frac{\rho}{M}\lambda_k\right)^{-1} > M2^{-R/M}\Big\}$,

$$\mathbb{P}\Big[\mathrm{Tr}\Big[\Big(\mathbf{I} + \frac{\rho}{M}\mathbf{H}^*\mathbf{H}\Big)^{-1}\Big] > M2^{-R/M}\Big] = \int_{\mathcal{B}_0} p(\lambda_1, \ldots, \lambda_M) d\lambda_1 \ldots d\lambda_M. \tag{2.10}$$

We now introduce $\mu_m = \sup_{(\lambda_1,\ldots,\lambda_M)\in\mathcal{B}_0}\{\rho\,\lambda_m\}$ and prove by contradiction that $\mu_m < +\infty$. If $\mu_m = +\infty$, there exists a sequence $(\lambda_1^{(n)}, \lambda_2^{(n)}, \ldots, \lambda_M^{(n)})_{n\in\mathbb{N}}$ such that $\lambda_k^{(n)} \to +\infty$ for any $k \geq m$. Besides,

$$M2^{-R/M} < \sum_{k=1}^{M}\Big(1 + \frac{\rho}{M}\lambda_k^{(n)}\Big)^{-1} \leq (m-1) + \sum_{k=m}^{M}\Big(1 + \frac{\rho}{M}\lambda_k^{(n)}\Big)^{-1}.$$

In particular $M2^{-R/M} < (m-1) + \sum_{k=m}^{M}\big(1 + \frac{\rho}{M}\lambda_k^{(n)}\big)^{-1}$, which, taking the limit when $n \to +\infty$, leads to $m-1 \geq M2^{-R/M}$, a contradiction with the assumption $m-1 < M2^{-R/M}$. Hence, $\mu_m < +\infty$.

We introduce the set $\mathcal{B}_1 = \{\lambda_1 \leq \lambda_2 \ldots \leq \lambda_M,\ 0 < \lambda_k \leq \frac{\mu_m}{\rho},\ k = 1, \ldots, m\}$, which verifies $\mathcal{B}_0 \subset \mathcal{B}_1$. Using (2.9) and (2.10), this implies that

$$\mathbb{P}(I < R) \leq \int_{\mathcal{B}_1} p(\lambda_1, \ldots, \lambda_M) d\lambda_1 \ldots d\lambda_M,$$

which is shown to be asymptotically smaller than $\rho^{-m(N-M+m)}$ in the sense of (2.1) in Appendix 2.B. The diversity is thus lower bounded by $m(N-M+m)$, ending the proof. □

2.4 Frequency selective MIMO channels with cyclic prefix

We consider a frequency selective MIMO channel with L independent taps. We consider a block transmission cyclic prefix scheme, with a block length of K. The output of the MIMO channel at time t is given by

$$\mathbf{y}_t = \sqrt{\frac{\rho}{ML}}\sum_{l=0}^{L-1}\mathbf{H}_l\mathbf{x}_{t-l} + \mathbf{n}_t = \sqrt{\frac{\rho}{ML}}\,[\mathbf{H}(z)]\mathbf{x}_t + \mathbf{n}_t$$

where $\mathbf{x}_t$ is the channel input vector at time t, $\mathbf{n}_t \sim \mathcal{CN}(\mathbf{0}, \mathbf{I}_N)$ the additive white Gaussian noise, $\mathbf{H}_l$ is the $N \times M$ channel matrix associated to l^{th} channel tap, for $l \in \{0, \ldots, L-1\}$, and $\mathbf{H}(z)$ denotes the

transfer function of the discrete-time equivalent channel defined by

$$\mathbf{H}(z) = \sum_{l=0}^{L-1} \mathbf{H}_l \, z^{-l}.$$

We make the common assumption that the entries of $\mathbf{H}_l$ are i.i.d and $\mathcal{CN}(0,1)$ distributed. Note that, thanks to the cyclic prefix, the output during one transmission block of length K can be written

$$\begin{bmatrix} \mathbf{y}_0 \\ \vdots \\ \mathbf{y}_{K-1} \end{bmatrix} = \mathcal{H} \begin{bmatrix} \mathbf{x}_0 \\ \vdots \\ \mathbf{x}_{K-1} \end{bmatrix} + \mathbf{n}, \tag{2.11}$$

where $\mathbf{n} \sim \mathcal{CN}(\mathbf{0}, \sigma^2 \mathbf{I}_{NK})$ is the equivalent white Gaussian noise and where $KN \times KM$ matrix $\mathcal{H}$ is the traditional block circulant matrix constructed from coefficients $\mathbf{H}_0, \mathbf{H}_1, \ldots, \mathbf{H}_{L-1}$. We can now state the second diversity theorem of the chapter.

Theorem 7. *Assume that the non restrictive condition $K > M^2(L-1)$ holds, ensuring that $\log \frac{M}{m} < -\log\left(\frac{m-1}{M} + \frac{(L-1)(M-(m-1))}{K}\right)$ for any $m = 1, \ldots, M$. Then, for a rate R verifying*

$$\log \tfrac{M}{m} < \tfrac{R}{M} < -\log\left(\tfrac{m-1}{M} + \tfrac{(L-1)(M-(m-1))}{K}\right), \tag{2.12}$$

$m \in \{1, \ldots, M\}$, the outage probability verifies

$$\mathbb{P}(I < R) \doteq \rho^{-m(LN-M+m)}, \tag{2.13}$$

that is a diversity of $m(LN - M + m)$.

The diversity of the MMSE receiver is thus $m(LN - M + m)$, corresponding to a flat fading MIMO channel with M transmit antennas and LN receive antennas. For a large block length K, the upper bound for rate R is close to the bound of the previous flat fading case $\log \frac{M}{m-1}$. Concerning data rates verifying $-\log\left(\frac{m-1}{M} + \frac{L-1}{K}(M-(m-1))\right) < \frac{R}{M} < \log \frac{M}{m-1}$, the $m(LN-M+m)$ diversity is only an upper bound; nevertheless the diversity is also lower bounded by $(m-1)(LN-M+(m-1))$.

Proof. Similarly to previous section the capacity of the MIMO MMSE system is written

$$I = \sum_{j=1}^{M} \log(1 + \beta_j),$$

where β_j is the SINR for the jth stream of $\mathbf{x}_t$. It is standard material that in MIMO frequency selective channel with cyclic prefix the SINR of the MMSE receiver is given by

$$\beta_j = \frac{1}{\frac{1}{K}\sum_{k=1}^{K} \left[\left(\mathbf{S}\left(\frac{k-1}{K}\right)\right)^{-1}\right]_{jj}} - 1, \tag{2.14}$$

where $\mathbf{S}(\nu) = \mathbf{I}_N + \frac{\rho}{M}\mathbf{H}(e^{2i\pi\nu})^* \mathbf{H}(e^{2i\pi\nu})$.

2.4.1 Outage probability lower bound

We assume that $R/M > \log(M/m)$.

One can show that function $\mathbf{A} \mapsto (\mathbf{A}^{-1})_{jj}$, defined over the set of positive-definite matrices, is convex. Using Jensen's inequality then yields

$$\begin{aligned}\frac{1}{K}\sum_{k=1}^{K}\left[\left(\mathbf{S}\left(\tfrac{k-1}{K}\right)\right)^{-1}\right]_{jj} &\geq \left(\left[\frac{1}{K}\sum_{k=1}^{K}\mathbf{S}\left(\tfrac{k-1}{K}\right)\right]^{-1}\right)_{jj} \\ &= \left(\left[\mathbf{I}_N + \sum_{l=0}^{L-1}\frac{\rho}{M}\mathbf{H}_l^*\mathbf{H}_l\right]^{-1}\right)_{jj}.\end{aligned}$$

The last equality follows from the fact that $\frac{1}{K}\sum_{k=1}^{K} e^{2i\pi\frac{k-1}{K}(l-n)} = \delta_{ln}$. Using this inequality in the SINR expression (2.14) gives

$$1+\beta_j \leq \left(\left(\left[\mathbf{I}_N + \sum_{l=0}^{L-1}\frac{\rho}{M}\mathbf{H}_l^*\mathbf{H}_l\right]^{-1}\right)_{jj}\right)^{-1}.$$

We now come back to the capacity I of the system; similarly to (2.4), using Jensen's inequality yields

$$\begin{aligned}I &\leq M\log\left[\frac{1}{M}\sum_{j=1}^{M}(1+\beta_j)\right] \\ &\leq M\log\left[\frac{1}{M}\sum_{j=1}^{M}\left(\left(\left[\mathbf{I}_N + \frac{\rho}{M}\sum_{l=0}^{L-1}\mathbf{H}_l^*\mathbf{H}_l\right]^{-1}\right)_{jj}\right)^{-1}\right].\end{aligned}$$

We can now use the results of section 2.3.1 by simply replacing $N \times M$ matrix $\mathbf{H}$ in (2.5) by $LN \times M$ matrix $\tilde{\mathbf{H}} = [\mathbf{H}_0^T, \mathbf{H}_1^T, \ldots, \mathbf{H}_{L-1}^T]^T$. They lead to the following lower bound for the outage capacity, for a rate R verifying $R/M > \log(M/m)$:

$$\mathbb{P}(I < R) \dot{\geq} \frac{1}{\rho^{m(LN-M+m)}}.$$

2.4.2 Outage probability upper bound

We assume that $\frac{R}{M} < -\log\left(\frac{m-1}{M} + \frac{(L-1)(M-(m-1))}{K}\right)$, that is $2^{-R/M} < \frac{m-1}{M} + \frac{L-1}{K}(M-(m-1))$.

We first derive a lower bound for the capacity I.

$$\begin{aligned}I &= -\sum_{j=1}^{M}\log\left(\frac{1}{K}\sum_{k=1}^{K}\left(\left[\mathbf{S}\left(\tfrac{k-1}{K}\right)\right]^{-1}\right)_{jj}\right) \\ &\geq -M\log\left(\frac{1}{KM}\sum_{k=1}^{K}\mathrm{Tr}\left(\left[\mathbf{S}\left(\tfrac{k-1}{K}\right)\right]^{-1}\right)\right)\end{aligned}$$

The latter inequality follows once again from Jensen's inequality on function $x \mapsto \log x$.

We now analyze $\mathrm{Tr}\left(\mathbf{S}(\nu)^{-1}\right)$. To that end, we write $LN \times M$ matrix $\tilde{\mathbf{H}} = [\mathbf{H}_0^T, \ldots, \mathbf{H}_{L-1}^T]^T$ under the form $\tilde{\mathbf{H}} = \mathbf{\Theta}(\tilde{\mathbf{H}}^*\tilde{\mathbf{H}})^{1/2}$, where $\mathbf{\Theta} = [\mathbf{\Theta}_0^T, \ldots, \mathbf{\Theta}_{L-1}^T]^T$ and $\mathbf{\Theta}^*\mathbf{\Theta} = \mathbf{I}_M$. Besides, we note $\mathbf{U}^*\Lambda\mathbf{U}$ the SVD of $\tilde{\mathbf{H}}^*\tilde{\mathbf{H}}$ with $\Lambda = \mathrm{diag}(\lambda_1, \ldots, \lambda_M)$, $\lambda_1 \leq \ldots \leq \lambda_M$. Hence,

$$\mathbf{H}(e^{2i\pi\nu}) = \mathbf{\Theta}(e^{2i\pi\nu})\mathbf{U}^*\Lambda^{1/2}\mathbf{U},$$

where $\mathbf{\Theta}(z) = \sum_{l=0}^{L-1} \mathbf{\Theta}_l z^{-l}$. Using this parametrization,

$$\begin{aligned}\mathrm{Tr}\left(\mathbf{S}(\nu)^{-1}\right) &= \mathrm{Tr}\left[\left(\mathbf{I} + \frac{\rho}{M}\mathbf{U}\mathbf{\Theta}^*(e^{2i\pi\nu})\mathbf{\Theta}(e^{2i\pi\nu})\mathbf{U}^*\Lambda\right)^{-1}\right] \\ &\leq \mathrm{Tr}\left[\left(\mathbf{I} + \frac{\rho}{M}\gamma(e^{2i\pi\nu})\Lambda\right)^{-1}\right],\end{aligned}$$

where $\gamma(\nu) = \lambda_{\min}(\mathbf{\Theta}^*(e^{2i\pi\nu})\mathbf{\Theta}(e^{2i\pi\nu}))$. Coming back to the outage probability,

$$\begin{aligned}\mathbb{P}(I < R) \leq& \mathbb{P}\left[\frac{1}{K}\sum_{k=0}^{K-1}\sum_{j=1}^{M}\left(1 + \frac{\rho\lambda_j}{M}\gamma\left(\frac{k}{K}\right)\right)^{-1} > M2^{-R/M}\right] \\ =& \mathbb{P}\left[\tilde{\mathbf{H}} \in \mathcal{B}_0\right],\end{aligned} \tag{2.15}$$

where $\mathcal{B}_0 = \left\{\tilde{\mathbf{H}}, \frac{1}{K}\sum_{k=0}^{K-1}\sum_{j=1}^{M}\left(1 + \frac{\rho\lambda_j}{M}\gamma\left(\frac{k}{K}\right)\right)^{-1} > M2^{-R/M}\right\}$.

We now prove by contradiction that $\mu_m < +\infty$, where $\mu_m = \sup_{\tilde{\mathbf{H}} \in \mathcal{B}_0}\{\rho\lambda_m\}$. If $\mu_m = +\infty$ there exists a sequence of matrices $\tilde{\mathbf{H}}^{(n)} \in \mathcal{B}_0$ such that $\rho\lambda_m^{(n)} \to +\infty$. Besides,

$$\begin{aligned}M2^{-\frac{R}{M}} <& \frac{1}{K}\sum_{k=0}^{K-1}\sum_{j=1}^{M}\left(1 + \frac{\rho\lambda_j^{(n)}}{M}\gamma^{(n)}\left(\frac{k}{K}\right)\right)^{-1} \\ \leq& (m-1) + \frac{1}{K}\sum_{k=0}^{K-1}\sum_{j=m}^{M}\left(1 + \frac{\rho\lambda_j^{(n)}}{M}\gamma^{(n)}\left(\frac{k}{K}\right)\right)^{-1}\end{aligned} \tag{2.16}$$

As $\mathbf{\Theta}^{(n)}$ belongs to a compact we can extract a subsequence $\mathbf{\Theta}^{(\psi(n))}$ which converges towards a matrix $\mathbf{\Theta}_\infty$. For this subsequence, inequality (2.16) becomes

$$M2^{-\frac{R}{M}} \leq (m-1) + \frac{1}{K}\sum_{k=0}^{K-1}\sum_{j=m}^{M}\left(1 + \frac{\rho\lambda_j^{(\psi(n))}}{M}\gamma^{(\psi(n))}\left(\frac{k}{K}\right)\right)^{-1} \tag{2.17}$$

Let γ_∞ be the function defined by $\gamma_\infty(\nu) = \lambda_{\min}(\mathbf{\Theta}_\infty^*(e^{2i\pi\nu})\mathbf{\Theta}_\infty(e^{2i\pi\nu}))$ and $k_1, \ldots, k_p$ be the integers for which $\gamma_\infty(k_j/K) = 0$. Then $\det\mathbf{\Theta}_\infty(z) = \det\left(\sum_{l=0}^{L-1}\mathbf{\Theta}_{\infty,l}z^{-l}\right) = 0$ for all $z \in \left\{e^{2i\pi k_j/K}, j = 1, \ldots, p\right\}$. Nevertheless, polynomial $z \mapsto \sum_{l=0}^{L-1}\mathbf{\Theta}_{\infty,l}z^{-l}$ has a maximum degree of $M(L-1)$, therefore

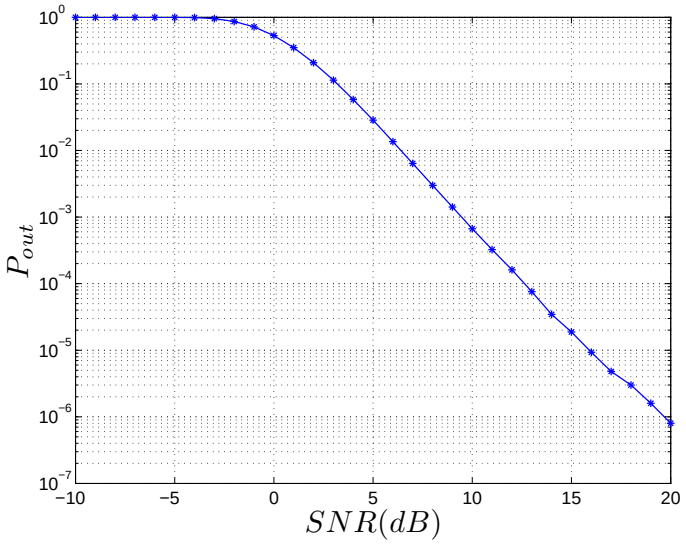

Figure 2.2: Outage probability of the MMSE receiver, L=2, K=64, M=N=2

$p \leq M(L-1)$. Inequality (2.17) then leads to

$$M2^{-\frac{R}{M}} \leq (m-1) + \frac{M(L-1)}{K} + \frac{1}{K} \sum_{k \notin \{k_1,\ldots,k_p\}} \sum_{j=m}^{M} \left(1 + \frac{\rho \lambda_j^{(\psi(n))}}{M} \gamma^{(\psi(n))}\left(\frac{k}{K}\right)\right)^{-1} \tag{2.18}$$

Moreover, if $k \notin \{k_1, \ldots, k_p\}$, $\lambda_j^{(\psi(n))} \gamma^{(\psi(n))}(\frac{k}{K}) \to +\infty$ for $j \geq m$, as $\gamma^{(\psi(n))}\big(\frac{k}{K}\big) \to \gamma_\infty\big(\frac{k}{K}\big) \neq 0$ for $k \notin \{k_1, \ldots, k_p\}$. Therefore taking the limit of (2.18) when $n \to +\infty$ gives

$$M2^{-\frac{R}{M}} \leq (m-1) + \frac{M(L-1)}{K},$$

which is in contradiction with the original assumption $2^{-R/M} < \frac{m-1}{M} + \frac{L-1}{K}(M-(m-1))$. Hence $\mu_m < +\infty$, and $\mathcal{B}_0 \subset \mathcal{B}_1 = \{\tilde{\mathbf{H}}, \rho\lambda_m(\tilde{\mathbf{H}}^*\tilde{\mathbf{H}}) < \mu_m\}$. Using (2.15), we thus have

$$\mathbb{P}(I < R) \leq \mathbb{P}(\tilde{\mathbf{H}} \in \mathcal{B}_1),$$

which, by Appendix 2.B, is asymptotically smaller than $\rho^{-m(NL-M+m)}$ in the sense of (2.1), therefore ending the proof. □

2.5 Numerical Results

We here illustrate the derived diversity in the frequency selective case. In the conducted simulation we took a block length of $K = 64$, a number of transmitting and receiving antennas $M = N = 2$, $L = 2$

channel taps and a target data rate $R = 3$ bits/s/Hz. Rate R then verifies (2.12) with $m = 1$, therefore the expected diversity is $LN - M + 1 = 3$. The outage probability is displayed on Fig. 2.2 as a function of SNR. We observe a slope of -10^{-3} per decade, hence a diversity of 3, confirming the result stated in section 2.4.

2.6 Conclusion

In this chapter we provided rigorous proofs regarding the diversity of the MMSE receiver at fixed rate, in both flat fading and frequency selective MIMO channels. The higher the target rate the less diversity is achieved; in particular, for sufficiently low rates, the MMSE receiver achieves full diversity in both MIMO channel cases, hence its great interest. Nonetheless, in frequency selective channels, the diversity bounds are not tight for some specific rates; this could probably be improved. Simulations corroborated our results.

Appendices

2.A Asymptotic lower bound for $\mathbb{P}(\sum_{k=1}^{m} \rho\lambda_k < b)$

We prove in this appendix that, for $b > 0$, $\mathbb{P}(\sum_{k=1}^{m} \rho\lambda_k < b) \dot{\geq} \rho^{-m(N-M+m)}$.

We note $\mathcal{C}_m$ the set defined by $\mathcal{C}_m = \{\lambda_1, \ldots, \lambda_m : \ 0 < \lambda_1 \leq \ldots \leq \lambda_m, \ \sum_{k=1}^{m} \rho\lambda_k < b\}$. As the λ_i verify $0 < \lambda_1 \leq \ldots \leq \lambda_M$, we can write

$$\mathbb{P}\left(\sum_{k=1}^{m} \rho\lambda_k < b\right) = \int_{(\lambda_1,\ldots,\lambda_m)\in\mathcal{C}_m} \int_{\lambda_m}^{+\infty} \cdots \int_{\lambda_{M-1}}^{+\infty} p_{M,N}(\lambda_1, \ldots, \lambda_M)\, d\lambda_1 \ldots d\lambda_M, \tag{2.19}$$

where $p_{M,N} : \mathbb{R}^M \to \mathbb{R}$ is the joint probability density function of the ordered eigenvalues of a $M \times M$ Wishart matrix with scale matrix $\mathbf{I}_M$ and N degrees of freedom, given by (see, e.g., [22]):

$$p_{M,N} = K_{M,N}^{-1} \prod_{i=1}^{M} \left(\lambda_i^{N-M} e^{-\lambda_i}\right) \prod_{i<j} (\lambda_i - \lambda_j)^2, \tag{2.20}$$

where $K_{M,N}$ is a normalizing constant. We now try to separate the integral in (2.19) in two integrals, one over $\lambda_1, \ldots, \lambda_m$, the other over $\lambda_{m+1}, \ldots, \lambda_M$. As we have $(\lambda_1, \ldots, \lambda_m) \in \mathcal{C}_m$ in (2.19), $\lambda_m < b/\rho$ and thus

$$\begin{aligned} &\int_{\lambda_m \leq \lambda_{m+1} \leq \ldots \leq \lambda_M} p_{M,N}(\lambda_1, \ldots, \lambda_M)\, d\lambda_{m+1} \ldots d\lambda_M \\ &\qquad \geq \int_{(\lambda_{m+1},\ldots,\lambda_M)\in\mathcal{D}} p_{M,N}(\lambda_1, \ldots, \lambda_M)\, d\lambda_{m+1} \ldots d\lambda_M \end{aligned} \tag{2.21}$$

where $\mathcal{D} = \{(\lambda_{m+1}, \ldots, \lambda_M) \in \mathbb{R}_+^{M-m};\ b/\rho \leq \lambda_{m+1} \leq \ldots \leq \lambda_M\}$. This integral can be simplified by noticing that $p_{M,N}(\lambda_1, \ldots, \lambda_M)$ explicit expression (2.20) is invariant by permutation of its parameters $\lambda_1, \ldots, \lambda_M$, in particular by permutation of its parameters $\lambda_{m+1}, \ldots, \lambda_M$. Therefore, noting $\mathcal{S} = \mathrm{Sym}(\{\lambda_{m+1}, \ldots, \lambda_M\})$ the group of permutations over the finite set $\{\lambda_{m+1}, \ldots, \lambda_M\}$, we get

$$\begin{aligned} &\int_{b/\rho}^{+\infty} \cdots \int_{b/\rho}^{+\infty} p_{M,N}(\lambda_1, \ldots, \lambda_M)\, d\lambda_{m+1} \ldots d\lambda_M \\ &\qquad = \sum_{s\in\mathcal{S}} \int_{s(\lambda_{m+1},\ldots,\lambda_M)\in\mathcal{D}} p_{M,N}(\lambda_1, \ldots, \lambda_M)\, d\lambda_{m+1} \ldots d\lambda_M \\ &\qquad = \mathrm{Card}(\mathcal{S}) \int_{(\lambda_{m+1},\ldots,\lambda_M)\in\mathcal{D}} p_{M,N}(\lambda_1, \ldots, \lambda_M)\, d\lambda_{m+1} \ldots d\lambda_M \\ &\qquad = (M-m)! \int_{(\lambda_{m+1},\ldots,\lambda_M)\in\mathcal{D}} p_{M,N}(\lambda_1, \ldots, \lambda_M)\, d\lambda_{m+1} \ldots d\lambda_M. \end{aligned} \tag{2.22}$$

Using (2.21) and (2.22) in (2.19), we obtain

$$\mathbb{P}\left(\sum_{k=1}^{m}\rho\lambda_k < b\right) \geq \frac{1}{(M-m)!}\int_{\mathcal{C}_m}\int_{b/\rho}^{+\infty}\cdots\int_{b/\rho}^{+\infty} p_{M,N}(\lambda_1,\ldots,\lambda_M)\,d\lambda_1\ldots d\lambda_M.$$

We now replace $p_{M,N}$ by its explicit expression (2.20) and then try to separate the m first eigenvalues from the others. Note that we can drop the constants $(M-m)!$ and $K_{M,N}$ as we only need an asymptotic lower bound.

$$\begin{aligned}\mathbb{P}\left(\sum_{k=1}^{m}\rho\lambda_k < b\right) &\dot{\geq} \int_{\mathcal{C}_m}\int_{b/\rho}^{+\infty}\cdots\int_{b/\rho}^{+\infty}\prod_{i=1}^{M}\left(\lambda_i^{N-M}e^{-\lambda_i}\right)\prod_{i<j}(\lambda_i-\lambda_j)^2\,d\lambda_1\ldots d\lambda_M \\ &= \int_{\mathcal{C}_m}\int_{b/\rho}^{+\infty}\cdots\int_{b/\rho}^{+\infty}\left(\prod_{i=1}^{m}\left(\lambda_i^{N-M}e^{-\lambda_i}\right)\prod_{i<j\leq m}(\lambda_i-\lambda_j)^2\right) \\ &\quad\cdot\left(\prod_{i=m+1}^{M}\left(\lambda_i^{N-M}e^{-\lambda_i}\right)\prod_{i\leq m<j}(\lambda_i-\lambda_j)^2\prod_{m<i<j}(\lambda_i-\lambda_j)^2\right)d\lambda_1\ldots d\lambda_M\end{aligned}$$

For $i \leq m < j$, we have that $\lambda_i \leq b/\rho$ and thus $(\lambda_i-\lambda_j)^2 \geq \left(\lambda_j-\frac{b}{\rho}\right)^2$. Hence,

$$\begin{aligned}\mathbb{P}\left(\sum_{k=1}^{m}\rho\lambda_k < b\right) &\dot{\geq} \left(\int_{\mathcal{C}_m}\prod_{i=1}^{m}\left(\lambda_i^{N-M}e^{-\lambda_i}\right)\prod_{i<j\leq m}(\lambda_i-\lambda_j)^2\,d\lambda_1\ldots d\lambda_m\right) \\ &\quad\cdot\left(\int_{b/\rho}^{+\infty}\cdots\int_{b/\rho}^{+\infty}\prod_{i=m+1}^{M}\left(\lambda_i^{N-M}e^{-\lambda_i}\right)\prod_{j=m+1}^{M}\left(\lambda_j-\frac{b}{\rho}\right)^{2m}\prod_{m<i<j}(\lambda_i-\lambda_j)^2\,d\lambda_{m+1}\ldots d\lambda_M\right)\end{aligned} \tag{2.23}$$

We now have two separate integrals. We first consider the second one, in which we make the substitution $\beta_i = \lambda_i - b/\rho$ for $i = m+1,\ldots,M$.

$$\begin{aligned}&\int_{b/\rho}^{+\infty}\cdots\int_{b/\rho}^{+\infty}\prod_{i=m+1}^{M}\left(\lambda_i^{N-M}e^{-\lambda_i}\right)\prod_{j=m+1}^{M}\left(\lambda_j-\frac{b}{\rho}\right)^{2m}\prod_{m<i<j}(\lambda_i-\lambda_j)^2\,d\lambda_{m+1}\ldots d\lambda_M \\ &\quad= e^{-(M-m)b/\rho}\int_{0}^{+\infty}\cdots\int_{0}^{+\infty}\prod_{i=m+1}^{M}\left(\left(\beta_i+\tfrac{b}{\rho}\right)^{N-M}e^{-\beta_i}\beta_i^{2m}\right)\prod_{m<i<j}(\beta_i-\beta_j)^2\,d\beta_{m+1}\ldots d\beta_M \\ &\quad\geq \frac{1}{2}\int_{0}^{+\infty}\cdots\int_{0}^{+\infty}\prod_{i=m+1}^{M}\left(\beta_i^{N-M+2m}e^{-\beta_i}\right)\prod_{m<i<j}(\beta_i-\beta_j)^2\,d\beta_{m+1}\ldots d\beta_M\end{aligned} \tag{2.24}$$

for ρ large enough, i.e. such that $e^{-(M-m)b/\rho} > 1/2$. It is straightforward to see that the integral in (2.24) is nonzero, finite, independent from ρ and therefore asymptotically equivalent to 1 in the sense of (2.1). Hence, we can drop the second integral in (2.23), leading to:

$$\mathbb{P}\left(\sum_{k=1}^{m}\rho\lambda_k < b\right) \dot{\geq} \int_{\mathcal{C}_m}\prod_{i=1}^{m}\left(\lambda_i^{N-M}e^{-\lambda_i}\right)\prod_{i<j\leq m}(\lambda_i-\lambda_j)^2\,d\lambda_1\ldots d\lambda_m. \tag{2.25}$$

Making the substitution $\alpha_i = \rho\lambda_i$ for $i = 1, \ldots, m$ in (2.25) and noting $\mathcal{C}'_m = \{\alpha_1, \ldots, \alpha_m : \ 0 < \alpha_1 \leq \ldots \leq \alpha_m, \ \sum_{k=1}^m \alpha_k < b\}$ we then have

$$\mathbb{P}\left(\sum_{k=1}^m \rho\lambda_k < b\right) \dot{\geq} \left(\rho^{-m-m(N-M)-m(m-1)} \int_{\mathcal{C}'_m} \prod_{i=1}^m \left(\alpha_i^{N-M} e^{-\alpha_i/\rho}\right) \prod_{i<j\leq m} (\alpha_i - \alpha_j)^2 \, d\alpha_1 \ldots d\alpha_m\right)$$

$$\geq \rho^{-m(N-M+m)} \int_{\mathcal{C}'_m} \prod_{i=1}^m \left(\alpha_i^{N-M} e^{-\alpha_i}\right) \prod_{i<j\leq m} (\alpha_i - \alpha_j)^2 \, d\alpha_1 \ldots d\alpha_m \tag{2.26}$$

for $\rho \geq 1$, as we have then $e^{-\alpha_i/\rho} \geq e^{-\alpha_i}$ for $i = 1, \ldots, m$. As $b > 0$ it is straightforward to see that the integral in (2.26) is nonzero but also finite and independent from ρ; it is therefore asymptotically equivalent to 1 in the sense of (2.1), yielding

$$\mathbb{P}\left(\sum_{k=1}^m \rho\lambda_k < b\right) \dot{\geq} \rho^{-m(N-M+m)},$$

which concludes the proof.

2.B Asymptotic upper bound for $\mathbb{P}(\rho\lambda_m < b)$

We prove in this section that $\mathbb{P}(\mathcal{B}_1) \dot{\leq} \rho^{-m(M-N+m)}$, where the set $\mathcal{B}_1$ is defined by

$$\mathcal{B}_1 = \{\lambda_1 \leq \lambda_2 \ldots \leq \lambda_M, \, 0 < \lambda_k \leq b, \, k = 1, \ldots, m\},$$

with $b > 0$ and $\lambda_1, \ldots, \lambda_M$ the ordered eigenvalues of the Wishart matrix $\mathbf{H}^*\mathbf{H}$. We use the same approach as in Appendix 2.A. For we note $p_{M,N}$ the joint probability density function of the ordered eigenvalues of a $M \times M$ Wishart matrix with scale matrix $\mathbf{I}_M$ and N degrees of freedom, the probability $\mathbb{P}(\mathcal{B}_1)$ can be written as

$$\mathbb{P}(\mathcal{B}_1) = \int_{(\lambda_1,\ldots,\lambda_M)\in\mathcal{B}_1} p_{M,N}(\lambda_1, \ldots, \lambda_M) \, d\lambda_1 \ldots d\lambda_M.$$

Similarly to Appendix 2.A we try to upper bound $\mathbb{P}(\mathcal{B}_1)$ by the product of two integrals, one containing the m first eigenvalues and the other the $M - m$ remaining eigenvalues. We first replace $p_{M,N}$ by it explicit expression (2.20):

$$\mathbb{P}(\mathcal{B}_1) = K_{M,N}^{-1} \int_{(\lambda_1,\ldots,\lambda_M)\in\mathcal{B}_1} \prod_{i=1}^M \lambda_i^{N-M} e^{-\lambda_i} \prod_{i<j} (\lambda_i - \lambda_j)^2 \, d\lambda_1 \ldots d\lambda_M$$

$$\doteq \int_{(\lambda_1,\ldots,\lambda_M)\in\mathcal{B}_1} \left(\prod_{i=1}^m \left(\lambda_i^{N-M} e^{-\lambda_i}\right) \prod_{i<j\leq m} (\lambda_i - \lambda_j)^2\right)$$

$$\cdot \left(\prod_{i=m+1}^M \left(\lambda_i^{N-M} e^{-\lambda_i}\right) \prod_{i\leq m<j} (\lambda_i - \lambda_j)^2 \prod_{m<i<j} (\lambda_i - \lambda_j)^2\right) d\lambda_1 \ldots d\lambda_M.$$

Note that we dropped the normalizing constant $K_{M,N}$, as $K_{M,N}^{-1} \doteq 1$. For $i \leq m < j$, we have $|\lambda_i - \lambda_j| \leq \lambda_j$ and thus $\prod_{i\leq m<j}(\lambda_i-\lambda_j)^2 \leq \prod_{j=m+1}^{M} \lambda_j^{2m}$, yielding

$$\mathbb{P}(\mathcal{B}_1) \dot{\leq} \int_0^{b/\rho}\int_{\lambda_1}^{b/\rho}\cdots\int_{\lambda_{m-1}}^{b/\rho}\int_{\lambda_m}^{+\infty}\cdots\int_{\lambda_{M-1}}^{+\infty}\left(\prod_{i=1}^{m}\left(\lambda_i^{N-M}e^{-\lambda_i}\right)\prod_{i<j\leq m}(\lambda_i-\lambda_j)^2\right)$$
$$\cdot\left(\prod_{i=m+1}^{M}\left(\lambda_i^{N+2m-M}e^{-\lambda_i}\right)\prod_{m<i<j}(\lambda_i-\lambda_j)^2\right)d\lambda_1\ldots d\lambda_M$$

In order to obtain two separate integrals we discard the λ_m in the integral bound simply by noticing that $\lambda_m > 0$, therefore

$$\mathbb{P}(\mathcal{B}_1) \dot{\leq} \left(\int_0^{b/\rho}\int_{\lambda_1}^{b/\rho}\cdots\int_{\lambda_{m-1}}^{b/\rho}\prod_{i=1}^{m}\left(\lambda_i^{N-M}e^{-\lambda_i}\right)\prod_{i<j\leq m}(\lambda_i-\lambda_j)^2\,d\lambda_1\ldots d\lambda_m\right)$$
$$\cdot\left(\int_0^{+\infty}\int_{\lambda_{m+1}}^{+\infty}\cdots\int_{\lambda_{M-1}}^{+\infty}\prod_{i=m+1}^{M}\left(\lambda_i^{N+2m-M}e^{-\lambda_i}\right)\prod_{m<i<j}(\lambda_i-\lambda_j)^2\,d\lambda_{m+1}\ldots d\lambda_M\right)$$

As the second integral (in λ_{m+1}, …, λ_M) is nonzero, finite and independent of ρ it is asymptotically equivalent to 1 in the sense of (2.1). Hence,

$$\mathbb{P}(\mathcal{B}_1) \dot{\leq} \int_0^{b/\rho}\int_{\lambda_1}^{b/\rho}\cdots\int_{\lambda_{m-1}}^{b/\rho}\prod_{i=1}^{m}\left(\lambda_i^{N-M}e^{-\lambda_i}\right)\prod_{i<j\leq m}(\lambda_i-\lambda_j)^2\,d\lambda_1\ldots d\lambda_m. \tag{2.27}$$

We now make the substitutions $\alpha_i = \rho\lambda_i$ for $i = 1, \ldots, m$ inside the remaining integral.

$$\begin{aligned}
&\int_0^{b/\rho}\int_{\lambda_1}^{b/\rho}\cdots\int_{\lambda_{m-1}}^{b/\rho}\prod_{i=1}^{m}\left(\lambda_i^{N-M}e^{-\lambda_i}\right)\prod_{i<j\leq m}(\lambda_i-\lambda_j)^2\,d\lambda_1\ldots d\lambda_m \\
&= \rho^{-m(N-M+m)}\int_0^{b}\int_{\alpha_1}^{b}\cdots\int_{\alpha_{m-1}}^{b}\prod_{i=1}^{m}\left(\alpha_i^{N-M}e^{-\alpha_i/\rho}\right)\prod_{i<j\leq m}(\alpha_i-\alpha_j)^2\,d\alpha_1\ldots d\alpha_m \\
&\leq \rho^{-m(N-M+m)}\int_0^{b}\int_{\alpha_1}^{b}\cdots\int_{\alpha_{m-1}}^{b}\prod_{i=1}^{m}\alpha_i^{N-M}\prod_{i<j\leq m}(\alpha_i-\alpha_j)^2\,d\alpha_1\ldots d\alpha_m,
\end{aligned} \tag{2.28}$$

as $e^{-\alpha_i/\rho} \leq 1$. The remaining integral in (2.28) is nonzero ($b > 0$), finite and does not depend on ρ; therefore, (2.28) is asymptotically equivalent to $\rho^{-m(N-M+m)}$ in the sense of (2.1). Coming back to (2.27) we obtain

$$\mathbb{P}(\mathcal{B}_1) \dot{\leq} \rho^{-m(N-M+m)}.$$

2.C Angular parameterization of $\mathbf{u}_{M-1}$

In this appendix, we review the results of [80, 81] for the reader's convenience.

It has been shown in [80] that any $n \times n$ unitary matrix A_n can be written as

$$A_n = d_n \mathcal{O}_n \begin{bmatrix} 1 & 0 \\ 0 & A_{n-1} \end{bmatrix}, \tag{2.29}$$

with A_{n-1} a $(n-1) \times (n-1)$ unitary matrix, d_n a diagonal phases matrix, that is $d_n = \mathrm{diag}(e^{i\varphi_1}, \ldots, e^{i\varphi_n})$ with $\varphi_1, \ldots, \varphi_n \in [0, 2\pi]$, and $\mathcal{O}_n$ an orthogonal matrix (the angles matrix). Matrix $\mathcal{O}_n$ can be written in terms of parameters $\theta_1, \ldots, \theta_n \in [0, \frac{\pi}{2}]$ thanks to the following decomposition:

$$\mathcal{O}_n = J_{n-1,n} J_{n-2,n-1} \ldots J_{1,2},$$

where

$$J_{i,i+1} = \begin{bmatrix} \mathbf{I}_{i-1} & 0 & 0 & 0 \\ 0 & \cos\theta_i & -\sin\theta_i & 0 \\ 0 & \cos\theta_i & -\sin\theta_i & 0 \\ 0 & 0 & 0 & \mathbf{I}_{n-i-1} \end{bmatrix}.$$

Let $\mathbf{U}_M$ be a $M \times M$ unitary Haar distributed matrix. Then, using decomposition (2.29),

$$\mathbf{U}_M = \mathbf{D}_M(\boldsymbol{\varphi}_1) \mathbf{V}_M(\boldsymbol{\theta}_1) \begin{bmatrix} 1 & 0 \\ 0 & \mathbf{U}_{M-1} \end{bmatrix},$$

with $\boldsymbol{\varphi}_1 = (\varphi_{1,1}, \ldots, \varphi_{1,M}) \in [0, 2\pi]^M$, $\boldsymbol{\theta}_1 = (\theta_{1,1}, \ldots, \theta_{1,M-1}) \in [0, \frac{\pi}{2}]^{M-1}$, $\mathbf{D}_M(\boldsymbol{\varphi}_1)$ the diagonal matrix defined by $\mathbf{D}_M(\boldsymbol{\varphi}_1) = \mathrm{diag}(e^{i\varphi_{1,1}}, \ldots, e^{i\varphi_{1,M}})$, $\mathbf{V}_M(\boldsymbol{\theta}_1)$ the orthogonal matrix defined by $\mathbf{V}_M(\boldsymbol{\theta}_1) = J_{M-1,M} J_{M-2,M-1} \ldots J_{1,2}$ and $\mathbf{U}_M$ a $M-1 \times M-1$ unitary matrix. Matrix $\mathbf{U}_{M-1}$ can naturally be similarly factorized.

Similarly to [81], we can show that, in order $\mathbf{U}_M$ to be a Haar matrix it is sufficient that $(\varphi_{1,i})_{i=1,\ldots,M}$ are i.i.d. random variables uniformly distributed over interval $[0, 2\pi[$, that $\theta_{1,1}, \ldots, \theta_{1,M-1}$ are independent with densities respectively equal to $(\sin\theta_1)^{M-2}$, $(\sin\theta_2)^{M-3}$, …, $(\sin\theta_{M-2})$, 1 and independent from $\boldsymbol{\varphi}_1$ and that $\mathbf{U}_{M-1}$ is Haar distributed and independent from $\boldsymbol{\varphi}_1$ and $\boldsymbol{\theta}_1$. The proof consists in first showing, by a simple variable change, that if the $(\varphi_{1,i})_{i=1,\ldots,M}$ and the $\theta_{1,1}, \ldots, \theta_{1,M-1}$ follow the mentioned distributions then $\mathbf{D}_M(\boldsymbol{\varphi}_1)\mathbf{V}_M(\boldsymbol{\theta}_1)$ is uniformly distributed over the unity sphere of $\mathbb{C}^M$. The proof is then completed by showing that if $\mathbf{U}_{M-1}$ is a Haar matrix independent from $\boldsymbol{\varphi}_1$ and θ_1 then $\mathbf{U}_M$ is Haar distributed.

Finally one can parameterize a Haar matrix $\mathbf{U}_M$ by $\boldsymbol{\varphi}_1$, θ_1 and $\mathbf{U}_{M-1}$. Repeating the same parameterization for $\mathbf{U}_{M-1}$ we obtain that $\mathbf{U}_M$ can be parameterized by the M^2 following independent variables

$$(\varphi_{1,1}, \ldots, \varphi_{1,M}), (\theta_{1,1}, \ldots, \theta_{1,M-1}), (\varphi_{2,1}, \ldots, \varphi_{2,M-1}), (\theta_{2,1}, \ldots, \theta_{2,M-2}), \ldots,$$
$$(\varphi_{M-2,1}, \varphi_{M-2,2}), \theta_{M-2,1}, \varphi_{M-1,1},$$

whose probability laws are almost surely positive.

Chapter 3

The SAIC/MAIC Alamouti concept

ORTHOGONAL space-time block codes (STBC), and the Alamouti scheme in particular, are of particular interest in Multiple-Input Multiple-Output (MIMO) systems since they achieve full spatial diversity over fading channels and are decoded from linear processing at the receiver. Nevertheless, due to the expensive spectral resource, increasing network capacity requires the development of interference cancellation techniques allowing several users to share the same spectral resources without impacting the transmission quality. In this context several interference cancellation schemes have been developed during this last decade, where each user is equipped with multiple antennas and employs STBC at transmission. However, these IC techniques require multiple antennas at reception, which remains a challenge at the handset level due to cost and size limitations. For this reason, low complexity Single Antenna Interference Cancellation (SAIC) techniques, currently operational in GSM handsets, have been developed recently for single antenna users using real-valued modulations or complex filtering of real-valued modulations, by using a widely linear (WL) filtering at reception. Extension to multiple antennas at reception is called Multiple Antenna Interference Cancellation (MAIC) technique. The purpose of this chapter is to extend the SAIC/MAIC technology to users using both real-valued constellations, such as Amplitude Shift Keying (ASK) constellations, and the Alamouti scheme at transmission.

3.1 Introduction

Increasing network capacity without requiring additional bandwidth is a great challenge for wireless networks, due to the expensive spectral resource,. This motivates the development of IC techniques allowing several users to share the same spectral resources without impacting the transmission quality of each user. In this context several IC schemes allowing $P+1$ users to share the same channel at a given time, have been developed during this last decade, where each user is equipped with M antennas

and employs STBC at transmission [40–47, 82]. In such environments, it has been shown in [48] that each user can be demodulated with M-order diversity if the receiver is equipped with $N = MP + 1$ antennas. However the number of receiving antennas can be reduced if the STBC structure is exploited. Indeed, in this case, to provide M-order diversity gain and suppress P co-channel space-time users with M transmit antennas, the required number of antennas at the receiver becomes $N = P + 1$. Such an IC scheme has been proposed in [40, 42] for a two antennas receiver and for two co-channel users, each equipped with two transmit antennas and applying the Alamouti STBC [38]. A generalization of this scheme to a higher number of users from $N > P$ receive antennas has been proposed in [43], whereas alternative approaches are presented in [47]. A multi-user receiver having similar properties has been proposed in [82] for CDMA systems. Finally an IC scheme allowing a receiver with $N > P$ antennas to separate $P + 1$ transmitted signals, each equipped with $M > 2$ transmit antennas and employing quasi-orthogonal STBC [49, 50], is presented in [46]. As indicated above, available IC techniques compatible with STBC schemes at transmission require multiple antennas at reception. However, if this is not a strong constraint at the base station level, it remains a challenge at the handset level due to cost and size limitations. For this reason, SAIC techniques, alternative to the complex ML multi-user demodulation technique [51], are still of interest for 4G wireless networks using the MIMO technology and STBC in particular.

SAIC techniques have received significant attention in recent years for the reception of several single antenna and single carrier (SC) users [52–56]. Among these techniques, those which exploit the second order (SO) non-circularity [57] (or impropriety [83]) property of real-valued modulation, such as Binary Phase Shift Keying (BPSK) or Amplitude Shift Keying (ASK) modulations, or of modulations corresponding, after a derotation operation, to a complex filtering of real-valued modulations, such as Minimum Shift Keying (MSK), Gaussian MSK (GMSK) or Offset Quadrature Amplitude Modulations (OQAM) [58], have received a particular attention [52, 54–56]. These techniques implement an optimal WL filtering [59] of the observations and allow the separation of two users from only one receive antenna [54]. The powerfulness of this concept jointly with its low complexity are the reasons why the 3G Americas [60] has presented the SAIC technology as a great improvement for GSM mobile station receivers allowing significant network's capacity gains for the GSM system [55, 67]. This technology has been standardized in 2005 for GSM and is currently operational in most of GSM handsets. A further standardization of this technology, called MUROS (Multi-User Reusing One Slot), is currently under investigation to make several GSM users reuse the same TDMA slot. Extension of the SAIC concept to a multi-antennas reception is called MAIC [54] and is of great interest for GPRS networks in particular [61].

As SAIC technology remains of great interest for 4G wireless networks, an extension of this technology to Orthogonal Frequency Division Multiplex (OFDM) transmissions using one transmit antenna and the real-valued ASK modulation has been presented very recently in [62]. Despite of the fact that ASK

modulation is less power efficient than a corresponding complex QAM modulation, since only one real dimension is used for data transmission, additional degrees of freedom are available and can be exploited for interference suppression at the receiver. Besides, it has been reported in [63] for DS-CDMA transmissions, in [64] for V-BLAST-based MIMO systems and in [62] for OFDM links, that transmission with real-valued data symbols using a WL receiver can lead to a higher spectral efficiency than using a complex symbol alphabet with linear receivers in multiuser contexts. As a consequence, the use of ASK constellations coupled with WL receivers instead of complex ones with linear receivers does not seem to be a limitation and may even bring advantages in terms of error probability and spectral efficiency, in multi-user environments.

In the context of MIMO systems, WL receivers have been used very recently, implicitly or explicitly, in [64, 84–87] to improve the reception of an user which uses the V-BLAST spatial multiplexing technology [88]. In [84,87] a WL receiver is used to exploit the SO non-circularity property exhibited by the noise which is generated by the successive interference cancellation process used to jointly demodulate the parallel independent data streams generated by the V-BLAST scheme. In [64, 85, 86] a WL receiver is used to exploit the SO non-circularity of the transmitted symbols, assumed to be real-valued. For transmission with STBC, WL receivers have been used in [65, 89, 90] for equalization purposes of frequency selective propagation channels, in [91] to decode Linear Dispersion STBC and in [40, 42, 45, 47] for IC purposes. In [89, 90], the use of WL receivers is motivated by the presence of real-valued symbols at the transmitter whereas in [40, 42, 45, 47, 65, 91], WL receivers are used to exploit the structural SO non-circularity property of the signals generated by the Alamouti scheme or some linear dispersion STBC respectively. However, despite of these works, the extension of the SAIC/MAIC technology to transmission with STBC, such as the Alamouti scheme, has not been developed.

The purpose of this chapter is to extend the SAIC and MAIC technologies, currently available and described in [54] for Single-Input Single-Output (SISO) and Single-Input Multiple-Outputs (SIMO) links respectively, to Multiple-Inputs Single-Output (MISO) and MIMO links respectively, which use both real-valued constellations, such as ASK constellations, and the Alamouti scheme. Note that the Alamouti MIMO-MAIC technology allows to mitigate both intra-network Alamouti and external interferences. More precisely, we introduce in this chapter a WL MMSE receiver, completely new for IC purposes in the context of Alamouti transmissions, and we study its link with the ML Alamouti receiver. We show in particular that, in the presence of synchronous Alamouti intra-network interferences, this WL receiver implements the ML receiver and outperforms both the existing WL receivers of the literature and the SAIC/MAIC receiver described in [54]. The proposed WL receiver is shown to be able to separate up to $2N$ synchronous Alamouti users from a receiver with N antennas, displaying the capability to do, for $N = 1$, SAIC of one synchronous Alamouti intra-network interference. We then provide a simple geometrical interpretation of this receiver in order to better understand its behavior. A performance analysis, in terms of SINR and SER, in the presence of Alamouti intra-network interferences and an

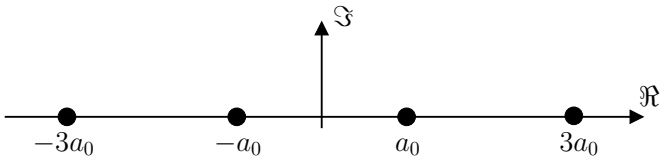

Figure 3.1: 4-ASK constellation

adaptive implementation of the proposed WL receiver complete the results.

After introducing the observation model, data statistics and WL filters in section 3.2, the proposed WL MMSE receiver jointly with its adaptive implementation are presented in section 3.3 and briefly compared with both the existing WL Alamouti receivers of the literature and the SAIC/MAIC receiver described in [54]. The link between the proposed WL MMSE receiver and the ML Alamouti receiver is analyzed in section 3.4. The maximal number of interferences which may be processed by the proposed WL MMSE receiver jointly with an analytical performance analysis of the latter in the presence of one or several synchronous Alamouti intra-network interferences respectively are presented in section 3.5. Finally, section 3.6 concludes the chapter. The main results of the chapter have been patented in [92] and presented in [93–95].

3.2 Problem Statement

In this section we first state the hypotheses required for our system model, before presenting three spatio-temporal observation models. We eventually define the second order statistics of the observations and of the total noise.

3.2.1 Hypotheses

We consider a radio communication system that employs a real-valued constellation (e.g. the 4-ASK constellation depicted on Fig. 3.1) and the well-known Alamouti scheme [38] with $M = 2$ transmit antennas and N receive antennas, as depicted on Fig. 3.2. We denote by T the symbol period. We assume either flat fading propagation channels with a single-carrier waveform and square-root Nyquist filter at both transmitter and receiver, or, equivalently, frequency selective propagation channels with an OFDM waveform, then considering the system sub-carrier by sub-carrier thanks to the Discrete Fourier

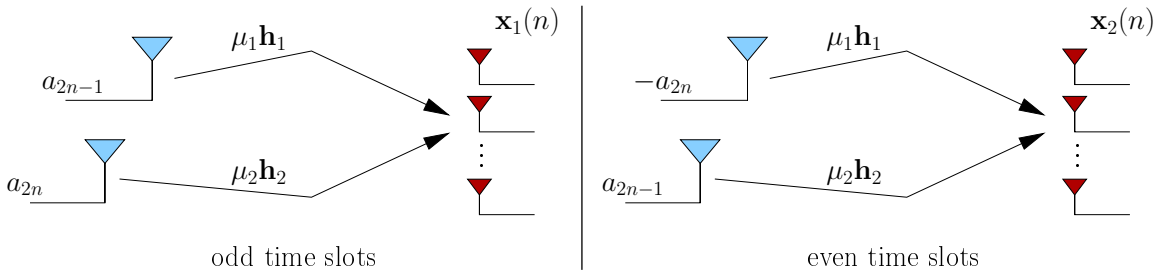

Figure 3.2: Alamouti scheme

Transform. The waveforms are assumed to be narrow-band at transmitter and receiver, that is the propagation delay between two transmit or two receive antennas reduces to a simple phase shift. The channel is assumed invariant over at least two successive symbol periods (and typically a burst). In addition we assume ideal timing and frequency information. Under these assumptions the observation vectors sampled at time $(2n-1)T$ and $2nT$, respectively denoted $\mathbf{x}_1(n)$ and $\mathbf{x}_2(n)$, can be written as

$$\begin{cases} \mathbf{x}_1(n) = \mu_1 a_{2n-1}\mathbf{h}_1 + \mu_2 a_{2n}\mathbf{h}_2 + \mathbf{b}_1(n) \\ \mathbf{x}_2(n) = -\mu_1 a_{2n}\mathbf{h}_1 + \mu_2 a_{2n-1}\mathbf{h}_2 + \mathbf{b}_2(n) \end{cases} \tag{3.1}$$

where $\mathbf{x}_1(n)$ and $\mathbf{x}_2(n)$ are the $N \times 1$ observation vectors at symbol periods $(2n-1)T$ and $2nT$ respectively, the quantities a_n are i.i.d real-valued random variables corresponding to the transmitted symbols, $\mu_{i\,(i=1,2)}$ is a real scalar which controls the power of the two transmitted signals received by the array of antennas; $\mathbf{h}_{i\,(i=1,2)}$, such that $\mathbb{E}[\mathbf{h}_i^H\mathbf{h}_i] = N$, is the normalized propagation channel vector between transmit antenna i and the receive array of antennas; $\mathbf{A}^H$ is the conjugate transpose of $\mathbf{A}$; $\mathbf{b}_1(n)$ and $\mathbf{b}_2(n)$ are the sampled total noise vector at sample times $(2n-1)T$ and $2nT$ respectively, potentially composed of intra-network interferences, external interferences (not generated by the network itself) and background noise.

All along this chapter, $\mathbf{R_{uv}}$ and $\mathbf{C_{uv}}$ are the correlation matrices defined by $\mathbf{R_{uv}} = \mathbb{E}_c[\mathbf{u}\mathbf{v}^H]$, $\mathbf{C_{uv}} = \mathbb{E}_c[\mathbf{u}\mathbf{v}^T]$, where $\mathbf{u}$ and $\mathbf{v}$ are vectors of same size, where $\mathbb{E}_c(\cdot)$ is the conditional expected value with respect to the channel vectors of the sources and where ^{T} means transpose. Moreover, we respectively denote by $\mathbf{R_v}$ and $\mathbf{C_v}$ the correlation matrices $\mathbf{R_{vv}}$ and $\mathbf{C_{vv}}$. Note that, in order to simplify the notations, we may not always mention the dependency in n of the variables.

3.2.2 Observation models

We here introduce the three spatio-temporal (ST) observation models used along this chapter, together with their associated filtering.

a) Basic observation model

We first note that the observation system (3.1) can be reduced into a simple observation vector $\mathbf{x}(n)$, where $\mathbf{x}(n)$ is the concatenation of $\mathbf{x}_1(n)$ and $\mathbf{x}_2(n)$:

$$\mathbf{x} = \begin{bmatrix} \mathbf{x}_1 \\ \mathbf{x}_2 \end{bmatrix}. \tag{3.2}$$

We note $\pi_s = \pi_a(\mu_1^2 + \mu_2^2)/2$, with $\pi_a = \mathbb{E}[a_n^2]$, the mean power of each useful symbol per receive antenna. Defining the $2N \times 1$ vectors, $\mathbf{x}(n)$, $\mathbf{b}(n)$, $\mathbf{f}_1$, $\mathbf{f}_2$ and the 2×1 vector $\mathbf{a}(n)$ by $\mathbf{x} = [\mathbf{x}_1^T, \mathbf{x}_2^T]^T$, $\mathbf{b} = [\mathbf{b}_1^T, \mathbf{b}_2^T]^T$, $\mathbf{f}_1 = \sqrt{\pi_a/\pi_s}[\mu_1 \mathbf{h}_1^T, \mu_2 \mathbf{h}_2^T]^T$, $\mathbf{f}_2 = \sqrt{\pi_a/\pi_s}[\mu_2 \mathbf{h}_2^T, -\mu_1 \mathbf{h}_1^T]^T$ and $\mathbf{a}(n) = [a_{2n-1}, a_{2n}]^T$, system (3.1) can be written in the following form:

$$\begin{aligned} \mathbf{x}(n) &= \sqrt{\pi_s/\pi_a}(a_{2n-1}\mathbf{f}_1 + a_{2n}\mathbf{f}_2) + \mathbf{b}(n) \\ &= \sqrt{\pi_s/\pi_a}\ \mathbf{F}\mathbf{a}(n) + \mathbf{b}(n), \end{aligned} \tag{3.3}$$

where the $2N \times 2$ matrix $\mathbf{F}$ is simply defined by $\mathbf{F} = [\mathbf{f}_1, \mathbf{f}_2]$. The filtering of $\mathbf{x}$ is called a linear filtering in the following.

b) Classical observation model

Nonetheless most of Alamouti receivers currently available for interference cancellation of intra-network interferences, see, e.g., [40, 42, 43, 82], use the classical observation model; they exploit the information contained in the $2N \times 1$ ST observation vector $\overline{\mathbf{x}}(n)$, defined by

$$\overline{\mathbf{x}} = \begin{bmatrix} \mathbf{x}_1 \\ \mathbf{x}_2^* \end{bmatrix}. \tag{3.4}$$

Defining the $2N \times 1$ vectors $\overline{\mathbf{b}}(n)$, $\mathbf{g}_1$ and $\mathbf{g}_2$ by $\overline{\mathbf{b}} = [\mathbf{b}_1^T, \mathbf{b}_2^H]^T$, $\mathbf{g}_1 = \sqrt{\pi_a/\pi_s}[\mu_1 \mathbf{h}_1^T, \mu_2 \mathbf{h}_2^H]^T$ and $\mathbf{g}_2 = \sqrt{\pi_a/\pi_s}[\mu_2 \mathbf{h}_2^T, -\mu_1 \mathbf{h}_1^H]^T$, and defining the $2N \times 2$ matrix $\mathbf{G}$ by $\mathbf{G} = [\mathbf{g}_1, \mathbf{g}_2]$, system (3.1) can be written in a more compact form.

$$\begin{aligned} \overline{\mathbf{x}}(n) &= \sqrt{\pi_s/\pi_a}\,(a_{2n-1}\mathbf{g}_1 + a_{2n}\mathbf{g}_2) + \overline{\mathbf{b}}(n), \\ &= \sqrt{\pi_s/\pi_a}\ \mathbf{G}\mathbf{a}(n) + \overline{\mathbf{b}}(n). \end{aligned} \tag{3.5}$$

The filtering of $\overline{\mathbf{x}}$ is hereafter called a partially Widely Linear (WL) filtering.

Table 3.1: Observation models

Observation	Expression	N_e	Filtering
$\mathbf{x} = \begin{bmatrix} \mathbf{x}_1 \\ \mathbf{x}_2 \end{bmatrix}$	$= \sqrt{\frac{\pi_s}{\pi_a}}(a_{2n-1}\mathbf{f}_1 + a_{2n}\mathbf{f}_2) + \mathbf{b}(n) \quad = \sqrt{\frac{\pi_s}{\pi_a}}\mathbf{F}\mathbf{a}(n) + \mathbf{b}(n)$	$2N$	linear
$\overline{\mathbf{x}} = \begin{bmatrix} \mathbf{x}_1 \\ \mathbf{x}_2^* \end{bmatrix}$	$= \sqrt{\frac{\pi_s}{\pi_a}}\,(a_{2n-1}\mathbf{g}_1 + a_{2n}\mathbf{g}_2) + \overline{\mathbf{b}}(n) \quad = \sqrt{\frac{\pi_s}{\pi_a}}\mathbf{G}\mathbf{a}(n) + \overline{\mathbf{b}}(n)$	$2N$	partially WL
$\tilde{\mathbf{x}} = \begin{bmatrix} \mathbf{x} \\ \mathbf{x}^* \end{bmatrix}$	$= \sqrt{\frac{\pi_s}{\pi_a}}\big(a_{2n-1}\tilde{\mathbf{f}}_1 + a_{2n}\tilde{\mathbf{f}}_2\big) + \tilde{\mathbf{b}}(n) \quad = \sqrt{\frac{\pi_s}{\pi_a}}\tilde{\mathbf{F}}\mathbf{a}(n) + \tilde{\mathbf{b}}(n)$	$4N$	fully WL

c) Extended observation model

We finally introduce the extended observation model, which is the basis of the receiver presented in this chapter. This observation model is the concatenation $\tilde{\mathbf{x}}$ of $\mathbf{x}_1$, $\mathbf{x}_2$, $\mathbf{x}_1^*$, $\mathbf{x}_2^*$, that is of $\mathbf{x}$ and $\mathbf{x}^*$:

$$\tilde{\mathbf{x}} = \begin{bmatrix} \mathbf{x} \\ \mathbf{x}^* \end{bmatrix}. \tag{3.6}$$

We then define the vectors $\tilde{\mathbf{f}}_1$, $\tilde{\mathbf{f}}_2$ and $\tilde{\mathbf{b}}(n)$ of size $4N \times 1$ by $\tilde{\mathbf{f}}_1 = [\mathbf{f}_1^T, \mathbf{f}_1^H]^T$, $\tilde{\mathbf{f}}_2 = [\mathbf{f}_2^T, \mathbf{f}_2^H]^T$ and $\tilde{\mathbf{b}} = [\mathbf{b}^T, \mathbf{b}^H]^T$ respectively. Eventually, defining the $4N \times 2$ matrix $\tilde{\mathbf{F}}$ by $\tilde{\mathbf{F}} = [\tilde{\mathbf{f}}_1, \tilde{\mathbf{f}}_2]$, observation vector $\tilde{\mathbf{x}}(n)$ becomes

$$\begin{aligned} \tilde{\mathbf{x}}(n) &= \sqrt{\pi_s/\pi_a}\big(a_{2n-1}\tilde{\mathbf{f}}_1 + a_{2n}\tilde{\mathbf{f}}_2\big) + \tilde{\mathbf{b}}(n) \\ &= \sqrt{\pi_s/\pi_a}\ \tilde{\mathbf{F}}\mathbf{a}(n) + \tilde{\mathbf{b}}(n) \end{aligned} \tag{3.7}$$

We call in the following fully Widely Linear (WL) filtering the filtering of $\tilde{\mathbf{x}}$.

d) Equivalent reception model

These three ST models, which are summed up in Table 3.1, can be seen as the equivalent reception at time nT_b, where $T_b = 2T$ is the duration of a block of two symbols, of two narrow-band uncorrelated sources (a_{2n-1} and a_{2n}) by a virtual array of N_e antennas, with a mean power per receiving antenna π_s. The number of virtual receiving antennas is $N_e = 2N$ for (3.3) and (3.5), $N_e = 4N$ for (3.7). The two sources mentioned are associated with the linearly independent virtual channel vectors $\mathbf{f}_1$ and $\mathbf{f}_2$ (3.3), $\mathbf{g}_1$ and $\mathbf{g}_2$ (3.5) and $\tilde{\mathbf{f}}_1$ and $\tilde{\mathbf{f}}_2$ (3.7) respectively, and corrupted by a total noise $\mathbf{b}$, $\overline{\mathbf{b}}$ and $\tilde{\mathbf{b}}$ respectively. Note that the channel vectors are orthogonal in models (3.5) and (3.7) but not in model (3.3).

3.2.3 Second order statistics

The SO (second order) statistics of the observation system $(\mathbf{x}_1, \mathbf{x}_2)$ (3.1) correspond to the six $N \times N$ matrices $\mathbf{R}_{\mathbf{x}_1}$, $\mathbf{R}_{\mathbf{x}_2}$, $\mathbf{R}_{\mathbf{x}_1\mathbf{x}_2}$, $\mathbf{C}_{\mathbf{x}_1}$, $\mathbf{C}_{\mathbf{x}_2}$ and $\mathbf{C}_{\mathbf{x}_1\mathbf{x}_2}$. Similarly the SO statistics of the total noise correspond to the six $N \times N$ matrices $\mathbf{R}_{\mathbf{b}_1}$, $\mathbf{R}_{\mathbf{b}_2}$, $\mathbf{R}_{\mathbf{b}_1\mathbf{b}_2}$, $\mathbf{C}_{\mathbf{b}_1}$, $\mathbf{C}_{\mathbf{b}_2}$ and $\mathbf{C}_{\mathbf{b}_1\mathbf{b}_2}$. To simplify notations they are respectively denoted $\mathbf{R}_1$, $\mathbf{R}_2$, $\mathbf{R}_{12}$, $\mathbf{C}_1$, $\mathbf{C}_2$ and $\mathbf{C}_{12}$ in the following. Using (3.1) we can now write the second order statistics of the observation as

$$\mathbf{R}_{\mathbf{x}_1} = \pi_a \left(\mu_1^2 \mathbf{h}_1 \mathbf{h}_1^H + \mu_2^2 \mathbf{h}_2 \mathbf{h}_2^H\right) + \mathbf{R}_1 \tag{3.8}$$

$$\mathbf{R}_{\mathbf{x}_2} = \pi_a \left(\mu_1^2 \mathbf{h}_1 \mathbf{h}_1^H + \mu_2^2 \mathbf{h}_2 \mathbf{h}_2^H\right) + \mathbf{R}_2 \tag{3.9}$$

$$\mathbf{R}_{\mathbf{x}_1\mathbf{x}_2} = \mu_1\mu_2\pi_a \left(\mathbf{h}_1 \mathbf{h}_2^H - \mathbf{h}_2 \mathbf{h}_1^H\right) + \mathbf{R}_{12} \tag{3.10}$$

$$\mathbf{C}_{\mathbf{x}_1} = \pi_a \left(\mu_1^2 \mathbf{h}_1 \mathbf{h}_1^T + \mu_2^2 \mathbf{h}_2 \mathbf{h}_2^T\right) + \mathbf{C}_1 \tag{3.11}$$

$$\mathbf{C}_{\mathbf{x}_2} = \pi_a \left(\mu_1^2 \mathbf{h}_1 \mathbf{h}_1^T + \mu_2^2 \mathbf{h}_2 \mathbf{h}_2^T\right) + \mathbf{C}_2 \tag{3.12}$$

$$\mathbf{C}_{\mathbf{x}_1\mathbf{x}_2} = \mu_1\mu_2\pi_a \left(\mathbf{h}_1 \mathbf{h}_2^T - \mathbf{h}_2 \mathbf{h}_1^T\right) + \mathbf{C}_{12} \tag{3.13}$$

Note that, in all six second order statistics, the part related to the useful signal of the observation is nonzero in general, except in $\mathbf{C}_{\mathbf{x}_1\mathbf{x}_2}$ for $N = 1$. Naturally, this would also be the case for the part generated by a synchronous intra-network interference, which thus generate non-circular noise [57].

The $2N \times 2N$ correlation matrices $\mathbf{R}_{\mathbf{x}}$, $\mathbf{C}_{\mathbf{x}}$ and $\mathbf{R}_{\overline{\mathbf{x}}}$ can be written in terms of the SO statistics of the observation introduced above, or in terms of the correlation matrices of the noise $\mathbf{R}_{\mathbf{b}}$, $\mathbf{C}_{\mathbf{b}}$ and $\mathbf{R}_{\overline{\mathbf{b}}}$.

$$\mathbf{R}_{\mathbf{x}} = \begin{bmatrix} \mathbf{R}_{\mathbf{x}_1} & \mathbf{R}_{\mathbf{x}_1\mathbf{x}_2} \\ \mathbf{R}_{\mathbf{x}_1\mathbf{x}_2}^H & \mathbf{R}_{\mathbf{x}_2} \end{bmatrix} = \pi_s \mathbf{F}\mathbf{F}^H + \mathbf{R}_{\mathbf{b}} \tag{3.14}$$

$$\mathbf{C}_{\mathbf{x}} = \begin{bmatrix} \mathbf{C}_{\mathbf{x}_1} & \mathbf{C}_{\mathbf{x}_1\mathbf{x}_2} \\ \mathbf{C}_{\mathbf{x}_1\mathbf{x}_2}^T & \mathbf{C}_{\mathbf{x}_2} \end{bmatrix} = \pi_s \mathbf{F}\mathbf{F}^T + \mathbf{C}_{\mathbf{b}} \tag{3.15}$$

$$\mathbf{R}_{\overline{\mathbf{x}}} = \begin{bmatrix} \mathbf{R}_{\mathbf{x}_1} & \mathbf{C}_{\mathbf{x}_1\mathbf{x}_2} \\ \mathbf{C}_{\mathbf{x}_1\mathbf{x}_2}^H & \mathbf{R}_{\mathbf{x}_2}^* \end{bmatrix} = \pi_s \mathbf{G}\mathbf{G}^H + \mathbf{R}_{\overline{\mathbf{b}}} \tag{3.16}$$

Similarly the statistics of the noise $\mathbf{R}_{\mathbf{b}}$, $\mathbf{C}_{\mathbf{b}}$ and $\mathbf{R}_{\overline{\mathbf{b}}}$ can be written blockwise in terms of the SO statistics of the noise introduced earlier

$$\mathbf{R}_{\mathbf{b}} = \begin{bmatrix} \mathbf{R}_1 & \mathbf{R}_{12} \\ \mathbf{R}_{12}^H & \mathbf{R}_2 \end{bmatrix};\ \mathbf{C}_{\mathbf{b}} = \begin{bmatrix} \mathbf{C}_1 & \mathbf{C}_{12} \\ \mathbf{C}_{12}^T & \mathbf{C}_2 \end{bmatrix};\ \mathbf{R}_{\overline{\mathbf{b}}} = \begin{bmatrix} \mathbf{R}_1 & \mathbf{C}_{12} \\ \mathbf{C}_{12}^H & \mathbf{R}_2^* \end{bmatrix}. \tag{3.17}$$

The MIMO receivers of the literature [40, 42, 43, 45, 47, 82] are based on partially WL filtering, hence only taking into account the information inside $\mathbf{R}_{\overline{\mathbf{x}}}$. By (3.16) and (3.17), we see that matrix $\mathbf{R}_{\overline{\mathbf{x}}}$ contains only three of the six second order matrices of the total noise, that is, matrices $\mathbf{R}_1$, $\mathbf{R}_2$ and $\mathbf{C}_{12}$. Therefore the receivers of the literature are expected to be second order suboptimal in the presence of

another Alamouti user, i.e. for internal interferences. On the opposite, the receiver which we introduce in this chapter is based on a fully WL filtering. It thus takes into account the information contained in the $4N \times 4N$ matrix $\mathbf{R}_{\tilde{\mathbf{x}}}$, which contain all six correlation matrices of the total noise. Indeed, matrix $\mathbf{R}_{\tilde{\mathbf{x}}}$ can be written as

$$\mathbf{R}_{\tilde{\mathbf{x}}} = \begin{bmatrix} \mathbf{R}_{\mathbf{x}} & \mathbf{C}_{\mathbf{x}} \\ \mathbf{C}_{\mathbf{x}}^* & \mathbf{R}_{\mathbf{x}}^* \end{bmatrix} = \pi_s \tilde{\mathbf{F}} \tilde{\mathbf{F}}^H + \mathbf{R}_{\tilde{\mathbf{b}}} \tag{3.18}$$

and matrix $\mathbf{R}_{\tilde{\mathbf{b}}}$ is given by

$$\mathbf{R}_{\tilde{\mathbf{b}}} = \begin{bmatrix} \mathbf{R}_{\mathbf{b}} & \mathbf{C}_{\mathbf{b}} \\ \mathbf{C}_{\mathbf{b}}^* & \mathbf{R}_{\mathbf{b}}^* \end{bmatrix}. \tag{3.19}$$

Note that, performing a blockwise inversion of $\mathbf{R}_{\tilde{\mathbf{b}}}$, we can write matrix $\mathbf{R}_{\tilde{\mathbf{b}}}^{-1}$, which we will use a lot in the following, under the following form:

$$\mathbf{R}_{\tilde{\mathbf{b}}}^{-1} = \begin{bmatrix} \mathbf{A} & \mathbf{D} \\ \mathbf{D}^* & \mathbf{A}^* \end{bmatrix}, \tag{3.20}$$

where the $2N \times 2N$ complex matrices $\mathbf{A}$ and $\mathbf{D}$ are given respectively by

$$\mathbf{A} = (\mathbf{R}_{\mathbf{b}} - \mathbf{C}_{\mathbf{b}} \mathbf{R}_{\mathbf{b}}^{-*} \mathbf{C}_{\mathbf{b}}^*)^{-1}, \tag{3.21}$$

$$\mathbf{D} = -\mathbf{A} \mathbf{C}_{\mathbf{b}} \mathbf{R}_{\mathbf{b}}^{-*}. \tag{3.22}$$

Matrices $\mathbf{A}$ and $\mathbf{D}$ respectively verify $\mathbf{A}^H = \mathbf{A}$ and $\mathbf{D}^T = \mathbf{D}$. Note that, as $\mathbf{R}_{\tilde{\mathbf{b}}}$ has the same block structure as $\mathbf{R}_{\tilde{\mathbf{x}}}$ (see (3.18)), we have a similar result for the structure of $\mathbf{R}_{\tilde{\mathbf{x}}}^{-1}$.

3.3 The MMSE Alamouti receivers

In this section we first recall some results about MMSE receivers, then present the MMSE Alamouti receivers of the literature before introducing a new WL MMSE Alamouti receiver called Fully WL MMSE Alamouti receiver. We outline the breakthrough of this new receiver. We finally present an adaptive implementation of the Fully WL MMSE Alamouti receiver. Note that all along this chapter we only consider the receivers for the estimation of symbol a_{2n-1}, as the analysis for the estimation of symbol a_{2n} is very similar, if not identical.

3.3.1 About MMSE receivers

A MMSE receiver implements a ML (Maximum Likelihood) estimation from the output y of a MMSE filter. The MMSE filter of $\mathbf{u}$ is the filter linear in $\mathbf{u}$ minimizing the Mean Square Error between its output

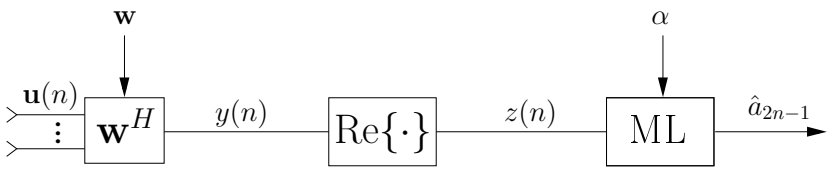

Figure 3.3: MMSE receiver structure

y and the symbol a to estimate. The MMSE filter of $\mathbf{u}$ for the estimation of symbol a_{2n-1} can be written as

$$\mathbf{w} = \mathbf{R}_{\mathbf{u}}^{-1}\mathbf{R}_{\mathbf{u}\,a_{2n-1}}. \tag{3.23}$$

We hereafter respectively call Linear MMSE, Partially WL MMMSE and Fully WL MMSE filters the MMSE filters of $\mathbf{x}$, $\overline{\mathbf{x}}$ and $\tilde{\mathbf{x}}$ for the estimation of symbol a_{2n-1}.

The vector carrying a_{2n-1} in $\mathbf{u}$ can be obtained by simply deriving $\mathbf{R}_{\mathbf{u}\,a_{2n-1}}/\pi_a$. Hence, looking at the output y of the MMSE filter, we have

$$\begin{aligned} y &= \mathbf{w}^H \frac{\mathbf{R}_{\mathbf{u}\,a_{2n-1}}}{\pi_a} a_{2n-1} + b(n) \\ &= \alpha\, a_{2n-1} + b(n), \end{aligned} \tag{3.24}$$

where $b(n)$ is the global noise at the output of the filter and where $\alpha = \mathbf{w}^H\mathbf{R}_{\mathbf{u}\,a_{2n-1}}/\pi_a = \mathbf{R}_{\mathbf{u}\,a_{2n-1}}^H \mathbf{R}_{\mathbf{u}}^{-1}\mathbf{R}_{\mathbf{u}\,a_{2n-1}}/\pi_a$. Parameter α is therefore real positive. Assuming the global noise $b(n)$ Gaussian, the ML estimation of a_{2n-1} from output y then generates the symbol a_{2n-1} minimizing $|\alpha\, a_{2n-1} - y(n)|^2$, or, equivalently, as α is real positive and as a_{2n-1} is real, minimizing the following metric:

$$C_{mmse}(a_{2n-1}) = \alpha\, a_{2n-1}^2 - 2a_{2n-1}\mathrm{Re}\{y(n)\}. \tag{3.25}$$

Hence, $z(n) = \mathrm{Re}\{y(n)\}$ is a sufficient statistic for the MMSE receiver. Furthermore, $z(n) = \mathrm{Re}\{\alpha\, a_{2n-1} + b(n)\} = \alpha\, a_{2n-1} + \mathrm{Re}\{b(n)\}$. Assuming that the real part of the global noise $\mathrm{Re}\{b(n)\}$ is Gaussian, the ML estimate of a_{2n-1} from $z(n)$ corresponds to the minimization of (3.25). We can therefore consider that $z(n)$ is the output of the MMSE receiver and thus display the MMSE receiver estimating a_{2n-1} from observation $\mathbf{u}$ as in Fig. 3.3.

As seen on Fig. 3.3, the MMSE receiver requires the knowledge of parameters α and $\mathbf{w}$. In practice the receiver needs to estimate these parameters from the observations. This is not restrictive in practice for the estimation of $\mathbf{w}$, nevertheless an accurate estimation of α generally requires a great number of training symbols. Therefore we also consider the Approximated MMSE receiver, which generates symbol a_{2n-1} minimizing (3.25), but where α has been replaced by 1, that is minimizing $a_{2n-1}^2 -$

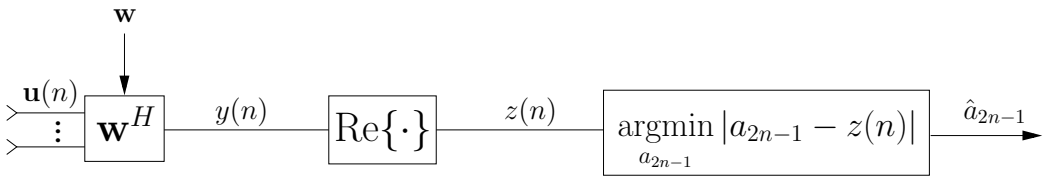

Figure 3.4: Approximated MMSE receiver structure

$2a_{2n-1}\mathrm{Re}\{y(n)\}$. Minimizing this metric is equivalent to minimizing $|a_{2n-1}-y(n)|^2$, or also, as a_{2n-1} is real, to minimizing the following Approximated MMSE metric:

$$C_{a-mmse}(a_{2n-1}) = |a_{2n-1} - z(n)|, \tag{3.26}$$

The structure of the MMSE receiver is therefore simplified and the Approximated MMSE receiver can be modeled by Fig. 3.4. Furthermore, if the Signal to Global noise ratio in $\mathbf{u}$ is high, we have $\mathbf{R}_{\mathbf{u}} \simeq \mathbf{R}_{\mathbf{u}\,a_{2n-1}}\mathbf{R}^H_{\mathbf{u}\,a_{2n-1}}/\pi_a$. Hence, for high Signal to Global noise ratios, $\alpha = \mathbf{R}^H_{\mathbf{u}\,a_{2n-1}}\mathbf{R}^{-1}_{\mathbf{u}}\mathbf{R}_{\mathbf{u}\,a_{2n-1}}/\pi_a \simeq 1$ and the approximated MMSE metric approximately corresponds to the MMSE metric.

3.3.2 Alamouti MMSE receivers of the literature

The Alamouti MMSE receivers available in the literature to demodulate symbol a_{2n-1} in the presence of internal interferences are all based on a partially WL MMSE filter [40, 42, 45, 47], which can be written as

$$\begin{aligned}\overline{\mathbf{w}}_{pwl} &= \mathbf{R}^{-1}_{\overline{\mathbf{x}}}\mathbf{R}_{\overline{\mathbf{x}}a_{2n-1}} \\ &= \sqrt{\pi_s\pi_a}\,\mathbf{R}^{-1}_{\overline{\mathbf{x}}}\mathbf{g}_1\end{aligned} \tag{3.27}$$

The output of this MMSE filter is then

$$\begin{aligned}y_{pwl}(n) &= \overline{\mathbf{w}}^H_{pwl}\overline{\mathbf{x}}(n) \\ &= \pi_s\left(a_{2n-1}\mathbf{g}_1^H\mathbf{R}^{-1}_{\overline{\mathbf{x}}}\mathbf{g}_1 + a_{2n}\mathbf{g}_1^H\mathbf{R}^{-1}_{\overline{\mathbf{x}}}\mathbf{g}_2\right) + \sqrt{\pi_s\pi_a}\,\mathbf{g}_1^H\mathbf{R}^{-1}_{\overline{\mathbf{x}}}\overline{\mathbf{b}}(n)\end{aligned} \tag{3.28}$$

We call the MMSE receiver related to $\overline{\mathbf{w}}_{pwl}$ the P-WL-MMSE (Partially WL MMSE) receiver. It generates the symbol a_{2n-1} minimizing the following metric:

$$C_{pwl}(a_{2n-1}) = \pi_s\mathbf{g}_1^H\mathbf{R}^{-1}_{\overline{\mathbf{x}}}\mathbf{g}_1 a^2_{2n-1} - 2a_{2n-1}z_{pwl}(n), \tag{3.29}$$

where z_{pwl} is defined as the real part of y_{pwl}:

$$z_{pwl} = \mathrm{Re}\{y_{pwl}\} = \mathrm{Re}\left\{\overline{\mathbf{w}}^H_{pwl}\overline{\mathbf{x}}(n)\right\} \tag{3.30}$$

This corresponds to a ML decision from the output $z_{pwl}(n)$; we therefore consider z_{pwl} as the output of the P-WL-MMSE receiver in the following. This P-WL-MMSE receiver only takes into account the information contained in $\mathbf{R}_{\overline{\mathbf{x}}}$. By (3.16) and (3.17), it therefore only considers the noise information contained in matrices $\mathbf{R}_1$, $\mathbf{R}_2$ and $\mathbf{C}_{12}$, but not the one in matrices $\mathbf{C}_1$, $\mathbf{C}_2$ and $\mathbf{R}_{12}$; it is thus sub-optimal in the presence of synchronous internal interferences in particular.

We now introduce the Approximated P-WL-MMSE receiver (AP-WL-MMSE). If the Signal to Global Noise Ratio is high, i.e. if $\mathbf{g}_1^H(\mathbf{R}_{\overline{\mathbf{b}}} + \pi_s \mathbf{g}_2 \mathbf{g}_2^H)^{-1}\mathbf{g}_1 \gg 1$, we have $\pi_s \mathbf{g}_1^H \mathbf{R}_{\overline{\mathbf{x}}}^{-1}\mathbf{g}_1 \simeq 1$. This justifies the Approximated MMSE receiver approach presented in 3.3.1, which corresponds here to minimizing the simple following metric:

$$C_{a-pwl}(a_{2n-1}) = |a_{2n-1} - z_{pwl}(n)| \tag{3.31}$$

where we recall that $z_{pwl} = \mathrm{Re}\{y_{pwl}\}$.

A possible alternative to the P-WL-MMSE receiver is the Linear MMSE (L-MMSE) receiver, based on the Linear MMSE filter $\mathbf{w}_{mmse}$ defined by

$$\mathbf{w}_{mmse} = \mathbf{R}_{\mathbf{x}}^{-1}\mathbf{R}_{\mathbf{x}a_{2n-1}} = \sqrt{\pi_s \pi_a}\, \mathbf{R}_{\mathbf{x}}^{-1}\mathbf{f}_1. \tag{3.32}$$

The L-MMSE receiver then generates symbol a_{2n-1} minimizing the following metric

$$C_l(a_{2n-1}) = \pi_s \mathbf{f}_1^H \mathbf{R}_{\mathbf{x}}^{-1}\mathbf{f}_1 a_{2n-1}^2 - 2a_{2n-1} z_l(n), \tag{3.33}$$

where $z_l(n)$ is the output of the Linear MMSE filter, defined by

$$z_l(n) = \mathrm{Re}\left\{\mathbf{w}_{mmse}^H \mathbf{x}(n)\right\}. \tag{3.34}$$

Nonetheless, such a receiver is not really considered in the literature, as the orthogonality of the Alamouti code is lost in this approach. Moreover, it only takes into account the information contained in $\mathbf{R}_{\mathbf{x}}^{-1}$, i.e. in matrices $\mathbf{R}_{\mathbf{x}_1}$, $\mathbf{R}_{\mathbf{x}_2}$ and $\mathbf{R}_{\mathbf{x}_1\mathbf{x}_2}$, but not the information contained in matrices $\mathbf{C}_{\mathbf{x}_1}$, $\mathbf{C}_{\mathbf{x}_2}$ and $\mathbf{C}_{\mathbf{x}_1\mathbf{x}_2}$. Hence, the L-MMSE receiver is also sub-optimal in the presence of synchronous internal interferences in particular. Note that an approximated version of the L-MMSE can also be considered.

3.3.3 The Fully WL MMSE receiver

In this section we introduce a new receiver, called the Fully WL MMSE (F-WL-MMSE) receiver, based on the extended observation vector $\tilde{\mathbf{x}}(n)$ (note that a similar fully WL MMSE receiver has already been introduced in [65] but for equalization purposes in frequency selective propagation channels). Such a receiver takes into account the information contained in all six second order correlation matrices $\mathbf{R}_{\mathbf{x}_1}$, $\mathbf{R}_{\mathbf{x}_2}$, $\mathbf{R}_{\mathbf{x}_1\mathbf{x}_2}$, $\mathbf{C}_{\mathbf{x}_1}$, $\mathbf{C}_{\mathbf{x}_2}$ and $\mathbf{C}_{\mathbf{x}_1\mathbf{x}_2}$. It is thus expected to outperform the P-WL-MMSE and L-MMSE

receivers in the presence of synchronous internal interferences in particular. The F-WL-MMSE receiver is based on the Fully WL MMSE filter $\tilde{\mathbf{w}}_{fwl}$ defined by

$$\begin{aligned}\tilde{\mathbf{w}}_{fwl} &= \mathbf{R}_{\tilde{\mathbf{x}}}^{-1}\mathbf{R}_{\tilde{\mathbf{x}}a_{2n-1}} \\ &= \sqrt{\pi_s\pi_a}\,\mathbf{R}_{\tilde{\mathbf{x}}}^{-1}\tilde{\mathbf{f}}_1\end{aligned} \tag{3.35}$$

The output of the Fully WL MMSE filter is then

$$\begin{aligned}z_{fwl}(n) &= \tilde{\mathbf{w}}_{fwl}^H\tilde{\mathbf{x}}(n) \\ &= \pi_s\left(a_{2n-1}\tilde{\mathbf{f}}_1^H\mathbf{R}_{\tilde{\mathbf{x}}}^{-1}\tilde{\mathbf{f}}_1 + a_{2n}\tilde{\mathbf{f}}_1^H\mathbf{R}_{\tilde{\mathbf{x}}}^{-1}\tilde{\mathbf{f}}_2\right) + \sqrt{\pi_s\pi_a}\,\tilde{\mathbf{f}}_1^H\mathbf{R}_{\tilde{\mathbf{x}}}^{-1}\tilde{\mathbf{b}}(n)\end{aligned} \tag{3.36}$$

Note that $z_{fwl}(n)$ is real. We have indeed $\tilde{\mathbf{w}}_{fwl} = [\mathbf{w}_{fwl}^T, \mathbf{w}_{fwl}^H]^T$, as $\mathbf{R}_{\tilde{\mathbf{x}}}^{-1}$ has the same block structure as $\mathbf{R}_{\tilde{\mathbf{b}}}^{-1}$ (3.20), yielding

$$z_{fwl}(n) = 2\mathrm{Re}\{y_{fwl}\}, \tag{3.37}$$

where $y_{fwl} = \mathbf{w}_{fwl}^H\mathbf{x}$. The F-WL-MMSE receiver implements a ML estimation from the output $z_{fwl}(n)$. The ML estimation generates the symbol a_{2n-1} minimizing the following (real) metric:

$$C_{fwl}(a_{2n-1}) = \pi_s\tilde{\mathbf{f}}_1^H\mathbf{R}_{\tilde{\mathbf{x}}}^{-1}\tilde{\mathbf{f}}_1 a_{2n-1}^2 - 2a_{2n-1}z_{fwl}(n). \tag{3.38}$$

As mentioned in 3.3.1, we also consider an approximated version of the F-WL-MMSE receiver. If the Signal to Global Noise Ratio is high, i.e. if $\tilde{\mathbf{f}}_1^H(\mathbf{R}_{\tilde{\mathbf{b}}} + \pi_s\tilde{\mathbf{f}}_2\tilde{\mathbf{f}}_2^H)^{-1}\tilde{\mathbf{f}}_1 \gg 1$, we have $\pi_s\tilde{\mathbf{f}}_1^H\mathbf{R}_{\tilde{\mathbf{x}}}^{-1}\tilde{\mathbf{f}}_1 \simeq 1$. In this case the metric (3.38) can be approximated by $a_{2n-1}^2 - 2a_{2n-1}z_{fwl}(n)$, giving rise to the so-called Approximated F-WL-MMSE receiver (AF-WL-MMSE). This Approximated MMSE receiver generates the symbol a_{2n-1} minimizing the simple following metric:

$$C_{a-fwl}(a_{2n-1}) = |a_{2n-1} - z_{fwl}(n)|. \tag{3.39}$$

3.3.4 The F-WL-MMSE receiver, a breakthrough

The available Alamouti receivers of the literature (the P-WL-MMSE receivers, see 3.3.2) fully exploit the orthogonal STBC structure of the Alamouti scheme but do not make good use of the real-valued nature of the constellations. They are therefore sub-optimal: they cannot separate more than N Alamouti users from N receive antennas. SAIC (Single Antenna Interference Cancellation, i.e. interference cancellation for $N = 1$) is thus impossible for these receivers.

On the opposite, the WL MMSE receiver presented in [54], introduced for synchronous single antenna users using real-valued constellations, fully exploits the real-valued nature of the sources symbols and is able to separate up to $2N$ single antenna users from N receive antennas, hence its SAIC capability of one internal interference. However this receiver is not exploiting the present STBC structure; the P

Alamouti users with real-valued symbols are seen as $2P$ uncorrelated single antenna users. Hence, it cannot separate more than N Alamouti users from N antennas and therefore cannot perform SAIC.

As for the F-WL-MMSE receiver, it exploits both the real-valued nature of the sources symbols and the orthogonal STBC nature of the Alamouti scheme. This breakthrough with respect to the receivers of the literature allows this new receiver to separate up to $2N$ Alamouti users from N receive antennas – this rejection capacity will be shown later in section 3.5.2. The F-WL-MMSE receiver can therefore perform SAIC of one intra-network Alamouti interference, giving rise to the Alamouti SAIC concept. Its extension to a number $N > 1$ of receiving antennas will be called the Alamouti MAIC (Multiple Antenna Interference Cancellation) concept.

3.3.5 Adaptive implementation of the MMSE Alamouti receivers

We already mentioned in section 3.3.1 that in situations of practical interest the considered MMSE receivers need to estimate several parameters:

- the associated MMSE filter,
- the parameter α which appears in the MMSE filter output.

We noted $\mathbf{w}$ the MMSE filter estimating a_{2n-1} from observation $\mathbf{u}$ in the general case; $\mathbf{w}$ is given by (3.23). Assuming the channels constant over the burst, the receivers need to perform the estimation for each burst. To that end the receiver uses M couples of training symbols (a_{2m-1}, a_{2m}) which are available for each burst. Noting M_0 the position of the first couple of training symbols in the burst we have $M_0 \leq m < M_0 + M$. In these conditions, an estimate $\widehat{\mathbf{w}}$ of the MMSE Alamouti filter $\mathbf{w}$ may be obtained by

$$\widehat{\mathbf{w}} = \widehat{\mathbf{R}}_{\mathbf{u}}^{-1} \widehat{\mathbf{R}}_{\mathbf{u}\, a_{2n-1}}, \tag{3.40}$$

where $\widehat{\mathbf{R}}_{\mathbf{u}}$ and $\widehat{\mathbf{R}}_{\mathbf{u}\, a_{2n-1}}$ are defined by

$$\widehat{\mathbf{R}}_{\mathbf{u}} = \frac{1}{M} \sum_{m=M_0}^{M_0+M-1} \mathbf{u}(m)\, \mathbf{u}(m)^H,$$

$$\widehat{\mathbf{R}}_{\mathbf{u}\, a_{2n-1}} = \frac{1}{M} \sum_{m=M_0}^{M_0+M-1} \mathbf{u}(m)\, a_{2m-1}.$$

The quick convergence speed of $\widehat{\mathbf{w}}$ will be later shown in the simulations by the Approximated MMSE receivers (section c)). An attempt to explain this result is that the estimation error in $\widehat{\mathbf{R}}_{\mathbf{u}}$ somehow compensates the estimation error in $\widehat{\mathbf{R}}_{\mathbf{u}\, a_{2n-1}}$, thanks to the inversion of matrix $\widehat{\mathbf{R}}_{\mathbf{u}}$.

An estimate $\widehat{\alpha}$ of parameter α can be similarly obtained. As $\alpha = \mathbf{w}^H \mathbf{R}_{\mathbf{u}\, a_{2n-1}}/\pi_a$, we can estimate α with $\widehat{\alpha}$, which is defined by:

$$\widehat{\alpha} = \frac{\widehat{\mathbf{w}}^H \widehat{\mathbf{R}}_{\mathbf{u}\, a_{2n-1}}}{\pi_a}. \tag{3.41}$$

However, contrary to the estimation of $\mathbf{w}$, an accurate estimation of α requires in practice a high number of training symbols, as already mentioned earlier in section 3.3.1.

3.4 MMSE Alamouti receivers vs. the ML Alamouti receiver

We outlined in previous section that the F-WL-MMSE receiver introduced is a breakthrough with respect to the receivers of the literature. We now prove that this new receiver is even optimal in the ML sense in some cases of practical interest. To that end we first introduce and analyze the ML Alamouti receiver before comparing it to the MMSE Alamouti receivers introduced in previous section.

3.4.1 The ML Alamouti receiver

We compute in this section the ML receiver for the demodulation of a real-valued Alamouti signal corrupted by potential intra-network and external interferences. As explained in section 3.2.3, in the presence of synchronous intra-network interferences matrix $\mathbf{C_b}$ is nonzero: the total noise vector $\mathbf{b}(n)$ becomes SO non-circular. Assuming a Gaussian and non-circular vector $\mathbf{b}(n)$, although the intra-network interferences are not Gaussian, the probability density of $\tilde{\mathbf{b}}(n)$, i.e. the joint probability density of the real and imaginary part of $\mathbf{b}(n)$, becomes [96, 97]:

$$p\left[\tilde{\mathbf{b}}(n)\right] = \left(\pi^{2N}\sqrt{\det(\mathbf{R}_{\tilde{\mathbf{b}}})\, \exp\left(\tilde{\mathbf{b}}^H \mathbf{R}_{\tilde{\mathbf{b}}}^{-1} \tilde{\mathbf{b}}\right)}\right)^{-1} \tag{3.42}$$

where $\det(\mathbf{A})$ means determinant of $\mathbf{A}$. Besides, as $\tilde{\mathbf{x}}(n) = \sqrt{\pi_s/\pi_a}\, \tilde{\mathbf{F}}\mathbf{a}(n) + \tilde{\mathbf{b}}(n)$ (see (3.7)), the ML receiver for the demodulation of vector $\mathbf{a}(n) = [a_{2n-1}, a_{2n}]^T$ in SO non-circular total noise is such that $\mathbf{a}(n)$ maximizes the ML criterion defined by

$$C_{nc-ml}(\mathbf{a}(n)) = p\left[\tilde{\mathbf{b}}(n) = \tilde{\mathbf{x}}(n) - \sqrt{\frac{\pi_s}{\pi_a}}\tilde{\mathbf{F}}\mathbf{a}(n) \Big/ \mathbf{a}(n)\right] \tag{3.43}$$

Using (3.42), we easily deduce that the maximization of (3.43) is equivalent to the minimization of the following ML criterion

$$\begin{aligned} C_{ml}(\mathbf{a}(n)) =& a_{2n-1}^2\, \tilde{\mathbf{f}}_1^H \mathbf{R}_{\tilde{\mathbf{b}}}^{-1} \tilde{\mathbf{f}}_1 + a_{2n}^2\, \tilde{\mathbf{f}}_2^H \mathbf{R}_{\tilde{\mathbf{b}}}^{-1} \tilde{\mathbf{f}}_2 + 2a_{2n-1}a_{2n} \tilde{\mathbf{f}}_1^H \mathbf{R}_{\tilde{\mathbf{b}}}^{-1} \tilde{\mathbf{f}}_2 \\ & - 2\sqrt{\frac{\pi_a}{\pi_s}} \left(a_{2n-1} \tilde{\mathbf{f}}_1^H \mathbf{R}_{\tilde{\mathbf{b}}}^{-1} \tilde{\mathbf{x}}(n) + a_{2n} \tilde{\mathbf{f}}_2^H \mathbf{R}_{\tilde{\mathbf{b}}}^{-1} \tilde{\mathbf{x}}(n)\right). \end{aligned} \tag{3.44}$$

Note that it is straightforward to see from (3.20) that $\tilde{\mathbf{f}}_1^H \mathbf{R}_{\tilde{\mathbf{b}}}^{-1} \tilde{\mathbf{f}}_2$, $\tilde{\mathbf{f}}_1^H \mathbf{R}_{\tilde{\mathbf{b}}}^{-1} \tilde{\mathbf{x}}(n)$ and $\tilde{\mathbf{f}}_2^H \mathbf{R}_{\tilde{\mathbf{b}}}^{-1} \tilde{\mathbf{x}}(n)$ are real-valued quantities. The ML receiver exploits all the information contained in $\mathbf{R}_{\tilde{\mathbf{b}}}$, i.e. in $\mathbf{R}_1$, $\mathbf{R}_2$, $\mathbf{R}_{12}$, $\mathbf{C}_1$, $\mathbf{C}_2$ and $\mathbf{C}_{12}$. It is a coupled receiver in the general case of arbitrary matrix $\mathbf{R}_{\tilde{\mathbf{b}}}$ and vectors $\mu_1 \mathbf{h}_1$ and $\mu_2 \mathbf{h}_2$, i.e. it requires the joint estimation of a_{2n-1} and a_{2n}. This generates K^2 tests for vector $\mathbf{a}(n)$, where K is the number of states of the constellation.

a) Decoupling condition of the ML receiver

We now derive the condition which decouples the ML receiver, i.e. the condition under which the ML receiver reduces to two separate and independent ML receivers for the estimation of a_{2n-1} and a_{2n} respectively. Indeed, as the MMSE Alamouti receivers estimate symbols a_{2n-1} and a_{2n} separately, the ML receiver needs to be decoupled in order to correspond to a MMSE Alamouti receiver.

We deduce from (3.44) that the minimization of $C_{ml}(\mathbf{a}(n))$ reduces to two independent minimizations of $C_{ml,1}(a_{2n-1})$ and $C_{ml,2}(a_{2n})$ when the following condition $C1$ is verified.

$$C1: \ \tilde{\mathbf{f}}_1^H \mathbf{R}_{\tilde{\mathbf{b}}}^{-1} \tilde{\mathbf{f}}_2 = 0 \tag{3.45}$$

The two metrics $C_{ml,1}(a_{2n-1})$ and $C_{ml,2}(a_{2n})$ are then defined by

$$C_{ml,1}(a_{2n-1}) = a_{2n-1}^2 \sqrt{\frac{\pi_s}{\pi_a}} \tilde{\mathbf{f}}_1^H \mathbf{R}_{\tilde{\mathbf{b}}}^{-1} \tilde{\mathbf{f}}_1 - 2\, a_{2n-1} \tilde{\mathbf{f}}_1^H \mathbf{R}_{\tilde{\mathbf{b}}}^{-1} \tilde{\mathbf{x}}(n) \tag{3.46}$$

$$C_{ml,2}(a_{2n}) = a_{2n}^2 \sqrt{\frac{\pi_s}{\pi_a}} \tilde{\mathbf{f}}_2^H \mathbf{R}_{\tilde{\mathbf{b}}}^{-1} \tilde{\mathbf{f}}_2 - 2\, a_{2n} \tilde{\mathbf{f}}_2^H \mathbf{R}_{\tilde{\mathbf{b}}}^{-1} \tilde{\mathbf{x}}(n) \tag{3.47}$$

It is shown in Appendix 3.A that condition $C1$ is in particular verified in the absence of interferences or in the presence of an arbitrary number of synchronous intra-network interferences. In such situations, the ML receiver becomes decoupled. This reduces in particular the complexity of the search procedure to the test of $2K$ possibilities for $\mathbf{a}(n)$ instead of K^2.

As in previous section we now focus on the estimation of a_{2n-1} through metric (3.46). Indeed, the analysis of the estimation of a_{2n} would provide the same results. To get a better insight of metric (3.46) we define the $4N \times 1$ fully WL filter $\tilde{\mathbf{w}}_{ml}$ defined by

$$\tilde{\mathbf{w}}_{ml} = \mathbf{R}_{\tilde{\mathbf{b}}}^{-1} \tilde{\mathbf{f}}_1.$$

Note that, thanks to $\mathbf{R}_{\tilde{\mathbf{b}}}^{-1}$ structure (3.20), filter $\tilde{\mathbf{w}}_{ml}$ can also be written as

$$\tilde{\mathbf{w}}_{ml} = \begin{bmatrix} \mathbf{w}_{ml} \\ \mathbf{w}_{ml}^* \end{bmatrix}, \tag{3.48}$$

where $\mathbf{w}_{ml} = [\mathbf{A}, \mathbf{D}]\tilde{\mathbf{f}}_1$. The output $z_{ml}(n)$ of this filter is therefore real-valued:

$$z_{ml}(n) = \tilde{\mathbf{w}}_{ml}^H \tilde{\mathbf{x}}(n) = 2\mathrm{Re}\{\mathbf{w}_{ml}^H \mathbf{x}(n)\}. \tag{3.49}$$

Using (3.7) this output can also be written

$$z_{ml}(n) = a_{2n-1}\sqrt{\frac{\pi_s}{\pi_a}}\,\tilde{\mathbf{f}}_1^H \mathbf{R}_{\tilde{\mathbf{b}}}^{-1}\tilde{\mathbf{f}}_1 + b_{ml}(n).$$

where $b_{ml}(n) = a_{2n}\sqrt{\frac{\pi_s}{\pi_a}}\,\tilde{\mathbf{f}}_1^H \mathbf{R}_{\tilde{\mathbf{b}}}^{-1}\tilde{\mathbf{f}}_2 + \tilde{\mathbf{f}}_1^H \mathbf{R}_{\tilde{\mathbf{b}}}^{-1}\tilde{\mathbf{b}}(n)$ is the global noise in the output z_{ml} for the estimation of symbol a_{2n-1}. Similarly to the MMSE receivers in section 3.3.1, assuming a Gaussian global noise $b_{ml}(n)$, an ML estimate of a_{2n-1} from $z_{ml}(n)$ generates the symbol a_{2n-1} minimizing $|a_{2n-1}\sqrt{\pi_s/\pi_a}\,\tilde{\mathbf{f}}_1^H \mathbf{R}_{\tilde{\mathbf{b}}}^{-1}\tilde{\mathbf{f}}_1 - z_{ml}(n)|^2$ or, equivalently, minimizing the following metric:

$$a_{2n-1}^2\sqrt{\frac{\pi_s}{\pi_a}}\,\tilde{\mathbf{f}}_1^H \mathbf{R}_{\tilde{\mathbf{b}}}^{-1}\tilde{\mathbf{f}}_1 - 2a_{2n-1}z_{ml}(n).$$

This is equivalent to minimizing $C_{ml,1}(a_{2n-1})$ defined in (3.46); the symbol a_{2n-1} which minimizes (3.46) therefore corresponds to the ML estimate of a_{2n-1} from $z_{ml}(n)$, which can thus be referred to as the output of the decoupled ML receiver.

b) Specific case of a SO circular temporally and spatially white noise

We now consider the particular case of a SO circular, temporally and spatially white background noise with no interferences. In such a case, $\mathbf{R}_{\mathbf{b}} = \sigma^2\mathbf{I}$ and $\mathbf{C}_{\mathbf{b}} = 0$, where σ^2 is the mean power of the noise per receive antenna. This generates $\mathbf{R}_{\tilde{\mathbf{b}}}$ such that $\mathbf{R}_{\tilde{\mathbf{b}}} = \sigma^2\mathbf{I}$. In this case, condition $C1$ is verified since

$$\tilde{\mathbf{f}}_1^H \mathbf{R}_{\tilde{\mathbf{b}}}^{-1}\tilde{\mathbf{f}}_2 = \frac{2}{\sigma^2}\,\mathrm{Re}\{\mathbf{f}_1^H\mathbf{f}_2\} = 0.$$

In this specific case, minimizing metric (3.46) is then equivalent to minimizing metric $C_{conv,1}(a_{2n-1})$, defined by

$$\begin{aligned} C_{conv,1}(a_{2n-1}) &= a_{2n-1}^2\sqrt{\frac{\pi_s}{\pi_a}}\,\mathbf{f}_1^H\mathbf{f}_1 - 2a_{2n-1}\,\mathrm{Re}\{\mathbf{f}_1^H\mathbf{x}(n)\} \\ &= a_{2n-1}^2\sqrt{\frac{\pi_s}{\pi_a}}\,\mathbf{g}_1^H\mathbf{g}_1 - 2a_{2n-1}\,\mathrm{Re}\{\mathbf{g}_1^H\overline{\mathbf{x}}(n)\}. \end{aligned} \tag{3.50}$$

This metric corresponds to the metric of the Conventional Alamouti receiver [38], that we hereafter denote CONV receiver. The symbol a_{2n-1} minimizing (3.50) corresponds to the ML estimate of a_{2n-1} from the output $y_{conv}(n)$ of filter $\mathbf{w}_{conv} = \mathbf{g}_1$ applied on observation $\overline{\mathbf{x}}(n)$, which can be written as

$$\begin{aligned} y_{conv}(n) &= \mathbf{g}_1^H\overline{\mathbf{x}}(n) \\ &= a_{2n-1}\sqrt{\frac{\pi_s}{\pi_a}}\,\mathbf{g}_1^H\mathbf{g}_1 + \mathbf{g}_1^H\overline{\mathbf{b}}(n), \end{aligned} \tag{3.51}$$

It also corresponds to the ML estimate of a_{2n-1} from $z_{conv}(n)$ defined by

$$z_{conv}(n) = \mathrm{Re}\{y_{conv}(n)\}. \tag{3.52}$$

We can thus consider z_{conv} as being the output of the CONV receiver. Note that $z_{conv}(n)$ is also equal to $\mathrm{Re}\{\mathbf{f}_1^H \mathbf{x}(n)\}$.

3.4.2 Optimality conditions of the F-WL-MMSE receiver

We analyze in this section the conditions under which the F-WL-MMSE Alamouti receiver corresponds to the ML Alamouti receiver. To that end, as $\mathbf{w}_{fwl}$ definition (3.35) involves matrix $\mathbf{R}_{\tilde{\mathbf{x}}}^{-1}$, we apply the matrix inversion Lemma to $\mathbf{R}_{\tilde{\mathbf{x}}} = \pi_s \mathbf{F}\mathbf{F}^H + \mathbf{R}_{\tilde{\mathbf{b}}} = \pi_s \tilde{\mathbf{f}}_1 \tilde{\mathbf{f}}_1^H + \pi_s \tilde{\mathbf{f}}_2 \tilde{\mathbf{f}}_2^H + \mathbf{R}_{\tilde{\mathbf{b}}}$ (3.18), yielding:

$$\mathbf{R}_{\tilde{\mathbf{x}}}^{-1} \tilde{\mathbf{f}}_1 = \frac{1}{1 + \pi_s \tilde{\mathbf{f}}_1^H \left(\pi_s \tilde{\mathbf{f}}_2 \tilde{\mathbf{f}}_2^H + \mathbf{R}_{\tilde{\mathbf{b}}} \right)^{-1} \tilde{\mathbf{f}}_1} \left(\mathbf{R}_{\tilde{\mathbf{b}}}^{-1} \tilde{\mathbf{f}}_1 - \frac{\pi_s \tilde{\mathbf{f}}_2^H \mathbf{R}_{\tilde{\mathbf{b}}}^{-1} \tilde{\mathbf{f}}_1}{1 + \pi_s \tilde{\mathbf{f}}_2^H \mathbf{R}_{\tilde{\mathbf{b}}}^{-1} \tilde{\mathbf{f}}_2} \mathbf{R}_{\tilde{\mathbf{b}}}^{-1} \tilde{\mathbf{f}}_2 \right). \tag{3.53}$$

We deduce from (3.53) that when condition $C1$, defined by (3.45), is verified, vectors $\tilde{\mathbf{w}}_{fwl} = \sqrt{\pi_s \pi_a}\, \mathbf{R}_{\tilde{\mathbf{x}}}^{-1} \tilde{\mathbf{f}}_1$ and $\tilde{\mathbf{w}}_{ml} = \mathbf{R}_{\tilde{\mathbf{b}}}^{-1} \tilde{\mathbf{f}}_1$ are collinear. This means that $z_{ml}(n)$, given by (3.49), and $z_{fwl}(n)$, given by (3.36), are proportional. A similar result would naturally be obtained for the filters involved in the demodulation of symbol a_{2n}. We then deduce that, when $C1$ is verified, the F-WL-MMSE receiver is optimal and corresponds to the ML receiver, whereas it remains generally sub-optimal otherwise.

For a given total noise vector $\mathbf{b}(n)$, condition $C1$ may be verified only for some particular channel vectors $\mu_1 \mathbf{h}_1$ and $\mu_2 \mathbf{h}_2$. Nevertheless, it is shown in Appendix 3.A that condition $C1$ is verified for all channel vectors $\mu_1 \mathbf{h}_1$ and $\mu_2 \mathbf{h}_2$ if and only if the total noise vector $\mathbf{b}(n)$ verifies the following condition:

$$C2 : \begin{cases} \mathbf{R}_1 = \mathbf{R}_2, \\ \mathbf{C}_1 = \mathbf{C}_2, \\ \mathbf{R}_{12}^H = -\mathbf{R}_{12}, \\ \mathbf{C}_{12}^T = -\mathbf{C}_{12}. \end{cases} \tag{3.54}$$

We deduce from (3.8), (3.9), (3.10), (3.11), (3.12) and (3.13) that condition $C2$ is in particular verified in the absence of interference for a SO circular, temporally and spatially white noise vector $\mathbf{b}(n)$. Indeed, $\mathbf{R}_1 = \mathbf{R}_2 = \sigma^2 \mathbf{I}$, $\mathbf{C}_1 = \mathbf{C}_2 = \mathbf{C}_{12} = \mathbf{R}_{12} = 0$ in this case. Condition $C2$ is also verified in the presence of one or several synchronous intra-network interferences plus SO circular, temporally and spatially white background noise. The six SO statistic matrices associated with an arbitrary synchronous intra-network interference have indeed the same algebraic structure as the six SO statistic matrices related to the useful signal in (3.8), (3.9), (3.10), (3.11), (3.12) and (3.13), which verify condition $C2$. Hence, condition $C2$ is verified in this case. Finally, condition $C2$ is still verified in the presence of external

interferences as long as $\mathbf{b}_1(n)$ and $\mathbf{b}_2(n)$ remain uncorrelated ($\mathbf{C}_{12} = \mathbf{R}_{12} = 0$) with the same SO statistics ($\mathbf{R}_1 = \mathbf{R}_2, \mathbf{C}_1 = \mathbf{C}_2$). Hence, the F-WL-MMSE receiver is optimal in numerous situations of practical interest.

3.4.3 Optimality conditions of the P-WL-MMSE and L-MMSE receivers

To give examples of situations for which the F-WL-MMSE receiver reduces to either a P-WL-MMSE or a L-MMSE receiver, we describe in this section the conditions under which the P-WL-MMSE and the L-MMSE Alamouti receivers correspond to the ML Alamouti receiver.

a) P-WL-MMSE receivers

As mentioned earlier, $\overline{\mathbf{w}}_{pwl} = \sqrt{\pi_s \pi_a}\, \mathbf{R}_{\overline{\mathbf{x}}}^{-1} \mathbf{g}_1$ only exploits the information contained in matrices $\mathbf{R}_1$, $\mathbf{R}_2$ and $\mathbf{C}_{12}$. A necessary condition for the ML/P-WL-MMSE equivalence is therefore $\mathbf{C}_1 = \mathbf{C}_2 = \mathbf{R}_{12} = 0$. We show in fact in Appendix 3.B that the P-WL-MMSE receiver is optimal and corresponds to the ML receiver if and only if condition $C3$ is verified, where $C3$ is defined by

$$C3 : \begin{cases} \mathbf{g}_1^H \mathbf{R}_{\overline{\mathbf{b}}}^{-1} \mathbf{g}_2 = 0, \\ \mathbf{C}_1 = \mathbf{C}_2 = \mathbf{R}_{12} = 0. \end{cases} \tag{3.55}$$

Otherwise, it remains generally sub-optimal.

Furthermore, we show in Appendix 3.C that condition $C3$ is verified for all channel vectors $\mu_1 \mathbf{h}_1$ and $\mu_2 \mathbf{h}_2$ if and only if the total noise vector $\mathbf{b}(n)$ verifies condition $C4$ defined by

$$C4 : \begin{cases} \mathbf{R}_1 = \mathbf{R}_2, \\ \mathbf{C}_1 = \mathbf{C}_2 = \mathbf{R}_{12} = 0. \\ \mathbf{C}_{12}^T = -\mathbf{C}_{12}. \end{cases} \tag{3.56}$$

In this case, the P-WL-MMSE receiver is optimal and the F-WL-MMSE receiver reduces in fact to a P-WL-MMSE receiver. Condition $C4$ is verified in particular in the absence of interferences for a circular, temporally and spatially white noise vector $\mathbf{b}(n)$. It is also verified in the presence of SO circular external interferences ($\mathbf{C}_1 = \mathbf{C}_2 = 0$) as long as $\mathbf{b}_1(n)$ and $\mathbf{b}_2(n)$ remain uncorrelated ($\mathbf{C}_{12} = \mathbf{R}_{12} = 0$) with the same SO statistics ($\mathbf{R}_1 = \mathbf{R}_2$, $\mathbf{C}_1 = \mathbf{C}_2$). However, the P-WL-MMSE receiver, used in [40, 42, 43, 45, 47], becomes sub-optimal in the presence of one or several synchronous intra-network interferences as we hen have $\mathbf{C}_1 = \mathbf{C}_2 \neq 0$ and $\mathbf{R}_{12} \neq 0$. It remains sub-optimal in the presence of external interferences which are either SO non-circular or such that $\mathbf{b}_1(n)$ and $\mathbf{b}_2(n)$ are correlated, which is in particular the case for very narrow-band external interferences.

b) L-MMSE receiver

Similarly, we show in Appendix 3.D that the L-MMSE receiver is optimal and corresponds to the ML receiver if and only if condition $C5$ defined by

$$C5 : \begin{cases} \mathbf{f}_1^H \mathbf{R}_{\mathbf{b}}^{-1} \mathbf{f}_2 = 0, \\ \mathbf{C}_1 = \mathbf{C}_2 = \mathbf{C}_{12} = 0. \end{cases} \tag{3.57}$$

is verified. Otherwise, it remains generally sub-optimal. Moreover, we prove in Appendix 3.E that condition $C5$ can never be optimal for all channel vectors $\mu_1 \mathbf{h}_1$ and $\mu_2 \mathbf{h}_2$, hence the interest of WL-MMSE receivers for the reception of real-valued Alamouti signals. In particular, in the presence of a SO circular, spatially and temporally white noise ($\mathbf{R}_{\mathbf{b}} = \sigma^2 \mathbf{I}$), (3.57) shows that the L-MMSE receiver is optimal only if $\mathbf{f}_1^H \mathbf{f}_2 = 0$, i.e. if $\mathrm{Im}\{\mathbf{h}_1^H \mathbf{h}_2\} = 0$, but becomes sub-optimal otherwise. In this latter case, the optimal receiver is the P-WL-MMSE receiver for which $\mathbf{g}_1^H \mathbf{g}_2 = 0$ in all cases (note that, as already mentioned, the F-WL-MMSE receiver then reduces to the P-WL-MMSE receiver).

3.5 Performance of Alamouti receivers in multiuser context

In this section we analyze the performance of the F-WL-MMSE Alamouti receiver in the presence of both synchronous intra-network and external interferences and we compare the latter to those of the receivers of the literature. We describe in a first part the total noise model. We then evaluate, in a second part, the maximal number of interferences which may be processed by the F-WL-MMSE receiver and the receivers of the literature, highlighting in particular the SAIC capability of one synchronous intra-network interference of the F-WL-MMSE Alamouti receiver. Finally, we discuss the performance of the previous receivers by first giving a simple geometrical interpretation of their behavior in the presence of one intra-network interference in a third part, then analyzing their output Signal to Interference plus Noise Ratio (SINR) and Symbol Error Rate (SER) in the presence of intra-network interferences in a fourth and fifth part respectively.

3.5.1 Total Noise Model

We assume in this section that the total noise vectors $\mathbf{b}_1(n)$ and $\mathbf{b}_2(n)$ are composed of $P = P_{int} + P_{ext}$ interferences and a background noise, where

- P_{int} is the number of synchronous intra-network (or internal) interferences, corresponding to other Alamouti users of the network with the same real-valued constellation as the useful signal,
- P_{ext} is the number of external interferences, coming from other networks or jamming.

We denote by $e_{i,n}$ the symbol n transmitted by the internal interference i and by $\mu_{2i+1}\mathbf{h}_{2i+1}$ (resp. $\mu_{2i+2}\mathbf{h}_{2i+2}$) the channel vector of internal interference i between the transmit antenna 1 (resp. 2) and the receive array of antennas. The scalar μ_{2i+1} and μ_{2i+2} are real parameters controlling the received power of the interference i coming from transmit antennas 1 and 2 respectively. The $N \times 1$ complex-valued vectors $\mathbf{h}_{2i+1}$ and $\mathbf{h}_{2i+2}$, such that $\mathbb{E}[\mathbf{h}_{2i+1}^H \mathbf{h}_{2i+1}] = \mathbb{E}[\mathbf{h}_{2i+2}^H \mathbf{h}_{2i+2}] = N$, are the associated normalized propagation channel vectors between transmit antenna 1 and 2 respectively and the receive array of antennas.

The external interference k is characterized by its complex envelope $m_k(t)$ and its $N \times 1$ complex-valued channel vector $\mathbf{j}_k$, constant over at least the duration $2T$ of a couple of symbols, and such that $\mathbb{E}[\mathbf{j}_k^H \mathbf{j}_k] = N$. An external interference k is said to be rectilinear if there exists a real ϕ_k such that $m_k(t)^* = m_k(t)e^{-j2\phi_k}$ and is said to be non-rectilinear otherwise. It is said to be coherent if there exists a real ψ_k such that $m_k(2nT) \simeq m_k((2n-1)T)e^{j\psi_k}$ and is said to be non-coherent otherwise. A coherent interference corresponds to a very narrow-band interference compared to the useful signal bandwidth. In this context, we assume that the P_{ext} external interferences are composed of

- $P_{r,c}$ rectilinear and coherent interferences,
- $P_{r,nc}$ rectilinear and non-coherent interferences,
- $P_{nr,c}$ non-rectilinear and coherent interferences,
- $P_{nr,nc}$ non-rectilinear and non coherent interferences,

such that $P_{ext} = P_{r,c} + P_{r,nc} + P_{nr,c} + P_{nr,nc}$. We also denote in the following

- $P_c = P_{r,c} + P_{nr,c}$ the number of coherent interferences,
- $P_{nc} = P_{r,nc} + P_{nr,nc}$ the number of non-coherent interferences,
- $P_{nr} = P_{nr,c} + P_{nr,nc}$ the number of non-rectilinear interferences.

3.5.2 Maximal number of interferences processed by the receivers

Under the previous assumptions, we deduce from the observation models (3.3), (3.5) and (3.7) that an internal interference generates two statistically uncorrelated interferences in vectors $\mathbf{b}(n)$, $\overline{\mathbf{b}}(n)$ and $\tilde{\mathbf{b}}(n)$ As for an external interference, it is easy to verify that the number of different interferences which

is generated in vectors $\mathbf{b}(n)$, $\overline{\mathbf{b}}(n)$ and $\tilde{\mathbf{b}}(n)$, denoted by $P_{\mathbf{b}}$, $P_{\overline{\mathbf{b}}}$ and $P_{\tilde{\mathbf{b}}}$ respectively, is such that

$$\left.\begin{array}{l} P_{\mathbf{b}} = 2P_{int} + P_c + 2P_{nc}, \\ P_{\overline{\mathbf{b}}} = 2P_{int} + P_{r,c} + 2(P_{r,nc} + P_{nr}), \\ P_{\tilde{\mathbf{b}}} = 2P_{int} + P_{r,c} + 2(P_{r,nc} + P_{nr,c}) + 4P_{nr,nc}. \end{array}\right\} \tag{3.58}$$

The F-WL-MMSE and the ML Alamouti receivers exploit in different ways the information contained in matrices $\mathbf{R}_{\tilde{\mathbf{x}}}$ or $\mathbf{R}_{\tilde{\mathbf{b}}}$ (see (3.35) and (3.44)), i.e. in the correlation matrix of the extended observation model (3.7), with or without the useful signal part. This model is associated with a virtual array of $N_e = 4N$ virtual antennas, as explained in section d), and the number of degrees of freedom available to reject interferences contained in $\tilde{\mathbf{b}}(n)$ is $N_e - 2$ for the two latter receivers. Indeed, for the ML receiver and in the absence of background noise, as one can see in (3.44) the space spanned by the interferences contained in $\tilde{\mathbf{b}}(n)$ has to be orthogonal to both vectors $\mathbf{R}_{\tilde{\mathbf{b}}}^{-1}\tilde{\mathbf{f}}_1$ and $\mathbf{R}_{\tilde{\mathbf{b}}}^{-1}\tilde{\mathbf{f}}_2$, which are not collinear in the general case. The maximal rank of this space is then $N_e - 2$. For the F-WL-MMSE receiver, one degree of freedom is used to keep one useful symbol in (3.7). Another degree of freedom is used to reject the other useful symbol, which is an interference for the first one. Hence there are $N_e - 2$ residual degrees of freedom to reject the interferences in $\tilde{\mathbf{b}}(n)$. The maximal number of interferences which may be rejected by the two previous receivers is then such that $N_e - 2 = P_{\tilde{\mathbf{b}}}$. A similar analysis may be done for both the P-WL-MMSE and the L-MMSE receivers giving rise to $N_e - 2 = P_{\overline{\mathbf{b}}}$ and $N_e - 2 = P_b$ respectively with $N_e = 2N$. Using (3.58), we obtain that the maximal number of interferences which may be processed by the previous receivers is such that

$$\left.\begin{array}{ll} 2(N-1) = 2P_{int} + P_c + 2P_{nc} & \text{for L-MMSE} \\ 2(N-1) = 2P_{int} + P_{r,c} + 2(P_{r,nc} + P_{nr}) & \text{for P-WL-MMSE} \\ 2(2N-1) = 2P_{int} + P_{r,c} + 2(P_{r,nc} + P_{nr,c}) + 4P_{nr,nc} & \text{for ML, F-WL-MMSE} \end{array}\right\} \tag{3.59}$$

These expressions show in particular that the L-MMSE and P-WL-MMSE receivers, i.e. the receivers of the literature, are not able to process more than $N - 1$ internal interferences from an array of N sensors. They cannot thus process any interference, internal or external, from $N = 1$ antenna. On the contrary, the F-WL-MMSE Alamouti receiver that we proposed and the ML Alamouti receiver are able to process up to $2N - 1$ internal interferences from N antennas. Hence, they can both perform SAIC of one synchronous intra-network Alamouti interference for $N = 1$. Besides, these latter receivers may also process up to $2N - 1$ rectilinear or coherent, and up to $4N - 2$ rectilinear and coherent external interferences from N antennas, hence the SAIC of one rectilinear or coherent external interference and of two rectilinear and coherent interferences respectively. Finally any of the considered receivers is able to process more than $N - 1$ non-rectilinear and non-coherent external interferences from N antennas.

3.5.3 Geometrical interpretation

For a better understanding of the structure of the receivers we subsequently assume in this section that the total noise is composed of $P = P_{int} = 1$ synchronous internal interference plus a spatially and temporally white background noise. The observation model is described in a first part, the Conventional Alamouti receiver (CONV) is analyzed in a second part and the F-WL-MMSE receiver in a third part.

a) Observation model

Under the previous assumption and using notations of section 3.5.1, the vectors $\mathbf{x}_1$ and $\mathbf{x}_2$ of (3.1) can be written as

$$\begin{cases} \mathbf{x}_1(n) = \mu_1 a_{2n-1}\mathbf{h}_1 + \mu_2 a_{2n}\mathbf{h}_2 + \mu_3 e_{2n-1}\mathbf{h}_3 + \mu_4 e_{2n}\mathbf{h}_4 + \mathbf{b}_{\nu 1}(n) \\ \mathbf{x}_2(n) = -\mu_1 a_{2n}\mathbf{h}_1 + \mu_2 a_{2n-1}\mathbf{h}_2 - \mu_3 e_{2n}\mathbf{h}_3 + \mu_4 e_{2n-1}\mathbf{h}_4 + \mathbf{b}_{\nu 2}(n) \end{cases} \tag{3.60}$$

We recall that $\mu_3\mathbf{h}_3$ and $\mu_4\mathbf{h}_4$ have been defined in section 3.5.1. Note that $e_{1,n}$ introduced in section 3.5.1 for internal interference 1 has been replaced by e_n to simplify notations. Vectors $\mathbf{b}_{\nu 1}$ and $\mathbf{b}_{\nu 2}$ are the $N \times 1$ background noise vectors in $\mathbf{x}_1$ and $\mathbf{x}_2$ respectively, such that the $2N \times 1$ vector $\mathbf{b}_\nu = [\mathbf{b}_{\nu 1}^T, \mathbf{b}_{\nu 2}^T]^T$ is SO circular, temporally and spatially white, i.e. such that $\mathbf{R}_{\mathbf{b}_\nu} = \sigma^2\mathbf{I}$ and $\mathbf{C}_{\mathbf{b}_\nu} = \mathbf{0}$. The observation system (3.60) gives rise to the following expressions for the total noise vectors $\mathbf{b}(n)$, $\overline{\mathbf{b}}(n)$ and $\tilde{\mathbf{b}}(n)$:

$$\mathbf{b}(n) = \sqrt{\frac{\pi_I}{\pi_a}}\,(e_{2n-1}\mathbf{f}_3 + e_{2n}\mathbf{f}_4) + \mathbf{b}_\nu(n), \tag{3.61}$$

$$\overline{\mathbf{b}}(n) = \sqrt{\frac{\pi_I}{\pi_a}}\,(e_{2n-1}\mathbf{g}_3 + e_{2n}\mathbf{g}_4) + \overline{\mathbf{b}}_\nu(n), \tag{3.62}$$

$$\tilde{\mathbf{b}}(n) = \sqrt{\frac{\pi_I}{\pi_a}}\left(e_{2n-1}\tilde{\mathbf{f}}_3 + e_{2n}\tilde{\mathbf{f}}_4\right) + \tilde{\mathbf{b}}_\nu(n), \tag{3.63}$$

where the scalar $\pi_I = \pi_a(\mu_3^2 + \mu_4^2)/2$ corresponds to the mean power of each interfering symbol per receive antenna, where the vectors $\mathbf{f}_3$, $\mathbf{f}_4$, $\mathbf{g}_3$, $\mathbf{g}_4$, $\tilde{\mathbf{f}}_3$, $\tilde{\mathbf{f}}_4$ are defined similarly to $\mathbf{f}_1$, $\mathbf{f}_2$, $\mathbf{g}_1$, $\mathbf{g}_2$, $\tilde{\mathbf{f}}_1$ and $\tilde{\mathbf{f}}_2$ respectively and where $\overline{\mathbf{b}}_\nu = [\mathbf{b}_{\nu 1}^T, \mathbf{b}_{\nu 2}^H]^T$, $\tilde{\mathbf{b}}_\nu = [\mathbf{b}_\nu^T, \mathbf{b}_\nu^H]^T$.

It was established in section 3.5.2 that the F-WL-MMSE receiver processes up to $P_{int} = 2N - 1$ internal interferers. As we consider only $P = P_{int} = 1$ internal interferer, corresponding to another Alamouti user of the network, we expect the F-WL-MMSE receiver to properly cancel this interferer. The purpose of this paper is to analyze the behavior of the conventional Alamouti receiver and of the F-WL-MMSE receiver to understand how the latter properly cancels the internal interference.

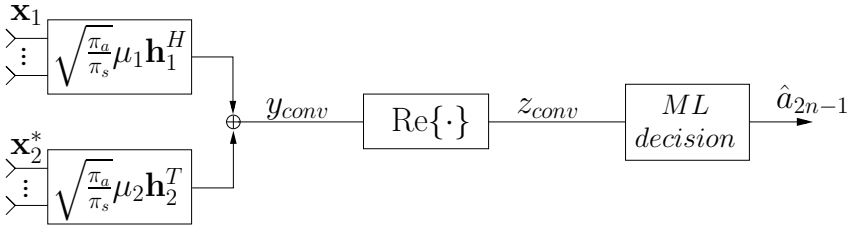

Figure 3.5: Scheme of the Conventional Alamouti receiver (CONV)

b) Conventional Alamouti receiver

We recall the definition of the Conventional Alamouti receiver described in section b) through Fig. 3.5. The Conventional Alamouti receiver is based on filter $\mathbf{w}_{conv} = \mathbf{g}_1 = \sqrt{\pi_a/\pi_s}[\mu_1\mathbf{h}_1^T,\ \mu_2\mathbf{h}_2^H]^T$. We can derive the output $y_{conv}(n)$ of filter $\mathbf{w}_{conv}$, defined in (3.51):

$$y_{conv}(n) = \sqrt{\frac{\pi_a}{\pi_s}}\left(\mu_1\mathbf{h}_1^H\mathbf{x}_1(n) + \mu_2\mathbf{h}_2^T\mathbf{x}_2(n)^*\right) \tag{3.64}$$

$$= a_{2n-1}\left(\mu_1^2\mathbf{h}_1^H\mathbf{h}_1 + \mu_2^2\mathbf{h}_2^T\mathbf{h}_2^*\right) + a_{2n}\mu_1\mu_2\left(\mathbf{h}_1^H\mathbf{h}_2 - \mathbf{h}_2^T\mathbf{h}_1^*\right) + \mathbf{g}_1^H\overline{\mathbf{b}}(n) \tag{3.65}$$

$$= a_{2n-1}\left(\mu_1^2\mathbf{h}_1^H\mathbf{h}_1 + \mu_2^2\mathbf{h}_2^T\mathbf{h}_2^*\right) + \mathbf{g}_1^H\overline{\mathbf{b}}(n) \tag{3.66}$$

Using the total noise model (3.62), we can also write y_{conv} as

$$y_{conv}(n) = \sqrt{\frac{\pi_s}{\pi_a}}a_{2n-1}\mathbf{g}_1^H\mathbf{g}_1 + \sqrt{\frac{\pi_I}{\pi_a}}\left(e_{2n-1}\mathbf{g}_1^H\mathbf{g}_3 + e_{2n}\mathbf{g}_1^H\mathbf{g}_4\right) + \mathbf{g}_1^H\overline{\mathbf{b}}_\nu(n). \tag{3.67}$$

And eventually, the output of the Conventional Alamouti receiver $z_{conv}(n) = \mathrm{Re}\{y_{conv}(n)\}$ can be written

$$z_{conv}(n) = \sqrt{\frac{\pi_s}{\pi_a}}a_{2n-1}\mathbf{g}_1^H\mathbf{g}_1 + \sqrt{\frac{\pi_I}{\pi_a}}\left(e_{2n-1}\mathrm{Re}\{\mathbf{g}_1^H\mathbf{g}_3\} + e_{2n}\mathrm{Re}\{\mathbf{g}_1^H\mathbf{g}_4\}\right) + \mathrm{Re}\{\mathbf{g}_1^H\overline{\mathbf{b}}_\nu(n)\} \tag{3.68}$$

We deduce from expressions (3.64) and (3.65) that the Conventional Alamouti receiver first implements a filter matched, in amplitude and phase, to the useful symbol channel in both $\mathbf{x}_1(n)$ and $\mathbf{x}_2(n)^*$ before summing the associated outputs, $\mu_1\mathbf{h}_1^H\mathbf{x}_1(n)$ and $\mu_2\mathbf{h}_2^T\mathbf{x}_2(n)^*$. This operation generates the output $y_{conv}(n)$ in which the Signal to background Noise Ratio (SNR) is maximized. This maximization is kept in $z_{conv}(n)$ due to the SO circularity of the background noise. Moreover, due to the orthogonality structure of the Alamouti scheme, these matched filtering operations generate opposite contributions of symbol a_{2n} in their outputs, as seen in (3.65). The contribution of symbol a_{2n} is thus automatically removed in $y_{conv}(n)$, hence in $z_{conv}(n)$. Unfortunately, $z_{conv}(n)$ still contains the real part of the residual interferences e_{2n-1} and e_{2n} in $y_{conv}(n)$, which have no reasons to be canceled in the general case. The internal interference thus degrades the output performance. This receiver exploits the orthogonality of

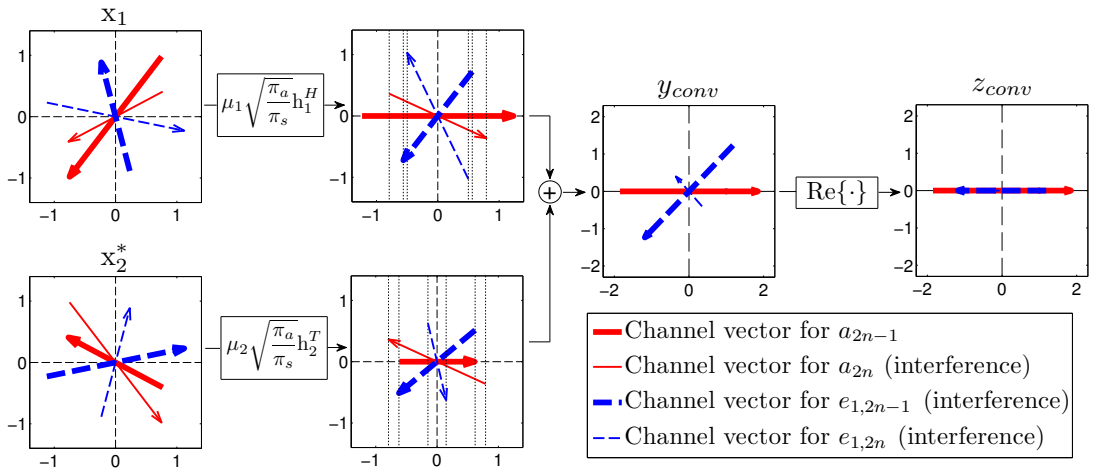

Figure 3.6: Constellations variation inside CONV receiver

Alamouti code but does not exploit the structure of the noise. As a consequence, it cannot cancel any intra-network interfering Alamouti user.

The results of the different steps on both the useful symbol a_{2n-1} and the associated interferences a_{2n}, e_{2n-1} and e_{2n} contained in $\mathbf{x}_1(n)$ and $\mathbf{x}_2(n)$ are illustrated in Fig. 3.6 for $N = 1$, $\pi_s/\sigma^2 = 0$dB, $\pi_I/\sigma^2 = 20$dB and fixed propagation channels, where large and thin full lines are associated with a_{2n-1} and a_{2n} respectively whereas large and thin dotted lines are associated with e_{2n-1} and e_{2n} respectively. Note in particular the matched filtering in $\mathbf{x}_1$ and $\mathbf{x}_2^*$ for the useful symbol channel and the opposite channels in $\mathbf{x}_1$ and $\mathbf{x}_2^*$ for the interference generated by a_{2n}.

Note that, for $N = 1$ and $P = 1$, the P-WL-MMSE receiver reduces to the CONV receiver; indeed Appendix 3.C shows that for internal interferences $\overline{\mathbf{w}}_{pwl}$ is proportional to $\mathbf{R}_{\overline{\mathbf{b}}}^{-1}\mathbf{g}_1$. Moreover, it is easy to check that $\mathbf{R}_{\overline{\mathbf{b}}}^{-1}$ is proportional to $\mathbf{I}_2$ for $N = 1$ and $P = 1$ (using the expression (3.96) of $\mathbf{R}_{\overline{\mathbf{b}}}^{-1}$ derived in the next section). Hence, the P-WL-MMSE receiver also provides the constellation variations of Fig. 3.6.

c) F-WL-MMSE receiver

In this section we prove that the F-WL-MMSE receiver is properly canceling the internal interferences for the estimation of symbol a_{2n-1} at high INR. We first derive the expression of filter $\tilde{\mathbf{w}}_{fwl}$ for the considered total noise model and then derive the contributions of useful and interfering symbols in the output of the F-WL-MMSE receiver. We recall from section 3.3.3 that the F-WL-MMSE receiver implements a ML decision from the output $z_{fwl} = 2\mathrm{Re}\{y_{fwl}\}$ where $y_{fwl}(n) = \mathbf{w}_{fwl}^H\mathbf{x}(n)$. Noting $\mathbf{w}_{fwl} = [\mathbf{w}_{fwl,1}^T, \mathbf{w}_{fwl,2}^T]^T$, we can display the F-WL-MMSE receiver as on Fig. 3.7.

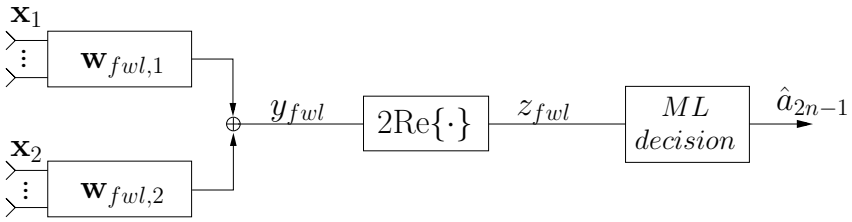

Figure 3.7: Scheme of the F-WL-MMSE receiver

Deriving filter $\tilde{\mathbf{w}}_{fwl}$:

We have proved in Appendix 3.A that condition $C1$ was verified in the case of internal interferences. Moreover, it has been shown in section 3.4.2 that under condition $C1$, the filter $\tilde{\mathbf{w}}_{fwl}$ is proportional to $\tilde{\mathbf{w}}_{ml} = \mathbf{R}_{\tilde{\mathbf{b}}}^{-1}\tilde{\mathbf{f}}_1$:

$$\tilde{\mathbf{w}}_{fwl} = k\tilde{\mathbf{w}}_{ml} = k\mathbf{R}_{\tilde{\mathbf{b}}}^{-1}\tilde{\mathbf{f}}_1, \tag{3.69}$$

with $k = \left(1 + \pi_s \tilde{\mathbf{f}}_1^H \left(\pi_s \tilde{\mathbf{f}}_2 \tilde{\mathbf{f}}_2^H + \mathbf{R}_{\tilde{\mathbf{b}}}\right)^{-1} \tilde{\mathbf{f}}_1\right)^{-1} > 0$. In the following we thus derive filter $\tilde{\mathbf{w}}_{ml}$ instead of $\tilde{\mathbf{w}}_{fwl}$. Using the extended observation model (3.63), the correlation matrix of the noise $\tilde{\mathbf{b}}(n)$ can be written as $\mathbf{R}_{\tilde{\mathbf{b}}} = \pi_a(\tilde{\mathbf{f}}_3\tilde{\mathbf{f}}_3^H + \tilde{\mathbf{f}}_4\tilde{\mathbf{f}}_4^H) + \sigma^2\mathbf{I}$. Thanks to the orthogonality of $\tilde{\mathbf{f}}_3$ and $\tilde{\mathbf{f}}_4$, a direct application of the Woodbury matrix identity yields its inverse:

$$\mathbf{R}_{\tilde{\mathbf{b}}}^{-1} = \frac{1}{\sigma^2}\left(\mathbf{I} - \frac{2\varepsilon_I}{1+2\varepsilon_I}\left(\frac{\tilde{\mathbf{f}}_3\tilde{\mathbf{f}}_3^H}{\|\tilde{\mathbf{f}}_3\|^2} + \frac{\tilde{\mathbf{f}}_4\tilde{\mathbf{f}}_4^H}{\|\tilde{\mathbf{f}}_4\|^2}\right)\right) \tag{3.70}$$

where $\varepsilon_I = \|\mathbf{f}_3\|^2\pi_I/\sigma^2 = \frac{1}{2}\|\tilde{\mathbf{f}}_3\|^2\pi_I/\sigma^2$ corresponds to the ratio between the interference power and the background noise power received by the array. We can now write $\tilde{\mathbf{w}}_{ml}$ under the following form:

$$\tilde{\mathbf{w}}_{ml} = \frac{1}{\sigma^2}\left(\tilde{\mathbf{f}}_1 - \frac{2\varepsilon_I}{1+2\varepsilon_I}\left(\frac{\tilde{\mathbf{f}}_3^H\tilde{\mathbf{f}}_1}{\|\tilde{\mathbf{f}}_3\|^2}\tilde{\mathbf{f}}_3 + \frac{\tilde{\mathbf{f}}_4^H\tilde{\mathbf{f}}_1}{\|\tilde{\mathbf{f}}_4\|^2}\tilde{\mathbf{f}}_4\right)\right). \tag{3.71}$$

We obtain the expression of $\tilde{\mathbf{w}}_{fwl}$ by multiplying (3.71) by k. We have seen that $\tilde{\mathbf{w}}_{fwl} = [\mathbf{w}_{fwl}^T,\ \mathbf{w}_{fwl}^H]^T$ in section 3.3.3. Using (3.71), vector $\mathbf{w}_{fwl}$ can be written as:

$$\mathbf{w}_{fwl} = \frac{k}{\sigma^2}\left(\mathbf{f}_1 - \frac{2\varepsilon_I}{1+2\varepsilon_I}\left(\frac{\tilde{\mathbf{f}}_3^H\tilde{\mathbf{f}}_1}{\|\tilde{\mathbf{f}}_3\|^2}\mathbf{f}_3 + \frac{\tilde{\mathbf{f}}_4^H\tilde{\mathbf{f}}_1}{\|\tilde{\mathbf{f}}_4\|^2}\mathbf{f}_4\right)\right). \tag{3.72}$$

We deduce from (3.72) the expressions of $\mathbf{w}_{fwl,1}$ and $\mathbf{w}_{fwl,2}$, defined by $\mathbf{w}_{fwl} = [\mathbf{w}_{fwl,1}^T,\ \mathbf{w}_{fwl,2}^T]^T$.

$$\mathbf{w}_{fwl,1} = \frac{k}{\sigma^2}\left(\mathbf{h}_1 - \frac{2\varepsilon_I}{1+2\varepsilon_I}\left(\frac{\tilde{\mathbf{f}}_3^H\tilde{\mathbf{f}}_1}{\|\tilde{\mathbf{f}}_3\|^2}\mathbf{h}_3 + \frac{\tilde{\mathbf{f}}_4^H\tilde{\mathbf{f}}_1}{\|\tilde{\mathbf{f}}_4\|^2}\mathbf{h}_4\right)\right) \tag{3.73}$$

$$\mathbf{w}_{fwl,2} = \frac{k}{\sigma^2}\left(\mathbf{h}_2 - \frac{2\varepsilon_I}{1+2\varepsilon_I}\left(\frac{\tilde{\mathbf{f}}_3^H\tilde{\mathbf{f}}_1}{\|\tilde{\mathbf{f}}_3\|^2}\mathbf{h}_4 - \frac{\tilde{\mathbf{f}}_4^H\tilde{\mathbf{f}}_1}{\|\tilde{\mathbf{f}}_4\|^2}\mathbf{h}_3\right)\right) \tag{3.74}$$

The filter $\mathbf{w}_{fwl}$ generates the output $y_{fwl}(n)$ given by

$$y_{fwl}(n) = \mathbf{w}_{fwl,1}^H \mathbf{x}_1(n) + \mathbf{w}_{fwl,1}^H \mathbf{x}_1(n) \tag{3.75}$$

$$= \sqrt{\frac{\pi_s}{\pi_a}} \left(a_{2n-1} \mathbf{w}_{fwl}^H \mathbf{f}_1 + a_{2n} \mathbf{w}_{fwl}^H \mathbf{f}_2 \right) + \sqrt{\frac{\pi_I}{\pi_a}} \left(e_{2n-1} \mathbf{w}_{fwl}^H \mathbf{f}_3 + e_{2n} \mathbf{w}_{fwl}^H \mathbf{f}_4 \right) + \mathbf{w}_{fwl}^H \mathbf{b}_\nu(n). \tag{3.76}$$

Case where $\tilde{\mathbf{f}}_1$ belongs to $\mathrm{span}\{\tilde{\mathbf{f}}_3, \tilde{\mathbf{f}}_4\}$:
Let us first consider the case where $\tilde{\mathbf{f}}_1$ belongs to the space spanned by the orthogonal vectors $\tilde{\mathbf{f}}_3$ and $\tilde{\mathbf{f}}_4$. Noting $\tilde{\gamma}$ the angle between $\tilde{\mathbf{f}}_1$ and the space spanned by $\tilde{\mathbf{f}}_3$ and $\tilde{\mathbf{f}}_4$, this means that

$$\cos^2 \tilde{\gamma} = 1. \tag{3.77}$$

Angle $\tilde{\gamma}$ is defined by the following relation:

$$\cos^2 \tilde{\gamma} = \frac{|\tilde{\mathbf{f}}_1^H \tilde{\mathbf{f}}_3|^2 + |\tilde{\mathbf{f}}_1^H \tilde{\mathbf{f}}_4|}{\|\tilde{\mathbf{f}}_1\|^2 \|\tilde{\mathbf{f}}_3\|^2} \tag{3.78}$$

Note that, using spatial correlation coefficients $\alpha_{13} = \frac{\mathbf{g}_1^H \mathbf{g}_3}{\|\mathbf{g}_1\| \|\mathbf{g}_3\|}$ and $\alpha_{13} = \frac{\mathbf{g}_1^H \mathbf{g}_4}{\|\mathbf{g}_1\| \|\mathbf{g}_3\|}$, $\cos^2 \tilde{\gamma}$ can also be written as

$$\cos^2 \tilde{\gamma} = \mathrm{Re}\{\alpha_{13}\}^2 + \mathrm{Re}\{\alpha_{14}\}^2. \tag{3.79}$$

Note also that condition (3.77) is equivalent to say that $\tilde{\mathbf{f}}_1$ is a linear combination with real-valued coefficients of $\tilde{\mathbf{f}}_3$ and $\tilde{\mathbf{f}}_4$, i.e., as $\tilde{\mathbf{f}}_3$ and $\tilde{\mathbf{f}}_4$ are orthogonal,

$$\tilde{\mathbf{f}}_1 = \frac{\tilde{\mathbf{f}}_3^H \tilde{\mathbf{f}}_1}{\|\tilde{\mathbf{f}}_3\|^2} \tilde{\mathbf{f}}_3 + \frac{\tilde{\mathbf{f}}_4^H \tilde{\mathbf{f}}_1}{\|\tilde{\mathbf{f}}_4\|^2} \tilde{\mathbf{f}}_3 \tag{3.80}$$

Under this assumption, we deduce from (3.72) that

$$\mathbf{w}_{fwl} = \frac{k}{\sigma^2 (1 + 2\varepsilon_I)} \mathbf{f}_1. \tag{3.81}$$

As $\mathrm{Re}\{\mathbf{f}_1^H \mathbf{x}(n)\} = \mathrm{Re}\{\mathbf{g}_1^H \overline{\mathbf{x}}(n)\}$, we deduce that $z_{conv}(n)$ and $z_{fwl}(n)$ are proportional, which means that the F-WL-MMSE receiver corresponds to the Conventional receiver, whose behavior is described in section b). The condition $\cos^2 \tilde{\gamma} = 1$ corresponds to the absence of both phase and spatio-temporal discrimination between the Alamouti useful signal and the interference. For $N = 1$, denoting by φ_i the phase of $\mathbf{h}_i$, such that $\mathbf{h}_i = |\mathbf{h}_i| e^{i\varphi_i}$, $i = 1, \ldots, 4$, it is straightforward to verify that this condition is in particular verified if $\varphi_1 = \varphi_2 = \varphi_3 = \varphi_4$, i.e. in the absence of phase diversity between the useful signal and interference.

Case where $\tilde{\mathbf{f}}_1$ does not belong to $\mathrm{span}\{\tilde{\mathbf{f}}_3, \tilde{\mathbf{f}}_4\}$:
Let us now assume that $\tilde{\mathbf{f}}_1$ does not belong to the space spanned by $\tilde{\mathbf{f}}_3$ and $\tilde{\mathbf{f}}_4$, which is equivalent to $\cos^2\tilde{\gamma} < 1$, i.e. there is a phase and/or a spatio-temporal discrimination between the Alamouti useful signal and interference. For $N = 1$, this occurs as soon as $(\varphi_1, \varphi_2) \neq (\varphi_3, \varphi_4)$ and/or $(\varphi_1, \varphi_2) \neq (\varphi_4, \varphi_3)$, i.e. as soon as there is a phase discrimination between the useful signal and interference. In order to understand the behavior of the F-WL-MMSE receiver, we analyze its output by deriving the contributions of the useful and interfering symbols.

Using (3.71) we directly derive the contribution of the useful signal a_{2n-1} in $z_{fwl} = \tilde{\mathbf{w}}_{fwl}^H \tilde{\mathbf{x}}$, i.e. $\tilde{\mathbf{w}}_{fwl}^H \tilde{\mathbf{f}}_1$.

$$\begin{aligned}\tilde{\mathbf{w}}_{fwl}^H \tilde{\mathbf{f}}_1 &= \frac{2k}{\sigma^2}\|\mathbf{f}_1\|^2\left(1 - \frac{2\varepsilon_I}{1+2\varepsilon_I}\cos^2\tilde{\gamma}\right)\\ &= \frac{2k}{\sigma^2}\|\mathbf{f}_1\|^2\left(\sin^2\tilde{\gamma} + \frac{1}{1+2\varepsilon_I}\cos^2\tilde{\gamma}\right)\end{aligned}$$

In Appendix 3.F, we derive the contribution of all interferences in y_{fwl}; the contributions of a_{2n}, e_{2n-1} and e_{2n} can be written as

$$\begin{aligned}\mathbf{w}_{fwl}^H \mathbf{f}_2 &= \frac{k}{\sigma^2}\beta_2 i,\\ \mathbf{w}_{fwl}^H \mathbf{f}_3 &= \frac{k}{\sigma^2}(\alpha_3 + i\beta_3),\\ \mathbf{w}_{fwl}^H \mathbf{f}_4 &= \frac{k}{\sigma^2}(\alpha_4 + i\beta_4),\end{aligned}$$

where $\beta_2,\ \alpha_3,\ \beta_3,\ \alpha_4,\ \beta_4 \in \mathbb{R}$ are defined by

$$\begin{aligned}\beta_2 &= \mathrm{Im}\left\{\frac{2\pi_a\mu_1\mu_2}{\pi_s}\mathbf{h}_1^H\mathbf{h}_2 - \frac{2\varepsilon_1}{1+2\varepsilon_1}\frac{\mathbf{f}_3^T\mathbf{f}_1^*\mathbf{f}_3^H\mathbf{f}_2}{\|\mathbf{f}_3\|^2}\right\},\\ \alpha_3 &= \frac{\mathrm{Re}\left\{\mathbf{f}_3^H\mathbf{f}_1\right\}}{1+2\varepsilon_1}, \qquad \beta_3 = \mathrm{Im}\left\{\mathbf{f}_1^H\mathbf{f}_3 - \frac{\pi_a\mu_3\mu_4}{\sigma^2}\frac{4\mathrm{Re}\left\{\mathbf{f}_4^H\mathbf{f}_1\right\}}{1+2\varepsilon_1}\mathbf{h}_4^H\mathbf{h}_3\right\},\\ \alpha_4 &= \frac{\mathrm{Re}\left\{\mathbf{f}_4^H\mathbf{f}_1\right\}}{1+2\varepsilon_1}, \qquad \beta_4 = \mathrm{Im}\left\{\mathbf{f}_1^H\mathbf{f}_4 - \frac{\pi_a\mu_3\mu_4}{\sigma^2}\frac{4\mathrm{Re}\left\{\mathbf{f}_3^H\mathbf{f}_1\right\}}{1+2\varepsilon_1}\mathbf{h}_3^H\mathbf{h}_4\right\}.\end{aligned}$$

We can now conclude by writing the output $z_{fwl} = 2\mathrm{Re}\{y_{fwl}\}$ of the F-WL-MMSE receiver.

$$\begin{aligned}z_{fwl} = \frac{2k}{\sigma^2}\Bigg(&(\|\mathbf{f}_1\|^2\sin^2\tilde{\gamma})a_{2n-1} + \frac{\left(\|\mathbf{f}_1\|^2\cos^2\tilde{\gamma}\right)a_{2n-1} + \mathrm{Re}\{\mathbf{f}_3^H\mathbf{f}_1\}\,e_{2n-1} + \mathrm{Re}\{\mathbf{f}_4^H\mathbf{f}_1\}\,e_{2n}}{1+2\varepsilon_I}\Bigg)\\ &+ 2\mathrm{Re}\{\mathbf{w}_{fwl}^H\mathbf{b}_\nu(n)\}\end{aligned} \tag{3.82}$$

First note that when $\cos^2\tilde{\gamma} < 1$, the contribution of the useful symbol a_{2n-1} in z_{fwl} cannot be zero, even for a strong interference ($\varepsilon_I \gg 1$). Moreover, due to the orthogonality structure of the Alamouti

scheme, (3.82) shows that $\mathbf{w}_{fwl}$ puts the contribution of symbol a_{2n} on the imaginary axis whatever the intra-network interference scenario. The contribution of symbol a_{2n} is thus completely removed in z_{fwl} by the real part operation. As for the interfering Alamouti user, $\mathbf{w}_{fwl}^H\mathbf{f}_3$ and $\mathbf{w}_{fwl}^H\mathbf{f}_4$ are approximately on the imaginary axis for $\cos^2\tilde{\gamma} < 1$ and $\varepsilon_I \gg 1$, as their real part is then negligible compared to $\tilde{\mathbf{w}}_{fwl}^H\tilde{\mathbf{f}}_1 \simeq \frac{2k}{\sigma^2}\|\mathbf{f}_1\|^2\sin^2\tilde{\gamma}$ ($\neq 0$), whatever the channel vectors $\mu_3\mathbf{h}_3$ and $\mu_4\mathbf{h}_4$. Hence, for a strong interference ($\varepsilon_I \gg 1$), the contribution of all interferences is properly canceled in $z_{fwl}(n)$ after the projection on the real axis. For $\varepsilon_I \gg 1$, the output $z_{fwl}(n)$ reduces to

$$z_{fwl} \simeq \frac{2k}{\sigma^2}\left(\|\mathbf{f}_1\|^2\sin^2\tilde{\gamma}\right)a_{2n-1} + 2\mathrm{Re}\{\mathbf{w}_{fwl}^H\mathbf{b}_\nu(n)\} \qquad (\varepsilon_I \gg 1,\ \cos^2\tilde{\gamma} < 1) \tag{3.83}$$

Note that in the particular case of $\cos^2\tilde{\gamma} = 0$, $\tilde{\mathbf{f}}_1$ is orthogonal to the space spanned by $\tilde{\mathbf{f}}_3$ and $\tilde{\mathbf{f}}_4$ and both the F-WL-MMSE receiver and the CONV receiver, which become equivalent, completely reject the interference.

The previous analysis shows that the F-WL-MMSE receiver cancels the intra-network interference, even for $N = 1$, by exploiting both the real-valued nature of the symbols and the particular structure of the Alamouti code. For this reason it is a breakthrough with respect to the WL Alamouti receivers of the literature [40–43,45,47,82]. More precisely, for $N = 1$, the number of degrees of freedom of the F-WL-MMSE receiver corresponds to the phases and moduli of both $\mathbf{w}_{fwl,1}$ and $\mathbf{w}_{fwl,2}$. One degree of freedom is used to keep the useful symbol a_{2n-1} in $z_{fwl}(n)$ while, for a strong intra-network interference, the three remaining degrees of freedom allow to generate in $\mathbf{w}_{fwl,1}^H\mathbf{x}_1(n)$ and $\mathbf{w}_{fwl,2}^H\mathbf{x}_2(n)$ contributions of interference symbols a_{2n}, e_{2n-1} and e_{2n} having an opposite real part, through homotheties and/or rotations on both $\mathbf{x}_1(n)$ and $\mathbf{x}_2(n)$. As a consequence, this puts on the imaginary axis the contribution in $y_{fwl}(n)$ of the three interference symbols a_{2n}, e_{2n-1} and e_{2n}, thus canceling these interferences in $z_{fwl}(n)$.

Fig. 3.8 sums up the previous different steps on the received constellations of both the useful symbol a_{2n-1} and the associated interferences a_{2n}, e_{2n-1} and e_{2n} in $\mathbf{x}_1(n)$ and $\mathbf{x}_2(n)$ for $N = 1$, $\pi_s/\sigma^2 = 0$dB, $\pi_I/\sigma^2 = 20$dB and fixed propagation channels, where large and thin full lines are associated with a_{2n-1} and a_{2n} respectively whereas large and thin dotted lines are associated with e_{2n-1} and e_{2n} respectively. Note in particular the opposite real part in $\mathbf{x}_1$ and $\mathbf{x}_2^*$ of the three interference channels associated to a_{2n}, e_{2n-1} and e_{2n}, which are therefore on the imaginary axis in $y_{fwl}(n)$ and hence canceled in z_{fwl}.

This section gave an enlightening geometrical interpretation of the Alamouti SAIC/MAIC concept, which extends, for synchronous Alamouti users, the SAIC/MAIC concept described in [54]. The WL MMSE receiver presented in [54] has been introduced for synchronous single antenna users using real-valued constellations; it fully exploits the real-valued nature of the sources symbols and is able to separate up to $2N$ single antenna users from N receive antennas, hence its SAIC capability of one internal interference for $N = 1$. It has been shown in [54] that, in the case of a strong INR (Interference to Noise

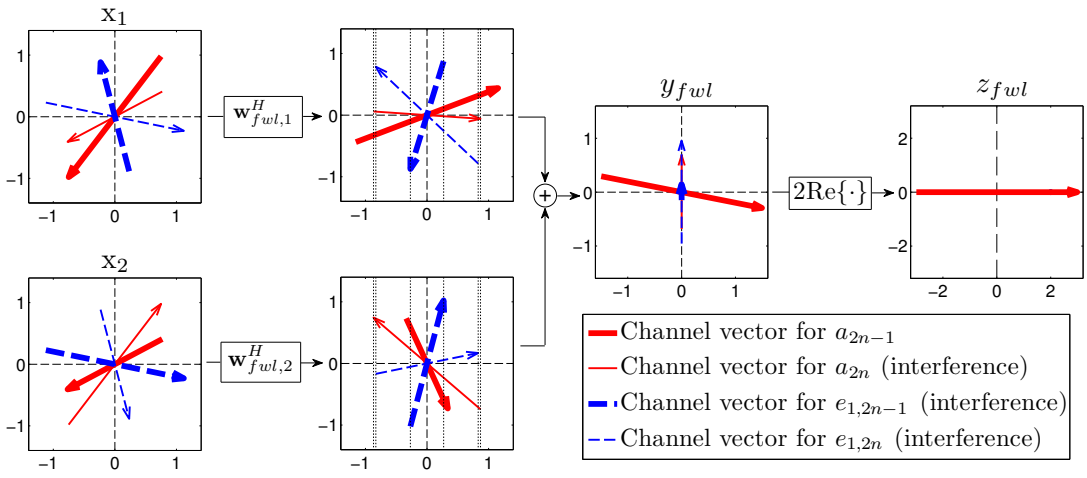

Figure 3.8: Constellations variation inside F-WL-MMSE receiver

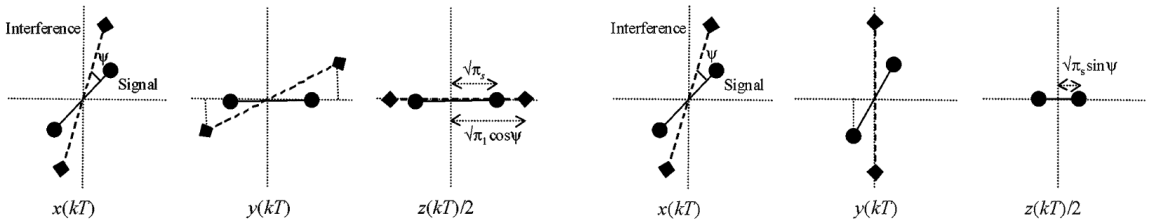

(a) Conventional MMSE receiver

(b) Fully-WL MMSE receiver

Figure 3.9: Constellations variations inside the mentioned receivers (SISO case) [54]

Ratio), the optimal WL filtering of this receiver can be seen as a rotation of the constellations followed by a projection on the I axis. The rotation puts the interferer constellation on the Q axis and the interference is therefore canceled by the projection (see Fig. 3.9(b) taken from [54]). On the opposite, the usual receiver just uses a rotation to put the constellation of the useful signal on the I axis; the interference constellation is not considered (see Fig. 3.9(a) taken from [54]). Note that the SAIC/MAIC concept corresponds to the previous results if taking $\mathbf{w}_{fwl,2} = 0$ and $\mu_2 = \mu_4 = 0$.

3.5.4 SINR performance

In this section, we want to quantify the performance of the F-WL-MMSE receiver in the presence of internal and/or external interferences for the demodulation of symbol a_{2n-1} and to highlight quantitatively the great interest of this receiver with respect to the receivers of the literature. To that end, we first compute the general expressions of the SINRs at the output of the F-WL-MMSE, P-WL-MMSE and CONV

receivers and then compare them for the particular case of one internal interference ($P = P_{int} = 1$). We finally analyze these SINRs in the case of $P = P_{int} \geq 1$, i.e. for any number of internal interferences.

a) General expressions of the SINRs

The SINRs of the F-WL-MMSE, P-WL-MMSE, L-MMSE and CONV receivers are respectively denoted by SINR_{fwl}, SINR_{pwl}, SINR_{l} and SINR_{conv}; they are defined as the ratio between the power of a_{2n-1} and the power of the global noise at the considered output. From the expressions of the outputs (3.36), (3.30), (3.34) and (3.52), we deduce the following results

$$\mathrm{SINR}_{fwl} = \frac{\pi_s(\tilde{\mathbf{f}}_1^H \mathbf{R}_{\tilde{\mathbf{x}}}^{-1} \tilde{\mathbf{f}}_1)^2}{\pi_s(\tilde{\mathbf{f}}_1^H \mathbf{R}_{\tilde{\mathbf{x}}}^{-1} \tilde{\mathbf{f}}_2)^2 + \tilde{\mathbf{f}}_1^H \mathbf{R}_{\tilde{\mathbf{x}}}^{-1} \mathbf{R}_{\tilde{\mathbf{b}}} \mathbf{R}_{\tilde{\mathbf{x}}}^{-1} \tilde{\mathbf{f}}_1} \tag{3.84}$$

$$\mathrm{SINR}_{pwl} = \frac{\pi_s(\mathbf{g}_1^H \mathbf{R}_{\overline{\mathbf{x}}}^{-1} \mathbf{g}_1)^2}{\pi_s(\mathrm{Re}\{\mathbf{g}_1^H \mathbf{R}_{\overline{\mathbf{x}}}^{-1} \mathbf{g}_2\})^2 + \frac{1}{2}(\mathbf{g}_1^H \mathbf{R}_{\overline{\mathbf{x}}}^{-1} \mathbf{R}_{\overline{\mathbf{b}}} \mathbf{R}_{\overline{\mathbf{x}}}^{-1} \mathbf{g}_1 + \mathrm{Re}\{\mathbf{g}_1^H \mathbf{R}_{\overline{\mathbf{x}}}^{-1} \mathbf{C}_{\overline{\mathbf{b}}} \mathbf{R}_{\overline{\mathbf{x}}}^{-*} \mathbf{g}_1^*\})} \tag{3.85}$$

$$\mathrm{SINR}_{l} = \frac{\pi_s(\mathbf{f}_1^H \mathbf{R}_{\mathbf{x}}^{-1} \mathbf{f}_1)^2}{\pi_s(\mathrm{Re}\{\mathbf{f}_1^H \mathbf{R}_{\mathbf{x}}^{-1} \mathbf{f}_2\})^2 + \frac{1}{2}(\mathbf{f}_1^H \mathbf{R}_{\mathbf{x}}^{-1} \mathbf{R}_{\mathbf{b}} \mathbf{R}_{\mathbf{x}}^{-1} \mathbf{f}_1 + \mathrm{Re}\{\mathbf{f}_1^H \mathbf{R}_{\mathbf{x}}^{-1} \mathbf{C}_{\mathbf{b}} \mathbf{R}_{\mathbf{x}}^{-*} \mathbf{f}_1^*\})} \tag{3.86}$$

$$\mathrm{SINR}_{conv} = \frac{2\pi_s(\mathbf{f}_1^H \mathbf{f}_1)^2}{\mathbf{f}_1^H \mathbf{R}_{\mathbf{b}} \mathbf{f}_1 + \mathrm{Re}\{\mathbf{f}_1^H \mathbf{C}_{\mathbf{b}} \mathbf{f}_1^*\}} \tag{3.87}$$

Note that when condition $C1$, defined by (3.45), is verified, SINR_{fwl} reduces to

$$\mathrm{SINR}_{fwl} = \pi_s \tilde{\mathbf{f}}_1^H \mathbf{R}_{\tilde{\mathbf{b}}}^{-1} \tilde{\mathbf{f}}_1. \tag{3.88}$$

If in addition the total noise is assumed to be SO circular, temporally and spatially white (i.e., $\mathbf{R}_{\tilde{\mathbf{b}}} = \sigma^2 \mathbf{I}$), we obtain the well-known result

$$\begin{aligned} \mathrm{SINR}_{fwl} &= \mathrm{SINR}_{pwl} = \mathrm{SINR}_{conv} \\ &= \frac{2\pi_s}{\sigma^2} \|\mathbf{f}_1\|^2 = \frac{2\pi_a}{\sigma^2} (\mu_1^2 \|\mathbf{h}_1\|^2 + \mu_2^2 \|\mathbf{h}_2\|^2). \end{aligned}$$

b) SINRs for $P = 1$ internal interference

We assume in this section that the total noise is composed of $P = P_{int} = 1$ internal interference plus a spatially and temporally white background noise. Under this assumption, we compute the SINR at the output of the F-WL-MMSE receiver and we compare it to the SINR at the output of both the P-WL-MMSE and the CONV receivers. We do not compute the SINR at the output of the L-MMSE receiver since this receiver is rarely used. The observation model is described in a first part, the SINRs are computed in a second part, discussed in a third part and illustrated in a fourth part.

Observation model:
As we suppose $P = P_{int} = 1$, the observation model is then the same as in section 3.5.3 a). We recall from (3.60) that the vectors $\mathbf{x}_1$ and x_2 of (3.1) can be written as

$$\begin{cases} \mathbf{x}_1(n) = \mu_1 a_{2n-1}\mathbf{h}_1 + \mu_2 a_{2n}\mathbf{h}_2 + \mu_3 e_{2n-1}\mathbf{h}_3 + \mu_4 e_{2n}\mathbf{h}_4 + \mathbf{b}_{\nu 1}(n), \\ \mathbf{x}_2(n) = -\mu_1 a_{2n}\mathbf{h}_1 + \mu_2 a_{2n-1}\mathbf{h}_2 - \mu_3 e_{2n}\mathbf{h}_3 + \mu_4 e_{2n-1}\mathbf{h}_4 + \mathbf{b}_{\nu 2}(n), \end{cases} \tag{3.89}$$

giving rise to the following expression for the observation vector $\mathbf{x}(n)$:

$$\mathbf{x}(n) = \sqrt{\frac{\pi_s}{\pi_a}}\left(a_{2n-1}\mathbf{f}_1 + a_{2n}\mathbf{f}_2\right) + \sqrt{\frac{\pi_I}{\pi_a}}\left(e_{2n-1}\mathbf{f}_3 + e_{2n}\mathbf{f}_4\right) + \mathbf{b}_\nu(n). \tag{3.90}$$

SINRs computation:
We derive in this section the SINRs for the CONV, P-WL-MMSE and F-WL-MMSE receivers under the previous assumptions.

In order to derive SINR_{conv} we first need to note that, for one internal interference, $\mathbf{R_b} = \pi_I(\mathbf{f}_3\mathbf{f}_3^H + \mathbf{f}_4\mathbf{f}_4^H) + \sigma^2\mathbf{I}$ and $\mathbf{C_b} = \pi_I(\mathbf{f}_3\mathbf{f}_3^T + \mathbf{f}_4\mathbf{f}_4^T)$. We can then derive the terms in the denominator of (3.87):

$$\mathbf{f}_1^H\mathbf{R_b}\mathbf{f}_1 = \sigma^2\|\mathbf{f}_1\|^2\left(1 + \varepsilon_I(|\alpha_{13}|^2 + |\alpha_{14}|^2)\right), \tag{3.91}$$

$$\mathbf{f}_1^H\mathbf{C_b}\mathbf{f}_1^* = \sigma^2\|\mathbf{f}_1\|^2\varepsilon_I\left(\alpha_{13}^2 + \alpha_{14}^2\right), \tag{3.92}$$

where we recall that the spatial correlation coefficients α_{13} and α_{14} are defined as

$$\alpha_{13} = \frac{\mathbf{g}_1^H\mathbf{g}_3}{\|\mathbf{g}_1\|\|\mathbf{g}_3\|}, \quad \alpha_{14} = \frac{\mathbf{g}_1^H\mathbf{g}_4}{\|\mathbf{g}_1\|\|\mathbf{g}_4\|} \tag{3.93}$$

and where ε_I (resp. ε_s) corresponds to the ratio between the interference power (resp. useful power) and the background noise power received by the array:

$$\varepsilon_I = \frac{\pi_I}{\sigma^2}\|\mathbf{f}_3\|^2 = \frac{\pi_a}{\sigma^2}\left(\mu_3^2\|\mathbf{h}_3\|^2 + \mu_4^2\|\mathbf{h}_4\|^2\right),$$
$$\varepsilon_s = \frac{\pi_s}{\sigma^2}\|\mathbf{f}_1\|^2 = \frac{\pi_a}{\sigma^2}\left(\mu_1^2\|\mathbf{h}_1\|^2 + \mu_2^2\|\mathbf{h}_2\|^2\right).$$

As $|z|^2 + \mathrm{Re}\{z^2\} = 2\mathrm{Re}\{z\}^2$ for any complex number z, using (3.91) and (3.92) in (3.87) leads to the following SINR expression:

$$\begin{aligned} \mathrm{SINR}_{conv} &= \frac{2\varepsilon_s}{1 + 2\varepsilon_I\left(\mathrm{Re}\{\alpha_{13}\}^2 + \mathrm{Re}\{\alpha_{14}\}^2\right)}, \\ &= \frac{2\varepsilon_s}{1 + 2\varepsilon_I\cos^2\tilde{\gamma}}. \end{aligned} \tag{3.94}$$

We recall that $\tilde{\gamma}$ is the angle formed by the vector $\tilde{\mathbf{f}}_1$ and the space spanned by the interfering vectors $\tilde{\mathbf{f}}_3$ and $\tilde{\mathbf{f}}_4$ (see (3.78), (3.79)).

Concerning the P-WL-MMSE receiver, it has been shown in Appendix 3.C that $\mathbf{g}_1^H \mathbf{R}_{\underline{\mathbf{b}}}^{-1} \mathbf{g}_2 = 0$ for internal interferences and that, as a consequence, $\mathbf{R}_{\underline{\mathbf{x}}}^{-1}\mathbf{g}_1$ and $\mathbf{R}_{\underline{\mathbf{b}}}^{-1}\mathbf{g}_1$ are collinear. Hence $\mathbf{g}_1^H \mathbf{R}_{\underline{\mathbf{b}}}^{-1} \mathbf{g}_2 = 0$ and the SINR derived in (3.85) can be written as

$$\mathrm{SINR}_{pwl} = \frac{2\pi_s (\mathbf{g}_1^H \mathbf{R}_{\underline{\mathbf{b}}}^{-1} \mathbf{g}_1)^2}{\mathbf{g}_1^H \mathbf{R}_{\underline{\mathbf{b}}}^{-1} \mathbf{g}_1 + \mathrm{Re}\{\mathbf{g}_1^H \mathbf{R}_{\underline{\mathbf{b}}}^{-1} \mathbf{C}_{\underline{\mathbf{b}}} \mathbf{R}_{\underline{\mathbf{b}}}^{-*} \mathbf{g}_1^*\}} \tag{3.95}$$

As we consider only one internal interference, $\mathbf{R}_{\underline{\mathbf{b}}} = \pi_I(\mathbf{g}_3\mathbf{g}_3^H + \mathbf{g}_4\mathbf{g}_4^H) + \sigma^2\mathbf{I}$. Besides, as interference vectors $\mathbf{g}_3$ and $\mathbf{g}_4$ are orthogonal, matrix $\mathbf{R}_{\underline{\mathbf{b}}}^{-1}$ is easily computed through a direct application of Woodbury matrix identity.

$$\mathbf{R}_{\underline{\mathbf{b}}}^{-1} = \frac{1}{\sigma^2}\left(\mathbf{I} - \frac{\varepsilon_I}{1+\varepsilon_I}\left(\frac{\mathbf{g}_3\mathbf{g}_3^H}{\|\mathbf{g}_3\|^2} + \frac{\mathbf{g}_4\mathbf{g}_4^H}{\|\mathbf{g}_4\|^2}\right)\right) \tag{3.96}$$

Using (3.96) we obtain the following expression for $\pi_s \mathbf{g}_1^H \mathbf{R}_{\underline{\mathbf{b}}}^{-1} \mathbf{g}_1$:

$$\pi_s \mathbf{g}_1^H \mathbf{R}_{\underline{\mathbf{b}}}^{-1} \mathbf{g}_1 = \varepsilon_s \left(1 - \frac{\varepsilon_I}{1+\varepsilon_I}\cos^2\overline{\gamma}\right), \tag{3.97}$$

where $\overline{\gamma}$, such that $\cos^2\overline{\gamma} = \frac{|\mathbf{g}_1^H\mathbf{g}_3|^2 + |\mathbf{g}_1^H\mathbf{g}_4|^2}{\|\mathbf{g}_1\|^2\|\mathbf{g}_3\|^2} = |\alpha_{13}|^2 + |\alpha_{14}|^2$, is the angle formed by the vector $\mathbf{g}_1$ and the space spanned by the interfering vectors $\mathbf{g}_3$ and $\mathbf{g}_4$. Moreover, as $\mathbf{C}_{\underline{\mathbf{b}}} = \pi_s(\mathbf{g}_3\mathbf{g}_3^T + \mathbf{g}_4\mathbf{g}_4^T)$, we can derive $\mathrm{Re}\{\mathbf{g}_1^H \mathbf{R}_{\underline{\mathbf{b}}}^{-1} \mathbf{C}_{\underline{\mathbf{b}}} \mathbf{R}_{\underline{\mathbf{b}}}^{-1*} \mathbf{g}_1^*\}$ using (3.96), leading to:

$$\begin{aligned}\mathrm{Re}\{\mathbf{g}_1^H \mathbf{R}_{\underline{\mathbf{b}}}^{-1} \mathbf{C}_{\underline{\mathbf{b}}} \mathbf{R}_{\underline{\mathbf{b}}}^{-1*} \mathbf{g}_1^*\} &= \frac{\varepsilon_s\varepsilon_I}{(1+\varepsilon_I)^2}\mathrm{Re}\{\alpha_{13}^2 + \alpha_{14}^2\}, \\ &= \frac{\varepsilon_s\varepsilon_I}{(1+\varepsilon_I)^2}\left(2\cos^2\tilde{\gamma} - \cos^2\overline{\gamma}\right).\end{aligned}$$

The last equality comes from the property $|z|^2 + \mathrm{Re}\{z^2\} = 2\mathrm{Re}\{z\}^2$ applied on α_{13} and α_{14}. We can now write (3.95) into the following form:

$$\mathrm{SINR}_{pwl} = \frac{2\varepsilon_s(1 - \frac{\varepsilon_I}{1+\varepsilon_I}\cos^2\overline{\gamma})^2}{1 - \frac{\varepsilon_I}{(1+\varepsilon_I)^2}\left(\varepsilon_I\cos^2\overline{\gamma} + 2\left(\cos^2\tilde{\gamma} - \cos^2\overline{\gamma}\right)\right)}. \tag{3.98}$$

We now derive the SINR at the output of the F-WL-MMSE receiver. We have previously seen that, in the case of internal interferences, condition $C1$ (3.45) is verified (see Appendix 3.A). Besides, we showed that under condition $C1$ the SINR of the F-WL-MMSE filter reduces to (3.88). Using the expression of $\mathbf{R}_{\tilde{\mathbf{b}}}^{-1}$ for $P = P_{int} = 1$ (see (3.70)) in (3.88) leads to

$$\mathrm{SINR}_{fwl} = 2\varepsilon_s\left(1 - \frac{2\varepsilon_I}{1+2\varepsilon_I}\cos^2\tilde{\gamma}\right), \tag{3.99}$$

where we recall that $\tilde{\gamma}$ is the angle formed by the vector $\tilde{\mathbf{f}}_1$ and the space spanned by the interfering vectors $\tilde{\mathbf{f}}_3$ and $\tilde{\mathbf{f}}_4$.

SINRs discussion:
In this section we discuss the SINRs depending on the values of $\cos^2\tilde{\gamma}$ and $\cos^2\overline{\gamma}$ (or equivalently, depending on $\tilde{\mathbf{f}}_1$ belonging or not to $\mathrm{span}\{\tilde{\mathbf{f}}_3, \tilde{\mathbf{f}}_4\}$ and on $\mathbf{g}_1$ belonging or not to $\mathrm{span}\{\mathbf{g}_3, \mathbf{g}_4\}$).

- **Case where $\tilde{\mathbf{f}}_1$ belongs to $\mathrm{span}\{\tilde{\mathbf{f}}_3, \tilde{\mathbf{f}}_4\}$:** This corresponds to $\tilde{\gamma}$ such that $\cos^2\tilde{\gamma} = 1$, or to (3.80) (i.e. $\tilde{\mathbf{f}}_1$ is a linear combination with real-valued coefficients of $\tilde{\mathbf{f}}_3$ and $\tilde{\mathbf{f}}_4$). In this case, there is no ST and no phase discrimination between the Alamouti useful signal and the interference. Furthermore, $\cos^2\overline{\gamma}$ is necessarily equal to 1 and expressions (3.94), (3.98) and (3.99) reduce to

$$\mathrm{SINR}_{fwl} = \mathrm{SINR}_{pwl} = \mathrm{SINR}_{conv} = \frac{2\varepsilon_s}{1+2\varepsilon_I} \tag{3.100}$$

  which decreases with ε_I and which tends to zero as ε_I becomes large. In this case, both the F-WL-MMSE and the P-WL-MMSE receivers behave like a CONV receiver, which does not reject the interference. In particular, for $N = 1$, denoting by φ_i the phase of $\mathbf{h}_i$, such that $\mathbf{h}_i = |\mathbf{h}_i|e^{i\varphi_i}$, $i = 1, \ldots, 4$, it is straightforward to verify that $\cos^2\tilde{\gamma} = 1$ is in particular verified if $\varphi_1 = \varphi_2 = \varphi_3 = \varphi_4$, i.e. in the absence of phase diversity between the useful signal and interference.

- **Case where $\tilde{\mathbf{f}}_1$ does not belong to $\mathrm{span}\{\tilde{\mathbf{f}}_3, \tilde{\mathbf{f}}_4\}$:** This is equivalent to $\cos^2\tilde{\gamma} < 1$, i.e. there is a ST and/or a phase discrimination between the Alamouti useful signal and the interference. In particular, for $N = 1$, this occurs as soon as $(\varphi_1, \varphi_2) \neq (\varphi_3, \varphi_4)$ and/or $(\varphi_1, \varphi_2) \neq (\varphi_4, \varphi_3)$, i.e. as soon as there is a phase discrimination between the Alamouti useful signal and the interference. In this case, expression (3.99) becomes, for a strong interference ($\varepsilon_I \gg 1$),

$$\mathrm{SINR}_{fwl} \simeq 2\varepsilon_s\left(1 - \cos^2\tilde{\gamma}\right) \qquad (\varepsilon_I \gg 1,\ \cos^2\tilde{\gamma} < 1). \tag{3.101}$$

  SINR_{fwl} then becomes independent of ε_I and is solely controlled by $2\varepsilon_s$ and $\cos^2\tilde{\gamma}$. This proves an interference rejection by the F-WL-MMSE receiver depending on parameter $\tilde{\gamma}$. For $N = 1$, (3.101) shows the SAIC capability of the F-WL-MMSE receiver as long as there is a phase discrimination between the Alamouti useful signal and the interference. Note that when $\cos^2\tilde{\gamma} < 1$ the quantity $\cos^2\overline{\gamma}$ may be equal to 1 or not.

- **Case where $\mathbf{g}_1$ belongs to $\mathrm{span}\{\mathbf{g}_3, \mathbf{g}_4\}$:** This is equivalent to $\cos^2\overline{\gamma} = 1$, which occurs in particular for $N = 1$. The P-WL-MMSE receiver then behaves like a CONV receiver: (3.98) reduces to (3.94). If $\cos^2\tilde{\gamma} = 0$ this receiver completely rejects the interference and coincide with the F-WL-MMSE receiver. Nonetheless, if $\cos^2\tilde{\gamma} \neq 0$, it does not reject the interference and its SINR decreases as ε_I becomes large, contrary to the F-WL-MMSE receiver, hence its sub-optimality.

- **Case where $\mathbf{g}_1$ does not to $\mathrm{span}\{\mathbf{g}_3, \mathbf{g}_4\}$:** This amounts to saying that $\cos^2\overline{\gamma} < 1$, which necessarily requires multiple receive antennas ($N > 1$). For a strong interference, (3.98) then reduces

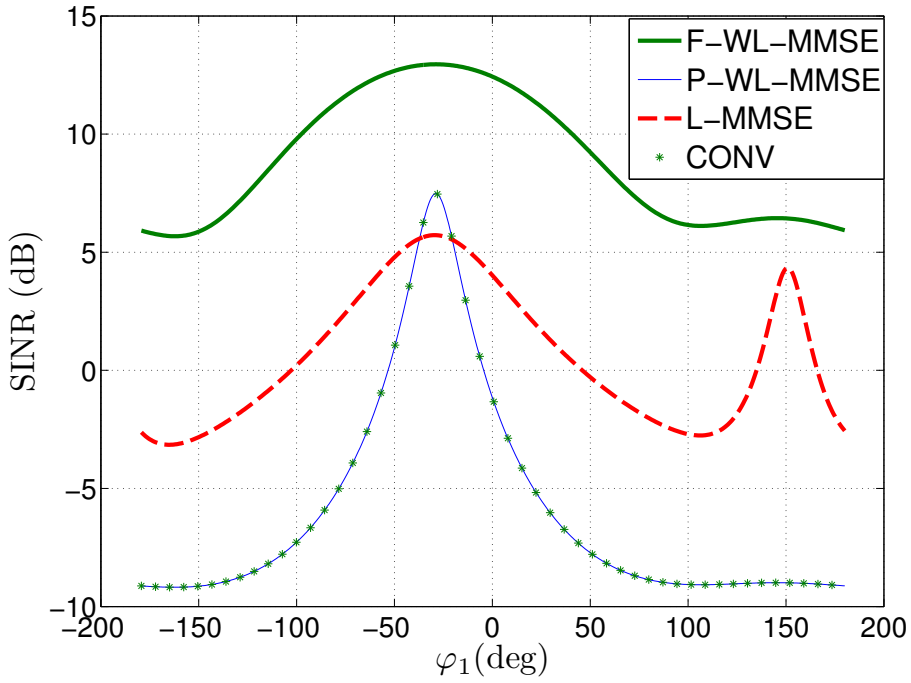

Figure 3.10: Receivers SINRs for $N = 1$

to

$$\mathrm{SINR}_{pwl} \simeq 2\varepsilon_s \left(1 - \cos^2 \overline{\gamma}\right) \qquad (\varepsilon_I \gg 1,\ \cos^2 \overline{\gamma} < 1). \tag{3.102}$$

SINR_{pwl} thus becomes independent of ε_I and is solely controlled by $2\varepsilon_s$ and $\cos^2 \overline{\gamma}$. This proves an interference rejection capability of the P-WL-MMSE receiver, contrary to the CONV receiver, depending on parameter $\overline{\gamma}$. However, despite of this rejection capability, since $\cos^2 \overline{\gamma} \geq \cos^2 \tilde{\gamma}$, we deduce from (3.101) and (3.102) that

$$\mathrm{SINR}_{pwl} \leq \mathrm{SINR}_{fwl}, \tag{3.103}$$

which proves the sub-optimality of the P-WL-MMSE receiver of the literature in general.

SINRs illustration:

The previous results are illustrated for $N = 1$ at Fig. 3.10, which shows the variations of SINR_{conv}, SINR_{l}, SINR_{pwl} and SINR_{fwl} as a function of φ_1, the phase of $\mathbf{h}_1$, when $\varphi_2 = -117.7°$, $\varphi_3 = 78.9°$,

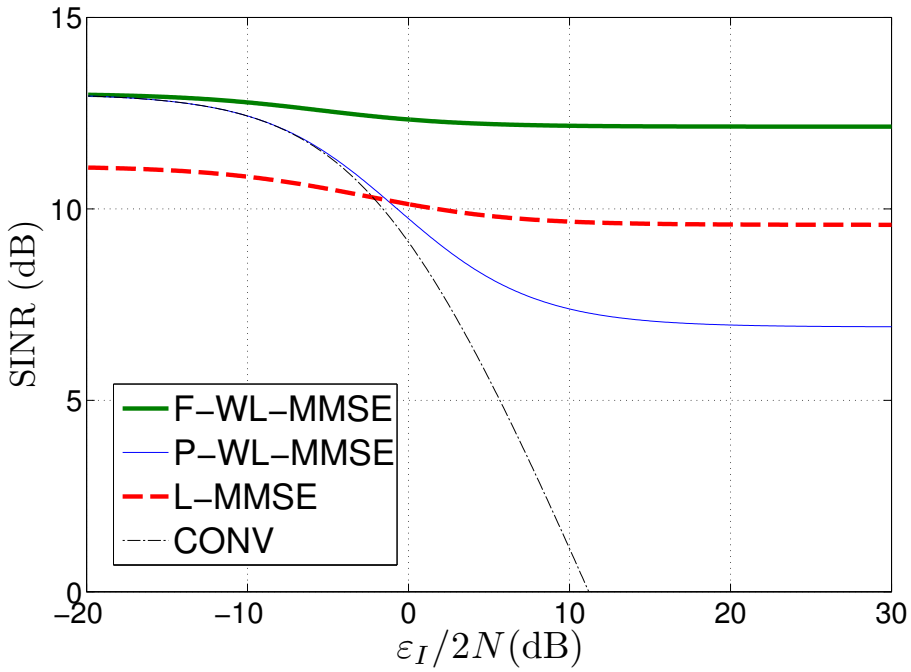

Figure 3.11: Receivers SINRs for $N = 2$

$\varphi_4 = -174.3°$, $\mu_1|\mathbf{h}_1| = 0.9$, $\mu_2|\mathbf{h}_2| = 0.48$, $\mu_3|\mathbf{h}_3| = 2.52$, $\mu_4|\mathbf{h}_4| = 2.02$, $\pi_a = 5$ (4-ASK constellation), $\sigma^2 = 0.5$, $\varepsilon_s = 10dB$ and $\varepsilon_I = 20dB$. We observe a much better performance of the F-WL-MMSE receiver with respect to the other receivers. Note the equivalent performance of the P-WL-MMSE and the CONV receivers. Note also the best performance of the L-MMSE with respect to the P-WL-MMSE receiver in most cases due, in the latter case, to the exploitation of information contained in $\mathbf{R}_{\mathbf{x}_1\mathbf{x}_2}$ in addition to the one contained in $\mathbf{R}_{\mathbf{x}_1}$ and $\mathbf{R}_{\mathbf{x}_2}$.

We also displayed the previous results for $N = 2$ on Fig. 3.11, which shows the variations of SINR_{conv}, SINR_l, SINR_{pwl} and SINR_{fwl} as a function of $\varepsilon_I/(2N)$, which corresponds to the mean Interference to noise ratio per antenna and per interference symbol at the input. We chose the following values for the simulation: $\mathbf{h}_1 = [0.89 - 0.71i,\ 1.15 + 0.21i]^T$, $\mathbf{h}_2 = [0.45 - 0.02i,\ -0.50 + 0.66i]^T$, $\mathbf{h}_3 = [-0.67 - 1.47i,\ 1.39 + 0.21i]^T$, $\mathbf{h}_4 = [0.19 + 0.14i,\ -0.05 - 0.77i]^T$, $\mu_1 = \mu_2 = 1$, $\mu_3 = \mu_4 = 1$, $\pi_a = 5$, $\varepsilon_s = 10dB$. We observe on Fig. 3.11 the optimality of the F-WL-MMSE, the P-WL-MMSE and the CONV receivers jointly with the sub-optimality of the L-MMSE receiver for a very low interference. Note the decreasing performance of the four receivers jointly with both the absence

of interference rejection of the CONV receiver (absence of a plateau) and the interference rejection of the other receivers (presence of a plateau) as $\varepsilon_I/(2N)$ increases. Note also the higher performance of the F-WL-MMSE receivers compared to the other receivers and the higher performance of the L-MMSE receiver with respect to the P-WL-MMSE for strong interference.

c) SINRs for $P > 1$ internal interference

In the presence of $P > 1$ internal interferences plus a spatially and temporally white background noise, condition $C1$ (3.45) is still verified, as shown in Appendix A. Therefore the F-WL-MMSE receiver still corresponds to the ML receiver, whose output SINR is given by (3.88). For interference number i, $i = 1, \ldots, P$, we define vectors $\mathbf{f}_{2i+1}$, $\mathbf{f}_{2i+2}$, $\mathbf{g}_{2i+1}$, $\mathbf{g}_{2i+2}$, $\tilde{\mathbf{f}}_{2i+2}$ and $\tilde{\mathbf{f}}_{2i+2}$ similarly to $\mathbf{f}_1$, $\mathbf{f}_2$, $\mathbf{g}_1$, $\mathbf{g}_2$, $\tilde{\mathbf{f}}_1$ and $\tilde{\mathbf{f}}_2$. It is straightforward to show that in the presence of $P > 1$ internal interferences, the SINR at the output of the CONV receiver is given by

$$\mathrm{SINR}_{conv} = \frac{2\varepsilon_s}{1 + \sum_{i=1}^{P} 2\varepsilon_{I,i} \cos^2 \tilde{\gamma}_i}, \tag{3.104}$$

where $\varepsilon_{I,i} = \pi_a \|\mathbf{f}_{2i+1}\|^2/\sigma^2$ corresponds to the ratio between the power of the i^{th} interference and the background noise power received by the antenna array, where $\tilde{\gamma}_i$, such that $\cos^2 \tilde{\gamma}_i = \big(|\tilde{\mathbf{f}}_1^H \tilde{\mathbf{f}}_{2i+1}|^2 + |\tilde{\mathbf{f}}_1^H \tilde{\mathbf{f}}_{2i+2}|^2\big)/\big(\|\tilde{\mathbf{f}}_1\|^2 \|\tilde{\mathbf{f}}_{2i+1}\|^2\big)$, is the angle formed by the vector $\tilde{\mathbf{f}}_1$ and the space spanned by the interfering vectors $\tilde{\mathbf{f}}_{2i+1}$ and $\tilde{\mathbf{f}}_{2i+2}$. Note that, similarly to the case $P = 1$, SINR_{conv} decreases with $\varepsilon_{I,i}$ and tends to zero as $\varepsilon_{I,i}$ becomes large.

On the opposite, using well-known array processing results [98] and assuming strong interferences ($\varepsilon_{I,i} \gg 1$, $i = 1, \ldots, P$), the SINR at the output of the P-WL-MMSE and F-WL-MMSE receivers become

$$\mathrm{SINR}_{pwl} \simeq 2\varepsilon_s \left(1 - \cos^2 \overline{\gamma}_I\right) \qquad (\varepsilon_{I,i} \gg 1,\ \cos^2 \overline{\gamma}_I < 1) \tag{3.105}$$

$$\mathrm{SINR}_{fwl} \simeq 2\varepsilon_s \left(1 - \cos^2 \tilde{\gamma}_I\right) \qquad (\varepsilon_{I,i} \gg 1,\ \cos^2 \tilde{\gamma}_I < 1) \tag{3.106}$$

where $\overline{\gamma}_I$ is the angle formed by the vector $\mathbf{g}_1$ and the space spanned by all $2P$ interfering vectors $\mathbf{g}_{2i+1}$, $\mathbf{g}_{2i+2}$, $i = 1, \ldots, P$, and where $\tilde{\gamma}_I$ is the angle formed by the vector $\tilde{\mathbf{f}}_1$ and the space spanned by all $2P$ interfering vectors $\tilde{\mathbf{f}}_{2i+1}$, $\tilde{\mathbf{f}}_{2i+2}$, $i = 1, \ldots, P$. Both SINRs are then solely controlled by ε_s and the angle $\overline{\gamma}_I$ or $\tilde{\gamma}_I$, showing the rejection capability of both considered receivers. Note that we still have $\mathrm{SINR}_{pwl} \leq \mathrm{SINR}_{fwl}$, as $\cos^2 \overline{\gamma}_I \geq \cos^2 \tilde{\gamma}_I$ holds.

3.5.5 SER performance

In this section we analyze the SER performance of all the receivers considered in this chapter. We present the total noise model in a first part, then compute the SER for the CONV, P-WL-MMSE and

F-WL-MMSE receivers in a second part and finally display in the last part the SER performances of all the considered receivers thanks to numerical simulations.

a) Observation model

We consider $P = P_{int} \geq 1$ internal interferences plus a spatially and temporally white background noise. Note that under these assumptions condition $C1$ (3.45) is still verified, as shown in Appendix A, and therefore the F-WL-MMSE receiver corresponds to the ML receiver. Using the notations of section 3.5.1, the observation vectors $\mathbf{x}_1$ and $\mathbf{x}_2$ of (3.1) can be written as

$$\begin{cases} \mathbf{x}_1(n) = \mu_1 a_{2n-1}\mathbf{h}_1 + \mu_2 a_{2n}\mathbf{h}_2 + \sum_{i=1}^{P} (\mu_{2i+1} e_{i,2n-1}\mathbf{h}_{2i+1} + \mu_{2i+2} e_{i,2n}\mathbf{h}_{2i+2}) + \mathbf{b}_{\nu 1}(n), \\ \mathbf{x}_2(n) = -\mu_1 a_{2n}\mathbf{h}_1 + \mu_2 a_{2n-1}\mathbf{h}_2 + \sum_{i=1}^{P} (-\mu_{2i+1} e_{i,2n}\mathbf{h}_{2i+1} + \mu_{2i+2} e_{i,2n-1}\mathbf{h}_{2i+2}) + \mathbf{b}_{\nu 2}(n). \end{cases} \tag{3.107}$$

We recall that $e_{i,n}$, $\mu_{2i+1}\mathbf{h}_{2i+1}$ and $\mu_{2i+2}\mathbf{h}_{2i+2}$ have been defined in section 3.5.1. Like in the previous sections vectors $\mathbf{b}_{\nu 1}$ and $\mathbf{b}_{\nu 2}$ are the $N \times 1$ background noise vectors in $\mathbf{x}_1$ and $\mathbf{x}_2$ respectively, such that the $2N \times 1$ vector $\mathbf{b}_\nu = [\mathbf{b}_{\nu 1}^T, \mathbf{b}_{\nu 2}^T]^T$ is SO circular, temporally and spatially white, i.e. such that $\mathbf{R}_{\mathbf{b}_\nu} = \sigma^2\mathbf{I}$ and $\mathbf{C}_{\mathbf{b}_\nu} = \mathbf{0}$. We define, for the i^{th} internal interference, $i = 1, \ldots, P$, vectors $\mathbf{g}_{2i+1}$, $\mathbf{g}_{2i+2}$, $\mathbf{G}_i$, $\tilde{\mathbf{f}}_{2i+2}$, $\tilde{\mathbf{f}}_{2i+2}$ and $\tilde{\mathbf{F}}_i$ similarly to $\mathbf{g}_1$, $\mathbf{g}_2$, $\mathbf{G}$, $\tilde{\mathbf{f}}_1$, $\tilde{\mathbf{f}}_2$ and $\tilde{\mathbf{F}}$. The observation system (3.107) gives rise to the following expressions for the total noise vectors $\overline{\mathbf{b}}(n)$ and $\tilde{\mathbf{b}}(n)$:

$$\overline{\mathbf{b}}(n) = \sum_{i=1}^{P} \sqrt{\frac{\pi_{I,i}}{\pi_a}} (e_{i,2n-1}\mathbf{g}_{2i+1} + e_{i,2n}\mathbf{g}_{2i+2}) + \overline{\mathbf{b}}_\nu(n) = \sum_{i=1}^{P} \sqrt{\frac{\pi_{I,i}}{\pi_a}} \mathbf{G}_i\mathbf{e}_i + \overline{\mathbf{b}}_\nu(n), \tag{3.108}$$

$$\tilde{\mathbf{b}}(n) = \sum_{i=1}^{P} \sqrt{\frac{\pi_{I,i}}{\pi_a}} \left(e_{i,2n-1}\tilde{\mathbf{f}}_{2i+1} + e_{2n}\tilde{\mathbf{f}}_{2i+2}\right) + \tilde{\mathbf{b}}_\nu(n) = \sum_{i=1}^{P} \sqrt{\frac{\pi_{I,i}}{\pi_a}} \tilde{\mathbf{F}}_i\mathbf{e}_i + \tilde{\mathbf{b}}_\nu(n), \tag{3.109}$$

where the scalars $\pi_{I,i} = \pi_a(\mu_{2i+1}^2 + \mu_{2i+2}^2)/2$ correspond to the mean power of each interfering symbol from the i^{th} interference per receive antenna, and where $\overline{\mathbf{b}}_\nu = [\mathbf{b}_{\nu 1}^T, \mathbf{b}_{\nu 2}^H]^T$, $\tilde{\mathbf{b}}_\nu = [\mathbf{b}_\nu^T, \mathbf{b}_\nu^H]^T$.

b) SER computation

We consider a $2L$-ASK constellation $\mathcal{A} = \{\pm 1, \pm 3, ..., \pm(2L-1)\}$. Supposing all symbols equally likely, for interferers signals as for the useful signal, we derive the following expression of the SER valid for the CONV, P-WL-MMSE and F-WL-MMSE receivers:

$$\text{SER} = k_L \sum_{\substack{e_{1,1}, e_{1,2}, ..., \\ e_{P,1}, e_{P,2} \in \mathcal{A}}} Q\left(\frac{\sqrt{\text{SNR}}}{\sqrt{\pi_a}} + \sum_{i=1}^{P} \mathbf{u}_i^H\mathbf{e}_i \frac{\sqrt{\text{INR}_i}}{\sqrt{\pi_a}}\right) \tag{3.110}$$

Table 3.2: SNR, INR$_i$ and $\mathbf{u}_i$ definitions

	CONV receiver	P-WL-MMSE receiver	F-WL-MMSE receiver
SNR	$\frac{2\pi_s}{\sigma^2}\|\mathbf{g}_1\|^2$	$\frac{2\pi_s(\mathbf{g}_1^H\mathbf{R}_{\underline{\mathbf{b}}}^{-1}\mathbf{g}_1)^2}{\sigma^2\mathbf{g}_1^H\mathbf{R}_{\underline{\mathbf{b}}}^{-2}\mathbf{g}_1}$	$\frac{\pi_s(\tilde{\mathbf{f}}_1^H\mathbf{R}_{\tilde{\mathbf{b}}}^{-1}\tilde{\mathbf{f}}_1)^2}{\sigma^2\tilde{\mathbf{f}}_1^H\mathbf{R}_{\tilde{\mathbf{b}}}^{-2}\tilde{\mathbf{f}}_1}$
INR$_i$	$\frac{2\pi_I\|\mathrm{Re}\{\mathbf{g}_1^H\mathbf{G}_i\}\|^2}{\sigma^2\|\mathbf{g}_1\|^2}$	$\frac{2\pi_I\|\mathrm{Re}\{\mathbf{g}_1^H\mathbf{R}_{\underline{\mathbf{b}}}^{-1}\mathbf{G}_i\}\|^2}{\sigma^2\mathbf{g}_1^H\mathbf{R}_{\underline{\mathbf{b}}}^{-2}\mathbf{g}_1}$	$\frac{\pi_I\|\tilde{\mathbf{f}}_1^H\mathbf{R}_{\tilde{\mathbf{b}}}^{-1}\tilde{\mathbf{F}}_i\|^2}{\sigma^2\tilde{\mathbf{f}}_1^H\mathbf{R}_{\tilde{\mathbf{b}}}^{-2}\tilde{\mathbf{f}}_1}$
$\mathbf{u}_i^H$	$\frac{\mathrm{Re}\{\mathbf{g}_1^H\mathbf{G}_i\}}{\|\mathrm{Re}\{\mathbf{g}_1^H\mathbf{G}_i\}\|}$	$\frac{\mathrm{Re}\{\mathbf{g}_1^H\mathbf{R}_{\underline{\mathbf{b}}}^{-1}\mathbf{G}_i\}}{\|\mathrm{Re}\{\mathbf{g}_1^H\mathbf{R}_{\underline{\mathbf{b}}}^{-1}\mathbf{G}_i\}\|}$	$\frac{\tilde{\mathbf{f}}_1^H\mathbf{R}_{\tilde{\mathbf{b}}}^{-1}\tilde{\mathbf{F}}_i}{\|\tilde{\mathbf{f}}_1^H\mathbf{R}_{\tilde{\mathbf{b}}}^{-1}\tilde{\mathbf{F}}_i\|}$

where

- $\mathbf{e}_i = [e_{i,1},\, e_{i,2}]^T$ refers to the signal of interferer i,
- $Q(u)$ is the Gaussian tail function $Q(u) = (\int_u^{+\infty} e^{-v^2/2}dv)/\sqrt{2\pi}$,
- $k_l = 2(2L-1)/(2L)^{2P+1}$
- SNR is the Signal to Noise Ratio at the output of the considered receiver,
- INR$_i$ is the Interference to Noise Ratio induced by interferer i at the output of the considered receiver,
- $\mathbf{u}_i$ is the unitary vector induced by interferer i at the output of the considered receiver.

The SNR, the INR$_i$ and the $\mathbf{u}_i$ are defined in Table 3.2, where we denoted $\mathrm{Re}\{\mathbf{v}\}$ the vector whose components are the real part of the components of vector $\mathbf{v}$. Note that, thanks to the orthogonality of the Alamouti code, there is no interference produced by symbol a_{2n}. Equation (3.110) extends the SER expression $\left(Q(\sqrt{SNR}+\sqrt{INR}) + Q(\sqrt{SNR}-\sqrt{INR})\right)/2$ of the SISO case with BPSK constellation derived in [54].

c) SER illustration

We consider a 4-ASK ($L = 2$) Alamouti radio communication link perturbed by $P = 1$ synchronous 4-ASK Alamouti interference. The channel vectors, $\mathbf{h}_i$, $i = 1, \ldots, 4$ of the sources are assumed to be constant over a burst duration but are random vectors from a burst to another and correspond to independent realizations of a zero mean vectorial complex and circular Gaussian law whose covariance matrix is $\mathbf{I}$. The sources are such that $\mu_1 = \mu_2$ and $\mu_3 = \mu_4$ are constant for each burst and such that $\pi_I/\sigma^2 = \pi_s/\sigma^2 + 10$dB. For a given receiver the SER has been computed for each burst and then averaged over 10^6 bursts. Under these assumptions, Fig. 3.12(a) and 3.12(b) show the variations of these average

SERs at the output of the CONV, the P-WL-MMSE, the F-WL-MMSE and the estimated AF-WL-MMSE (EAF-WL-MMSE) receivers as a function of the SNR π_s/σ^2, for $N = 1$ and 2 respectively. The EAF-WL-MMSE(M) receiver corresponds to the approximated F-WL-MMSE receiver estimated from M couples of training symbols inserted in each burst, as described in section 3.3.5, which is assumed to also contain 2×56 information symbols. We added the SERs computed directly from (3.110), which are perfectly in line with the average SERs. On these figures we also displayed as a reference curve the average SER at the output of the CONV receiver without any interference. Moreover, for Figure 3.12(b), we added the SERs of the P-WL-MMSE, F-WL-MMSE and E-AF-WL-MMSE receivers in the presence of one internal and one external circular non-coherent interference whose power per antenna is equal to $\pi_E = 20\pi_s$.

As expected from the SINR comparison, we can see that the F-WL-MMSE receiver performs better than the other receivers in terms of SER. For $N = 1$ (Fig. 3.12(a)), the P-WL-MMSE receiver does not handle the interference while the F-WL-MMSE performs SAIC, as stated in (3.59). For $N = 2$ (Fig. 3.12(b)), both receivers handle the internal interference, but the F-WL-MMSE requires a lower π_s/σ^2 than the P-WL-MMSE for a given SER; e.g. the F-WL-MMSE has a 3 dB gain over the P-WL-MMSE at a SER of 10^{-2}. Moreover, for $N = 2$ receiving antennas, the F-WL-MMSE receiver can handle one external interference together with one internal interference, whereas the P-WL-MMSE cannot, as predicted by (3.59). Note also the quick convergence of the EAF-WL-MMSE. These figures highlight the F-WL-MMSE capability to perform SAIC of one internal interference and its robustness to both internal and external interferences.

3.6 Conclusion

In this chapter, a WL MMSE receiver, called the F-WL-MMSE receiver, completely new for IC purposes in the context of radio communications using the Alamouti scheme, has been introduced, analyzed and compared to the available receivers of the literature for the demodulation of an Alamouti signal using real-valued constellations, such as ASK constellations, in the presence of both synchronous intra-network and external interferences. This WL MMSE receiver is a breakthrough with respect to the receivers of the literature since it jointly exploits both the real-valued nature of the sources symbols and the ST structure of the Alamouti scheme. As a consequence, it has been shown to outperform the existing receivers of the literature, to be easy to implement, to converge quickly and to implement the ML receiver in the presence of synchronous intra-network interferences. In particular, this receiver has been shown to be able to separate up to $2N$ synchronous Alamouti users from N receiving antennas, displaying its capability to perform SAIC of one synchronous Alamouti intra-network interference for $N = 1$, thanks to a phase discrimination exploitation between the useful signal and interference. This Alamouti

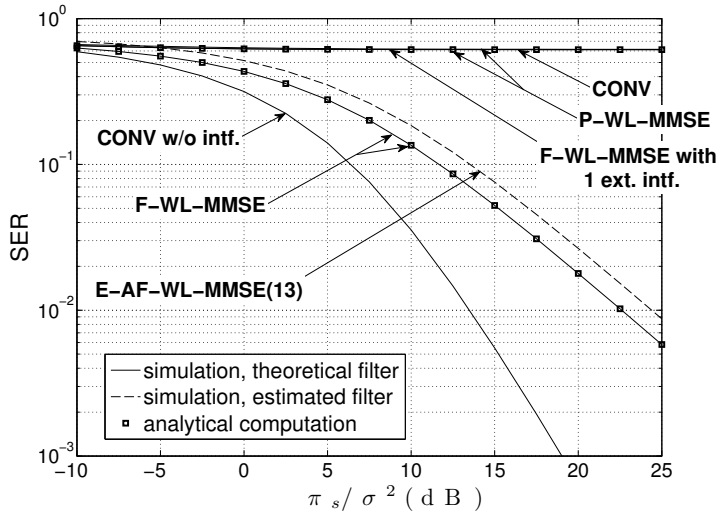

(a) $N = 1$

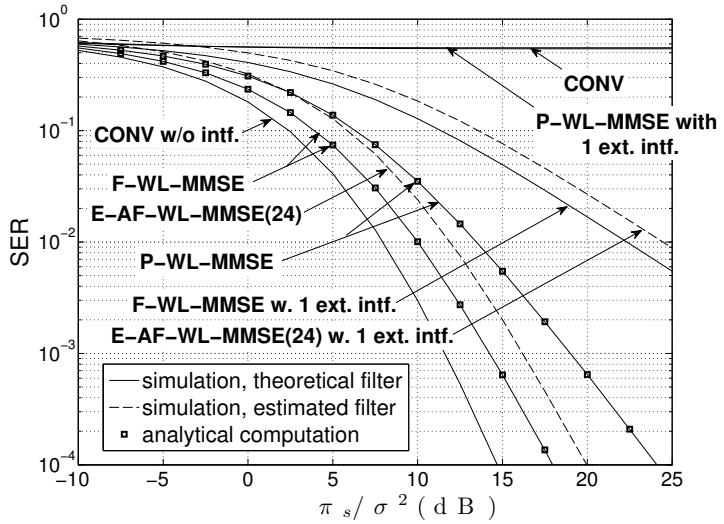

(b) $N = 2$

Figure 3.12: Theoretical and simulated SERs

SAIC/MAIC concept extends, for users with two transmit antennas using the Alamouti scheme, the SAIC/MAIC concept already available for single carrier users and SISO/SIMO links presented in [54]. A geometrical interpretation of this new SAIC/MAIC Alamouti concept has been given, highlighting the simple behavior of the receiver. Performance, in terms of output SINR and SER, of the F-WL-MMSE receiver in the presence of internal interferences have been computed analytically and compared with

those of the receivers of the literature. These computations have shown the great interest of the F-WL-MMSE receiver, for both $N = 1$ (SAIC Alamouti concept) and $N > 1$ (MAIC Alamouti concept). In particular, this new receiver allows to mitigate both intra-network and external interferences for $N > 1$. An adaptive implementation of the F-WL-MMSE receiver from training symbols has also been proposed. Thanks to its properties and low complexity, the F-WL-MMSE receiver opens up new prospects for interference management in radio communication networks using the Alamouti scheme. Indeed, this receiver may be used for many applications, such as 4G communication networks, for both downlink and uplink, providing SAIC capability for handsets with one receiving antenna but also MAIC capability for handsets with more than one antenna and for base stations, or such as military ad hoc networks, as they require simple and robust systems (here ensured by the SAIC/MAIC capability and the open-loop system) enhancing the range (here provided by the diversity through the Alamouti scheme).

Appendices

3.A Developing condition $C1 : \tilde{\mathbf{f}}_1^H \mathbf{R}_{\tilde{\mathbf{b}}}^{-1} \tilde{\mathbf{f}}_2 = 0$

In this part, we show that condition $C1$, defined by (3.45), is verified for all channel vectors $\mu_1 \mathbf{h}_1$ and $\mu_2 \mathbf{h}_2$ if and only if condition $C2$, defined by (3.54) is verified. We recall the blockwise expression (3.20) of $\mathbf{R}_{\tilde{\mathbf{b}}}^{-1}$:

$$\mathbf{R}_{\tilde{\mathbf{b}}}^{-1} = \begin{bmatrix} \mathbf{A} & \mathbf{D} \\ \mathbf{D}^* & \mathbf{A}^* \end{bmatrix}, \tag{3.111}$$

with $\mathbf{A}^H = \mathbf{A}$ and $\mathbf{D}^T = \mathbf{D}$. We can write matrices $\mathbf{A}$ and $\mathbf{D}$ under the following form:

$$\mathbf{A} = \begin{bmatrix} \mathbf{A}_1 & \mathbf{A}_{12} \\ \mathbf{A}_{12}^H & \mathbf{A}_2 \end{bmatrix}; \ \mathbf{D} = \begin{bmatrix} \mathbf{D}_1 & \mathbf{D}_{12} \\ \mathbf{D}_{12}^T & \mathbf{D}_2 \end{bmatrix}, \tag{3.112}$$

where the $N \times N$ complex matrices $\mathbf{A}_1, \mathbf{A}_2, \mathbf{A}_{12}, \mathbf{D}_1, \mathbf{D}_2$ and $\mathbf{D}_{12}$ are such that $\mathbf{A}_1^H = \mathbf{A}_1$, $\mathbf{A}_2^H = \mathbf{A}_2$, $\mathbf{D}_1^T = \mathbf{D}_1$ and $\mathbf{D}_2^T = \mathbf{D}_2$. We then deduce from (3.111) and (3.112) that

$$\begin{aligned} \tilde{\mathbf{f}}_1^H \mathbf{R}_{\tilde{\mathbf{b}}}(n)^{-1} \tilde{\mathbf{f}}_2 =& 2\mathrm{Re}\left[\mathbf{f}_1^H \mathbf{A} \mathbf{f}_2\right] + 2\mathrm{Re}\left[\mathbf{f}_1^T \mathbf{D}^* \mathbf{f}_2\right] \\ =& 2\frac{\pi_a}{\pi_s}\Big\{\mu_1\mu_2 \mathrm{Re}\left[\mathbf{h}_1^H(\mathbf{A}_1 - \mathbf{A}_2)\mathbf{h}_2 + \mathbf{h}_1^H(\mathbf{D}_1 - \mathbf{D}_2)\mathbf{h}_2^*\right] \\ & - \mu_1^2 \mathrm{Re}\left[\mathbf{h}_1^H(\mathbf{A}_{12}\mathbf{h}_1 + \mathbf{D}_{12}\mathbf{h}_1^*)\right] + \mu_2^2 \mathrm{Re}\left[\mathbf{h}_2^H(\mathbf{A}_{12}^H\mathbf{h}_2 + \mathbf{D}_{12}^T\mathbf{h}_2^*)\right]\Big\}. \end{aligned} \tag{3.113}$$

It is straightforward to show from (3.113) that quantity $\tilde{\mathbf{f}}_1^H \mathbf{R}_{\tilde{\mathbf{b}}}^{-1}(n) \tilde{\mathbf{f}}_2$ is equal to zero whatever $\mu_1 \mathbf{h}_1$ and $\mu_2 \mathbf{h}_2$ if and only if the four following equalities hold:

$$\mathbf{A}_1 - \mathbf{A}_2 = 0, \tag{3.114}$$

$$\mathbf{D}_1 - \mathbf{D}_2 = 0, \tag{3.115}$$

$$\mu_1^2 \mathrm{Re}\left[\mathbf{h}_1^H(\mathbf{A}_{12}\mathbf{h}_1 + \mathbf{D}_{12}\mathbf{h}_1^*)\right] = 0 \quad \forall \mu_1 \mathbf{h}_1, \tag{3.116}$$

$$\mu_2^2 \mathrm{Re}\left[\mathbf{h}_2^H(\mathbf{A}_{12}^H\mathbf{h}_2 + \mathbf{D}_{12}^T\mathbf{h}_2^*)\right] = 0 \quad \forall \mu_2 \mathbf{h}_2. \tag{3.117}$$

By considering vectors $\mu_1 \mathbf{h}_1$ of the form $\mu_1 \mathbf{h}_1 = \gamma \mathbf{e}_k + \zeta \mathbf{e}_l$, $(1 \leq k, l \leq N)$, where $\mathbf{e}_k$ is the $N \times 1$ vector whose k^{th} component is 1 while the others are zero, and by choosing successively particular couples (γ, ζ) such that $(\gamma, \zeta) \in \{(1,0), (j,0), (-j,0), (1,1), (j,j), (-j,-j), (1,j)\}$, we find that if (3.117) is verified, then necessarily $\mathbf{A}_{12} = -\mathbf{A}_{12}^H$ and $\mathbf{D}_{12} = -\mathbf{D}_{12}^T$. Conversely if $\mathbf{A}_{12} = -\mathbf{A}_{12}^H$ and $\mathbf{D}_{12} = -\mathbf{D}_{12}^T$, it is easy to verify that (3.117) is verified. Consequently Condition $C1$ is verified for all

channel vectors $\mu_1\mathbf{h}_1$ and $\mu_2\mathbf{h}_2$ if and only if

$$\begin{cases} \mathbf{A}_1 = \mathbf{A}_2; \\ \mathbf{D}_1 = \mathbf{D}_2; \\ \mathbf{A}_{12}^H = -\mathbf{A}_{12}; \\ \mathbf{D}_{12}^T = -\mathbf{D}_{12}. \end{cases}$$

It is straightforward to check that this condition is equivalent to condition $C2$ (3.54).

In the case of a total noise composed of an arbitrary number of synchronous intra-network interferences plus a SO circular, temporally and spatially white background noise, we can check using (3.8), (3.9), (3.10), (3.11), (3.12) and (3.13) that $\mathbf{R}_1 = \mathbf{R}_2$, $\mathbf{R}_{12}^H = -\mathbf{R}_{12}$, $\mathbf{C}_1 = \mathbf{C}_2$ and $\mathbf{C}_{12}^T = -\mathbf{C}_{12}$. Condition $C2$ (3.54) is verified and thus condition $C1$ (3.45) is also verified.

3.B Deriving a condition for the ML/P-WL-MMSE equivalence

In this section we derive a necessary and sufficient condition for the P-WL-MMSE receiver to correspond to the ML receiver.

As mentioned in 3.3.2, the partially WL MMSE filter $\overline{\mathbf{w}}_{pwl}$ only exploits the information contained in matrices $\mathbf{R}_1$, $\mathbf{R}_2$ and $\mathbf{C}_{12}$ but not the one in $\mathbf{C}_1$, $\mathbf{C}_2$ and $\mathbf{R}_{12}$. A necessary condition for the ML/P-WL-MMSE equivalence is therefore

$$\mathbf{C}_1 = \mathbf{C}_2 = \mathbf{R}_{12} = 0. \tag{3.118}$$

This condition is equivalent to

$$\mathbf{D}_1 = \mathbf{D}_2 = \mathbf{A}_{12} = 0. \tag{3.119}$$

where $\mathbf{D}_1$, $\mathbf{D}_2$ and $\mathbf{A}_{12}$ are defined in (3.112). Under this condition, matrices $\mathbf{R}_{\tilde{\mathbf{b}}}$ and $\mathbf{R}_{\tilde{\mathbf{b}}}^{-1}$ can then be written as:

$$\mathbf{R}_{\tilde{\mathbf{b}}} = \begin{bmatrix} \mathbf{R}_1 & 0 & 0 & \mathbf{C}_{12} \\ 0 & \mathbf{R}_2 & \mathbf{C}_{12}^T & 0 \\ 0 & \mathbf{C}_{12}^* & \mathbf{R}_1^* & 0 \\ \mathbf{C}_{12}^H & 0 & 0 & \mathbf{R}_2^* \end{bmatrix} ; \; \mathbf{R}_{\tilde{\mathbf{b}}}^{-1} = \begin{bmatrix} \mathbf{A}_1 & 0 & 0 & \mathbf{D}_{12} \\ 0 & \mathbf{A}_2 & \mathbf{D}_{12}^T & 0 \\ 0 & \mathbf{D}_{12}^* & \mathbf{A}_1^* & 0 \\ \mathbf{D}_{12}^H & 0 & 0 & \mathbf{A}_2^* \end{bmatrix}. \tag{3.120}$$

We now complete the previous necessary condition (3.118) to make it sufficient. In order to have the equivalence between the ML and the P-WL-MMSE receivers, their outputs before the ML decision need

to be proportional. We first derive z_{ml} from (3.49) and (3.120), assuming (3.118) is verified:

$$\begin{aligned} z_{ml} &= (\mathbf{R}_{\tilde{\mathbf{b}}}^{-1} \tilde{\mathbf{f}}_1)^H \tilde{\mathbf{x}} \\ &= 2\mathrm{Re}\left\{ \mathbf{f}_1^H \begin{bmatrix} \mathbf{A}_1 & 0 \\ 0 & \mathbf{A}_2 \end{bmatrix} \mathbf{x} + \mathbf{f}_1^T \begin{bmatrix} 0 & \mathbf{D}_{12}^* \\ \mathbf{D}_{12}^H & 0 \end{bmatrix} \mathbf{x} \right\} \\ &= 2\mathrm{Re}\left\{ \mathbf{g}_1^H \begin{bmatrix} \mathbf{A}_1 & \mathbf{D}_{12} \\ \mathbf{D}_{12}^H & \mathbf{A}_2^* \end{bmatrix} \overline{\mathbf{x}} \right\}. \end{aligned} \tag{3.121}$$

Besides, writing $\mathbf{R}_{\tilde{\mathbf{b}}}^{-1} \mathbf{R}_{\tilde{\mathbf{b}}} = \mathbf{I}$ with (3.120) leads to

$$\begin{bmatrix} \mathbf{A}_1 & \mathbf{D}_{12} \\ \mathbf{D}_{12}^H & \mathbf{A}_2^* \end{bmatrix} \begin{bmatrix} \mathbf{R}_1 & \mathbf{C}_{12} \\ \mathbf{C}_{12}^H & \mathbf{R}_2^* \end{bmatrix} = \mathbf{I},$$

where we recognize $\mathbf{R}_{\underline{\mathbf{b}}}$ expression (3.17). We derived this way the inverse of $\mathbf{R}_{\underline{\mathbf{b}}}$, which in fact corresponds to the matrix in (3.121). Hence,

$$z_{ml} = 2\mathrm{Re}\left\{ (\mathbf{R}_{\underline{\mathbf{b}}}^{-1} \mathbf{g}_1)^H \overline{\mathbf{x}} \right\} \tag{3.122}$$

As for the output of the P-WL-MMSE receiver, it can be written using (3.27) and (3.28) under the following form:

$$z_{pwl} = \mathrm{Re}\left\{ \sqrt{\pi_s \pi_a} (\mathbf{R}_{\overline{\mathbf{x}}}^{-1} \mathbf{g}_1)^H \overline{\mathbf{x}} \right\}. \tag{3.123}$$

Therefore, in order to have z_{ml} and z_{pwl} proportional, vectors $\mathbf{R}_{\overline{\mathbf{x}}}^{-1} \mathbf{g}_1$ and $\mathbf{R}_{\underline{\mathbf{b}}}^{-1} \mathbf{g}_1$ need to be collinear. Applying the matrix inversion Lemma to $\mathbf{R}_{\overline{\mathbf{x}}} = \pi_s \mathbf{G}\mathbf{G}^H + \mathbf{R}_{\underline{\mathbf{b}}} = \pi_s \mathbf{g}_1 \mathbf{g}_1^H + \pi_s \mathbf{g}_2 \mathbf{g}_2^H + \mathbf{R}_{\underline{\mathbf{b}}}$, we obtain

$$\mathbf{R}_{\overline{\mathbf{x}}}^{-1} \mathbf{g}_1 = \frac{1}{1 + \pi_s \mathbf{g}_1^H \left(\mathbf{R}_{\underline{\mathbf{b}}} + \pi_s \mathbf{g}_2 \mathbf{g}_2^H \right)^{-1} \mathbf{g}_1} \left[\mathbf{R}_{\underline{\mathbf{b}}}^{-1} \mathbf{g}_1 - \frac{\pi_s \mathbf{g}_2^H \mathbf{R}_{\underline{\mathbf{b}}}^{-1} \mathbf{g}_1}{1 + \pi_s \mathbf{g}_2^H \mathbf{R}_{\underline{\mathbf{b}}}^{-1} \mathbf{g}_2} \mathbf{R}_{\underline{\mathbf{b}}}^{-1} \mathbf{g}_2 \right]. \tag{3.124}$$

We deduce from (3.124) that $\mathbf{g}_1^H \mathbf{R}_{\underline{\mathbf{b}}}^{-1} \mathbf{g}_2$ have to be equal to 0 to have vectors $\mathbf{R}_{\overline{\mathbf{x}}}^{-1} \mathbf{g}_1$ and $\mathbf{R}_{\underline{\mathbf{b}}}^{-1} \mathbf{g}_1$ collinear. We have thus obtained the following necessary condition for the ML/P-WL-MMSE receivers equivalence:

$$C3 : \begin{cases} \mathbf{g}_1^H \mathbf{R}_{\underline{\mathbf{b}}}^{-1} \mathbf{g}_2 = 0, \\ \mathbf{C}_1 = \mathbf{C}_2 = \mathbf{R}_{12} = 0. \end{cases} \tag{3.125}$$

It is straightforward to check that condition $C3$ is moreover sufficient.

3.C Developing condition $\mathbf{g}_1^H \mathbf{R}_{\underline{\mathbf{b}}}^{-1} \mathbf{g}_2 = 0$

In this section, we show that the condition $\mathbf{g}_1^H \mathbf{R}_{\underline{\mathbf{b}}}^{-1} \mathbf{g}_2 = 0$ is verified for all channel vectors $\mu_1 \mathbf{h}_1$ and $\mu_2 \mathbf{h}_2$, if and only if $\mathbf{R}_1 = \mathbf{R}_2$ and $\mathbf{C}_{12}^T = -\mathbf{C}_{12}$. We can show that $\mathbf{R}_{\underline{\mathbf{b}}}^{-1}$ has the same block structure of

$\mathbf{R}_{\overline{\mathbf{b}}}$, that is

$$\mathbf{R}_{\overline{\mathbf{b}}}^{-1} = \begin{bmatrix} \mathbf{A}_1 & \mathbf{D}_{12} \\ \mathbf{D}_{12}^H & \mathbf{A}_2^* \end{bmatrix},$$

where the $N \times N$ complex matrices $\mathbf{A}_1$ and $\mathbf{A}_2$ are such that $\mathbf{A}_1^H = \mathbf{A}_1$ and $\mathbf{A}_2^H = \mathbf{A}_2$. Note that these matrices do not correspond to those of Appendices 3.A and 3.B in general. We then obtain

$$\mathbf{g}_1^H \mathbf{R}_{\overline{\mathbf{b}}}^{-1} \mathbf{g}_2 = \frac{\pi_a}{\pi_s} \left[\mu_1 \mu_2 \mathbf{h}_1^H \left(\mathbf{A}_1 - \mathbf{A}_2 \right) \mathbf{h}_2 - \mu_1^2 \mathbf{h}_1^H \mathbf{D}_{12} \mathbf{h}_1^* + \mu_2^2 \mathbf{h}_2^T \mathbf{D}_{12}^H \mathbf{h}_2 \right] \tag{3.126}$$

We first assume that $\mathbf{g}_1^H \mathbf{R}_{\overline{\mathbf{b}}}^{-1} \mathbf{g}_2 = 0$ for all channel vectors $\mu_1 \mathbf{h}_1$ and $\mu_2 \mathbf{h}_2$. In particular, considering $(\mu_2 \mathbf{h}_2, \mu_1 \mathbf{h}_1) = (\mathbf{0}, \mathbf{e}_k)$ and $(\mu_2 \mathbf{h}_2, \mu_1 \mathbf{h}_1) = (\mathbf{0}, \mathbf{e}_k + \mathbf{e}_l)$ with $k \neq l$, we find that $\mathbf{g}_1^H \mathbf{R}_{\overline{\mathbf{b}}}^{-1} \mathbf{g}_2 = 0$ implies

$$\mathbf{D}_{12}^T = -\mathbf{D}_{12}.$$

Then, (3.126) becomes

$$\mathbf{g}_1^H \mathbf{R}_{\overline{\mathbf{b}}}^{-1} \mathbf{g}_2 = \frac{\pi_a}{\pi_s} \mu_1 \mu_2 \mathbf{h}_1^H \left(\mathbf{A}_1 - \mathbf{A}_2 \right) \mathbf{h}_2.$$

We now consider $(\mu_2 \mathbf{h}_2, \mu_1 \mathbf{h}_1) = (\mathbf{e}_k, \mathbf{e}_l)$, $(1 \leq k, l \leq N)$, which yields $\mathbf{A}_1 = \mathbf{A}_2$.

Conversely if $\mathbf{A}_1 = \mathbf{A}_2$ and $\mathbf{D}_{12} = -\mathbf{D}_{12}^T$, it is straightforward to verify that (3.126) is verified. Consequently $\mathbf{g}_1^H \mathbf{R}_{\overline{\mathbf{b}}}^{-1} \mathbf{g}_2 = 0$ for all channel vectors $\mu_1 \mathbf{h}_1$ and $\mu_2 \mathbf{h}_2$, if and only if $\mathbf{A}_1 = \mathbf{A}_2$ and $\mathbf{D}_{12}^T = -\mathbf{D}_{12}$. One can check by blockwise inversion that this is equivalent to

$$\begin{cases} \mathbf{R}_1 = \mathbf{R}_2, \\ \mathbf{C}_{12}^T = -\mathbf{C}_{12}. \end{cases}$$

In the case of a total noise composed of an arbitrary number of synchronous intra-network interferences plus a SO circular, temporally and spatially white background noise, we have thus $\mathbf{g}_1^H \mathbf{R}_{\overline{\mathbf{b}}}^{-1} \mathbf{g}_2 = 0$. Indeed, we can check using (3.8), (3.9) and (3.13) that we then have $\mathbf{R}_1 = \mathbf{R}_2$, and $\mathbf{C}_{12}^T = -\mathbf{C}_{12}$. We recall that, from (3.124), this implies that vectors $\mathbf{R}_{\overline{\mathbf{x}}}^{-1} \mathbf{g}_1$ and $\mathbf{R}_{\overline{\mathbf{b}}}^{-1} \mathbf{g}_1$ are then collinear.

We can now conclude: condition $C3$, defined by (3.55), is therefore equivalent to condition $C4$ defined by

$$C4 : \begin{cases} \mathbf{R}_1 = \mathbf{R}_2, \\ \mathbf{C}_1 = \mathbf{C}_2 = \mathbf{R}_{12} = 0, \\ \mathbf{C}_{12}^T = -\mathbf{C}_{12}. \end{cases} \tag{3.127}$$

3.D Deriving a condition for the ML/L-MMSE equivalence

In this section we derive a necessary and sufficient condition for the Linear MMSE receiver to correspond to the ML receiver.

As mentioned in 3.3.2, the Linear MMSE filter $\mathbf{w}_{mmse}$ only exploits the information contained in matrices $\mathbf{R}_1$, $\mathbf{R}_2$ and $\mathbf{R}_{12}$ but not the one in $\mathbf{C}_1$, $\mathbf{C}_2$ and $\mathbf{C}_{12}$. Hence, a necessary condition for the ML/P-WL-MMSE equivalence is that

$$\mathbf{C}_1 = \mathbf{C}_2 = \mathbf{C}_{12} = 0, \tag{3.128}$$

is verified, i.e. that $b(n)$ is SO circular. This condition is equivalent to $\mathbf{D} = 0$, where $\mathbf{D}$ is defined in (3.22).

We now complete the previous necessary condition (3.128) to make it sufficient. In order to have the equivalence between the ML and the Linear MMSE receivers, their outputs before the ML decision need to be proportional. We first derive z_{ml} from (3.49) and (3.19), assuming (3.128) is verified:

$$\begin{aligned} z_{ml} &= (\mathbf{R}_{\tilde{\mathbf{b}}}^{-1} \tilde{\mathbf{f}}_1)^H \tilde{\mathbf{x}} \\ &= 2\mathrm{Re}\left\{ \mathbf{f}_1^H \mathbf{R}_{\mathbf{b}}^{-1} \mathbf{x} \right\}. \end{aligned} \tag{3.129}$$

$$z_{ml} = 2\mathrm{Re}\left\{ (\mathbf{R}_{\overline{\mathbf{b}}}^{-1} \mathbf{g}_1)^H \overline{\mathbf{x}} \right\} \tag{3.130}$$

As for the output of the Linear MMSE receiver, it can be written using (3.32) under the following form:

$$z_l = \mathrm{Re}\left\{ \sqrt{\pi_s \pi_a} (\mathbf{R}_{\mathbf{x}}^{-1} \mathbf{f}_1)^H \mathbf{x} \right\}. \tag{3.131}$$

Therefore, in order to have z_{ml} and z_{pwl} proportional, vectors $\mathbf{R}_{\mathbf{x}}^{-1}\mathbf{f}_1$ and $\mathbf{R}_{\mathbf{b}}^{-1}\mathbf{f}_1$ need to be collinear. Applying the matrix inversion Lemma to $\mathbf{R}_{\mathbf{x}} = \pi_s \mathbf{F}\mathbf{F}^H + \mathbf{R}_{\mathbf{b}} = \pi_s \mathbf{f}_1 \mathbf{f}_1^H + \pi_s \mathbf{f}_2 \mathbf{f}_2^H + \mathbf{R}_{\mathbf{b}}$, we obtain

$$\mathbf{R}_{\mathbf{x}}^{-1}\mathbf{f}_1 = \frac{1}{1 + \pi_s \mathbf{f}_1^H (\mathbf{R}_{\mathbf{b}} + \pi_s \mathbf{f}_2 \mathbf{f}_2^H)^{-1} \mathbf{f}_1} \left[\mathbf{R}_{\mathbf{b}}^{-1}\mathbf{f}_1 - \frac{\pi_s \mathbf{f}_2^H \mathbf{R}_{\mathbf{b}}^{-1} \mathbf{f}_1}{1 + \pi_s \mathbf{f}_2^H \mathbf{R}_{\mathbf{b}}^{-1} \mathbf{f}_2} \mathbf{R}_{\mathbf{b}}^{-1} \mathbf{f}_2 \right] \tag{3.132}$$

We deduce from (3.132) that $\mathbf{f}_1^H \mathbf{R}_{\mathbf{b}}^{-1} \mathbf{f}_2$ has to be equal to 0 in order to have vectors $\mathbf{R}_{\mathbf{x}}^{-1}\mathbf{f}_1$ and $\mathbf{R}_{\mathbf{b}}^{-1}\mathbf{f}_1$ collinear. We have thus obtained the following necessary condition for the ML/Linear MMSE receivers equivalence:

$$C5 : \begin{cases} \mathbf{f}_1^H \mathbf{R}_{\mathbf{b}}^{-1} \mathbf{f}_2 = 0, \\ \mathbf{C}_1 = \mathbf{C}_2 = \mathbf{C}_{12} = 0. \end{cases} \tag{3.133}$$

It is straightforward to check that condition $C5$ is moreover sufficient.

3.E Developing condition $\mathbf{f}_1^H \mathbf{R}_{\mathbf{b}}^{-1} \mathbf{f}_2 = 0$

In this section, we show that we cannot have $\mathbf{f}_1^H \mathbf{R}_{\mathbf{b}}^{-1} \mathbf{f}_2 = 0$ for all channel vectors $\mu_1 \mathbf{h}_1$ and $\mu_2 \mathbf{h}_2$.

The structure of $\mathbf{R}_{\mathbf{b}}^{-1}$ matrix is given by

$$\mathbf{R}_{\mathbf{b}}^{-1} = \begin{bmatrix} \mathbf{A}_1 & \mathbf{A}_{12} \\ \mathbf{A}_{12}^H & \mathbf{A}_2 \end{bmatrix},$$

where the $N \times N$ complex matrices $\mathbf{A}_1$ and $\mathbf{A}_2$ are such that $\mathbf{A}_1^H = \mathbf{A}_1$ and $\mathbf{A}_2^H = \mathbf{A}_2$. Note that these matrices do not correspond in general to those of Appendices 3.A, 3.B, 3.C, 3.D. We can now derive $\mathbf{f}_1^H \mathbf{R}_{\mathbf{b}}^{-1} \mathbf{f}_2$.

$$\mathbf{f}_1^H \mathbf{R}_{\mathbf{b}}^{-1} \mathbf{f}_2 = \frac{\pi_a}{\pi_s} \left[\mu_1 \mu_2 \left[\mathbf{h}_1^H \mathbf{A}_1 \mathbf{h}_2 - \mathbf{h}_2^H \mathbf{A}_2 \mathbf{h}_1 \right] - \mu_1^2 \mathbf{h}_1^H \mathbf{A}_{12} \mathbf{h}_1 + \mu_2^2 \mathbf{h}_2^H \mathbf{A}_{12}^H \mathbf{h}_2 \right] \tag{3.134}$$

We assume that $\mathbf{f}_1^H \mathbf{R}_{\mathbf{b}}^{-1} \mathbf{f}_2 = 0$ for any channel vectors $\mu_1 \mathbf{h}_1$ and $\mu_2 \mathbf{h}_2$. In particular, considering first the case of $\mu_2 \mathbf{h}_2 = 0$ and then the case of $\mu_1 \mathbf{h}_1 = 0$, we obtain that

$$-\mu_1^2 \mathbf{h}_1^H \mathbf{A}_{12} \mathbf{h}_1 = \mu_2^2 \mathbf{h}_2^H \mathbf{A}_{12}^H \mathbf{h}_2 = 0 \quad \forall\, \mu_1 \mathbf{h}_1,\, \mu_2 \mathbf{h}_2.$$

Hence $\mathbf{A}_{12} = 0$. This result simplifies the expression of $\mathbf{f}_1^H \mathbf{R}_{\mathbf{b}}^{-1} \mathbf{f}_2$ given in (3.134), which can then be written as

$$\mathbf{f}_1^H \mathbf{R}_{\mathbf{b}}^{-1} \mathbf{f}_2 = \frac{\pi_a}{\pi_s} \mu_1 \mu_2 \left[\mathbf{h}_1^H \mathbf{A}_1 \mathbf{h}_2 - \mathbf{h}_2^H \mathbf{A}_2 \mathbf{h}_1 \right]. \tag{3.135}$$

We now consider the special cases $\mu_2 \mathbf{h}_2 = \mu_1 \mathbf{h}_1$ and $\mu_2 \mathbf{h}_2 = j \mu_1 \mathbf{h}_1$ in (3.135). They generate the following equality

$$\mu_1 \mathbf{h}_1^H \left(\mathbf{A}_1 - \mathbf{A}_2 \right) \mathbf{h}_1 = \mu_1 \mathbf{h}_1^H \left(\mathbf{A}_1 + \mathbf{A}_2 \right) \mathbf{h}_1 = 0 \quad \forall\, \mu_1 \mathbf{h}_1,$$

which implies that $\mathbf{A}_1 = \mathbf{A}_2 = 0$. As we also showed that $\mathbf{A}_{12} = 0$, we eventually have that $\mathbf{R}_{\mathbf{b}}^{-1} = 0$. Nonetheless we cannot have $\mathbf{R}_{\mathbf{b}}^{-1} = 0$ for finite entries of $\mathbf{R}_{\mathbf{b}}$. It would happen, e.g., for a Gaussian circular noise of infinite variance. Restricting ourselves to the study of finite power signals and noise, we can conclude that the ML receiver and the L-MMSE receiver never correspond.

3.F Interferences contribution at the F-WL-MMSE output

In this appendix we analyze the impact of the interferences in the output z_{fwl} of the F-WL-MMSE receiver for $P = P_{int} = 1$. We then derive the contributions of a_{2n}, e_{2n-1} and e_{2n} in $y_{fwl} = \mathbf{w}_{fwl}^H \mathbf{x}$. We recall that the output of the F-WL-MMSE receiver is given by $z_{fwl} = 2\mathrm{Re}\{y_{fwl}\}$ (3.37).

3.F.1 Contribution of the interfering signal a_{2n}

We derive the contribution of a_{2n} in y_1, which corresponds to $\mathbf{w}_{fwl}^H\mathbf{f}_2$.

$$\begin{aligned}\mathbf{w}_{fwl}^H\mathbf{f}_2 &= \frac{k}{\sigma^2}\left(\mathbf{f}_1^H\mathbf{f}_2 - \frac{2\varepsilon_I}{1+2\varepsilon_I}\frac{(\tilde{\mathbf{f}}_3^H\tilde{\mathbf{f}}_1)(\mathbf{f}_3^H\mathbf{f}_2)+(\tilde{\mathbf{f}}_4^H\tilde{\mathbf{f}}_1)(\mathbf{f}_4^H\mathbf{f}_2)}{\|\tilde{\mathbf{f}}_3\|^2}\right)\\ &= \frac{k}{\sigma^2}\left(\mathbf{f}_1^H\mathbf{f}_2 - \frac{2\varepsilon_I}{1+2\varepsilon_I}\frac{(\tilde{\mathbf{f}}_3^H\tilde{\mathbf{f}}_1)(\mathbf{f}_3^H\mathbf{f}_2)-(\tilde{\mathbf{f}}_3^H\tilde{\mathbf{f}}_2)(\mathbf{f}_3^H\mathbf{f}_1)}{\|\tilde{\mathbf{f}}_3\|^2}\right),\end{aligned}$$

as $\tilde{\mathbf{f}}_4^H\tilde{\mathbf{f}}_1 = -\tilde{\mathbf{f}}_3^H\tilde{\mathbf{f}}_2$ and $\mathbf{f}_4^H\mathbf{f}_2 = \mathbf{f}_3^H\mathbf{f}_1$. Eventually, as $\tilde{\mathbf{f}}_3^H\tilde{\mathbf{f}}_1 = \mathbf{f}_3^H\mathbf{f}_1 + (\mathbf{f}_3^H\mathbf{f}_1)^*$ and $\tilde{\mathbf{f}}_3^H\tilde{\mathbf{f}}_2 = \mathbf{f}_3^H\mathbf{f}_1 + (\mathbf{f}_3^H\mathbf{f}_1)^*$,

$$\mathbf{w}_{fwl}^H\mathbf{f}_2 = i\cdot\frac{k}{\sigma^2}\mathrm{Im}\left\{\frac{2\pi_a\mu_1\mu_2}{\pi_s}\mathbf{h}_1^H\mathbf{h}_2 - \frac{2\varepsilon_I}{1+2\varepsilon_I}\frac{(\mathbf{f}_3^H\mathbf{f}_1)^*\mathbf{f}_3^H\mathbf{f}_2}{\|\mathbf{f}_3\|^2}\right\}.$$

The interference induced by a_{2n} has a phase of $\pm\,\pi/2$ due to the orthogonality of the Alamouti code; its contribution in z_{fwl} is therefore canceled by the real part operation.

3.F.2 Contribution of the interfering signal through e_{2n-1} and e_{2n}

We now calculate the contribution induced by the interfering Alamouti user. The interfering symbol e_{2n-1} is carried by $\mathbf{w}_{fwl}^H\mathbf{f}_3$ in y_1 and

$$\begin{aligned}\mathbf{w}_{fwl}^H\mathbf{f}_3 &= \frac{k}{\sigma^2}\left(\mathbf{f}_1^H\mathbf{f}_3 - \frac{2\varepsilon_I}{1+2\varepsilon_I}\frac{(\tilde{\mathbf{f}}_3^H\tilde{\mathbf{f}}_1)(\mathbf{f}_3^H\mathbf{f}_3)+(\tilde{\mathbf{f}}_4^H\tilde{\mathbf{f}}_1)(\mathbf{f}_4^H\mathbf{f}_3)}{\|\tilde{\mathbf{f}}_3\|^2}\right)\\ &= \frac{k}{\sigma^2}\left(\mathbf{f}_1^H\mathbf{f}_3 - \frac{2\varepsilon_I}{1+2\varepsilon_I}\left(\mathrm{Re}\{\mathbf{f}_3^H\mathbf{f}_1\} + \frac{\mathrm{Re}\{\mathbf{f}_4^H\mathbf{f}_1\}\cdot i\,\mathrm{Im}\{\frac{2\pi_a\mu_3\mu_4}{\pi_I}\mathbf{h}_4^H\mathbf{h}_3\}}{\|\mathbf{f}_3\|^2}\right)\right)\\ &= \frac{k}{\sigma^2}\left(\frac{\mathrm{Re}\{\mathbf{f}_1^H\mathbf{f}_3\}}{1+2\varepsilon_I} + i\left(\mathrm{Im}\{\mathbf{f}_1^H\mathbf{f}_3\} - \frac{4\pi_a\mu_3\mu_4}{\sigma^2(1+2\varepsilon_I)}\mathrm{Re}\{\mathbf{f}_4^H\mathbf{f}_1\}\mathrm{Im}\{\mathbf{h}_4^H\mathbf{h}_3\}\right)\right).\end{aligned}$$

We similarly obtain the contribution of e_{2n} in y_1.

$$\mathbf{w}_{fwl}^H\mathbf{f}_4 = \frac{k}{\sigma^2}\left(\frac{\mathrm{Re}\{\mathbf{f}_1^H\mathbf{f}_4\}}{1+2\varepsilon_I} + i\left(\mathrm{Im}\{\mathbf{f}_1^H\mathbf{f}_4\} - \frac{4\pi_a\mu_3\mu_4}{\sigma^2(1+2\varepsilon_I)}\mathrm{Re}\{\mathbf{f}_3^H\mathbf{f}_1\}\mathrm{Im}\{\mathbf{h}_3^H\mathbf{h}_4\}\right)\right).$$

Conclusion

THIS thesis aimed to study the frequency selective channels for single-carrier transmitters on two levels: mutual information and diversity. We concentrated on the optimization of the input covariance matrix w.r.t. the ergodic mutual information in a first part before studying the diversity for fixed target rate and MMSE receivers in a second part. We completed in a third part these results by studying a way to achieve optimal diversity: the use of orthogonal STBC such as the Alamouti code, which was analyzed in multiuser context with a new kind of MMSE receiver at the receiver.

Capacity optimization

In chapter 1 we have confirmed the validity of the asymptotic approximation of the ergodic mutual information derived by Moustakas and Simon thanks to a rigorous proof. We have also shown that the approximation error was a $\mathcal{O}\left(1/t\right)$ term, where t is the number of transmit antennas. Besides, we established that the approximation is a strictly concave function of the input covariance matrix and that the average mutual information evaluated at the argmax of the approximation is equal to the capacity of the channel up to a $\mathcal{O}\left(1/t\right)$ term. This latter result justified our indirect maximization approach which consists in optimizing the approximation instead of the ergodic mutual information. To that end we proposed an algorithm based on an iterative waterfilling scheme and we studied its convergence to some extent. We also illustrated our results by numerical simulations which showed the relevance of our algorithm: the new approach provides the same results as the direct approach – i.e., maximizing the ergodic mutual information – even for a small number of transmit and receive antennas.

Following these results, it would be interesting to conduct a similar approach for optimizing the mutual information of a MIMO system using a MMSE receiver at reception. Indeed, our approach assume an optimal receiver at reception, that is, a ML receiver, whose complexity compared to the MMSE receivers is in practice dissuasive. In fact we easily derived a large system approximation of the

ergodic mutual information, which can be written as

$$\overline{I}_{mmse}(\mathbf{Q}) = -\sum_{j=1}^{t} \log \left[\left(\mathbf{I}_t + \mathbf{K}^H \left(\sum_{l=1}^{L} \delta_l(\mathbf{Q}) \tilde{\mathbf{C}}^{(l)} \right) \mathbf{K} \right)^{-1} \right]_{jj},$$

where $\mathbf{K}$ is the precoder, i.e., $\mathbf{K}\mathbf{s}(n)$ is sent at the transmitter, where $\mathbf{s}(n)$ components are i.i.d. with unit variance, hence, the input covariance is $\mathbf{Q} = \mathbf{K}\mathbf{K}^H$. Nevertheless its optimization is different from the previous case; we showed that the optimization is equivalent to optimizing the following term:

$$\log \left| \mathbf{I}_t + \mathbf{Q} \left(\sum_{l=1}^{L} \delta_l(\mathbf{Q}) \tilde{\mathbf{C}}^{(l)} \right) \right|.$$

Unfortunately the iterative waterfilling algorithm is not relevant anymore for the optimization of this term, even though in all conducted simulations $\overline{\mathbf{Q}}_*$ which maximizes $\overline{I}(\mathbf{Q})$ was a local maximum for $\overline{I}_{mmse}(\mathbf{Q})$. A Newton algorithm, coupled with a barrier interior-point method, could then however be used. Once the optimal $\mathbf{Q}_{opt}$ matrix is obtained, the optimal precoding matrix $\mathbf{K}_{opt}$ is easily recovered: $\mathbf{K}_{opt} = \mathbf{Q}_{opt}^{1/2}\mathbf{U}_{opt}$, where $\mathbf{U}_{opt}$ is the eigenvectors unitary matrix of

$$\mathbf{Q}_{opt}^{1/2} \left(\sum_{l=1}^{L} \delta_l(\mathbf{Q}_{opt}) \mathbf{C}^{(l)} \right) \mathbf{Q}_{opt}^{1/2} = \mathbf{U}_{opt} \Delta \mathbf{U}_{opt}^H.$$

Hence, $\mathbf{K}_{opt}$ is the matrix such that $\mathbf{K}_{opt}^H \left(\sum_{l=1}^{L} \delta_l(\mathbf{Q}_{opt}) \mathbf{C}^{(l)} \right) \mathbf{K}_{opt}$ is diagonal and $\mathbf{Q}_{opt} = \mathbf{K}_{opt}\mathbf{K}_{opt}^H$. Nonetheless, we did not consider this approach since the Newton algorithm with barrier method is less attractive in terms of implementation.

MMSE Diversity Analysis

In chapter 2 we evaluated the maximal diversity of a MIMO system using a MMSE receiver. To that end we used the Diversity-Multiplexing Trade-off approach with a multiplexing gain of 0, i.e. for finite (w.r.t. the SNR) target rates $\mathbf{R}$. For frequency selective fading channels with cyclic prefix, we rigorously proved the surprising behavior observed by Hedayat et al. for finite rates R: in this case, the MMSE receiver causes the MIMO system to take several diversity values depending on the fixed target rate value, achieving in particular the full diversity MNL, which is the diversity of the ML receiver, for sufficiently low rates – M being the number of transmitting antennas, N the number of receiving antennas and L the number of independent taps.

The result stated for frequency selective fading channels with cyclic prefix could probably be improved. Indeed we assumed in the frequency selective case that the transmission data block length K

is large enough: $K > M^2(L-1)$. But most of all, the diversity has not been derived for rates R verifying $-\log\left(\frac{m-1}{M} + \frac{L-1}{K}(M-(m-1))\right) < \frac{R}{M} < \log\frac{M}{m-1}$ for a given $m \in \{1,\dots,M\}$. Actually the derived bounds are not tight in this case. This corresponds to the step from $m(LN-M+m)$ to $(m+1)(LN-M+(m+1))$, $m \in \{1,\dots,M-1\}$, of the diversity function. It would therefore be interesting to analyze how the diversity behaves in this rate range.

The SAIC/MAIC Alamouti concept

In chapter 3 we focused on the diversity implied by the use of the Alamouti orthogonal STBC. We introduced in the multiuser context, with users using real-valued modulations, the F-WL-MMSE receiver, which makes the most of the degrees of freedom available in the channel. We showed indeed that this receiver is robust to internal and external interferences; in particular it is able to separate $2N$ users of the network from N receiving antennas, hence its SAIC capability. In this sense, it extends the SAIC/MAIC concept to the MISO/MIMO cases. Besides, we proved that in the case of internal interferences the F-WL-MMSE receiver is optimal in the ML sense. Furthermore we derived its SINR and SER and showed that this receiver outperforms the receivers of the literature in terms of SINR and SER, highlighting its optimality. We also provided a geometrical interpretation of the SAIC/MAIC Alamouti concept which underlines its simple behavior. Lastly, an easy adaptive implementation of the F-WL-MMSE has been proposed, which converges quickly in practice. Thanks to these results, the F-WL-MMSE receiver offers new prospects for interference management in 4G communication networks and military ad hoc networks.

The analysis was however limited to the case of flat fading channels (or, equivalently, of frequency selective channels with an OFDM waveform). An interesting research topic, which was unfortunately not tackled in this thesis, would be to extend these results to frequency selective channels with single carrier waveforms, then using STBCs in the frequency domain. It would also be interesting to analyze the more common case of complex constellations, considering circular constellations but also non-circular constellations, whose relevance has recently been pointed out to some extent by [99]. This study is currently ongoing. Another worthwhile research point which is underway is the case of asynchronous interferences. Indeed, we assumed in this thesis that the internal interferences are synchronous, which rarely occurs in practice. It would be interesting to analyze how the asynchronism impacts the performance of the MMSE Alamouti receivers and to find a way to prevent the asynchronism consequences.

Bibliography

[1] E. Telatar, "Capacity of multi-antenna gaussian channels, technical memorandum," *Bell Labs Tech. Memo.*, 1995.

[2] ——, "Capacity of multi-antenna gaussian channels," *European transactions on telecommunications*, vol. 10, no. 6, pp. 585–595, 1999.

[3] A. Scaglione, P. Stoica, S. Barbarossa, G. Giannakis, and H. Sampath, "Optimal designs for space-time linear precoders and decoders," *IEEE Trans. Signal Processing*, vol. 50, no. 5, pp. 1051–1064, may 2002.

[4] E. Visotsky and U. Madhow, "Space-time transmit precoding with imperfect feedback," *IEEE Trans. Inform. Theory*, vol. 47, no. 6, pp. 2632–2639, sep 2001.

[5] E. Jorswieck and H. Boche, "Channel capacity and capacity-range of beamforming in MIMO wireless systems under correlated fading with covariance feedback," *IEEE Trans. Wireless Commun.*, vol. 3, no. 5, pp. 1543–1553, sep 2004.

[6] D. Hosli, Y. Kim, and A. Lapidoth, "Monotonicity results for coherent MIMO Rician channels," *IEEE Trans. Inform. Theory*, vol. 51, no. 12, pp. 4334–4339, Dec 2005.

[7] M. Vu and A. Paulraj, "Capacity optimization for Rician correlated MIMO wireless channels," in *Proc. Asilomar Conference*, 2005, pp. 133–138.

[8] A. Moustakas, S. Simon, and A. Sengupta, "MIMO capacity through correlated channels in the presence of correlated interferers and noise: A (not so) large N analysis," *IEEE Trans. Inform. Theory*, vol. 49, no. 10, pp. 2545–2561, 2003.

[9] A. Tulino, A. Lozano, and S. Verdú, "Impact of antenna correlation on the capacity of multiantenna channels," *IEEE Trans. Inform. Theory*, vol. 51, no. 7, pp. 2491–2509, jul 2005.

[10] W. Hachem, O. Khorunzhiy, P. Loubaton, J. Najim, and L. Pastur, "A new approach for capacity analysis of large dimensional multi-antenna channels," *IEEE Trans. Inform. Theory*, vol. 54, no. 9, pp. 3987–4004, Sep 2008.

[11] G. Taricco, "On the capacity of separately-correlated MIMO Rician channels," in *Proc. IEEE Globecom*, 2006.

[12] J. Dumont, W. Hachem, S. Lasaulce, P. Loubaton, and J. Najim, "On the capacity achieving covariance matrix for Rician MIMO channels: an asymptotic approach," *IEEE Trans. Inform. Theory*, vol. 56, no. 3, pp. 1048–1069, Mar 2010.

[13] C. Wen, P. Ting, and J. Chen, "Asymptotic analysis of MIMO wireless systems with spatial correlation at the receiver," *IEEE Trans. Commun.*, vol. 54, no. 2, pp. 349–363, Feb 2006.

[14] G. Taricco and E. Riegler, "On the ergodic capacity of the asymptotic separately-correlated Rician fading MIMO channel with interference," in *Proc. of ISIT (International Symposium on Information Theory)*, jun 2007, pp. 531–535.

[15] ——, "On the ergodic capacity of correlated Rician fading MIMO channels with interference," *IEEE Trans. Inform. Theory*, vol. 57, no. 7, pp. 4123–4137, jul 2011.

[16] H. Bolcskei, D. Gesbert, and A. Paulraj, "On the capacity of OFDM-based spatial multiplexing systems," *IEEE Trans. Commun.*, vol. 50, no. 2, pp. 225–234, Feb 2002.

[17] A. Moustakas and S. Simon, "On the outage capacity of correlated multiple-path MIMO channels," *IEEE Trans. Inform. Theory*, vol. 53, no. 11, p. 3887, Nov 2007.

[18] H. Witsenhausen, "A determinant maximization problem occurring in the theory of data communication," *SIAM Journal on Applied Mathematics*, vol. 29, no. 3, pp. 515–522, nov 1975.

[19] S. Zhou and G. Giannakis, "Single-carrier space-time block-coded transmissions over frequency-selective fading channels," *IEEE Trans. Inform. Theory*, vol. 49, no. 1, pp. 164–179, jan 2003.

[20] C. Tepedelenlioglu, "Maximum multipath diversity with linear equalization in precoded OFDM systems," *IEEE Trans. Inform. Theory*, vol. 50, no. 1, pp. 232–235, jan 2004.

[21] R. Schober, W. Gerstacker, and L. Lampe, "Performance analysis and design of stbcs for frequency-selective fading channels," *IEEE Trans. Wireless Commun.*, vol. 3, no. 3, pp. 734–744, may 2004.

[22] L. Zheng and D. Tse, "Diversity and multiplexing: A fundamental tradeoff in multiple-antenna channels," *IEEE Trans. Inform. Theory*, vol. 49, no. 5, pp. 1073–1096, 2003.

[23] L. Grokop and D. Tse, "Diversity/multiplexing tradeoff in ISI channels," in *Proc. of ISIT (International Symposium on Information Theory)*, jun 2004, p. 97.

[24] ——, "Diversity–multiplexing tradeoff in ISI channels," *Information Theory, IEEE Transactions on*, vol. 55, no. 1, pp. 109–135, jan 2009.

[25] A. Medles and D. Slock, "Optimal diversity vs multiplexing tradeoff for frequency selective MIMO channels," in *Proc. of ISIT (International Symposium on Information Theory)*. IEEE, 2005, pp. 1813–1817.

[26] D. Slock, "On the diversity-multiplexing tradeoff for frequency-selective MIMO channels," in *Proc. of Information Theory and Applications Workshop*, jan 2007, pp. 426–430.

[27] P. Coronel and H. Bolcskei, "Diversity-multiplexing tradeoff in selective-fading MIMO channels," in *Proc. of ISIT (International Symposium on Information Theory)*, jun 2007, pp. 2841–2845.

[28] K. Kumar, G. Caire, and A. Moustakas, "Asymptotic performance of linear receivers in MIMO fading channels," *IEEE Trans. Inform. Theory*, vol. 55, no. 10, pp. 4398–4418, oct. 2009.

[29] A. Hedayat, A. Nosratinia, and N. Al-Dhahir, "Linear equalizers for flat rayleigh MIMO channels," in *Proc. ICASSP Conference*, vol. 3, march 2005, pp. 445–448.

[30] ——, “Outage probability and diversity order of linear equalizers in frequency-selective fading channels,” in *Proc. Asilomar Conference*, vol. 2, nov. 2004, pp. 2032–2036.

[31] A. Tajer and A. Nosratinia, “Diversity order of MMSE single-carrier frequency domain linear equalization,” in *Proc. Globecom Conference*, nov. 2007, pp. 1524–1528.

[32] A. Mehana and A. Nosratinia, “Diversity of MMSE MIMO receivers,” in *Proc. of ISIT (International Symposium on Information Theory)*, june 2010, pp. 2163–2167.

[33] ——, “Diversity of MMSE MIMO Receivers,” 2011. [Online]. Available: http://arxiv.org/abs/1102.1462

[34] G. Foschini, “Layered space-time architecture for wireless communication in a fading environment when using multi-element antennas,” *Bell labs technical journal*, vol. 1, no. 2, pp. 41–59, 1996.

[35] P. Wolniansky, G. Foschini, G. Golden, and R. Valenzuela, “V-BLAST: An architecture for realizing very high data rates over the rich-scattering wireless channel,” in *Proc. of URSI ISSSE conference*, sep 1998, pp. 295–300.

[36] V. Tarokh, N. Seshadri, and A. Calderbank, “Space-time codes for high data rate wireless communication: Performance criterion and code construction,” *IEEE Trans. Inform. Theory*, vol. 44, no. 2, pp. 744–765, Mar 1998.

[37] V. Tarokh, H. Jafarkhani, and A. Calderbank, “Space-time block codes from orthogonal designs,” *IEEE Trans. Inform. Theory*, vol. 45, no. 5, pp. 1456–1467, Jul 1999.

[38] S. Alamouti, “A simple transmit diversity technique for wireless communications,” *IEEE J. Select. Areas Commun.*, vol. 16, no. 8, pp. 1451–1458, Oct 1998.

[39] S. Diggavi, N. Al-Dhahir, A. Stamoulis, and A. Calderbank, “Great expectations: The value of spatial diversity in wireless networks,” *Proc. IEEE*, vol. 92, no. 2, pp. 219–270, Feb 2004.

[40] A. Naguib, N. Seshadri, and A. Calderbank, “Applications of space-time block codes and interference suppression for high capacity and high data rate wireless systems,” in *Proc. Asilomar Conference*, nov 1998, pp. 1803–1810.

[41] V. Tarokh, A. Naguib, N. Seshadri, and A. Calderbank, “Combined array processing and space-time coding,” *IEEE Trans. Inform. Theory*, vol. 45, no. 4, pp. 1121–1128, 1999.

[42] A. Naguib, N. Seshadri, and A. Calderbank, “Increasing data rate over wireless channels,” *IEEE Signal Processing Mag.*, vol. 17, no. 3, pp. 76–92, 2000.

[43] A. Stamoulis, N. Al-Dhahir, and A. Calderbank, “Further results on interference cancellation and space-time blockcodes,” in *Proc. Asilomar Conference*, 2001, pp. 257–261.

[44] J. Li, K. Ben Letaief, and Z. Cao, “Co-channel interference cancellation for space-time coded OFDM systems,” *IEEE Trans. Wireless Commun.*, vol. 2, no. 1, pp. 41–49, Jan. 2003.

[45] Z. Zhang, Y. Gong, Y. Gong, Y. Ye, and C. Jin, “A simplified ML approach in suppression of directional interference for STBC MIMO system,” in *Proc. WiCom 2007*, Sept 2007, pp. 346–349.

[46] J. Kazemitabar and H. Jafarkhani, "Multiuser interference cancellation and detection for users with more than two transmit antennas," *IEEE Trans. Commun.*, vol. 56, pp. 574–583, 2008.

[47] S. Sirianunpiboon, A. Calderbank, and S. Howard, "Bayesian analysis of interference cancellation for Alamouti multiplexing," *IEEE Trans. Inform. Theory*, vol. 54, no. 10, pp. 4755–4761, Oct 2008.

[48] J. Winters, J. Salz, and R. Gitlin, "The impact of antenna diversity on the capacity of wireless communication systems," *IEEE Trans. Commun.*, vol. 42, no. 234, pp. 1740–1751, Feb 1994.

[49] H. Jafarkhani, "A quasi-orthogonal space-time block code," *IEEE Trans. Commun.*, vol. 49, no. 1, pp. 1–4, Jan 2001.

[50] W. Su and X. Xia, "Signal constellations for quasi-orthogonal space-time block codes with full diversity," *IEEE Trans. Inform. Theory*, vol. 50, no. 10, pp. 2331–2347, Oct 2004.

[51] S. Verdu, *Multiuser detection*. Cambridge Univ Pr, 1998.

[52] H. Trigui and D. Slock, "Performance bounds for cochannel interference cancellation within the current GSM standard," *Signal processing*, vol. 80, no. 7, pp. 1335–1346, 2000.

[53] M. Pukkila, G. Mattellini, and P. Ranta, "Cochannel interference suppression for constant modulus signals," in *Proc. IEEE Int. Conf. on Comm.*, vol. 5, Jun 2004, pp. 2548–2552.

[54] P. Chevalier and F. Pipon, "New insights into optimal widely linear array receivers for the demodulation of BPSK, MSK, and GMSK signals corrupted by noncircular interferences-application to SAIC," *IEEE Trans. Signal Processing*, vol. 54, no. 3, pp. 870–883, 2006.

[55] R. Meyer, W. Gerstacker, R. Schober, and J. Huber, "A single antenna interference cancellation algorithm for increased GSM capacity," *IEEE Trans. Wireless Commun.*, vol. 5, no. 7, pp. 1616–1621, 2006.

[56] P. Chevalier, F. Pipon, and F. Delaveau, "Second-order optimal array receivers for synchronization of BPSK, MSK, and GMSK signals corrupted by noncircular interferences," *EURASIP Journal on Advances in Signal Processing*, vol. 2007, no. 3, pp. 1–16, Dec 2007.

[57] B. Picinbono, "On circularity," *IEEE Trans. Signal Processing*, vol. 42, no. 12, pp. 3473–3482, Dec 1994.

[58] J. Proakis, *Digital communications*. New York: McGraw-Hill, Third Edition, 1995.

[59] B. Picinbono and P. Chevalier, "Widely linear estimation with complex data," *IEEE Trans. Signal Processing*, vol. 43, no. 8, pp. 2030–2033, 1995.

[60] M. Austin, "SAIC and synchronized networks for increased GSM capacity," *White Paper, 3G Americas' SAIC working group*, 2003.

[61] L. Popova, R. Meyer, W. Gerstacker, and W. Koch, "Downlink performance improvements in (a) synchronous GPRS networks using single/multiple antenna interference cancellation techniques," in *Proc. 12th European Wireless Conference*, Apr 2006, pp. 1–7.

[62] M. Konrad and W. Gerstacker, "Interference robust transmission for the downlink of an OFDM-based mobile communications system," *EURASIP Journal on Wireless Communications and Networking*, 2008.

[63] A. Lampe and M. Breiling, "Asymptotic analysis of widely linear MMSE multiuser detection - complex vs. real modulation," in *Proc. IEEE Information Theory Workshop (ITW'01)*, 2001, pp. 55–57.

[64] S. Buzzi, M. Lops, and S. Sardellitti, "Widely linear reception strategies for layered space-time wireless communications," *IEEE Trans. Signal Processing*, vol. 54, no. 6, pp. 2252–2262, Jun 2006.

[65] W. Gerstacker, F. Obernosterer, R. Schober, A. Lehmann, A. Lampe, and P. Gunreben, "Equalization concepts for Alamouti's space-time block code," *IEEE Trans. Commun.*, vol. 52, no. 7, pp. 1178–1190, 2004.

[66] A. H. Mehana and A. Nosratinia, "The diversity of MMSE receiver over frequency-selective MIMO channel," in *Proc. of ISIT (International Symposium on Information Theory)*, aug 2011, pp. 1121 –1125.

[67] A. Mostafa, R. Kobylinski, I. Kostanic, and M. Austin, "Single antenna interference cancellation (SAIC) for GSM networks," in *Proc. IEEE Vehicular Technology Conference (VTC)*, vol. 2, Oct 2003, pp. 1089–1093.

[68] A. Goldsmith, S. Jafar, N. Jindal, and S. Vishwanath, "Capacity limits of MIMO channels," *IEEE J. Select. Areas Commun.*, vol. 21, no. 5, pp. 684–702, Jun 2003.

[69] J. Dumont, W. Hachem, S. Lasaulce, P. Loubaton, and J. Najim, "On the capacity achieving covariance matrix for Rician MIMO channels: an asymptotic approach," 2007, extended version of [12]. [Online]. Available: http://arxiv.org/abs/0710.4051

[70] C. Artigue, P. Loubaton, and B. Mouhouche, "On the ergodic capacity of frequency selective MIMO systems equipped with MMSE receivers: An asymptotic approach," in *Proc. Globecom*, 2008.

[71] R. Horn and C. Johnson, *Matrix analysis*. Cambridge Univ Pr, 1990.

[72] ——, *Topics in matrix analysis*. Cambridge Univ Pr, 1994.

[73] J. Borwein and A. Lewis, *Convex analysis and nonlinear optimization : theory and examples*. New York: Springer Verlag, 2000.

[74] M. Kreĭn and A. Nudel'man, *The Markov moment problem and extremal problems*. Translations of Mathematical Monographs, American Mathematical Society, Providence, 1977, vol. 50.

[75] W. Hachem, P. Loubaton, and J. Najim, "Deterministic equivalents for certain functionals of large random matrices," *Ann. Appl. Probab.*, vol. 17, no. 3, pp. 875–930, 2007.

[76] L. Pastur, "A simple approach to the global regime of Gaussian ensembles of random matrices," *Ukrainian Math. J.*, vol. 57, no. 6, pp. 936–966, Jun 2005.

[77] E. Novikov, "Functionals and the random-force method in turbulence theory," *Soviet Physics-JETP*, vol. 20, pp. 1290–1294, 1965.

[78] W. Hachem, P. Loubaton, and J. Najim, "A CLT for information-theoretic statistics of Gram random matrices with a given variance profile," *Ann. Appl. Probab.*, vol. 18, no. 6, pp. 2071–2130, Dec 2008.

[79] Y. Jiang, M. Varanasi, and J. Li, "Performance analysis of ZF and MMSE equalizers for MIMO systems: an in-depth study of the high SNR regime," *IEEE Trans. Inform. Theory*, vol. 57, no. 4, pp. 2008–2026, apr. 2011.

[80] P. Diţă, "Factorization of unitary matrices," *J. Phys. A: Math. Gen.*, vol. 36, pp. 2781–2789, 2003.

[81] M. Lundberg and L. Svensson, "The Haar measure and the generation of random unitary matrices," in *Proc. IEEE Sensor Array and Multichannel Signal Processing Workshop*, 2004, pp. 114–118.

[82] H. Li, X. Lu, and G. Giannakis, "Capon Multiuser Receiver for CDMA Systems With Space-Time Coding," *IEEE Trans. Signal Processing*, vol. 50, no. 5, pp. 1193–1204, 2002.

[83] F. Neeser and J. Massey, "Proper complex random processes with applications to information theory," *IEEE Trans. Inform. Theory*, vol. 39, no. 4, pp. 1293–1302, Jul 1993.

[84] R. Fischer and C. Windpassinger, "Real versus complex-valued equalisation in V-BLAST systems," *Electronics Letters*, vol. 39, no. 5, pp. 470–471, Mar 2003.

[85] C. Pietsch, S. Sand, W. Teich, and J. Lindner, "Modeling and performance evaluation of multiuser MIMO systems using real-valued matrices," *IEEE J. Select. Areas Commun.*, vol. 21, no. 5, pp. 744–753, Jun 2003.

[86] S. Sfar, R. Murch, and K. Letaief, "Layered space-time multiuser detection over wireless uplink systems," *IEEE Trans. Wireless Commun.*, vol. 2, no. 4, pp. 653–668, Jul 2003.

[87] M. Witzke, "Linear and widely linear filtering applied to iterative detection of generalized MIMO signals," in *Annales des télécommunications*, vol. 60, no. 1-2, Jan 2005, pp. 147–168.

[88] G. Foschini, G. Golden, R. Valenzuela, and P. Wolniansky, "Simplified processing for high spectral efficiency wireless communication employing multi-element arrays," *IEEE J. Select. Areas Commun.*, vol. 17, no. 11, pp. 1841–1852, Nov 1999.

[89] D. Mattera, L. Paura, and F. Sterle, "Widely linear decision-feedback equalizer for time-dispersive linear MIMO channels," *Signal Processing, IEEE Transactions on*, vol. 53, no. 7, pp. 2525–2536, July 2005.

[90] K. Carson Pun and T. Nguyen, "Widely linear filter bank equalizer for real STBC," *IEEE Trans. Signal Processing*, vol. 56, no. 9, pp. 4544–4548, Sep 2008.

[91] A. Aghaei, K. Plataniotis, and S. Pasupathy, "Widely linear MMSE receivers for linear dispersion space-time block-codes," *IEEE Trans. Wireless Commun.*, vol. 9, no. 1, pp. 8–13, Jan 2010.

[92] P. Chevalier and F. Dupuy, "Procédé et dispositif de réception mono et multi antennes pour liaisons de type alamouti," french Patent FR 09.05 263, Nov 3, 2009.

[93] ——, "Single and multiple antennas Alamouti receivers for the reception of real-valued signals corrupted by interferences," in *Proc. Asilomar Conference*, Nov 2009.

[94] ——, "Widely linear Alamouti receivers for the reception of real-valued constellations corrupted by interferences – the Alamouti SAIC/MAIC concept," *IEEE Trans. Signal Processing*, July 2011.

[95] F. Dupuy and P. Chevalier, "Performance analysis of WL Alamouti receivers for real-valued constellations in multiuser context," in *Proc. of EUSIPCO conference*, sep 2011.

[96] A. van den Bos, "The multivariate complex normal distribution-a generalization," *IEEE Trans. Inform. Theory*, vol. 41, no. 2, pp. 537–539, 1995.

[97] B. Picinbono, "Second-order complex random vectors and normal distributions," *IEEE Trans. Signal Processing*, vol. 44, no. 10, pp. 2637–2640, Oct 1996.

[98] P. Chevalier, “Optimal separation of independent narrow-band sources: Concept and performance,” *Signal processing*, vol. 73, no. 1-2, pp. 27–47, feb 1999.

[99] M. Lipardi, D. Mattera, and F. Sterle, “Constellation design for widely linear transceivers,” *EURASIP Journal on Advances in Signal Processing*, vol. 2010, 2010.